REPORT

Drainage Åknes

HYDROGEOLOGICAL REPORT

DOC.NO. 20180662-06-R
REV.NO. 1 / 2021-01-14

NORWEGIAN GEOTECHNICAL INSTITUTE
NGI.NO

Project

Project title:	Drainage Åknes
Document title:	Hydrogeological report
Document no.:	20180662-06-R
Date:	2020-06-11
Revision no. /rev. date:	1 / 2021-01-14

Client

Client:	NVE
Client contact person:	Gustav Pless
Contract reference:	Research and development contract, signed 12 September 2018

for NGI

Project manager:	Kristin H. Holmøy
Prepared by:	Kristin H. Holmøy, Tore Ingvald Bjørnarå, Mahdi Shabanimashcool, Henrik Langeland
Reviewed by:	Vidar Kveldsvik

NORWEGIAN GEOTECHNICAL INSTITUTE
NGI.NO

Main office
PO Box 3930 Ullevaal St.
NO-0806 Oslo
Norway

Trondheim office
PO Box 5687 Torgarden
NO-7485 Trondheim
Norway

T 22 02 30 00
F 22 23 04 48
NGI@ngi.no

BIC NO. DNBANOKK
IBAN NO26 5096 05 01281
ORGANISATION NO.
958 254 318MVA

ISO 9001/14001
CERTIFIED BY BSI
FS 32989/EMS 612006

Summary

NGI is engaged by Norwegian water resources and energy directorate (NVE) to carry out stability analysis of the Åknes rock slide. This report is presenting and analysing the most important investigations and monitoring, such as packer tests and piezometer measurements in both open boreholes and boreholes with packers dividing the borehole in sections. A hydrogeological model is presented.

The main conclusions are:

- Water head on the sliding plane are small, only small peaks up to 3-4 meter over short periods of time are monitored. For most of the boreholes the water table is several meters below the main sliding plane.
- The hydraulic communication in the slope is high. It seems like the hydraulic system is fed from a bigger area, not only the backscarp.

Contents

1 Background and introduction 6
2 Results from hydrogeological borehole investigations 8
2.1 Packer tests in boreholes 8
2.2 Variable head tests in boreholes 15
2.3 Piezometer measurements in boreholes 15
3 Hydrological analysis 30
3.1 Analysis of water pressure in the boreholes from 2017 and 2018 30
3.2 Hydraulic conductivity from Lugeon-tests 40
3.3 Rock mass fracture analysis 41
4 Hydrogeological model 49
4.1 Saturated flow: Darcy's law 49
4.2 Unsaturated flow: Richards' equation 50
4.3 Unsaturated flow: variables 53
4.4 Anisotropy 56
4.5 Results fluid flow 57
4.6 Surface flow 60
5 Discussion of results and concluding remarks 62
5.1 Hydraulic communications in the slope 62
5.2 Water pressure on main sliding plane 67
5.3 Concluding remarks 69
6 References 70

Appendix

Appendix A Packer test interpretation KH-02-2017, KH-01-2018 and KH-02-2018
Appendix B Details on position of packers and piezometers in the four boreholes
Appendix C Water pressure variation versus precipitation in the boreholes from 2017 and 2018
Appendix D Illustration of Profile W2
Appendix E Weather data: Precipitation and temperature
Appendix F Hydraulic conductivity and fracture statistics
Appendix G Variable head tests in boreholes

Review and reference page

1 Background and introduction

NGI is engaged by Norwegian water resources and energy directorate (NVE) to carry out stability analysis of the Åknes rock slide. The stability analysis will include water pressure as one important input parameter in a coupled hydromechanical stability analysis. This report is presenting and analysing the most important investigations and monitoring, such as packer tests and piezometer measurements in both open boreholes and boreholes with packer dividing the borehole in sections.

Hydrogeological analysis is carried out, and main emphasis has been on the monitoring done in the boreholes KH-01-2017, KH-02-2017, KH-01-2018 and KH-02-2018 drilled during autumn 2017 and autumn 2018 (see Figure 1). The purpose is to understand how the water flows and how to implement the water pressure in the coupled hydro-mechanical stability analysis. The stability analysis will be done in UDEC code with explicitly considering discontinuities in the models. The code can model rock mass with joint sets plus sliding planes. Since water is flowing through the discontinuities (joints / foliations / sliding planes/ faults) the focus is to find how high the water pressure in the main sliding plane is and how it varies over time.

The results from this report will give input data for boundary conditions for water table and water pressure in the UDEC model.

Revision No. 1 dated 11th January 2021 has included new analysis of water pressure in the sectioned boreholes from 2017 and 2018. Boundary conditions for the hydro-geological model is added. In addition, some figures are enlarged. At last, the discussion and conclusion chapters are rewritten slightly.

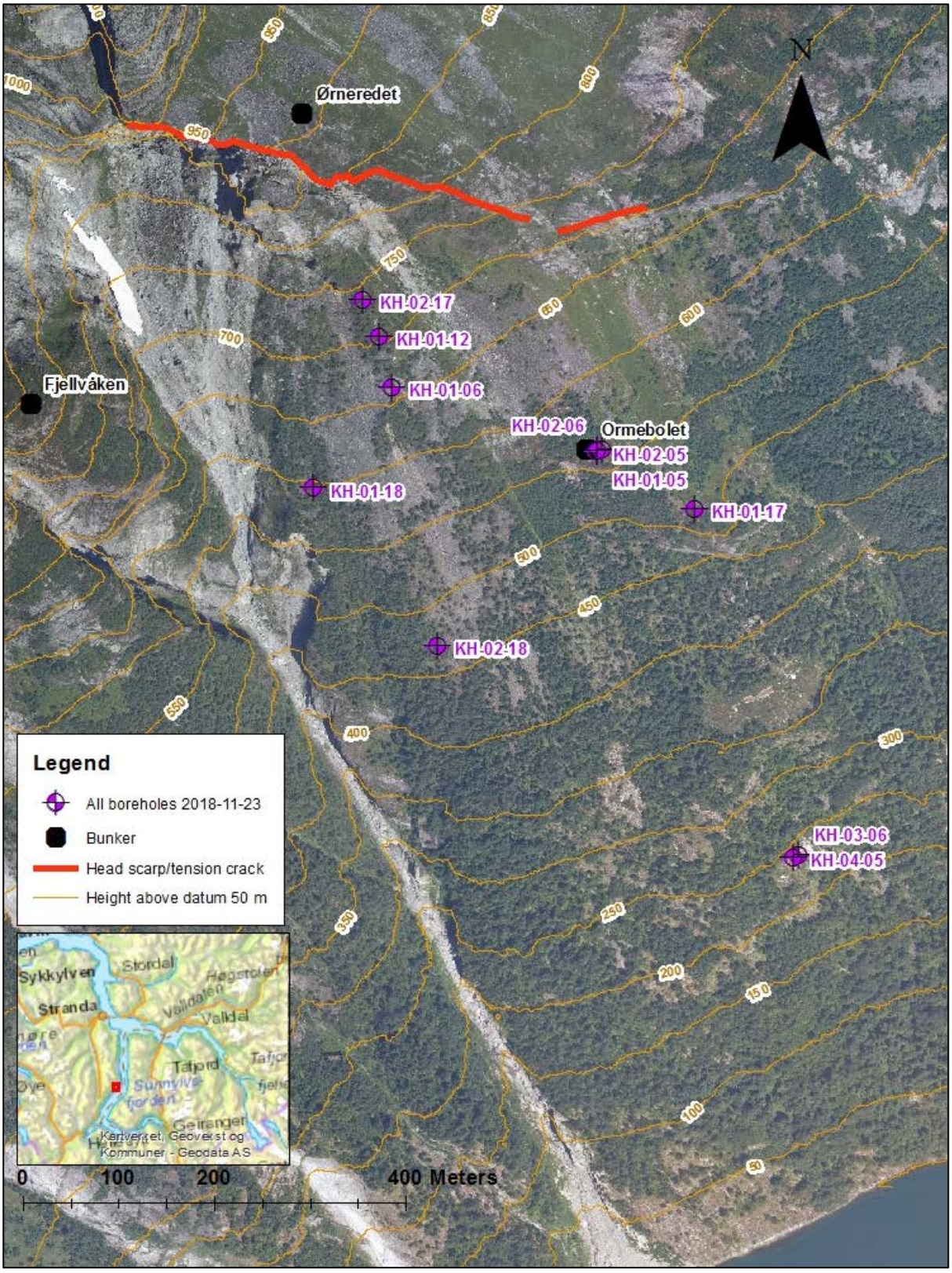

Figure 1 Overview of the Åknes rock slope with borehole locations.

Several borehole/drilling core investigations and tests have been used to log the boreholes and rock cores (Table 1).

Table 1. Investigations and tests in borehole and on rock cores from boreholes -2017 and -2018.

No.	Borehole / Investigation	KH-01-2017	KH-02-2017	KH-01-2018	KH-02-2018
1	Optical televiewer and borehole deviation	X	X	X	X
2	Temperature	X	X	X	X
3	Fluid conductivity and pH	X		X (not pH)	X (not pH)
4	Natural gamma	X	X	X	X
5	Rock resistivity	X	X	X	X
6	Seismic velocity	X	X	X	X
7	Flowmeter	X	X (down to 137m)	X	X
8	Packer test (lugeon test)	X	X	X	X
9	Variable head tests		X		
10	Engineering geological corelogging	X	X	X	X
11	Heat tracing tests	X	X	X	X

The work is summarized in following reports:

- Investigation no. 1-7: NGU (2018)
- Investigation 8: NGI (2019d)
- Investigation 9: Summarized in this report (Chapter 2.2)
- Investigation 10: NGI (2018) and NGI (2019a-c)
- Investigation 11: Bengt Dahlgren AB; Acuna et al. (2018)

2 Results from hydrogeological borehole investigations

2.1 Packer tests in boreholes

2.1.1 Method

Packer tests, sometimes named Lugeon test after Maurice Lugeon (Lugeon, 1933), were performed in all -2017 and -2018 boreholes. The entire borehole length is not tested in any of the boreholes.

NGIs technical note 20180662-01-TN (2019d) summarize test methods used and results from the packer tests in borehole KH-01-17, KH-02-17, KH-01-18 and KH-02-18.

The packer test was originally developed for assessing the need for foundation grouting at dam sites and the test have been modified from its original method (Houlsby, 1976). Fell et al. (2015) describe the test as: "The use of successive rising and falling test

pressures establishes the relationship between the volume of water accepted into the section and the pressure, to provide an estimation of permeability, and indicate water flow mechanisms. As rock substance is generally almost impermeable, the permeability determined in this test represents an indication of the number, continuity and opening of the rock defects which intersect the wall of the borehole in the test section".

The permeability is expressed in terms of Lu (Lugeon units), which is empirically defined as the hydraulic conductivity required to achieve a flow rate of 1 liter/minute per meter of test interval at a reference pressure of 1 MPa (Houlsby, 1976, Quiñones-Rozo, 2010, Fell et al., 2015):

$$Lu = V_L \frac{p_{ref}}{P} \qquad \textit{Eq. 1}$$

where V_L (l/min/m) is the water taken in test, p_{ref} (1 MPa) is the reference pressure and P (MPa) is the pressure of the test.

From the packer test, hydraulic conductivity K (m/s) can be calculated (NS-EN, 2012):

$$K = \frac{Q ln\left(\frac{R}{r_0}\right)}{2LH_p\pi} \qquad \textit{Eq. 2}$$

where L (m) is length of test section, R is radius of influence (typically equal to L), r_0 is radius of the borehole (m) and Q is flowrate (m^3/s). H_p is net injection pressure head in the test section.

$$H_p = \frac{P}{\rho g} \qquad \textit{Eq. 3}$$

where ρ (kg/m^3) is density of water and g (m/s^2) is the gravity constant.

Initially the packer test practice was to test at only one test pressure during the test, but the current test practise is to perform a multi-step procedure with at least 3 stages, changing the injection pressure every stage (Beale and Read, 2013). A normal practice is the sequence A-B-C-B-A with maximum pressure at stage C. A multi-step practice enables an interpretation of the possible changing of natural conditions in the borehole due to the increasing, and subsequent decreasing, applied pressure. The interpretation practice is based on Houlsby (1976), where Houlsby proposed that representative hydraulic conductivity values should be selected by interpretation of the flow behaviour from calculated Lugeon values at each test stage (Houlsby, 1976, Quiñones-Rozo, 2010, Beale and Read, 2013).

The program AquiferTest Pro 9.0 (Aquifer Test, 2020) have been used for packer test interpretation.

2.1.2 Results - Borehole KH-01-2017 and KH-02-2017

Table 2 gives an overview of test sections and type of packer test (1 stage or 5 stages). When interpreting the tests, the Lugeon-value depends on flow behaviour while the estimated hydraulic conductivity is an average of all the stages in each interval.

Table 2. Overview of test sections and type of packer test (1 stage or 5 stage) in 2017 boreholes. The Packer test-column indicates how many test-stages that were performed in the interval.

Zone	Packer test	Packer placement		Length zone	Ground-water before test	Ground-water after test	Test status
		From	To				
		meter	meter	meter	meter	meter	
KH-01-2017							
Zone 1	1 stage	-84	-88,9	4,90	-	-	Wrecked (upper) packer
Zone 2	1 stage	-69	-88,9	19,90	-	-	Wrecked (upper) packer
KH-02-2017							
Zone 1	1 stage	-66,50	-73,50	7,00	-70,00	-	Successful
Zone 2	5 stage	-84,50	-87,00	2,50	-78,50	-76,20	Successful
Zone 3	1 stage	-88,20	-90,50	2,30	-77,00	-	Successful
Zone 4	1 stage	-111,30	-114,30	3,00	-77,00	-	Successful
Zone 5	5 stage	-120,50	-123,50	3,00	-77,60	-76,10	Successful
Zone 6	1 stage	-268,00	-271,50	3,50	-77,40	-74,50	Successful

Table 3 summarize test results from the 2017 boreholes. Details are shown in Appendix A. Interpretation is not performed for KH-01-2017, due to wrecking of packer during test.

Table 3. Results from packer tests in 2017 boreholes, with average hydraulic conductivity values for all test stages.

Zone	Packer test	Length (m)	Lugeon (l/min/m)	Flow	Hydraulic conductivity (m/s)
KH-01-2017					
Zone 1	1 st	4.9	0,81	NA	NA
Zone 2	1 st	19.9	2,36	NA	NA
KH-02-2017					
Zone 1	1 stage	7	11,63	Laminar	1,51E-06
Zone 2	5 stage	2.5	8	Turbulent	9,46E-07
Zone 3	1 stage	2.3	45,219	Laminar	4,55E-06
Zone 4	1 stage	3	2	Laminar	2,15E-07
Zone 5	5 stage	3	12	Turbulent	1,22E-06
Zone 6	1 stage	3.5	3,14	Laminar	3,51E-07

2.1.3 Results - Borehole KH-01-2018 and KH-02-2018

Table 4 and Table 5 give an overview of test sections and type of packer-test (only 5 stage-test in 2018 boreholes).

Table 4. Overview of test sections and type of packer test in borehole KH-01-18 .

Zone	Packer test	Packer placement		Length zone	Groundwater before test	Groundwater after test	Test status
		From	To				
		meter	meter	meter	meter	meter	
KH-01-2018							
Zone 1	5 stage	41	47	6	5,3	-	Successful
Zone 2	5 stage	47,9	53,9	6	5,3	-	Successful
Zone 3	5 stage	53,9	59,9	6	39,6	-	Successful
Zone 4	5 stage	65,5	71,5	6	41,2	-	Successful
Zone 5	5 stage	72,5	78,5	6	41,2	-	Successful
Zone 6	5 stage	84,5	90,5	6	41,2	-	Successful
Zone 7	5 stage	141	147	6	41,2	-	Successful
Zone 8	5 stage	158,9	164,9	6	65,7	-	Successful
Zone 9	5 stage	164,8	170,8	6	-	-	Successful
Zone 10	5 stage	170,8	176,8	6	61	-	Successful
Zone 11	5 stage	176,8	182,9	6,1	61	-	Successful
Zone 12	5 stage	182,9	188,9	6	57	-	Successful
Zone 13	5 stage	188,9	194,9	6	57	-	Successful

Zone	Packer test	Packer placement		Length zone	Groundwater before test	Groundwater after test	Test status
		From	To				
		meter	meter	meter	meter	meter	
Zone 14	5 stage	194,9	200,9	6	56	-	Successful
Zone 15	5 stage	200,9	206,9	6	56	-	Successful
Zone 16	5 stage	206,9	212,9	6	56	-	Successful
Zone 17	5 stage	212,9	218,9	6	50	-	Successful
Zone 18	5 stage	218,9	222,6	3,7	50	-	Successful

Table 5. Overview of test sections and type of packer test in KH-02-18 borehole.

Zone	Packer test	Packer placement		Length zone	Groundwater before test	Groundwater after test	Test status
		From	To				
		meter	meter	meter	meter	meter	
KH-02-2018							
Zone 1	5 stage	30	36	6	-	-	Successful
Zone 2	5 stage	35,8	41,8	6	-	-	Successful
Zone 3	5 stage	51	57,1	6,1	-	-	Successful
Zone 4	5 stage	57	63	6	-	-	Successful
Zone 5	5 stage	63	69	6	-	-	Successful
Zone 6	5 stage	69	76	7	-	-	Successful
Zone 7	5 stage	75,5	82,5	7	-	-	Successful
Zone 8	5 stage	82,5	88	5,5	-	-	Successful
Zone 9	5 stage	93	99	6	-	-	Successful
Zone 10	5 stage	101	109,5	8,5	-	-	Successful
Zone 11	5 stage	122	130,5	8,5	-	-	Successful
Zone 12	5 stage	138	145	7	-	-	Successful
Zone 13	5 stage	148	154	6	-	-	Successful
Zone 14	5 stage	154	160	6	-	-	Successful
Zone 15	5 stage	160	166	6	-	-	Successful
Zone 16	5 stage	185	200	15	-	-	Successful

Table 6 and Table 7 summarize test results from the 2018 boreholes. Details are shown in Appendix A.

Table 6. Results from packer tests in KH-01-18 borehole, with average hydraulic conductivity values for all test stages.

Zone	Packer test	Length (m)	Lugeon (l/min/m)	Flow	Hydraulic conductivity (m/s)
KH-01-2018					
Zone 1	5 stage	6	6,43	Wash out	5,32E-07
Zone 2	5 stage	6	4,74	Dilation	8,54E-07
Zone 3	5 stage	6	11,43	Turbulent	1,5E-06
Zone 4	5 stage	6	1,5	Void filling	2,87E-07
Zone 5	5 stage	6	0	Laminar	0,00E+00
Zone 6	5 stage	6	0,1	Void filling	4,93E-08
Zone 7	5 stage	6	4,24	Turbulent	5,36E-07
Zone 8	5 stage	6	0	Laminar	0,00E+00
Zone 9	5 stage	6	0	Laminar	0,00E+00
Zone 10	5 stage	6	0	Laminar	0,00E+00
Zone 11	5 stage	6,1	0	Laminar	0,00E+00
Zone 12	5 stage	6	0	Laminar	0,00E+00
Zone 13	5 stage	6	0	Laminar	0,00E+00
Zone 14	5 stage	6	0	Laminar	0,00E+00
Zone 15	5 stage	6	0	Laminar	0,00E+00
Zone 16	5 stage	6	0	Laminar	0,00E+00
Zone 17	5 stage	6	0	Laminar	0,00E+00
Zone 18	5 stage	3,7	2,95	Void filling	3,71E-07

Table 7. Results from packer tests in KH-02-18 borehole, with average hydraulic conductivity values for all test stages.

Zone	Packer test	Length (m)	Lugeon (l/min/m)	Flow	Hydraulic conductivity (m/s)
KH-02-2018					
Zone 1	5 stage	6	0	Laminar	0,00E+00
Zone 2	5 stage	6	24,917	Turbulent	3,73E-06
Zone 3	5 stage	6,1	27,706	Turbulent	3,99E-06
Zone 4	5 stage	6	29,25	Turbulent	4,39E-06
Zone 5	5 stage	6	10,233	Laminar	1,29E-06
Zone 6	5 stage	7	0,536	Dilation	7,15E-08
Zone 7	5 stage	7	0	Dilation	1,18E-08
Zone 8	5 stage	5,5	0	Dilation	6,25E-09
Zone 9	5 stage	6	0,217	Dilation	2,47E-08

Zone	Packer test	Length (m)	Lugeon (l/min/m)	Flow	Hydraulic conductivity (m/s)
Zone 10	5 stage	8,5	0,436	Dilation	9,26E-08
Zone 11	5 stage	8,5	0,847	Dilation	1,09E-07
Zone 12	5 stage	7	0,171	Dilation	3,92E-08
Zone 13	5 stage	6	0	Void filling	2,51E-09
Zone 14	5 stage	6	0,567	Dilation	1,2E-07
Zone 15	5 stage	6	0	Laminar	0,00E+00
Zone 16	5 stage	15	0,6	Dilation	9,88E-08

The hydraulic conductivity depth-profiles of the packer-tests are shown in Figure 2.

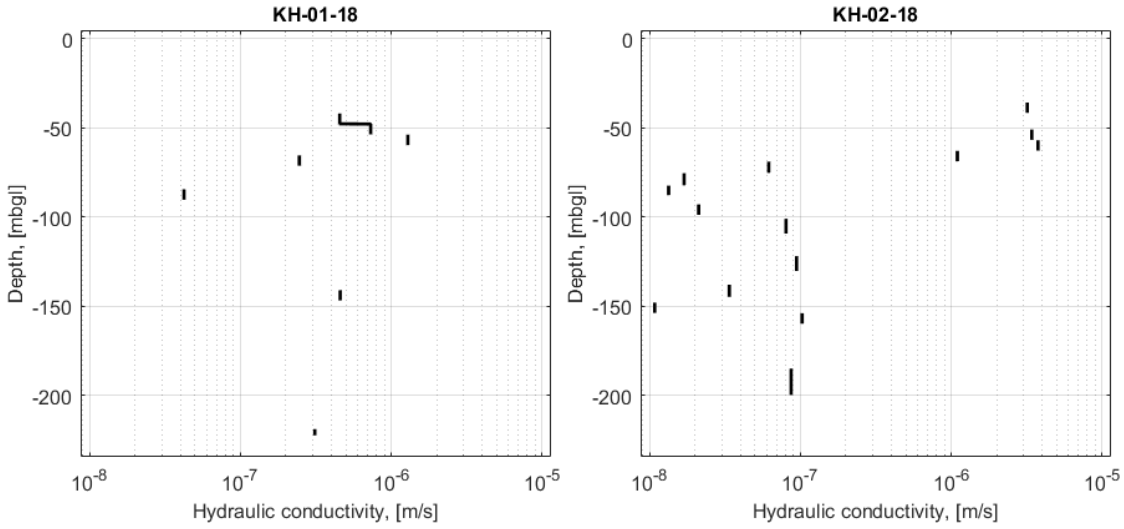

Figure 2 Hydraulic conductivity depth-profile of the 2018-boreholes.

Figure 2 presents the sections where the Lugeon values were measured and gave result above zero. In the other sections no water was penetrated in joints during the Lugeon measurement with the water pressure used. The results show that the hydraulic conductivity in general is higher in borehole KH-01-18, including deeper parts of the borehole, compared to KH-02-18. However, borehole KH-02-18 has higher hydraulic conductivity in the upper part of the borehole.

2.2 Variable head tests in boreholes

Variable head tests were only performed in KH-02-2017. The performed variable head test follow the procedure of Norwegian standard (ISO) (NS-EN 2012b) and Beale and Read (2013);

- Rising head test; rapidly empty the borehole (or borehole section) and measure time for recovery of head to original level
- Falling head test; instantaneous increase in head by pumping water into the borehole and then measure time for the head to decline to original level

Hydraulic conductivity can be calculated from the rate at which water returns to original depth (Beale and Read, 2013), where a fast recovery of water head indicates high hydraulic conductivity and slow recovery indicates low hydraulic conductivity.

There were several challenges with the tests, but some tests were successful and water head values that could be analysed were recorded. Although successful, the documentation is a bit unclear as to the conditions under the various tests, and the time stamps in the recorded data-files do not seem to match the documentation many places. This means that we cannot derive reliable values from the tests. Also, the shape of the falling head curves indicates complex flow patterns and simple analytical expressions cannot be applied to calculate the hydraulic conductivity, instead more rigorous analysis, possibly combined with back-calculation using numerical models, is needed. More details from the tests are described in Appendix G. The hydraulic conductivity of the rock mass will therefore rely on the Lugeon-tests described later in Section 2.1.

2.3 Piezometer measurements in boreholes

To understand the groundwater flow and potential build-up of water pressure in the jointed rock mass, it has been installed piezometers which measure the water pressure locally in boreholes. This is done using packers below and above the piezometers in the borehole. Location of boreholes are shown in Figure 3.

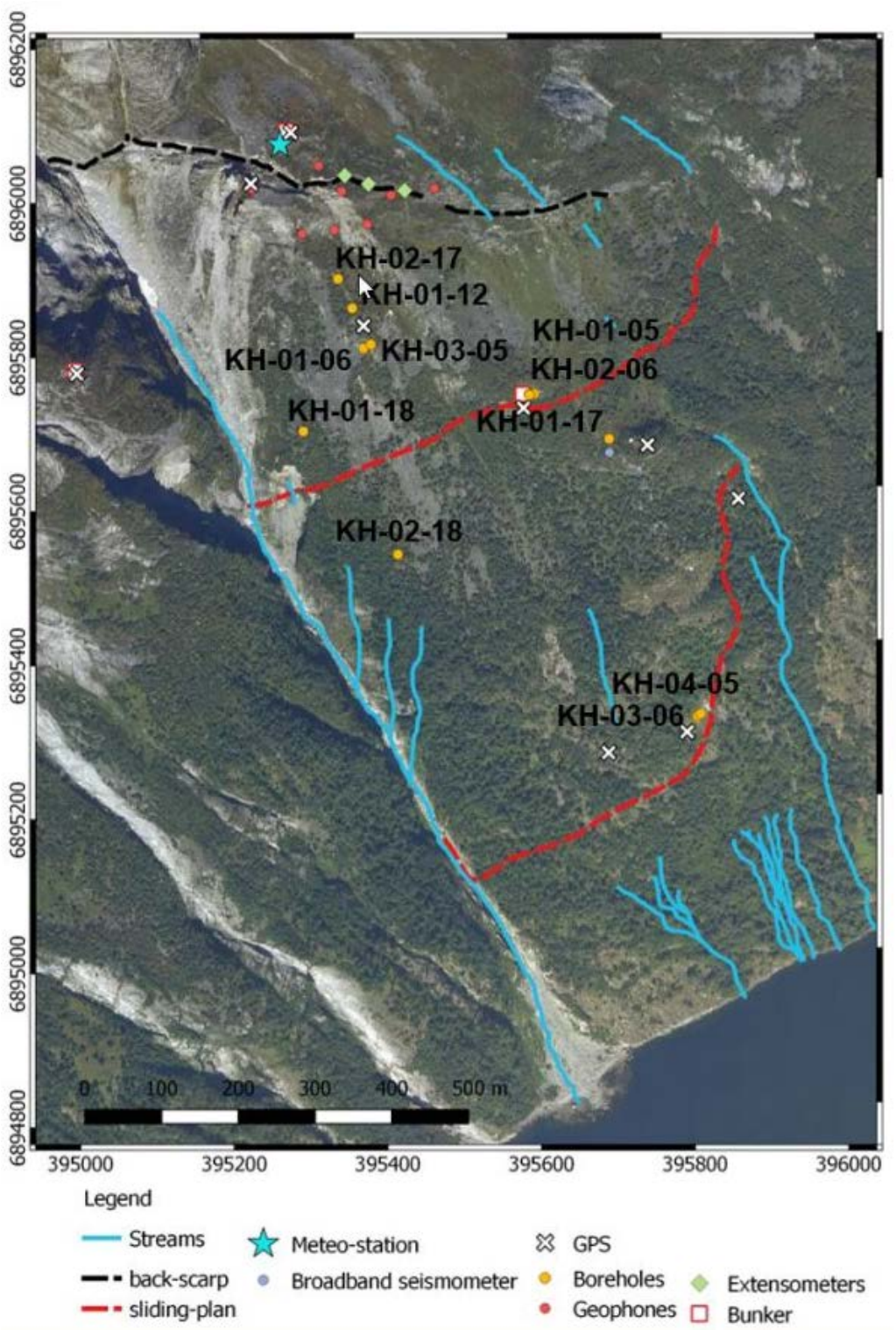

Figure 3 Illustration presenting location of boreholes, GPS, geophones, extensometer as well as suggested location of two sliding planes and registered streams (from Clara Sena's presentation, 28. Nov 2019).

Four boreholes, two boreholes from 2017 and two from 2018, are instrumented with the DMS system (Differential Monitoring of Stability), monitoring real time water pressure. In the 2017 boreholes, the piezometers are positioned 2 – 8 meters above the lowest packer of the two. While the piezometers in the 2018 boreholes are positioned directly above the lowest packer with varying distance up to the upper packer. Details on position of packers and piezometers in the four boreholes are presented in Appendix B. Figure 4 shows an example of how the positions of the piezometers and packers are illustrated in Appendix B.

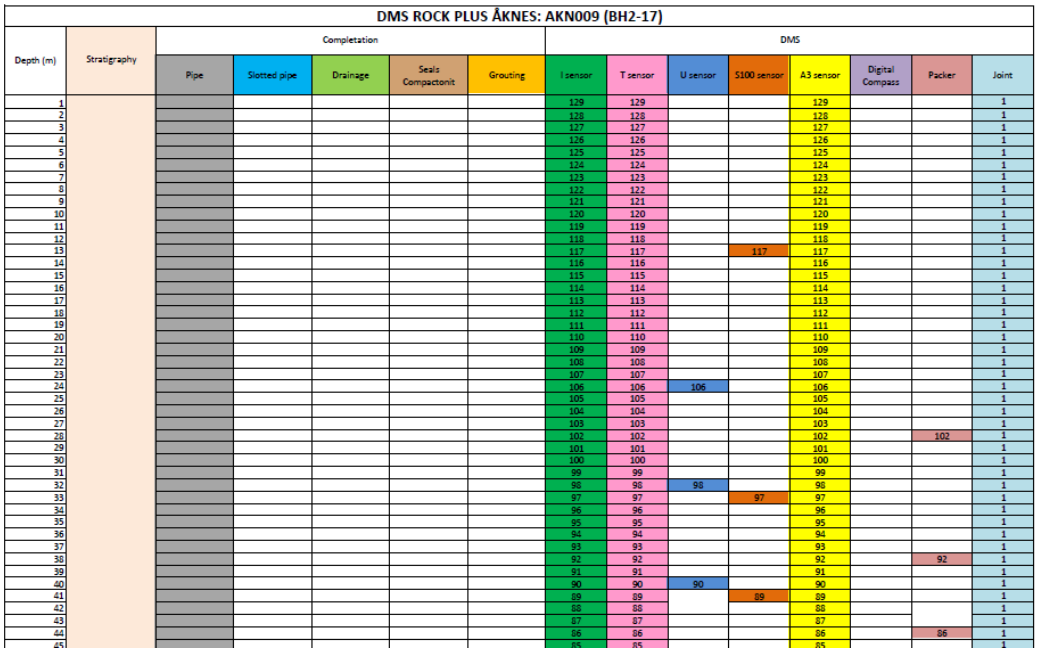

DMS ROCK PLUS ÅKNES: AKN009 (BH2-17)

Depth (m)	Stratigraphy	Completation					DMS							
		Pipe	Slotted pipe	Drainage	Seals Compactonit	Grouting	I sensor	T sensor	U sensor	S100 sensor	A3 sensor	Digital Compass	Packer	Joint
1							129	129			129			1
2							128	128			128			1
3							127	127			127			1
4							126	126			126			1
5							125	125			125			1
6							124	124			124			1
7							123	123			123			1
8							122	122			122			1
9							121	121			121			1
10							120	120			120			1
11							119	119			119			1
12							118	118			118			1
13							117	117		117	117			1
14							116	116			116			1
15							115	115			115			1
16							114	114			114			1
17							113	113			113			1
18							112	112			112			1
19							111	111			111			1
20							110	110			110			1
21							109	109			109			1
22							108	108			108			1
23							107	107			107			1
24							106	106	106		106			1
25							105	105			105			1
26							104	104			104			1
27							103	103			103			1
28							102	102			102		102	1
29							101	101			101			1
30							100	100			100			1
31							99	99			99			1
32							98	98	98		98			1
33							97	97		97	97			1
34							96	96			96			1
35							95	95			95			1
36							94	94			94			1
37							93	93			93			1
38							92	92			92		92	1
39							91	91			91			1
40							90	90	90		90			1
41							89	89		89	89			1
42							88	88			88			1
43							87	87			87			1
44							86	86			86		86	1
45							85	85			85			1

Figure 4 Snip from Appendix B showing the first 44 m of borehole KH-02-17. The dark blue-coloured cells illustrate the position of the piezometers with module No. 106, 98 and 90 at increasing depth, while the brownish coloured cells illustrate the position of the packers. See also Appendix B.

2.3.1 How to understand the piezometer measurements

The normal procedure is to locate a piezometer between two packers in the section of interest; such as highly jointed sections which have increased possibility for water inflow. Often the optical televiewer video is utilized to place the piezometers. Measured water pressure depends on several parameters; such as joint connectivity, opening of apertures and connection with water and waterflow from higher altitude or drainage to lower parts of the rock slope. In some areas the rock mass is highly jointed and much of the water is drained and water pressure is hardly ever built up. Figure 5 shows a sketch illustrating the difference between open borehole measuring water table directly and piezometers located between two packers along a borehole.

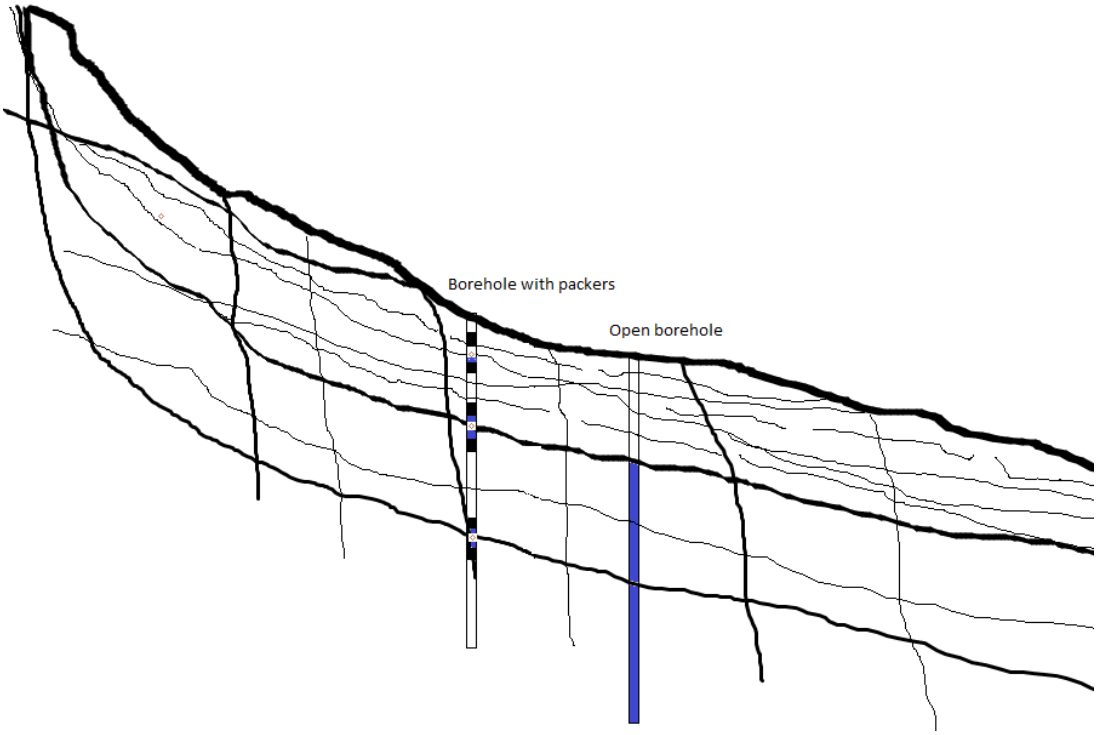

Figure 5 Sketch illustrating how the water-table in open boreholes is a direct measure of where the groundwater is located in the borehole. The piezometers are located between two packers measuring the local water pressure at the position of the piezometers along the borehole.

The Italian company CSG Geotechnical Monitoring (2020) has delivered the DMS-equipment and are responsible for the monitoring system. Each piezometer has a module number. and are positioned at a specific depth. Highest module No's are in the upper part of the borehole. For each piezometer the water pressure is registered over time. It is important that the packers have sufficiently air pressure to keep the sections separated and sealed from the rest of the borehole. The water pressure registered are automatically calculated to a corresponding water table given in meters below ground level (mbgl). Figure 6 shows an example where the water table vary between -74 and -76,8 mbgl (meter below ground level) from October 2018 to July 2019. This gives a water head (H_w) equal to 1,2 to 4 m at the depth of -78 mbgl.

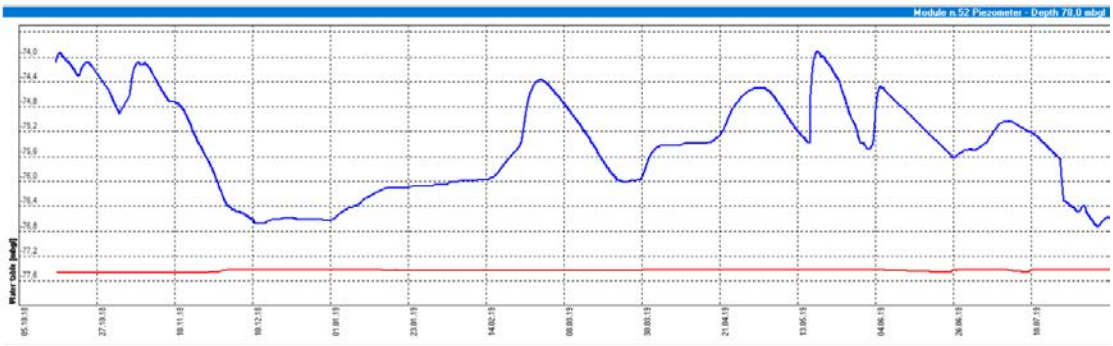

Figure 6 Water table (blue line) given in meters below ground level (mbgl) for Module No. 52 at depth 78 mbgl in borehole KH-02-17. Red line shows the temperature (scale is not shown).

The registered water pressure (called water table in the downloaded graphs) is a local water pressure obtained through water in connecting joints above the piezometer height.

2.3.2 Water table levels in open boreholes

There are recordings of water table levels in most of the boreholes, the newer boreholes from 2017 and 2018 have packers installed to measure water pressure in isolated borehole sections. The data from the active boreholes can be retrieved from a username/password protected DMS web-view portal (htpps://app.csgsrl.eu) or by using a software installed on local computers. Table 8 shows an overview of the monitored boreholes.

Table 8. Overview of boreholes and water table monitoring.

Borehole	Installation	Calibration	Stopped		Total depth (m)
KH-01-05	2007	NA	2017	Open	150
KH-02-05	No monitoring				150
KH-03-05	No monitoring				162
KH-04-05	2009	NA	2017	Open	151
KH-01-06	2007	NA	2013	Open	201
KH-02-06	22-05-2014	20-09-2015	Active	Open	202
KH-03-06	04-08-2015	18-09-2015	Active	Open	198
KH-01-12	22-05-2014	24-09-2015	Active	Open	200
KH-01-17	25-06-2019	06-11-2019	Active	Packers	304,5
KH-02-17	29-09-2018	15-10-2018	Active	Packers	300
KH-01-18	30-10-2019	08-11-2019	Active	Packers	222,6
KH-02-18	29-10-2019	08-11-2019	Active	Packers	199,4

Borehole KH-01-05 and KH-04-05 show relatively constant water table (Figure 7) with some degree of seasonal fluctuations (Figure 8). For well KH-01-05 the water table is at its lowest during the winter months and at its highest during (early) fall. The annual water table for well KH-04-05 is less consistent, but it seems to have a low-period during the winter months.

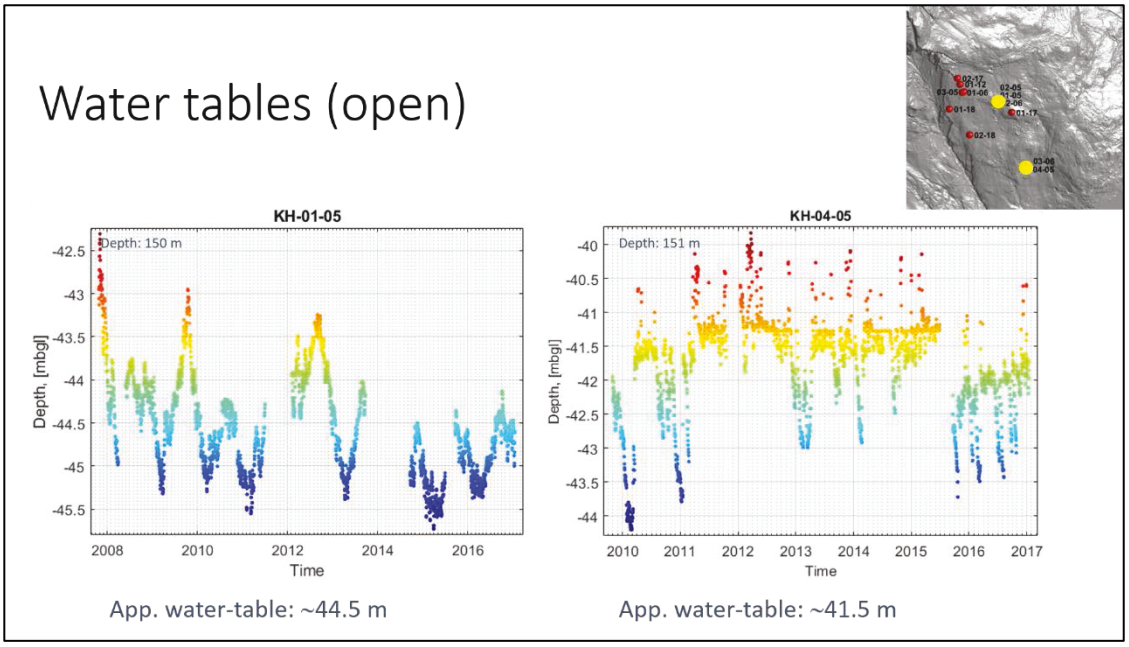

Figure 7 Water-table recordings from boreholes KH-01-05 and KH-04-05 (open boreholes). The locations of the boreholes are indicated in the upper-right inset and in Figure 3.

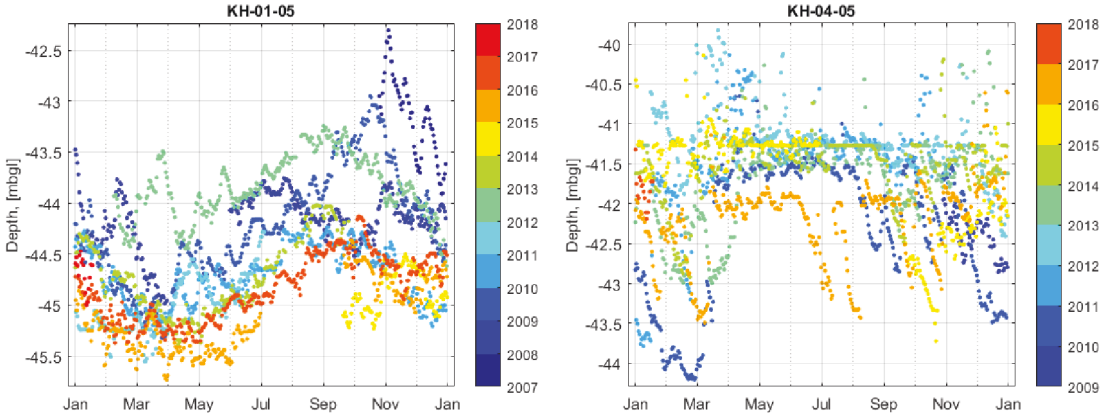

Figure 8 Annual water-table recordings from boreholes KH-01-05 and KH-04-05.

Borehole KH-01-06 shows a very irregular water-table (see Figure 9), and it is not known what is causing this. Despite this the water-table shows some seasonal trend of lower water-table readings in the winter and higher values in the fall, see Figure 10. Borehole KH-02-06 shows relatively constant water-table with some seasonal fluctuations with lower water-table in the winter compared to the fall, see Figure 10.

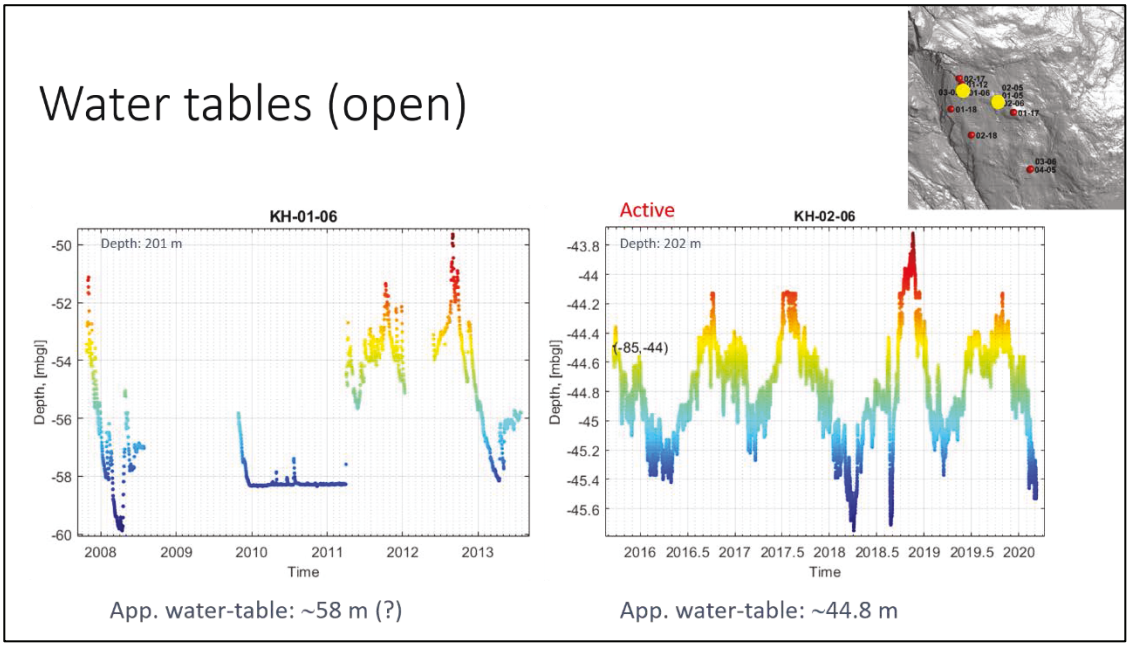

Figure 9 Water-table recordings of boreholes KH-01-06 and KH-02-06 (open boreholes). The location of the boreholes is indicated in the upper-right inset and in Figure 3.

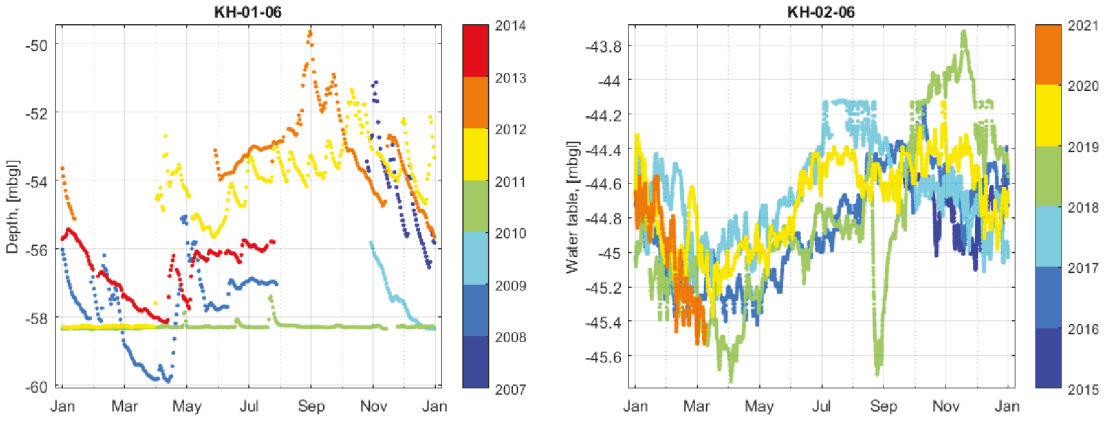

Figure 10 Annual water-table recordings from boreholes KH-01-06 and KH-02-06.

Borehole KH-03-06 and KH-01-12 have been active since 2015. For borehole KH-01-12 seasonal variations (Figure 11) with characteristic groundwater level decline during winter and recovery from March/April when the snow melting is high. For borehole KH-03-06 the water table trend seems to increase steadily over time, app. 1 m over a four-year period. The seasonal variations in KH-03-06 are more random, see Figure 12.

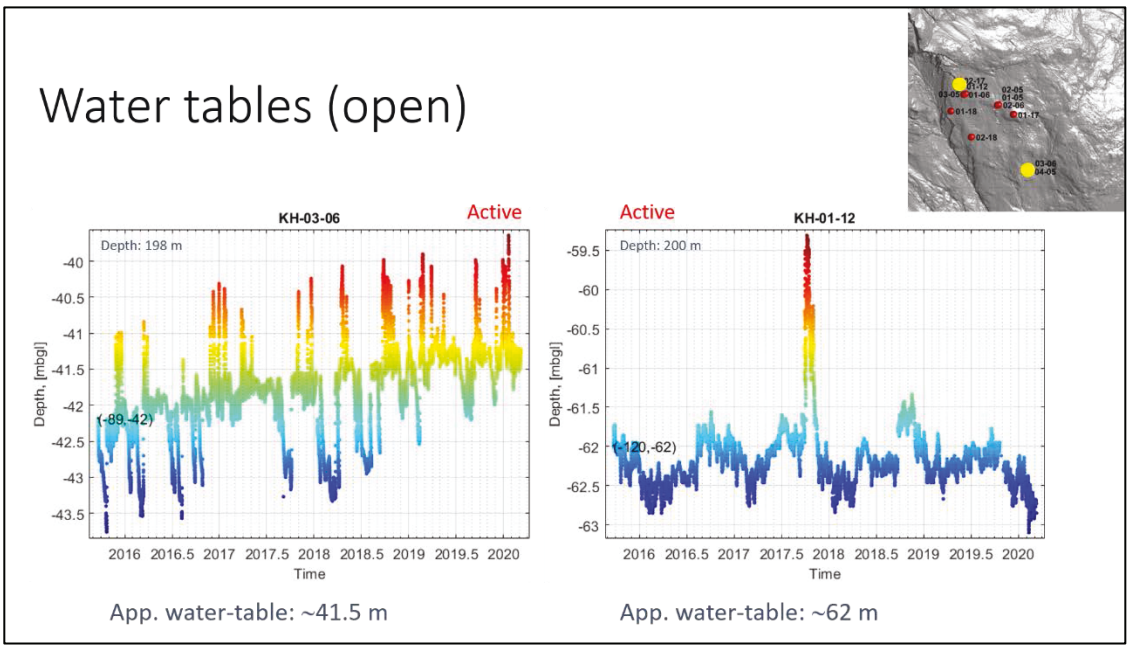

Figure 11 Water-table recordings of boreholes KH-03-06 and KH-01-12 (open boreholes). The location of the boreholes is indicated in the upper-right inset and in Figure 3.

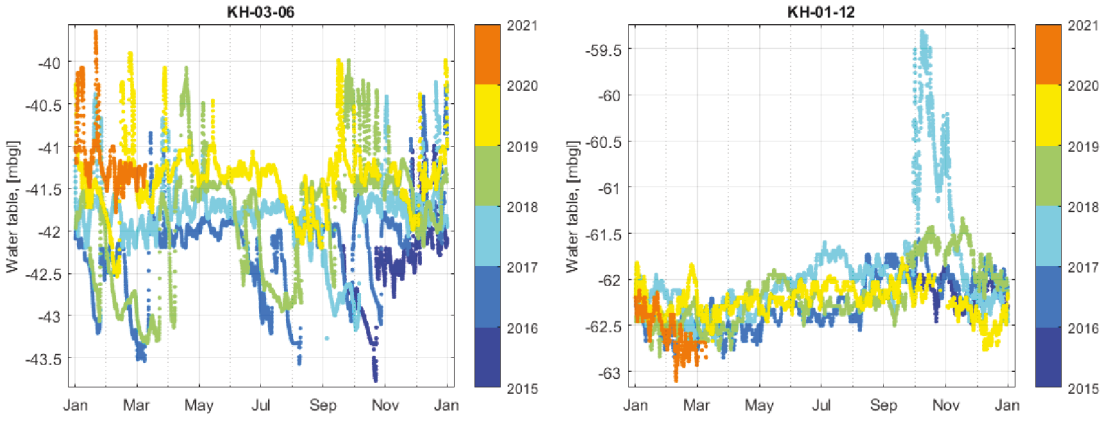

Figure 12 Annual water-table recordings from boreholes KH-03-06 and KH-01-12.

Figure 13 shows registered water table (mbgl) in more detail for borehole KH-01-12. One peak is seen in the period 11th to 15th October 2017.

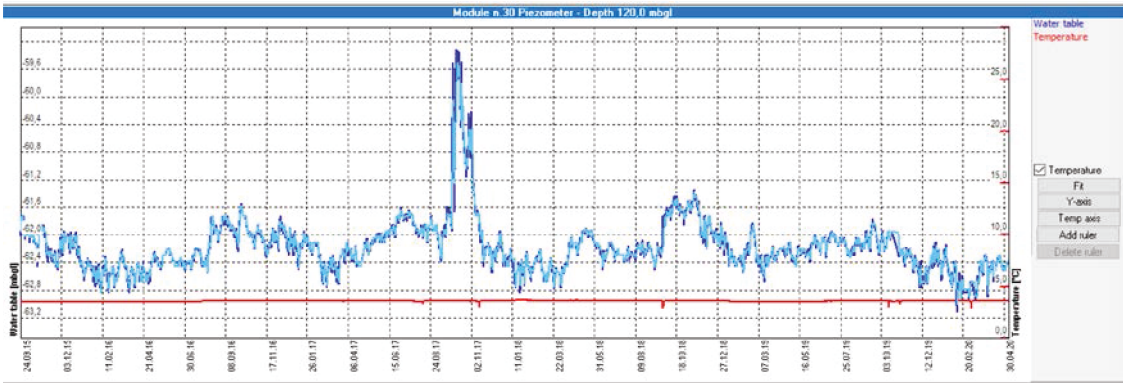

Figure 13 Water table in borehole KH-01-12 from September 2015 until May 2020.

The peak medio October may be due to heavy rain a few days earlier, with 35 mm daily rain the 6th October, see Figure 14. However, this peak in rainfall is not extra-ordinary and several rainy periods are registered without similar peaks in the water table.

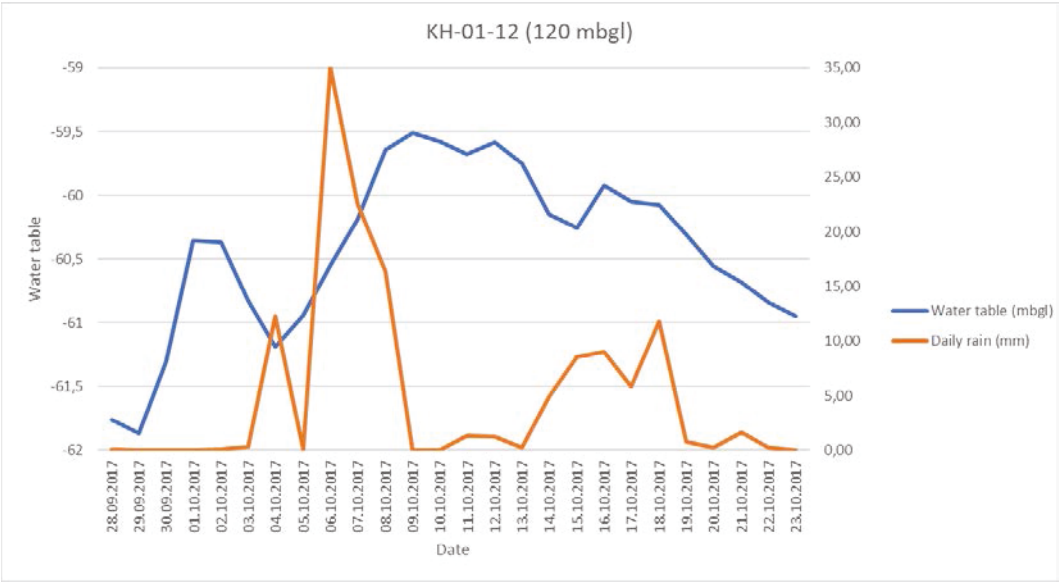

Figure 14 Water table as registered in piezometer (120 mbgl) compared with daily rain in October 2017.

A summary of the measured water tables is given in Table 9.

Table 9. Summary of observed water table data in open boreholes.

Borehole	Water table range, below surface, [m]	Note
KH-01-05	44.5	From 2007-2017, seasonal fluctuations
KH-02-05		Not monitored
KH-03-05		Not monitored
KH-04-05	40-44	From 2009-2017, irregular seasonal variations
KH-01-06	50-60	From 2007-2013, large irregular variations
KH-02-06	44.8	From 2015. Seasonal fluctuations. Possible correlation with precipitation
KH-03-06	40-43.5	From 2015. Irregular seasonal variations. Possible correlation with precipitation.
KH-01-12	62	From 2015. Seasonal fluctuations
KH-01-17	60	Before packers were installed.
KH-02-17	75	Before packers were installed.
KH-01-18	25	Before packers were installed.
KH-02-18	60	Before packers were installed.

2.3.3 Monitored water pressure in the boreholes from 2017 and 2018

In the four boreholes from 2017 and 2018 several piezometers are installed between two packers to measure water pressure in selected sections at various depths in the boreholes.

Before the packers were installed in **borehole KH-01-17** a water-table around 60 m below ground level was measured. After the packers were installed the piezometers at 65 m and below showed signs of hydraulic communication with water table between 65 to 70 mbgl. As can be seen in Figure 15 the piezometers were not in operation during spring and summer 2019. This was due to a snow avalanche winter 2019. When the monitoring started again autumn 2019, lower water tables were registered. Early in November, large fluctuations were registered in all the piezometers below 65 mbgl, possibly due to leakage between the packers. Furthermore, between 5th and 19th December some peaks/lows were registered in piezometers at 65 and 79 mbgl. These irregularities and rapid changes, particularly in the piezometer at 86 mbgl, seem to have connections with similar peaks/lows for the packer pressure (3 to 7,5 bar). Hence, the monitoring results for the lowest piezometers in borehole KH-01-17 is not giving correct values.

Borehole KH-02-17 is installed with packers at various depths in the borehole, see Figure 15. The piezometers installed deeper than 67 mbgl. seem to be hydraulically connected with a water-table between 75 and 80 m below ground level. This is in line with water table around 75 measured before the packers were installed. The exception is the bottom piezometer which shows periods of with low water pressure where the corresponding water table is approximately at the piezometer depth. Results from

borehole KH-02-17 shows rapid changes between 1st August to 5th November 2019 with peaks/lows in several piezometers. This is monitored in the lowermost piezometers 101, 121 and 129 mbgl. In the same period the packer pressure has rapid fluctuations, from 3 to 8 bar, which may be a reason for the abrupt changes.

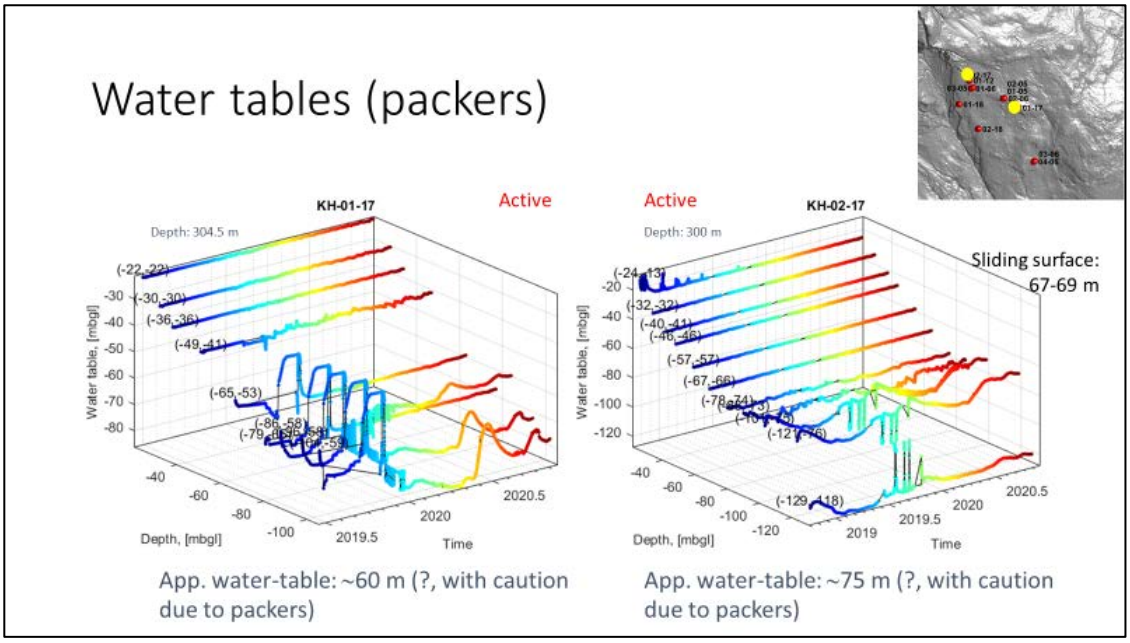

Figure 15 Water table recordings of boreholes KH-01-17 and KH-02-17. These boreholes have packers at various depths, indicated by the first coordinate in the various lines. First reading of water pressure is given in the second coordinate in the various lines. The location of the boreholes is indicated in the upper right inset and in Figure 3. The minor ticks indicate months. See App. C for more detailed curves.

Before the packers were installed (Figure 16), **borehole KH-01-18** had a water-table around 25 m below ground level. After the packers were installed the piezometers at 61 mbgl and below showed signs of hydraulic communication with higher water table, around 5 mbgl. The piezometers in the deepest sections of the borehole (from 94 mbgl and down) has the same pattern; high water table from start of monitoring 8th November until 26th December, where a gradual and stepwise decrease of water pressure starts.

In addition, precipitation rate and temperature level does not explain the unusual measuring high water head in the period of 8th November 2019 to 26th December 2019 in KH-01-2018, since the temperature is always below zero at the mentioned dates except one day during that period which eliminated possibility of snow melting.

The piezometers in the middle of borehole KH-01-18 (80, 61 and 53 mbgl) show rapid changes with similar patterns until end of December 2019. While in the upper part, the piezometer at 43 mbgl show variations around 33 mbgl and the piezometer at 24 mbgl shows a few peaks between 5th and 29th December 2019, before stabilising around 22

mbgl. It seems like the piezometer at 24 mbgl is partly drained as in periods no water pressure was registered autumn 2019.

After December 2019 it seems like the water pressure in the lowest piezometers gradually and stepwise start to decrease. In May 2020 the water pressure is registered around 33 mbgl, equivalent to the depth of the sliding plane. The packer pressure in the piezometers have had some fluctuations, typically between 13 and 21 bar (indicating failure to seal off sections). Two incidents, one the 12th and one the 27th December packer pressure was registered as 11,2 and 0 bar respectively. It is not analysed in detail how these fluctuations in packer pressure have influenced the monitoring of water pressure.

A water-table around 60 m was measured in **borehole KH-02-18**. before the packers were installed (Figure 16). After the packers were installed the piezometers at -67 mbgl and above appears to have small and sharp variations, probably the water pressure is changing rapidly due to precipitation/infiltration and drainage. Highest water head registered was around 5 m; corresponding to water table at 62 mbgl.

The piezometers in the deepest sections of the borehole (from 127 mbgl and down) has the same pattern and values; a stepwise slow increase of water pressure until 28th January 2020. The corresponding water table at 28th January is around 8-9 mbgl. Afterwards the water pressure gradually decreases down to 22 mbgl medio May 2020.

Two piezometers in the middle of the borehole (piezometers at 87 and 111 mbgl) have irregular patterns with abrupt decrease in pressure at the same time as the lower piezometers (mentioned above) have increase. After 30th January 2020 the water pressures have been stable with small decrease of pressure, ending with a water table around 61 and 64 mbgl.

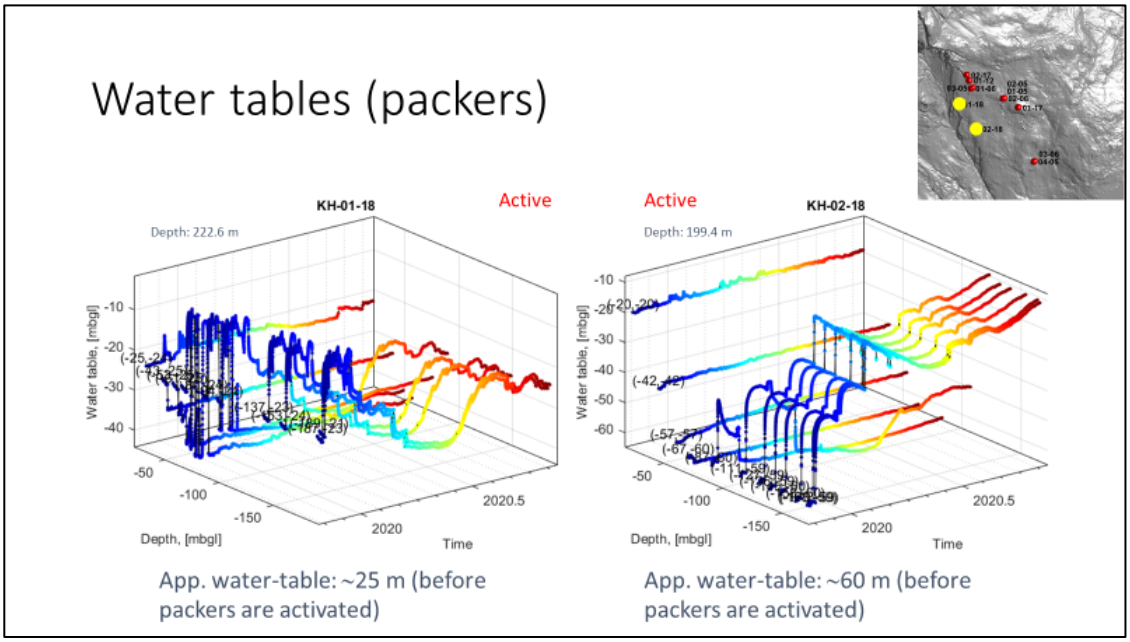

Figure 16 Water-table recordings of boreholes KH-01-18 and KH-02-18. These boreholes have packers at various depths, indicated by the first coordinate in the various lines. While first reading of water pressure is given in the second coordinate in the various lines. The location of the boreholes is indicated in the upper right figure inset and in Figure 3. The minor ticks indicate months. See App. C for more detailed curves.

2.3.4 Water pressure variation versus precipitation in the boreholes from 2017 and 2018

In the following figures; Figure 17, Figure 18, Figure 19, and Figure 20 registered water pressure in piezometers (mbgl) for the four boreholes from 2017 and 2018 are presented. Upper left graph is the lowermost piezometer (module 1), and the lower right graph presents measurements from the deepest piezometer (high module No.). Daily precipitation is presented in dark grey without scale for comparison. The figures are also presented in Appendix C.

Based on the monitoring results for the four boreholes described in Section 2.3.3 and the following figures rapid changes have been monitored in the deepest sections. These changes have no correlation with precipitation and are more likely due to changes in the packer pressure. However, it can look like the monitoring have stabilised and the values seem more correct lately (from March 2020).

In the middle part of the boreholes, some seasonal dependency can be seen, and the results are changing more naturally and not very fast. However, exceptions are found, which may be due to rapid changes in packer pressure locally.

In the upper parts of the boreholes some abrupt changes can be seen in the start of the monitoring, this may be due to packer pressure have some adjustments in the start. After

some time, the water pressure shows small (within 1 to 3 meters) and relatively fast changes most likely responding to precipitation / snow melt. These changes are seen above and just below the sliding planes in the respective boreholes.

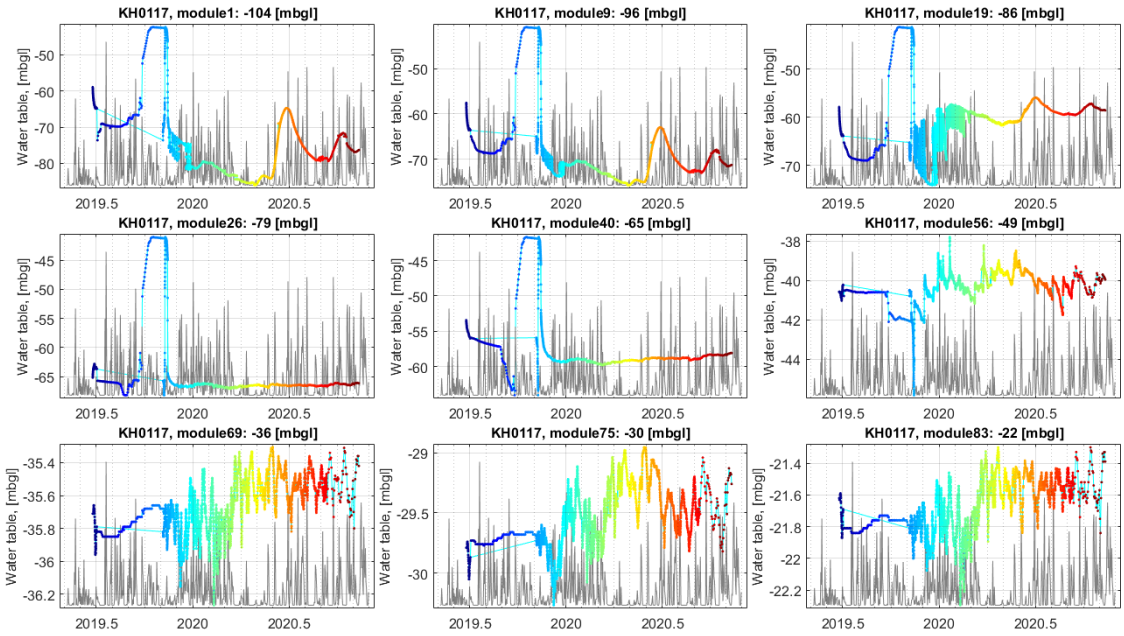

Figure 17 Water table recordings of boreholes KH-01-17 for each module. Vertical gridlines indicate one month in time. Dark grey lines indicate the precipitation in that period (without scale). Sliding plane is around 35,5 mbgl. See App. C for more detailed curves.

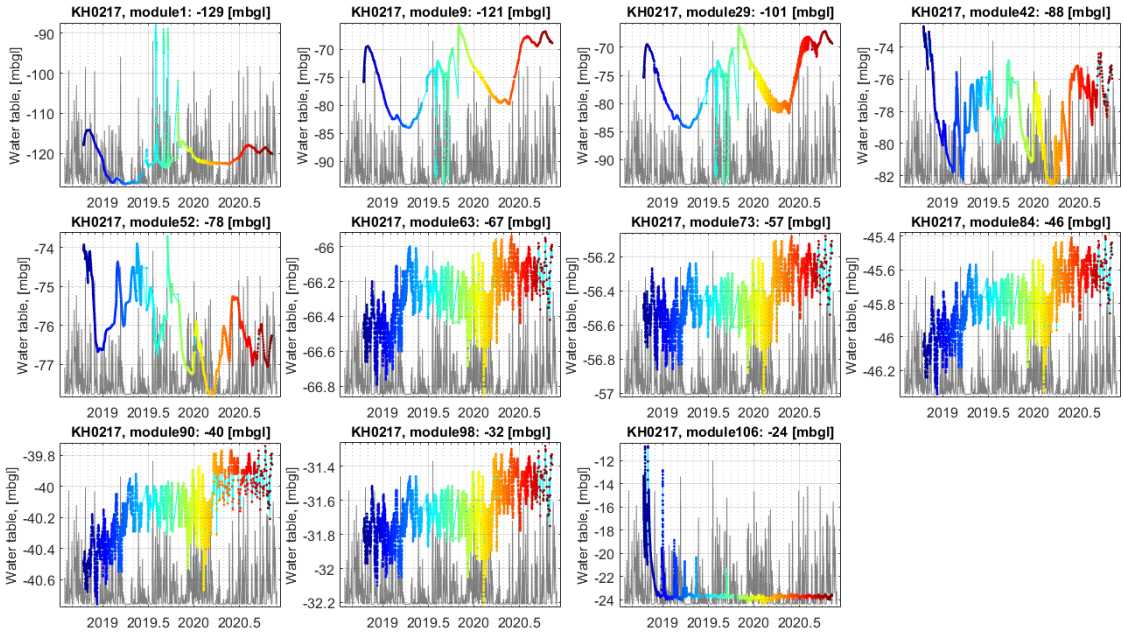

Figure 18 Water table recordings of boreholes KH-02-17 for each module. Vertical gridlines indicate a month in time. Dark grey lines indicate the precipitation in that period (without scale). Two sliding planes around 32 and 69 mbgl. See App. C for more detailed curves.

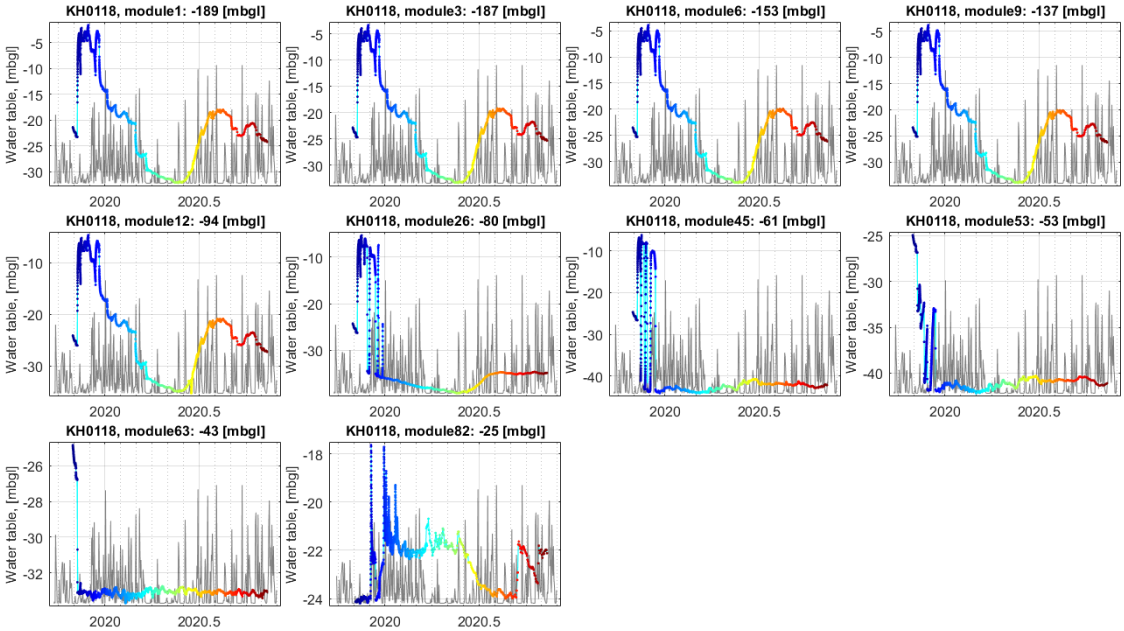

Figure 19 Water table recordings of boreholes KH-01-18 for each module. Vertical gridlines indicate a month in time. Dark grey lines indicate the precipitation in that period (without scale). Sliding plane around 34 mbgl. See App. C for more detailed curves.

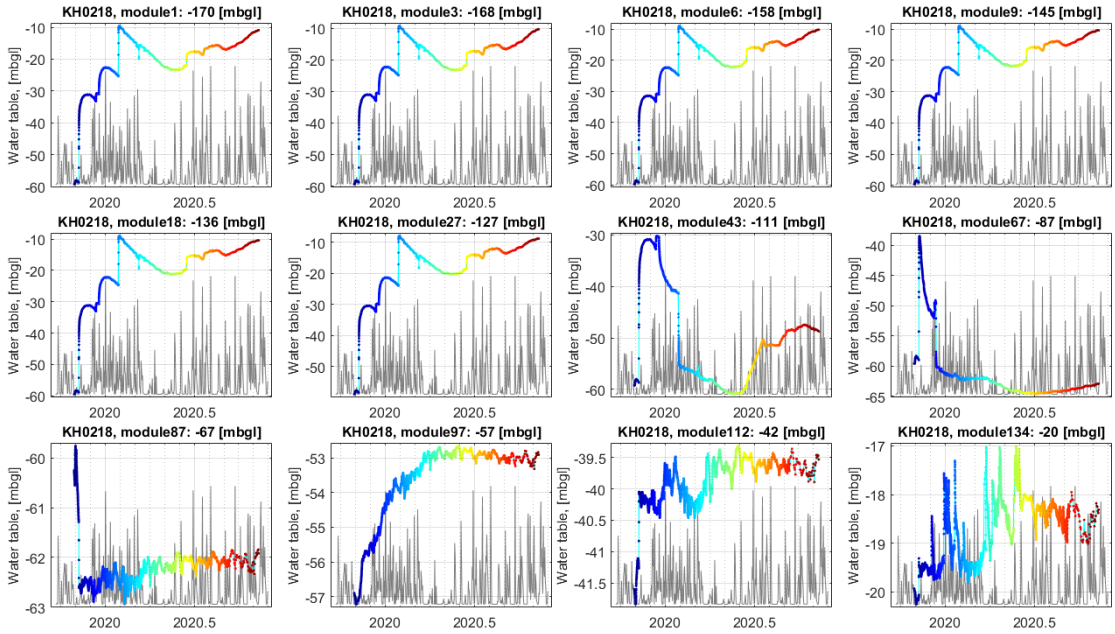

Figure 20 Water table recordings of boreholes KH-02-18 for each module. Vertical gridlines indicate a month in time. Dark grey lines indicate the precipitation in that period (without scale). Sliding plane around 15 mbgl. See App. C for more detailed curves.

3 Hydrological analysis

In the following chapter results from investigations and monitoring carried out in both open and sectioned boreholes are analysed. This is done to understand the hydro-geological situation of the Åknes rock slope.

3.1 Analysis of water pressure in the boreholes from 2017 and 2018

An analysis of the piezometer data from boreholes KH-01-17, KH-02-17, KH-01-18 and KH-02-18 is presented in the following section to investigate how the rock-mass is hydraulically connected along the length of the boreholes. The boreholes are divided in several isolated zones by packers and in each isolated zone one piezometer were installed (Figure 21). It is of interest to find out if sections along a borehole are hydraulically connected.

At first sight it might seem difficult to identify which sections in the boreholes are hydraulically connected. One approach is to find sections of the boreholes which are showing linear water head changes with a gradient of 1. For example, assume a borehole with several packers (see Figure 21), the depth of the piezometers is shown by X and the water table measured by each piezometer is shown as y_0 . Both X and y_0 are zero at the surface while increases with depth. Using the surface as datum, the water head measured in each piezometer can be calculated by:

$$H_w = X - y_0 \qquad \textit{Eq. 4}$$

If the water head is fluctuating just above the depth of the piezometer (and sometimes no water pressure is built up) the height of the water above the piezometer is close to zero ($H_w = 0$). A linear function can be fitted to data which shows H_w versus X. If the groundwater table was hydrostatically built-up, the equation should have gradient of 1 and the Y-intercept of the fitted linear function is the depth of the groundwater table (the depth at which $H_w = 0$).

Least square method is used to find the best fitting line which has gradient of 1. The correlation coefficient from the least square method, R^2, shows how much the data are close to linearity with the constrain we made (gradient equal to 1). R^2 will always be a number between 0 and 1, with values close to 1 indicating a good degree of fit (Albright et al., 2003). In this study we assumed that the data shows $R^2 > 0.9$ have acceptable linear correlations.

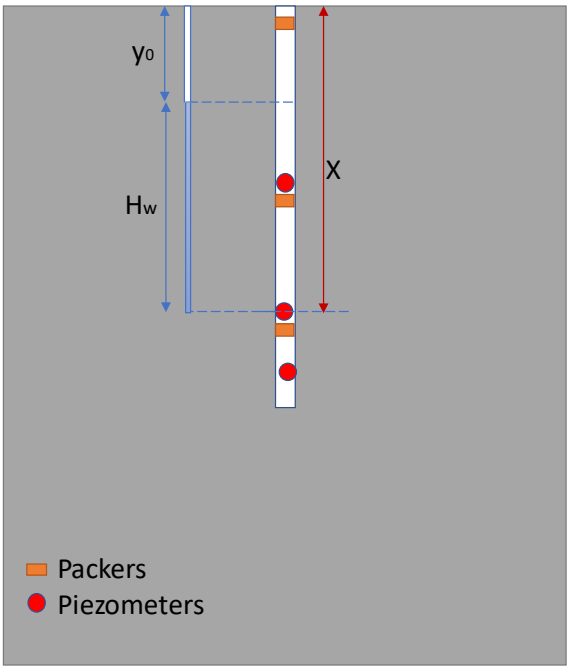

Figure 21 Water head evaluation in a borehole with straddle packers.

Water head values are studied in all four boreholes at three points in time (December 2019, March 2020 and September 2020) and plotted as explained above. These three points in time were chosen because they are expected to give a representative variation in the monitored water head in all the boreholes. Borehole KH-02-17 and KH-01-18 were analysed also medio May 2020, but no changes of results were seen.

If there exist several hydraulically connected zones in one borehole, different fragments of a linear graph might be possible to see for one borehole. Therefore, before fitting a linear function for the data, a visual inspection was done to divide the borehole in different zones if appropriate. Afterwards, it was tried to fit a linear equation on the data of the water head versus depth for sections of the borehole.

Figure 22 shows water head versus the depth of the piezometers for **borehole KH-01-17**. The orange points show that the upper part of the borehole down to around 40 mbgl is dry. Deeper in the borehole some sections may be hydraulically connected with a water table between 60 and 70 mbgl. Nevertheless, the data does not show a perfect linear correlation and it is not possible to drive any clear conclusion out of it. It should be added that the equipment of the borehole has experienced an incident of snow avalanche which might affect the quality of the measurements.

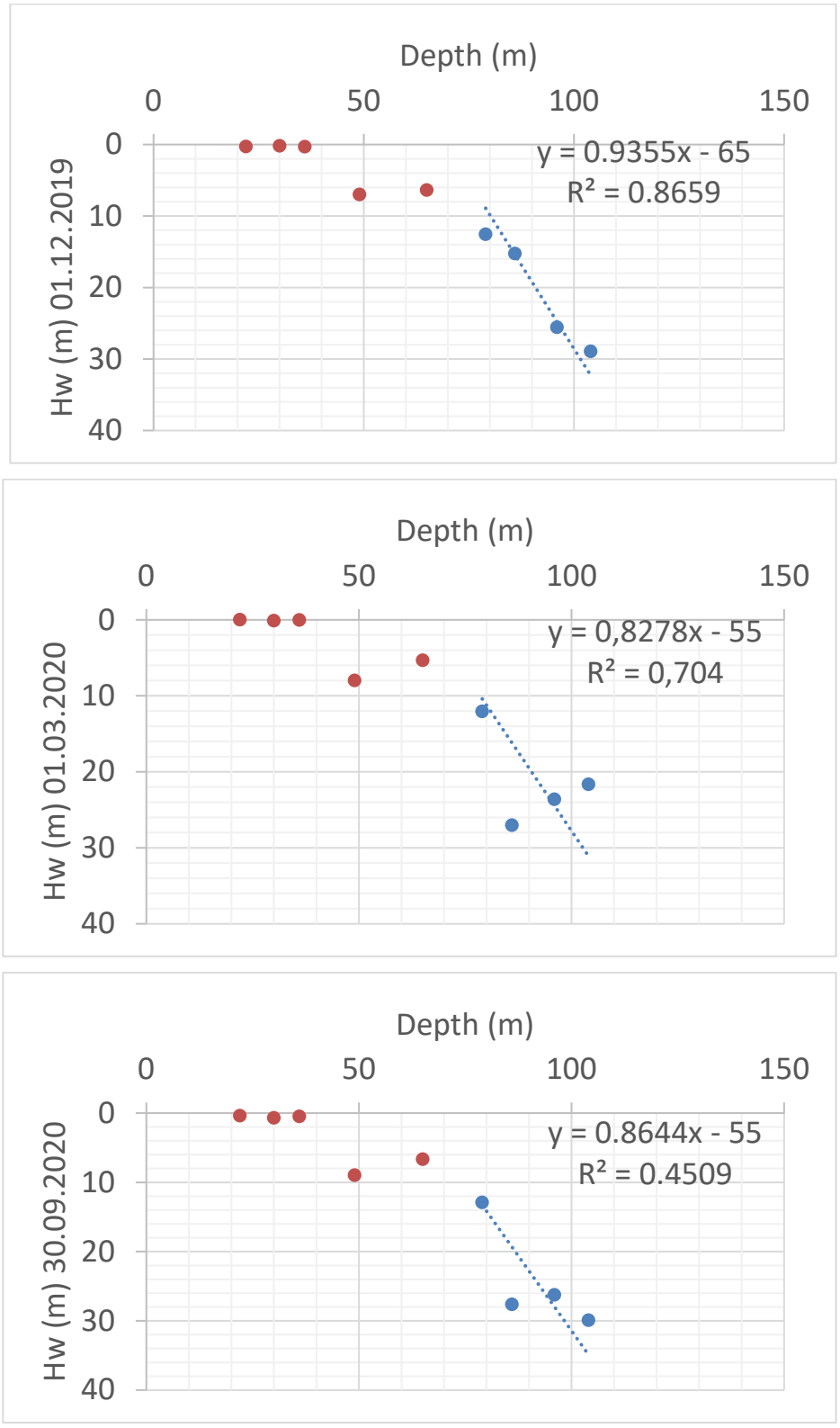

Figure 22 Water head versus depth for borehole KH-01-17. Water head values from December 2019, March 2020 and September 2020.

Borehole KH-02-17 (Figure 23) shows two zones, deeper one with hydraulically connection (blue points) and a dry unsaturated zone above it (orange points). The hydraulically connected zone has water table (water head $H_w = 0$) in depths of 73 and 80 mbgl for the first of December 2019 and March 2020/September 2020, respectively.

The deepest piezometer at 129 mbgl shows lower water pressure (green point in Figure 23). One reason can be that the deepest piezometer is installed without any packer below the piezometer. Since the borehole has a total length of 300 m, the measured water head is disturbed and is not representative for the rock mass at the depth of the piezometer (129 mbgl).

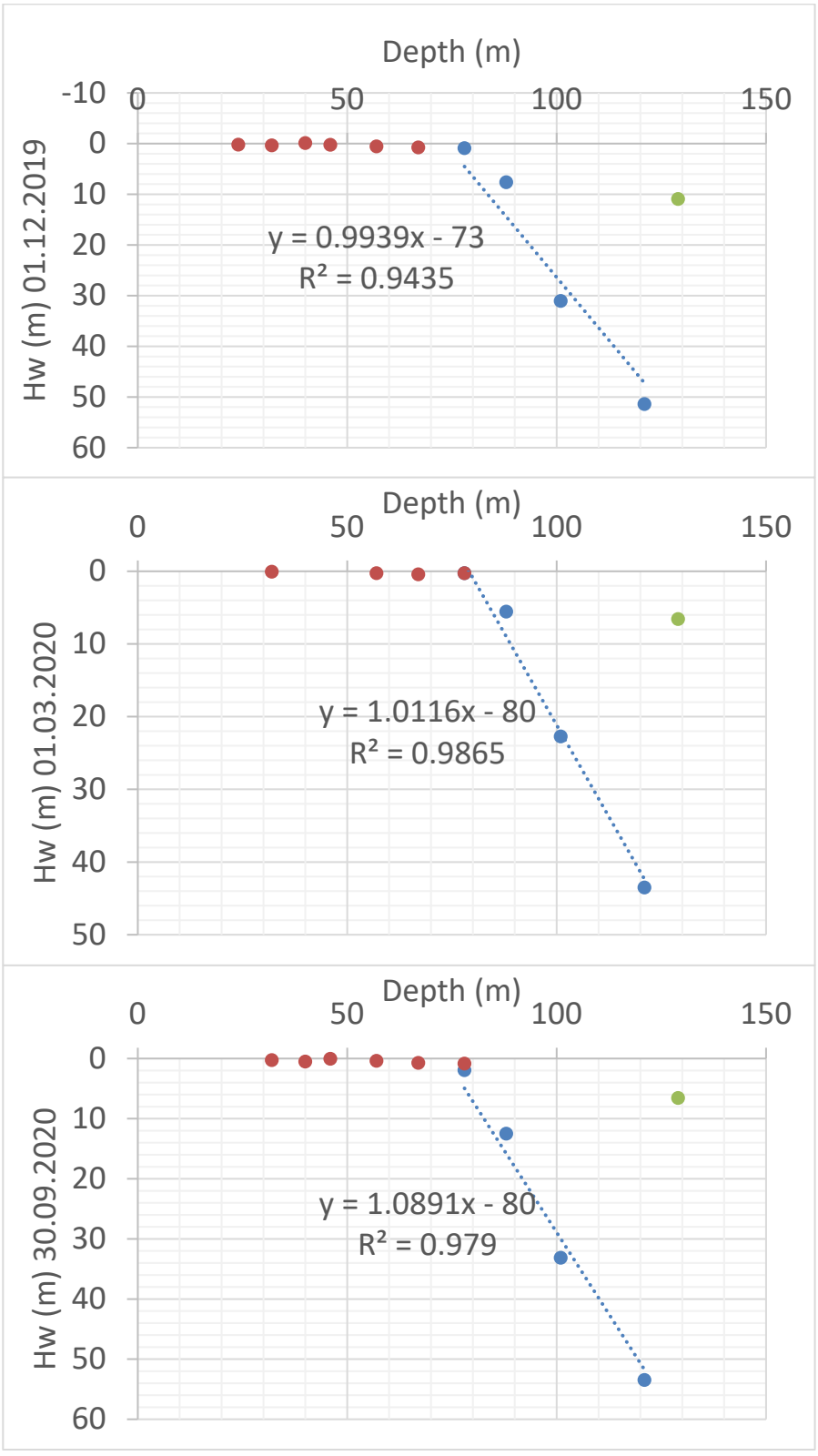

Figure 23 Water head versus depth for borehole KH-02-17. Water head values from December 2019, March 2020 and September 2020 are presented.

Figure 24 shows data for **borehole KH-01-18.** The data shows hydraulic connection in the depth bellow 22 m. The groundwater table is established between 10 and 30 mbgl in the first of December 2019 and March 2020/September 2020, respectively. In this borehole it may be that all data points are hydraulically connected.

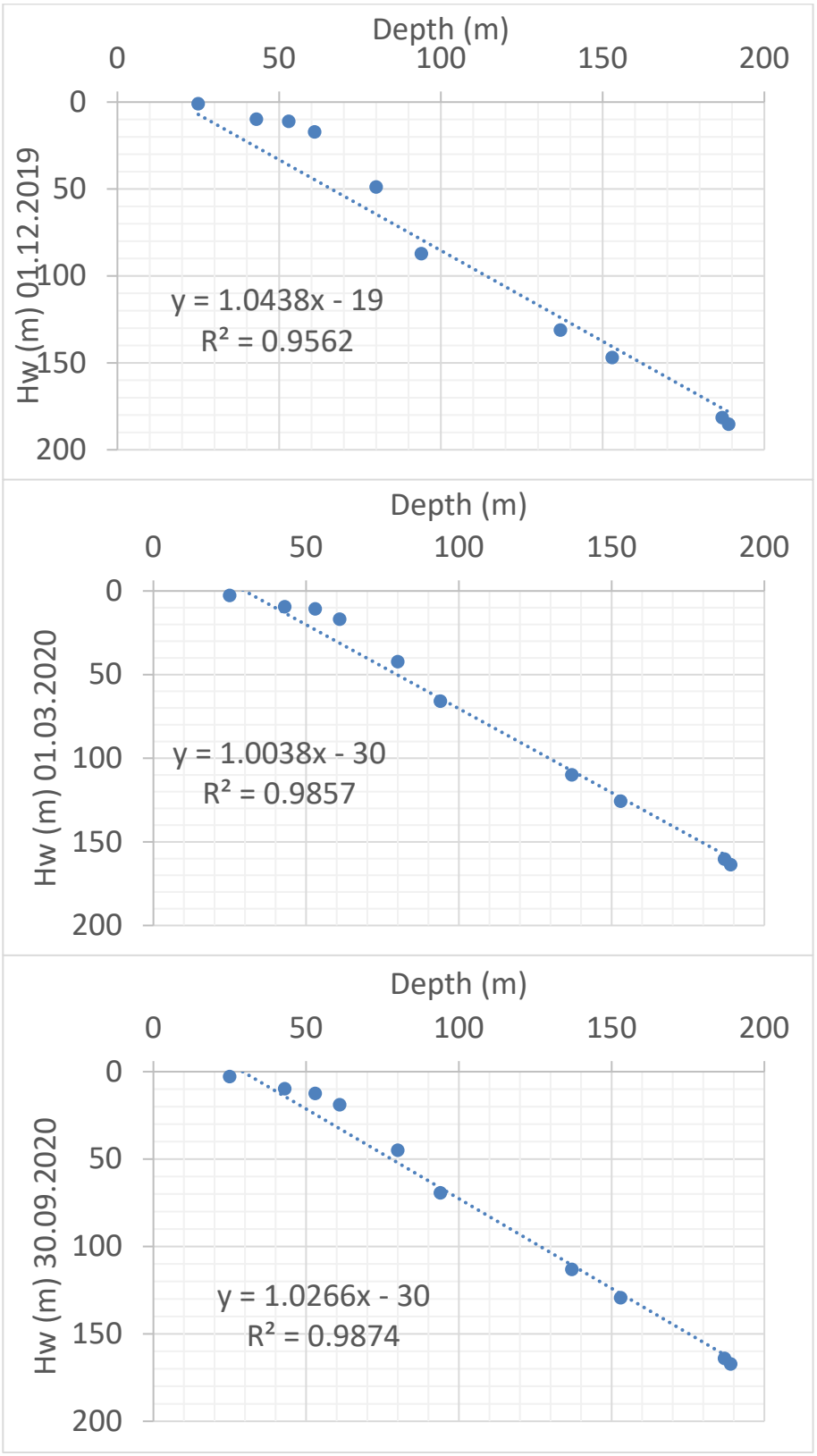

Figure 24 Water head versus depth for borehole KH-01-18. Water head values from December 2019, March 2020 and September 2020.

The data from **borehole KH-02-18** shows complex behaviour (Figure 25). Two different zones with connected hydraulic head can be identified with an unsaturated (dry) zone above depth of 20 m. The blue points show water table standing at depths of 31.7 and 16 mbgl for the first of December 2019 and March 2020/September, respectively. While the orange points show water table standing at the depth of 48 and 59 mbgl for the first of December 2019 and March 2020/September 2020, respectively.

However, the fitted linear equation on the orange points at the first of December 2019 is not fulfilling the criteria of $R^2 > 0.9$ (meaning that it is not linear). The blue points and orange points show to different sections which are hydraulically connected, but not with each other. This may be due to geological structures which make the water flow and drain easily in some places while water pressure builds up locally other places.

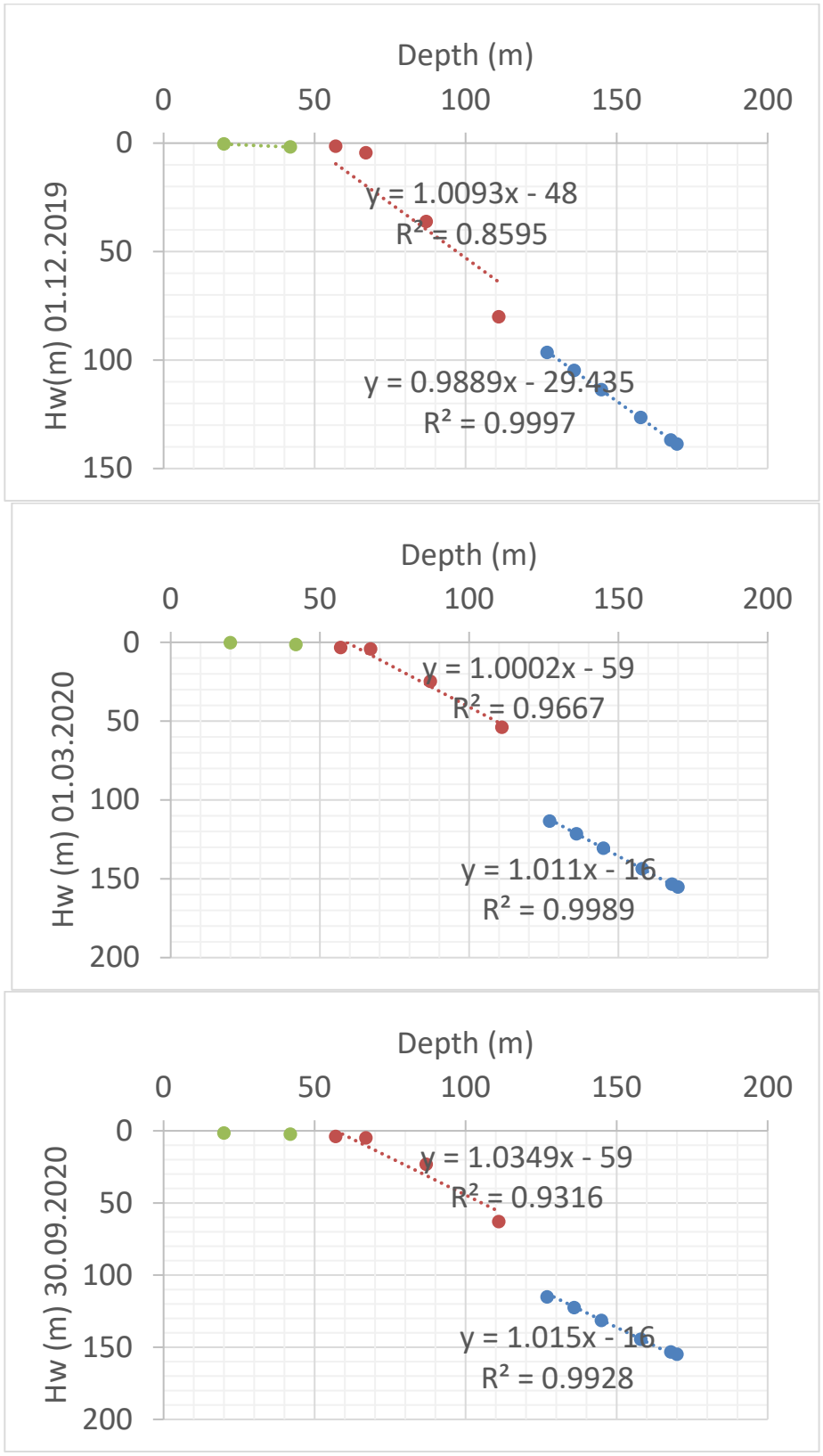

Figure 25 Water head versus depth for borehole KH-02-18. Water head values from December 2019, March 2020 and September 2020.

3.2 Hydraulic conductivity from Lugeon-tests

Several Lugeon-tests were performed in boreholes KH-02-17, KH-01-18 and KH-02-18 (Section 2.1.2 and 2.1.2). The distribution of values from different boreholes are shown in Figure 26. The result from the Lugeon-tests are analysed by (1) using one average value from every tested borehole-interval and (2) by using all the values from every pressurisation test that was performed at every test-interval. The analysis of the latter (2) is also shown in the figure and indicated with the keyword "ext" (for extended) in the title.

The data-set is very sparse, not many intervals were tested, but the data show some trends, and by analysing all the data combined, the data fits very well to a log-normal distribution function. The median value of the hydraulic conductivity of the rock mass from the Lugeon-tests is $0.25 \cdot 10^{-6}$ m/s (from "All data"-panel). With one standard deviation interval, the hydraulic conductivity of the rock mass is $0.04 \cdot 10^{-6}$ m/s to $1.5 \cdot 10^{-6}$ m/s).

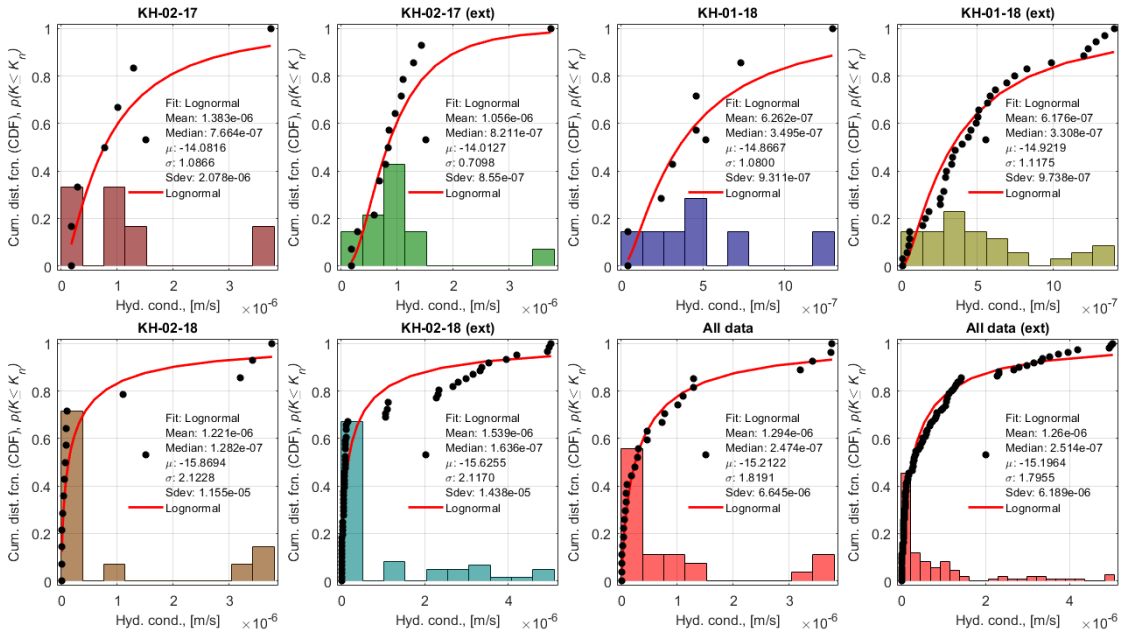

Figure 26 Bar plot of hydraulic conductivity fitted to a log-normal cumulative distribution function. The plots with (ext.) in the title contain all the measurement data in every Lugeon-test interval. See a bigger version of figure in Appendix F.

When fitting the results from the Lugeon-test with an empirical cumulative distribution function we get a curve that describes the probability p that the rock mass has a hydraulic conductivity that is smaller than or equal to a certain value K_i: $p(K \leq K_i)$. When only considering gravitational forces on the water in a rock mass: if the hydraulic conductivity is equal to the precipitation rate, the gravity is sufficient to transport the precipitation through the rock mass. This further implies that if the hydraulic conductivity is less than

the precipitation rate, then water will pond or run-off on the surface. Various levels of precipitation rates are indicated in Figure 27 by the grey rectangles: $0.04 \cdot 10^{-6}$ m/s (dark grey rectangle, equivalent to 3.5 mm/day, or 1.3 m/year, which is approximately the average yearly precipitation rate at Åknes) and various daily precipitation rates of 10, 20, 40 and 80 mm/day precipitation (equivalent to 0.12, 0.23, 0.46 and 0.95 µm/s, respectively). The implications of this at Åknes is neither fully understood nor analysed but could suggest some limits to what rates of precipitation that is expected to increase water table levels and increase water pressure on the weakness zones (sliding planes).

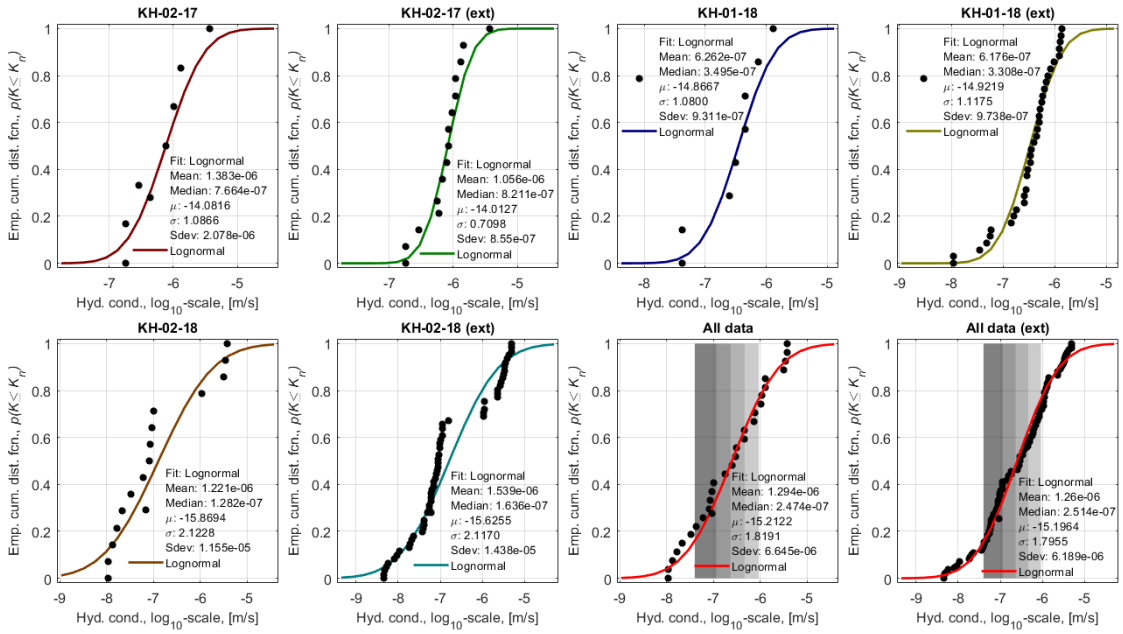

Figure 27 Hydraulic conductivity fitted to a log-normal empirical cumulative distribution function. The plots with (ext) in the title contain all the measurement data in every Lugeon-test interval. Four ranges of precipitation rates are represented by grey rectangles (from dark-grey to light-grey): 0.04-0.12 µm/s (equivalent to 3.5-10 mm/day), 0.12-0.23 µm/s (equivalent to 10-20 mm/day), 0.23-0.46 µm/s (equivalent to 20-40 mm/day), and finally 0.46-0.95 µm/s (equivalent to 40-80 mm/day). See a bigger version of figure in Appendix F.

3.3 Rock mass fracture analysis

Here we analyse the observed and measured fracturing of the rock-mass at Åknes and how the fracture frequency affects the choice of conceptual model and how it can be used to derive effective hydraulic properties.

The rock mass shows three distinct joint sets; the foliation joints and two sub-vertical joint sets with approximately N–S strike and E–W strike (Ganerød et al. 2008; Langeland, 2014). The jointed gneiss has typical block size 0.2-0.6 m^3 (block sizes up to 3 to 5 m^3 is reported by (Grimstad, 1989; Ringstad, 2019). Some properties for the intact rock are given in Table 10.

Table 10. Material properties for intact rock at Åknes.

Variable	Symbol	Value	Unit	Note
Density	ρ_s	2800	kg/m^3	Intact rock (Tønset, 2019)
Youngs modulus	E	40	GPa	Intact rock (Langeland, 2014)
Poisson's ratio	ν	0.2	-	Intact rock (Langeland, 2014)

The cores from the boreholes have been logged and the fracturing have been analysed. Several of the boreholes have also been logged using a televiewer (borehole camera), but only one of the televiewer data have been analysed here, borehole KH-01-17. In general, the fracture frequency becomes lower with increasing depth (Figure 28), but this is not analysed in detail here.

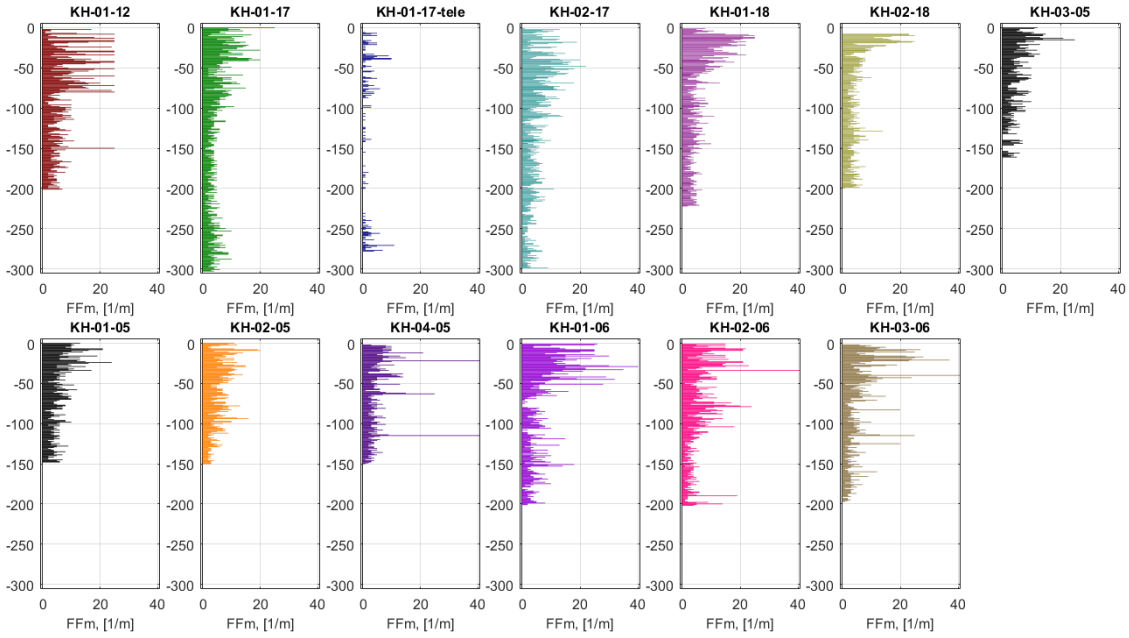

Figure 28 Fracture frequency (number of fractures per meter) with depth of various boreholes. The fracture frequency diagrams are based on core logging, except for KH-01-17 which is from a televiewer (from NGU and NGI reports, 2007 until 2019). See a bigger version of figure in Appendix F.

To analyse the fracture frequency, statistical methods were applied. It can be seen from Figure 29 that the average fracture frequency is around 6.5 with a standard deviation of 4.6. The statistical description of the fracture frequency typically fits good with a Negative Binomial distribution because it captures zones of more intensified fracturing.

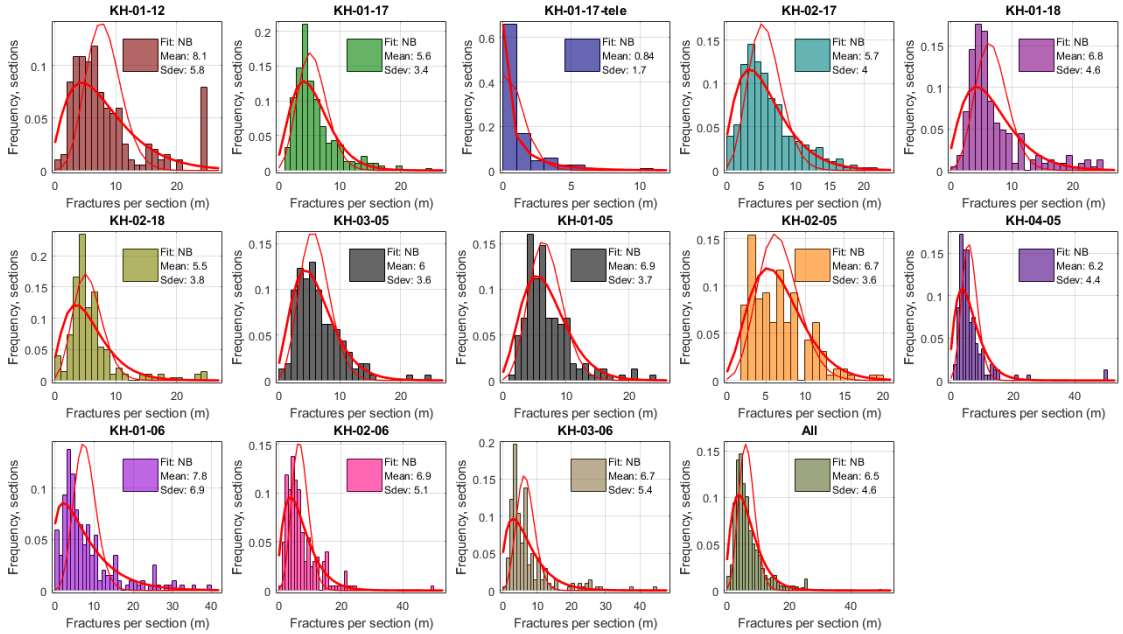

Figure 29 Bar plot of fracture frequency (number of fractures per meter) of various boreholes fitted to a Negative Binomial (NB) distribution function (thick red line) and a Poisson distribution function (thin red line). The last figure (lower right) is the statistical distribution of all the fracture datasets. The fracture frequency diagrams are based on core-logging, except for "KH-01-17-tele", which is from a televiewer. See a bigger version of figure in Appendix F.

When analysing the distribution at various depths the lower parts of the boreholes best fit a Poisson (random) distribution, while the highly fractured top 50-100 m contributes to improving the fit with the Negative Binomial distribution. This is also evident when considering the fit of the fracture frequency with cumulative distribution functions (Figure 30). The Poisson (random) distribution (thin green line) does not manage to obtain a good fit with the high fracture frequency numbers.

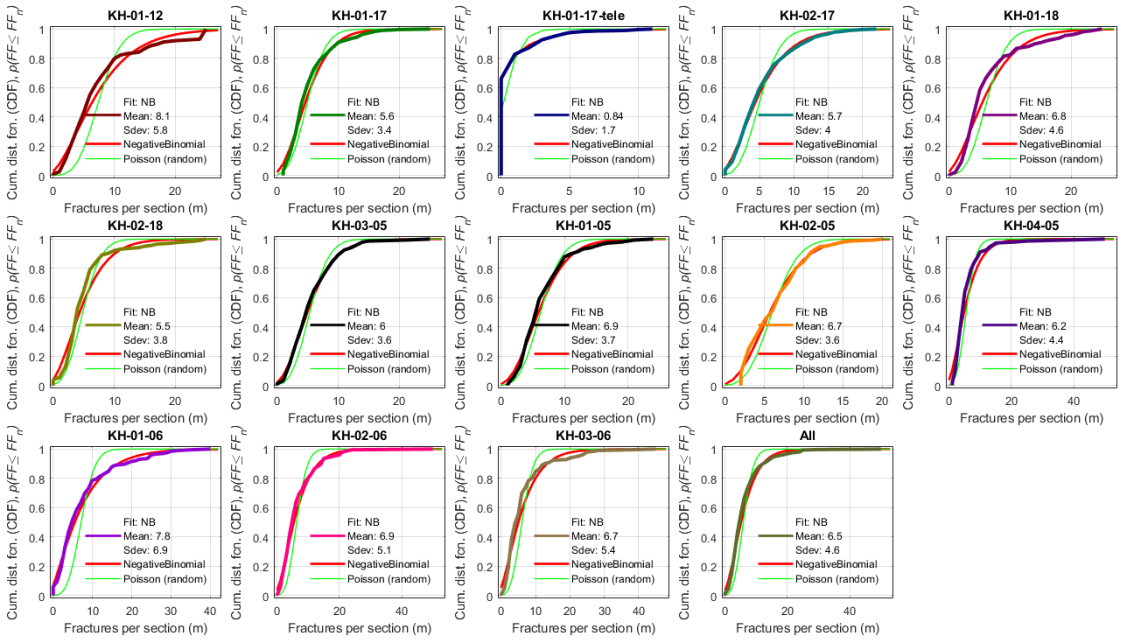

Figure 30 Cumulative distribution of fractures (number of fractures per meter) of various boreholes (thick coloured lines, not red) fitted to two cumulative distribution functions: Negative Binomial (thick red line) and Poisson (thin green line). The last figure (lower right) is the statistical distribution of all the fracture datasets. The frequency diagrams are based on core-logging, except for "KH-01-17-tele" which is from a televiewer.

3.3.1 Model concepts

The fracture frequency can indicate which type of model concept should be used to represent the real fracture system. Examples of model concepts are shown in Figure 31.

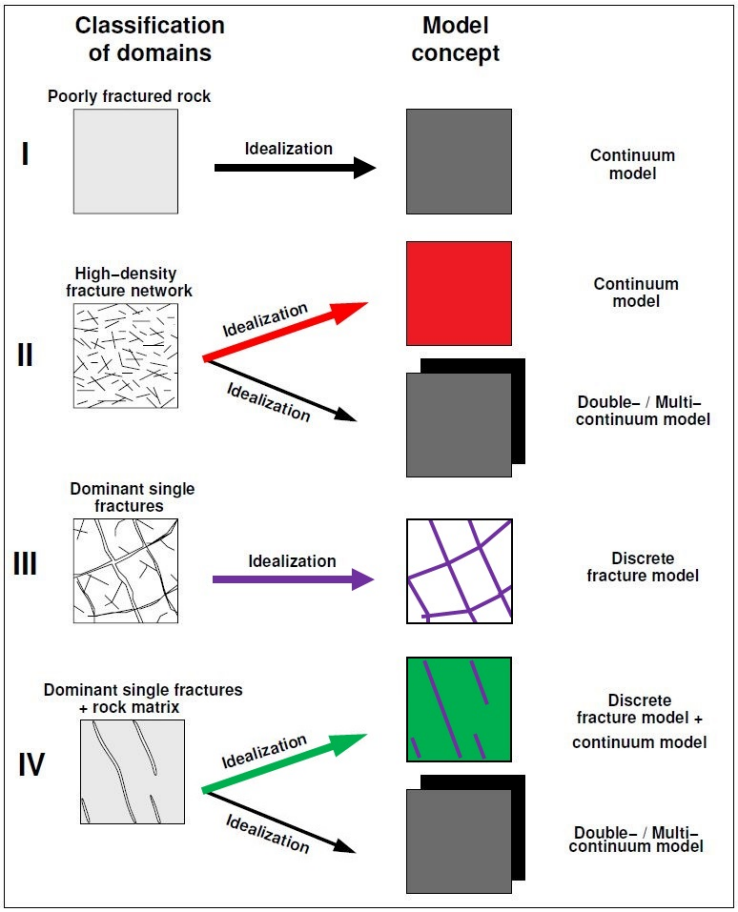

Figure 31 Model concepts. Figure modified from Dietrich et al. (2005).

Considering the physical extent of the Åknes rock mass (km-scale) and the fracture frequency, both model concept II (high-density fracture network, represented by fractured continuum model FCM) and model concept III (dominant single fractures, represented by discrete fracture network model DFN) are reasonable representations of the Åknes rock mass. FCM models are typically solved using a finite element, finite difference or finite volume method. The DFN models are typically solved using discrete element methods.

Here the FCM (using the finite element method) will be used in a conceptual model to illustrate the difference between saturated and unsaturated groundwater flow. In the unsaturated groundwater flow model, the air-phase is also considered (in addition to water) by introducing the concept of capillary pressure and relative permeability. This modifies the fluid flow equation with the consequence of a lower effective hydraulic conductivity in the rock-mass where air is present (unsaturated zone).

3.3.2 Hydraulic properties

The fracture frequency can be used to infer hydraulic properties of the rock mass. By first approximating that the fracture frequency can be converted to fracture spacing in each of the joint sets in the Åknes rock-mass, and then use correlations from Nelson (2001), some first-order estimate of fracture void fraction (fracture porosity) and fractured rock permeability can be obtained, see Figure 32.

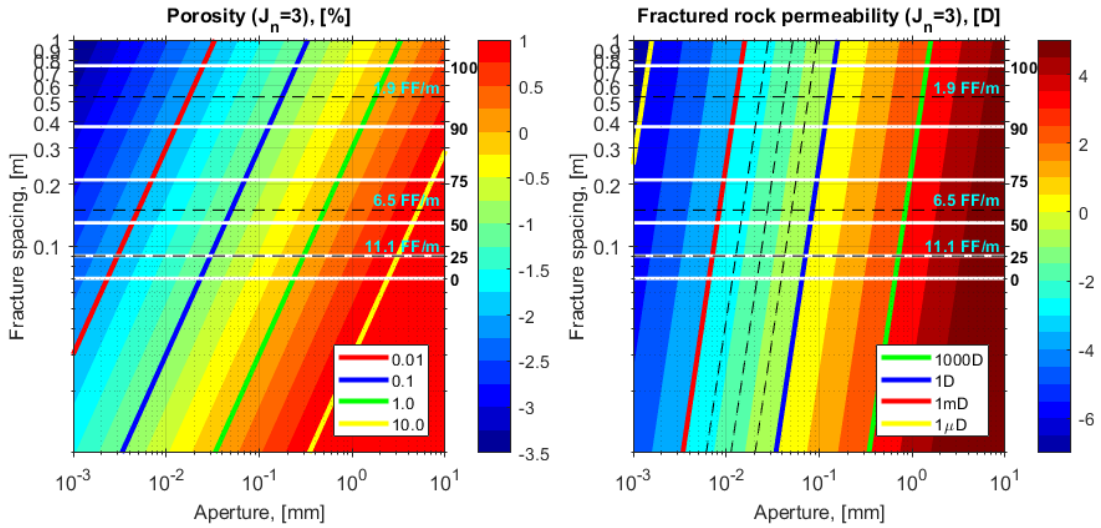

Figure 32 Fracture porosity and permeability (in Darcy, $1D \approx 1 \cdot 10^{-12}$ m²) from simple geometrical correlations when assuming three fracture sets ($J_n = 3$) (Nelson, 2001). White lines are RQD-values (Rock Quality Designation) from the Q-system (NGI, 2015): RQD < 25 corresponds to more than 27 fractures per m³, 25<RQD<50 corresponds to 20-27 fractures per m³, 50<RQD<75 corresponds to 13-19 fractures per m, 75<RQD<90 corresponds to 8-12 fractures per m³ and RQD>90 corresponds to 0-7 fractures per m³. Fracture permeability and porosity can be estimated from Eq. 5 and Eq. 6.

Fracture permeability k_f [m²] of a rock mass with three orthogonal fracture sets with the similar spacing and constant aperture in all directions, in the three-dimensional space, can be calculated as (Nelson, 2001):

$$k_f = \frac{J_n b^3}{12D} \qquad \textit{Eq. 5}$$

where $J_n = 3$ for three set of planes, b [m] is effective, or equivalent, hydraulic aperture of the fractures in the rock mass and D [m] is the average spacing between the fracture plane. Fracture porosity ϕ_{fr} [-] can be estimated by (Nelson, 2001):

$$\phi_{fr} = \frac{J_n b}{D} \qquad \textit{Eq. 6}$$

Figure 32 is created using the formulas of Eq. 5 and Eq. 6. Given a fracture density of 6.5 ± 4.6 fractures per meter (Figure 32) gives a fracture spacing D of 0.09-0.53 m. The hydraulic conductivity K [m/s] from the Lugeon-tests can be converted to permeability k [m^2] by using the following expression:

$$k = \frac{K\mu_w}{\rho_w g} \qquad \textit{Eq. 7}$$

where μ_w [Pa·s] and ρ_w [kg/m^3] are the viscosity and density of water, respectively, and g [m/s^2] is the gravity constant. Typical water properties that can be expected at Åknes for a temperature range of 5-10°C (representing ground water) and a pressure range of 2-50 bar (equivalent to hydraulic head of 20-500 m) are given in Table 11. Using values from this table, and the range of measured hydraulic conductivity (Lugeon-tests, described in Section 2.1 and results are analysed in Section 3.2) result in a permeability range of (0.0063-0.23)·10^{-12} m^2 and an average value of 0.038·10^{-12} m^2.

Table 11. Water properties at Åknes. Properties are based on temperature interval of 5-10 ℃ and pressure interval of 2-50 bar.

Variable	Symbol	Value	Unit	Note
Density	ρ_w	997-1002	kg/m^3	
Viscosity	μ_w	(1.3-1.5) ·10^{-3}	Pa·s	
Compressibility	c_f	0.47-0.49	1/GPa	
Thermal expansion	β_w	(1.6-10)·10^{-5}	1/K	Volumetric. Mainly sensitive to temperature.
Thermal conductivity	κ_w	0.57-0.58	W/(m·K)	
Heat capacity	C_{pw}	4.2	kJ/(kg·K)	At constant pressure.

Knowing the fracture spacing and permeability, Figure 32 (right) can be used to estimate an equivalent, hydraulic aperture b of the fractures in the rock mass: 12-75 μm.

Knowing the fracture spacing and the equivalent, hydraulic aperture b, Figure 32 (left) can be used to estimate a fracture porosity ϕ_{fr}: 0.01-0.3 %.

Note that the simplified analysis above is based on a fracture network that can be represented by three orthogonal joint sets and that the fracture frequency is assumed to be perpendicular to only one joint set. However, this is not the case here, the boreholes intersect the fractures (joint sets) at an angle and therefore intersects more than one joint

set, resulting in an overestimation of the fracture frequency, or underestimation of the fracture spacing. Therefore, the fracture spacing is probably higher than the estimated value of 0.09-0.53 m which implies that the fracture porosity should be slightly lower than estimated and the equivalent hydraulic aperture should be slightly higher (c.f. Eq. 5 and Eq. 6).

Furthermore, the connectivity factor 1/12 in Eq. 5 implies perfect hydraulic communication between all fractures and fracture sets. This is a good assumption for a highly fractured rock-mass. For a rock-mass with a low fracture frequency, the connectivity between the fractures is lower because some fracture may be isolated or not hydraulically connected to neighbouring fractures. This reduction in hydraulic connectivity can be reflected in a reduced connectivity factor <1/12 (with a lower limit of approximately 1/50, Figure 11 in Oda, 1986), implying that the equivalent hydraulic aperture can be up to 1.6 time larger than the estimated values in the analysis here (because of the exponent 3 in aperture in Eq. 5).

The derived hydraulic properties from the Lugeon-tests (Chapter 3.2) and the fracture frequency analysis above are summarized in Table 12

Table 12. Åknes rock mass fracture properties and hydraulic properties from Lugeon-tests and fracture frequency analysis.

Variable	Symbol	Value	Unit	Note
Spacing	D	0.09-0.53	m	Average fracture spacing, based on average fracture frequency. This value is probably underestimated*.
Hydraulic conductivity	K	Range: $(0.04\text{-}1.5)\cdot10^{-6}$ Avg.: $0.25\cdot10^{-6}$	m/s	From Lugeon tests, see Chapter 3.2
Permeability	k	Range: $(5.7\text{-}210)\cdot10^{-15}$ Avg.: $38\cdot10^{-15}$	m^2	Converted from hydraulic conductivity using Eq. 7.
Aperture	b	12-75	μm	Effective/equivalent hydraulic aperture. This value is probably underestimated*.
Fracture porosity	ϕ_{fr}	0.01-0.3	%	Effective/equivalent fracture void ratio fraction of rock mass. This value is probably overestimated*.

* The note on under- and overestimation refers to discussion above table.

4 Hydrogeological model

Here we present the hydrogeological model using the available data as described earlier. The focus here is to increase the understanding of the water-flow in Åknes. The water table is relatively constant in the rock-slope, see Section 2.3.2 on water table in open boreholes, implying that the top 25-75 m is relatively dry/drained.

The work presented here is a two-dimensional (2D cross-section) fractured continuum model (FCM, concept II in Figure 31) approximation of the rock mass at Åknes, see Figure 33 (right). The detailed topography of the cross-sections have been further simplified to straight lines/slopes with the average slope from Åknes rock slope.

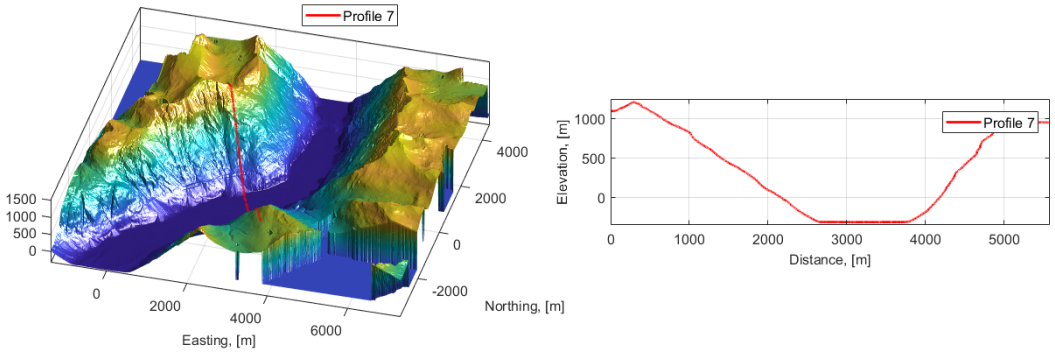

Figure 33 Topography and bathymetry of Åkneset. Sunnylvsfjorden is approximately 320 m deep, average slope of the Åknes rock mass is 33-38 °, depending on the orientation, but typically higher towards south-east and down-slope.

First, the governing equations for saturated and unsaturated flow are described.

4.1 Saturated flow: Darcy's law

The fluid flow in a saturated rock mass can be described by: the mass conservation equation for the water and the rock mass combined with Darcy's law. The derivation can be found in relevant textbooks, here we just formulate the governing equation for saturated flow:

$$\rho_w S \frac{\partial p}{\partial t} + \nabla \cdot (\rho_w \mathbf{q}_w) = 0 \qquad \textit{Eq. 8}$$

where S [1/Pa] is the storage coefficient for a saturated rock mass, p [Pa] is the fluid pressure, t [s] is time and the specific fluid discharge vector $\mathbf{q}_w$ [m/s] is described by Darcy's law:

$$\mathbf{q}_w = -\frac{\mathbf{k}}{\mu_w}(\nabla p + \rho_f \mathbf{g}) \qquad \textit{Eq. 9}$$

where $\mathbf{k}$ [m^2] is the permeability tensor, $\mathbf{g}$ [m/s^2] is the gravity vector. The storage coefficient that can be expressed (for a slightly deforming media):

$$S = \frac{(b - \phi_{fr})}{K_s} + \frac{\phi_{fr}}{K_w} + \frac{b^2}{M} \qquad \textit{Eq. 10}$$

where b [-] is the Biot's coefficient, K_s [Pa] is the bulk modulus of the solid constituents of the rock mass, K_w [Pa] is the inverse of the fluid compressibility c_w, M [Pa] is the p-wave modulus, or Oedometer modulus. For incompressible solids the storage coefficient is reduced to $S = \phi_{fr}/K_w$, for highly compressible rock mass the storage coefficient can be reduced to $S = 1/M$. The Biot's coefficient is typically expressed as:

$$b = 1 - \frac{K}{K_s} \qquad \textit{Eq. 11}$$

where K [Pa] is the bulk modulus of the rock mass. For homogeneous and isotropic linear elastic materials their mechanical moduli can be determined by any two moduli among these. Both p-wave modulus M and bulk modulus K can be expressed by Young's modulus E [Pa] and Poisson's ratio ν [-]:

$$K = \frac{E}{3(1-2\nu)}, \qquad M = \frac{E(1-\nu)}{(1+\nu)(1-2\nu)} \qquad \textit{Eq. 12}$$

4.2 Unsaturated flow: Richards' equation

The fluid flow in an unsaturated rock mass can be described by Richards' equation. Richards' equation is a two-phase flow equation where the air is assumed to be perfectly mobile such that the air pressure can be considered constant everywhere and the mass conservation equation for the air-phase can be eliminated from the system of governing equations. The remaining governing equation for unsaturated flow is:

$$\rho_w S_u \frac{\partial p}{\partial t} + \nabla \cdot (\rho_w \mathbf{q}_w) = 0 \qquad \textit{Eq. 13}$$

where S_u [1/Pa] is the storage coefficient for an unsaturated rock mass, which can be expressed (for a slightly deforming media):

$$S_u = \phi_{fr} \frac{ds_w}{dp} + s_w S \qquad \textit{Eq. 14}$$

where s_w [-] is the water saturation: the volume fraction of water in pore/fracture space of the rock mass. The specific fluid discharge vector $\mathbf{q}_w$ [m/s] is now described by Darcy-Buckingham's law:

$$\mathbf{q}_w = -\frac{k_r \mathbf{k}}{\mu_w}(\nabla p + \rho_w \mathbf{g}) \qquad \textit{Eq. 15}$$

where k_r [-] is the relative permeability. In an unsaturated rock mass, the wetting properties of the water becomes important, resulting in capillary suction. This capillary suction affects both the fluid pressure and the permeability of the water in the rock mass fractures. The effect on pressure is expressed through the capillary pressure function and the effect on relative permeability is an integral expression of the capillary pressure. A common expression for the capillary pressure is the relation by van Genuchten (1980):

$$p_c = p_d \left(\frac{1}{s_{ew}^{1/m}} - 1 \right)^{1/n} \qquad \textit{Eq. 16}$$

where p_d [Pa] is the entry pressure (roughly equivalent to the pressure needed to displace water with air) and m [-] and n [-] are fitting parameters (see later section). s_{ew} [-] is the effective saturation of the water in the rock-mass:

$$s_{ew} = \frac{s_w - s_{wr}}{1 - s_{wr}} \qquad \textit{Eq. 17}$$

where s_w [-] is the total fraction of water content in the rock-mass void-spaces (pores and fractures) and s_{wr} [-] is the residual (irreducible) saturation of water. In the following analysis we assume that $s_{wr} = 0$.

The relative permeability for the water is expressed by (van Genuchten, 1980):

$$k_r = s_{ew}^{1/2} \left(1 - \left(1 - s_{ew}^{1/m} \right)^m \right)^2 \qquad \textit{Eq. 18}$$

4.2.1 Boundary conditions

The geometry and the boundary conditions in the hydrogeological model are shown in Figure 34.

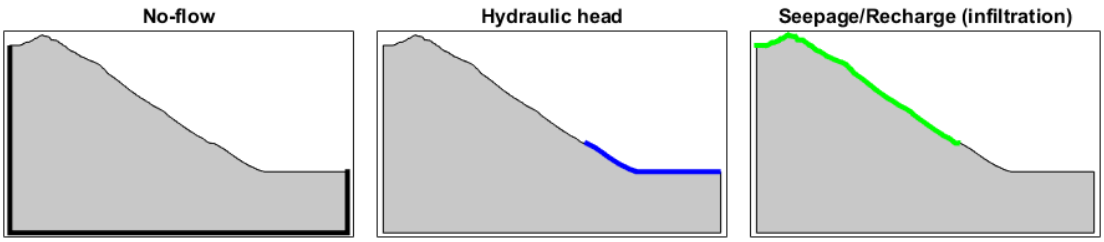

Figure 34. Boundary conditions used in the hydrogeological model: No-flow (black boundary), constant hydraulic head (blue) and seepage/recharge (infiltration) boundary flux (green).

No-flow boundary condition is used to describe boundaries with no flow across the boundary, it is also used to describe symmetric boundary conditions:

$$-\mathbf{n} \cdot \rho\mathbf{q} = 0 \qquad \textit{Eq. 19}$$

where **n** is the normal vector to the boundary.

Boundaries to Sunnylvsfjorden (blue boundaries in Figure 34) have a constant hydraulic head that corresponds to the water elevation, here the mean sea level, with a constant hydraulic head H [m]:

$$p = \rho g(H - D) \qquad \textit{Eq. 20}$$

where D [m] is the reference elevation (here $D = 0$ m).

Water infiltration q_n [kg/(m^2·s)] depends on the precipitation $R(t)$ [m^3/(m^{2}s)] (noting that the unit m^3/(m^{2}s) is a volume flux and is typically simplified to m/s, or mm/dag for precipitation). Although not all of the precipitation infiltrates the ground (some evaporates), it is assumed in the simulations here that the maximum infiltration is equivalent to the average precipitation rate.

In the model it is further assumed that the infiltration q_n can neither be larger than the precipitation R nor result in a hydraulic head larger than the elevation:

$$\begin{cases} q_n = R(t), & H < z_0 \\ H = z_0, & H \geq z_0 \end{cases} \qquad \textit{Eq. 21}$$

where z_0 [m] is the elevation of the surface. Mathematically this can also be expressed as:

$$q_n = -\mathbf{n} \cdot \mathbf{q} = \min\left(R(t), -\frac{K_b}{L}(H - z_0 + L \cdot |n_z|)\right) \qquad \textit{Eq. 22}$$

where K_b [m/s] is the hydraulic conductivity of a boundary layer with the thickness L [m] and n_z is the vertical component of the unit normal-vector that corrects the gravitational contribution to the infiltration on sloping surface. The boundary layer can be different from the rock mass. e.g. a thin sedimentary layer, but in the model, it is assumed to be an extension of the rock mass. The last term in Eq. 22 is a linearization of Darcy's equation, Eq. 9, in one dimension. Note further that this boundary condition (as it is defined) only considers whether precipitation can infiltrate the rock mass or if water is flowing out of the surface, it does not keep track of run-off that might infiltrate further down-slope.

4.3 Unsaturated flow: variables

Estimating entry pressure, p_d, is critical in capillary pressure modelling. Based on almost 100 samples with various lithologies, porosity and permeability, Wu (2005) proposed the following relationship between entry pressure, porosity and permeability:

$$p_d = \exp\left[5.458 - 1.255 \ln\sqrt{\frac{k}{\phi_{fr}}} + 0.081\left(\ln\sqrt{\frac{k}{\phi_{fr}}}\right)^2\right] \qquad \textit{Eq. 23}$$

This correlation is plotted in Figure 35. This correlation is not based on fractured rock samples, but porous rocks (sandstone, shaly sandstone and carbonate rocks), but we apply it here as a first order approximation.

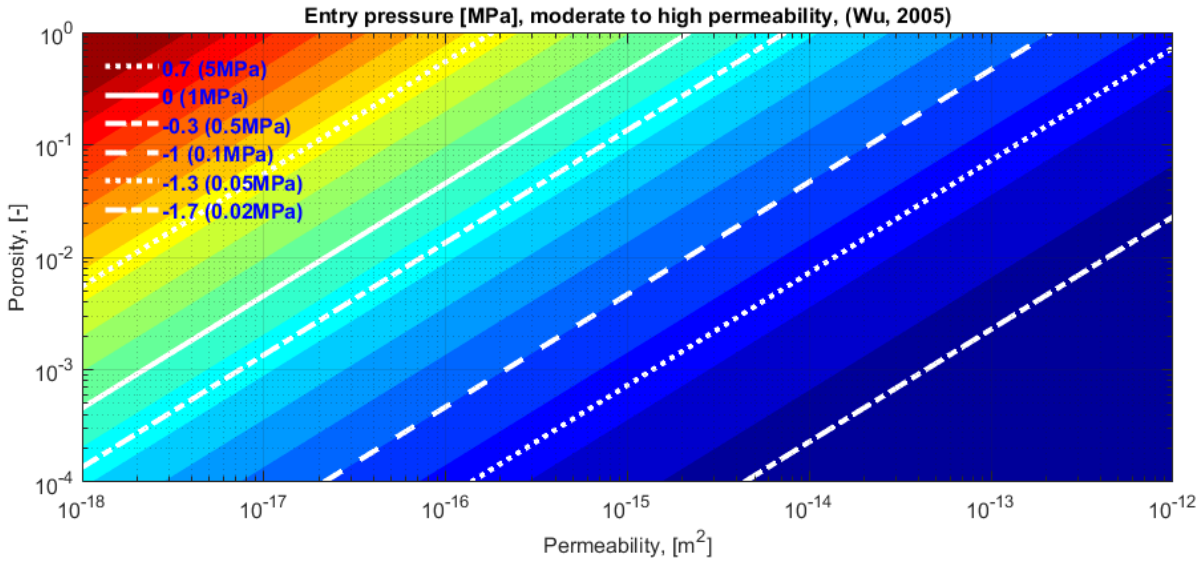

Figure 35 Entry pressure (for capillary pressure functions), using correlation by Wu (2005) in Eq. 23.

Entry pressure can also be derived directly for a fractured media. There is some literature on this in relation to storage of nuclear waste, e.g. Jarsjö et al. (2017). Characteristic relations correlating capillary pressure, water saturation and relative permeability in soils are typically used described by van Genuchten relations (van Genuchten, 1980). In fracture media these relations are aperture based, and although these relations are very similar in shape to the traditional van Genuchten-curves, their parameters differ from the van Genuchten-type of parameterizations that are integrated in most state-of-the art numerical codes for unsaturated flow. By matching the van Genuchten-curves to the fracture aperture based characteristic curves, Jarsjö et al. (2017) showed that the van Genuchten-parameters could unambiguously be determined from the fracture characteristics (mean aperture and standard deviation of fracture aperture). These correlations are shown in Figure 36.

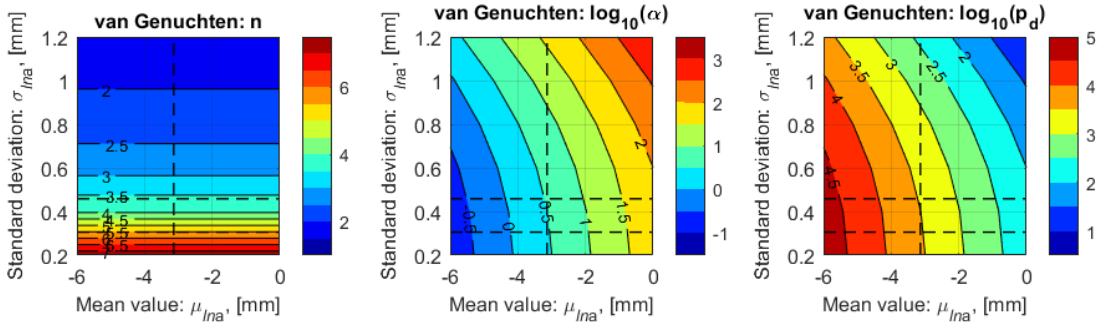

Figure 36 Matching values of the van Genuchten parameters n [-] and α [1/m] (m=0.5 in all cases) for reproducing unsaturated flow characteristics for aperture-based relations based on mean fracture aperture (log-scale, μ_{lna}) and standard deviation of fracture aperture (log-scale, σ_{lna}). Note that α in the figure refers to fracture aperture and that $p_d = \rho_f g/\alpha$. The dashed lines indicate the range of values from effective hydraulic aperture range in Table 12.

Using the average fracture aperture (43.5 mm) value in Table 12, we obtain that $\mu_{lna} = -3.13$. To estimate the standard deviation, we assume that the aperture range in Table 12 covers four-six standard deviations (app. 95 % to 99 % probability that the effective hydraulic fracture aperture is within the given range, respectively), then $\sigma_{lna} = 0.31 - 0.46$. The values for μ_{lna} and σ_{lna} results in the corresponding van Genuchten parameter-values $n \approx 3.6 - 5.5$ and $p_d \approx 3.2$ kPa. These parameters describe a very sharp saturation profile and a relative permeability of the water that drops very fast, see Figure 37.

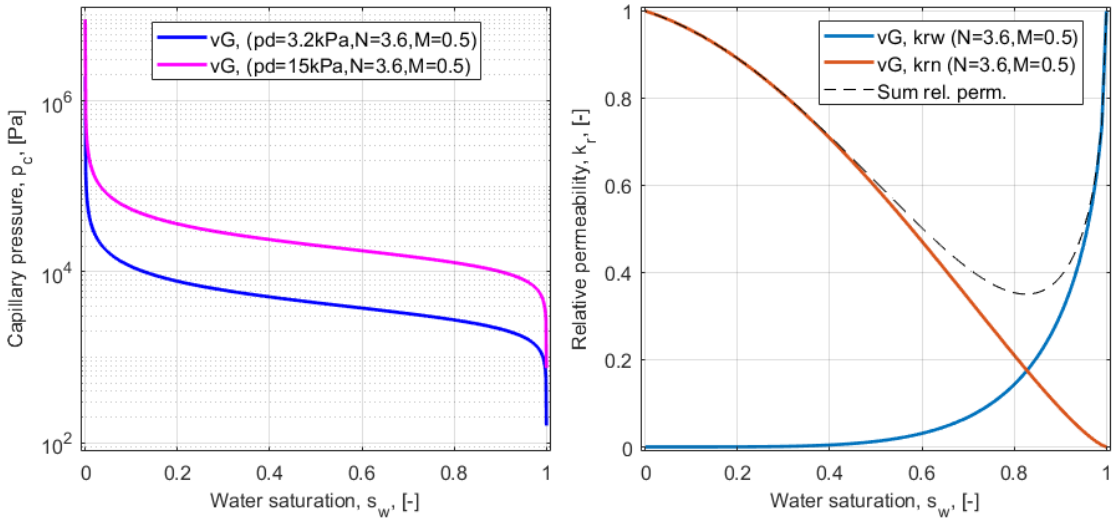

Figure 37 Capillary pressure and relative permeability for the rock mass at Åknes.

Table 13. Åknes rock mass unsaturated hydraulic properties, van Genuchten-parameters.

Variable	Symbol	Value	Unit	Note
Entry pressure	p_d	3.2, 15	kPa	Depends on method: 15 kPa using Wu (2005) and 3.2 kPa by using Jarsjö et al. (2017)
n-parameter	n	3.6	-	Jarsjö et al. (2017)
m-parameter	m	0.5	-	Jarsjö et al. (2017)

A low entry pressure p_d implies a sharp interface between saturated and unsaturated flow: the lower value the sharper the interface, requiring a very fine discretisation (dense calculation grid). Additionally, low entry pressure is (notoriously) difficult to solve numerically, hence in the following simulations we use a higher entry pressure value of 50 kPa.

4.4 Anisotropy

The fracture network consists of three fracture planes: two sub-vertical and one almost parallel with the rock slope surface (similar to the foliation joints). Fracture orientation determines the direction of preferred flow-path, differences in the joint sets will therefore imply anisotropy in the hydraulic conductivity of the rock-mass. We do not have any data that allows us to determine the anisotropy, or the ratio between the various directional components in the hydraulic conductivity tensor, hence a natural initial assumption is that the hydraulic conductivity of the rock mass is isotropic. However, in the conceptual model presented in the following section we distinguish between the hydraulic conductivity along the foliation and the joint set perpendicular to the morphology of the surface (sub-vertical). This means that the hydraulic conductivity will be anisotropic with a sub-vertical and a "sub-slope-parallel" component. The "sub-slope-parallel" component follows approximately the topography. In the numerical model this is represented by an anisotropy tensor as illustrated by the blue and red arrows in Figure 38.

Since there is no data to back up anisotropy in the hydraulic conductivity, a somewhat arbitrarily chosen ratio of 1:5 between the hydraulic conductivity in the sub-vertical direction (the blue arrow in Figure 38) and the "sub-slope-parallel" direction (the red arrows in Figure 38) to achieve a significant effect compared to an isotropic rock-mass.

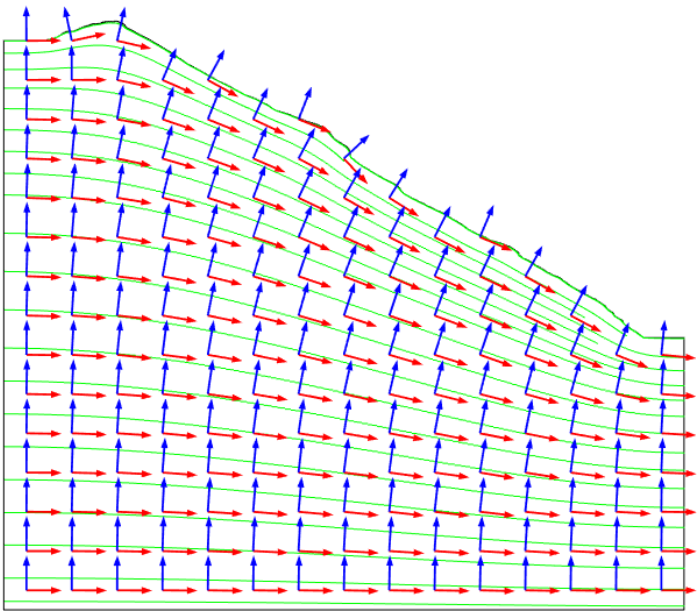

Figure 38 Illustration of the anisotropy used in the hydrogeological model of Åknes. The green streamlines and red arrows represent the direction of the sub-slope-parallel fracture plane and its resulting sub-horizontal anisotropy-component following the topography. The blue arrows indicate the sub-vertical anisotropy-component.

The effect of various anisotropy ratios has not been investigated.

4.5 Results fluid flow

In the following we present some result of both saturated and unsaturated flow to illustrate the similarities and the differences between the two approaches. In general, the two approaches result in similar solutions under steady-state conditions, but the main difference is observed when the two approaches are compared in time, e.g. days-months when draining the rock mass. The saturated (Darcy) flow-approach assumes hydraulic communication everywhere while the unsaturated (Richards) flow-approach considers reduced hydraulic communication in areas with reduced saturation (dry areas). The latter approach (Richards) will therefore drain slower compared to the former (Darcy).

Before continuing the presentation of the modelling results we describe the details in the presented figure. The contours and lines in the following results are explained and described in Figure 39.

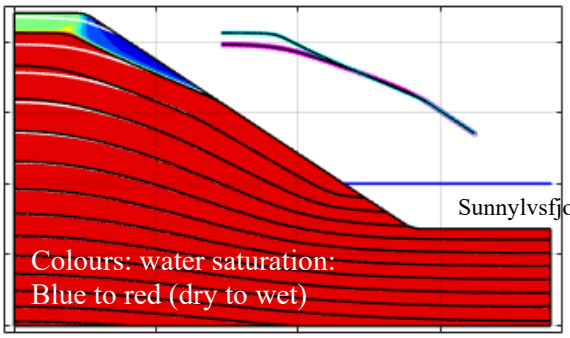

Magenta line: water table (hydraulic head contour at 0 m), saturated (Darcy) flow.

Cyan line: water table (hydraulic head contour at 0 m), unsaturated (Richards) flow.

Note that the contours are shifted to the right for visualisation purposes and the thin black lines indicate the initial water-table before drainage.

Black contours: hydraulic head (200 m interval), unsaturated flow

White contours: hydraulic head (200 m interval), saturated flow

Figure 39 Explanation of contours and lines in result-plots.

The first results show the steady-state solution of constant infiltration. To simplify the analysis a linear relative permeability function is used ($k_r = s_{ew}$, compared with Eq. 18). This simplifies the following analysis because the depth to water-table will be proportional to the ratio of the constant precipitation (rain) rate and the hydraulic conductivity of the rock mass. For instance, the saturation of the rock mass will be the same when the precipitation rate and hydraulic conductivity of the rock mass are 4 mm/day and 0.4 µm/s, respectively, or 16 mm/day and 1.6 µm/s. The average precipitation in Åknes is approximately 1300 mm/year, or approximately 4 mm/day (data from MET.no, see Appendix E). In Figure 40 the result of two cases are shown but note that these results scale linearly according to the discussion above.

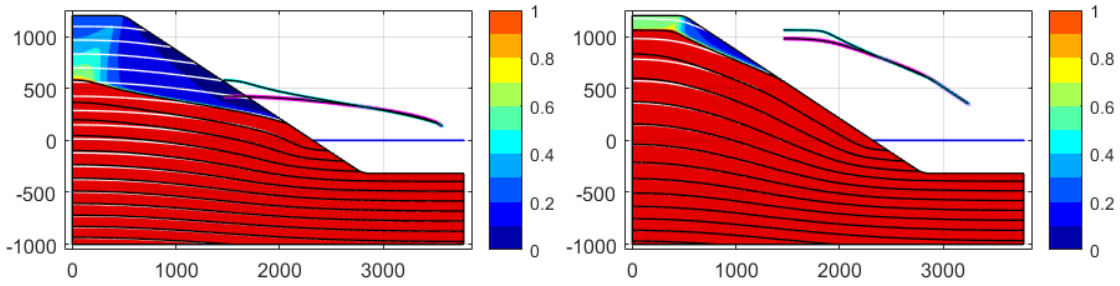

Figure 40 Steady-state solution (saturation) of constant infiltration. In both figures the precipitation has a constant rate of 4 mm/day but the hydraulic conductivity is (left figure) 8 μm/s and (right figure) 4 μm/s. See Figure 39 for explanation of the plots.

In practice the precipitation infiltrates (in-flow) the rock mass in the unsaturated (blue) areas, where the water table (magenta/cyan line) is below the surface, while the drainage (out-flow) occurs in the saturated (red) areas and into the fjord (Sunnylvsfjorden), the saturated areas below the water table (magenta/cyan line).

To demonstrate the difference between steady state solution and transient solution in time for the two approaches (Darcy and Richards), the solution from a steady state solution is used as initial condition (the solution in Figure 40, right), at time t=0 the precipitation is turned off (simulating a dry period), and the results for a selection of elapsed time steps are shown in Figure 41.

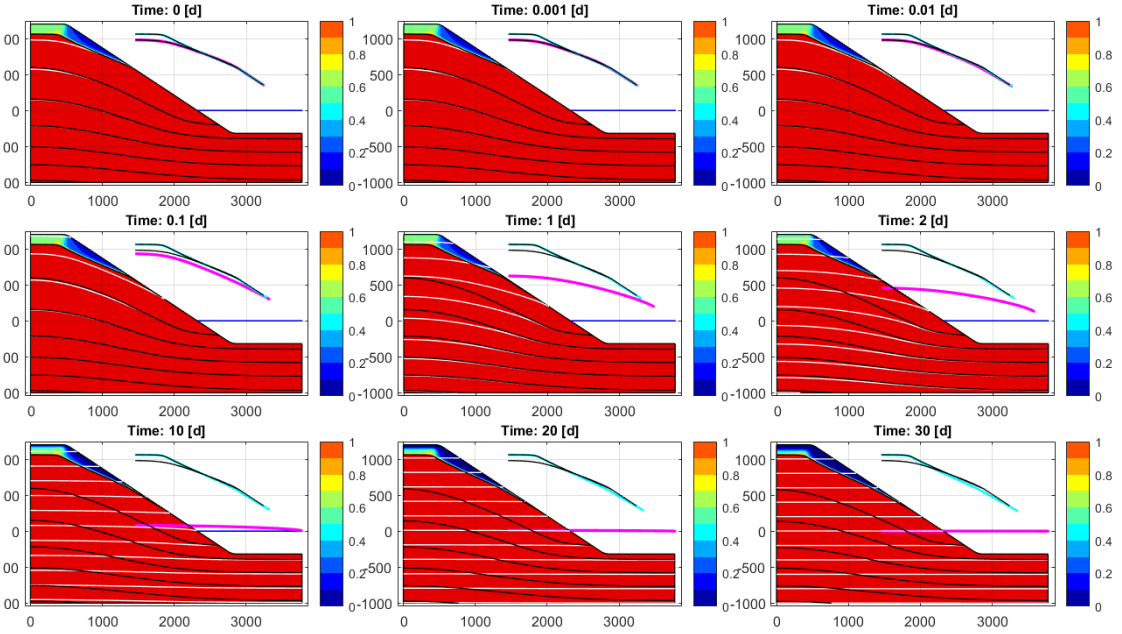

Figure 41 Transient simulation of drainage at Åknes. The panels show the solution of saturated (Darcy) and unsaturated (Richards) flow at various times after drainage starts.

By comparing the shifted water-table contour lines of the two approaches (cyan for unsaturated and magenta for the saturated) it can be seen how quickly the water table in the saturated approach drops compared to the unsaturated approach. After 10 days the rock mass is almost completely drained as the water table is almost at the level with Sunnylvsfjorden (compare cyan curve to the blue horizontal line that illustrates the water level in the fjord). Note that drainage will scale with the rock mass permeability, a high-permeable rock mass drains faster. It can be seen in the results for the unsaturated approach (Richards) that the water table is almost not dropping at all. The reason that the water table in the unsaturated approach drops slower compared to the saturated approach (Darcy) is because of the relative permeability that effectively reduces the permeability in the rock mass (low-permeable rock mass drains slower).

The important take-away from this comparison is that if the rock mass do not have a constant water table on the left boundary (e.g. in Instevatnet behind the ridge above Åknes) and the capillary forces are neglected, the rock-mass could practically drain completely within weeks in periods of no precipitation and large fluctuations in the water table between periods of low/high precipitation is expected. But, note that this depends on the permeability and porosity (or void ratio) of the rock mass, e.g. halve the permeability and double the porosity will slow down the drainage process four-fold. A big assumption in the model is that the rock mass is homogeneous, heterogeneities in the rock mass with contrasts in permeability (e.g. lower) and storativity (e.g. higher) can smooth out fluctuations in water table due to varying degree of infiltration, this has not been explored here.

The model above is a strong indicator that the capillary forces are significant, and that unsaturated flow needs to be considered, since it can explain the relatively stable water table data. Alternatively, or additionally, this could indicate that there exist water-bearing joints giving hydraulic connectivity also high in the mountain-side towards Instevatnet keeping the rock-mass from draining completely during times of little/no precipitation. When the cross-section of Åkneset is extended to the Instevatn lake behind the mountain ridge, a hypothetical water table (here linear) can be drawn from the lake down towards the Åknes rock slope (where the streams come out of the rock mass around 400 masl) and towards the Sunnylvsfjord, see Figure 42. This will be further discussed in Chapter 5.1. The extended profile intersects with the boreholes KH-01-06, KH-01-12 and KH-02-17 and slightly to the side of KH-02-18.

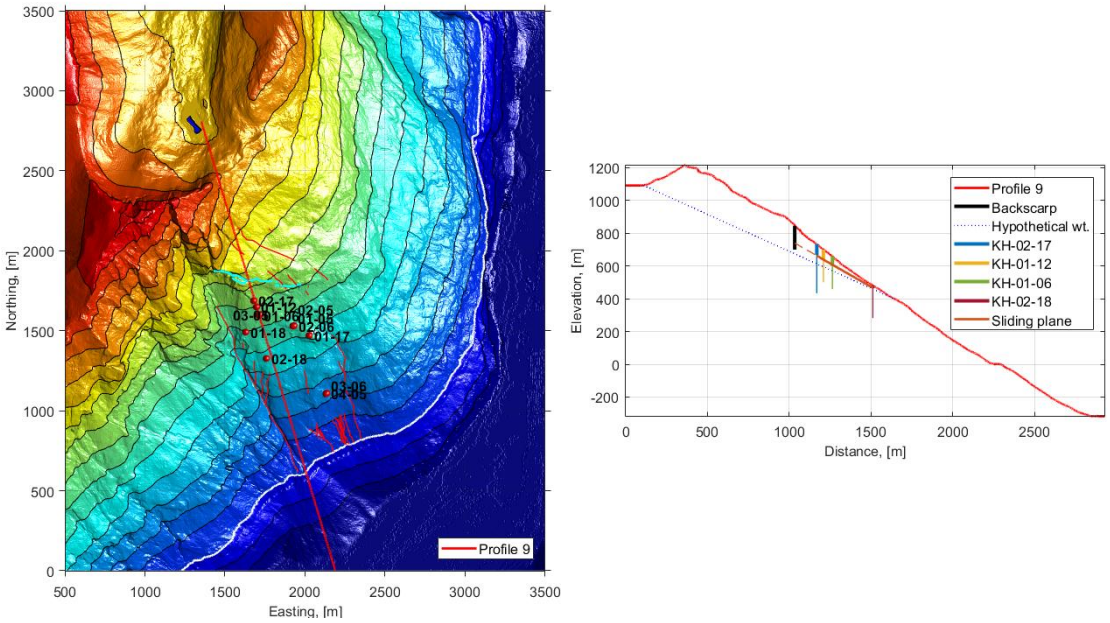

Figure 42 Left: topography of Åknes with the location of the wells, streams, backscarp and an indication of a cross section (red, straight line) between Instevatn lake and the fjord. Right: The cross-section of Åknes along profile indicated in the left figure. Thick line indicating the depth of the water table see Table 14 and Table 15. For more details see Figure 44.

4.6 Surface flow

A surface flow simulation was performed to investigate the surface run-off patterns and see where the water in the Åknes slope is coming from. The simulation shows where water will flow due to gravity and surface slope when no water can infiltrate the rock mass. The results are shown in Figure 43, and the calculated surface streamlines (black lines) coincide well with the red lines which are mapped streams (perennial and ephemeral).

The Figure 43 (right) can be used to approximate where the water that feeds the back scarp of the Åknes is coming from. It can be seen that the surface area that feeds the backscarp, is a relatively small area.

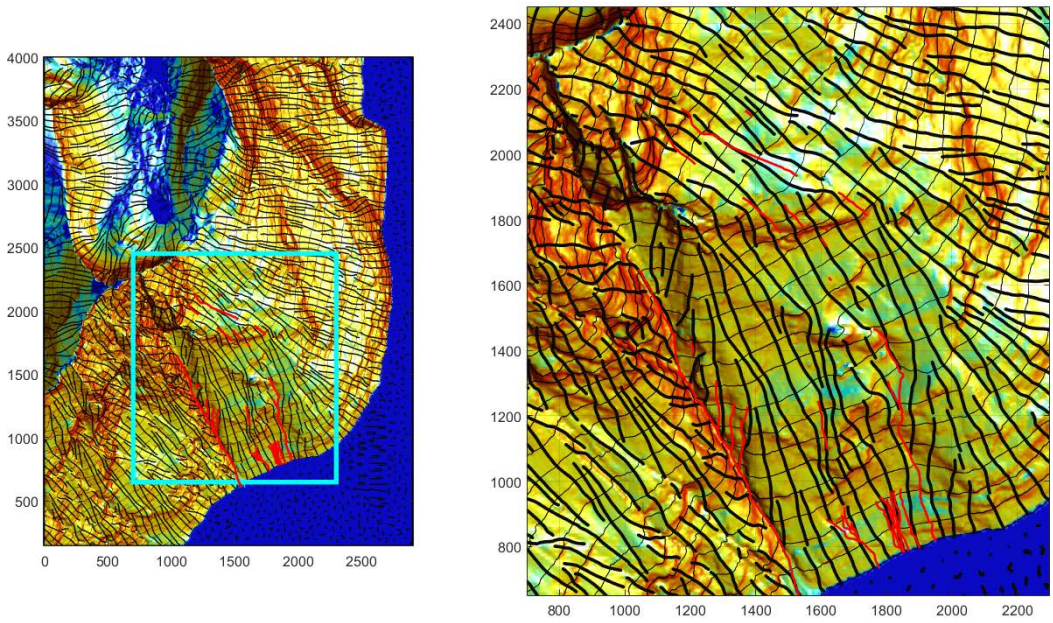

Figure 43 Surface flow-simulation where all precipitation is modelled as run-off. The color represents the slope (from flat, blue, to steep slope, red). The calculated surface streamlines (black lines) coincide well with the red lines which are mapped streams (perennial and ephemeral).

5 Discussion of results and concluding remarks

In this chapter a discussion of results from field investigations, monitoring and outcomes from hydrogeological analyses are presented. An understanding of how the hydraulic communication in the rock slope might be, is discussed. Further, some concluding remarks on the ground water pressure on the sliding planes are given. The conclusions from this report will be used as inputs for the hydromechanical stability analysis of Åknes rock slope.

5.1 Hydraulic communications in the slope

The analysis of the water head in the boreholes from 2017 and 2018 (Figure 22 to 25), show example of linear build-up of water pressure with depth. In the time periods analysed in this report this is a clear pattern. Only in borehole 02-17 the deepest piezometer (129 mbgl) shows lower water pressure. One explanation can be that this piezometer is installed without any packer below the piezometer, and therefore the water pressure is not building up as in the other sections with packers below the piezometers.

If an extended profile is drawn upwards to the lake Instevatn a hypothetical water table can be drawn from the lake down towards the Åknes rock slope and towards the Sunnylvsfjord, see Figure 44. In the extended profile the boreholes KH-02-17, KH-01-12, KH-01-06 and KH-02-18 are located with estimated water table at the point where the thick part of the lines indicating the boreholes are ending. There exists no water table as such in hard rock, since the water flows along the discontinuities. And joint connectivity and the degree of opening of apertures are controlling the waterflow. The groundwater table is defined as the transition between the unsaturated zone and the zone below where the open joints are saturated with groundwater.

In the Åknes rock slope the water pressure at different heights are measured in sectioned borehole and several springs are mapped at different locations. In the drawn profile in Figure 44 many springs are located at height approximately 400 and 460 meters above sea level. From the monitoring the water table seems to be located just above the hypothetical groundwater table. Most likely infiltration of water from the surface and particularly the backscarp results in a water table close and just below the sliding plane. However, the rock mass above and partly below the sliding plane is highly jointed resulting in water flowing out in springs in the toe area for the main sliding plane.

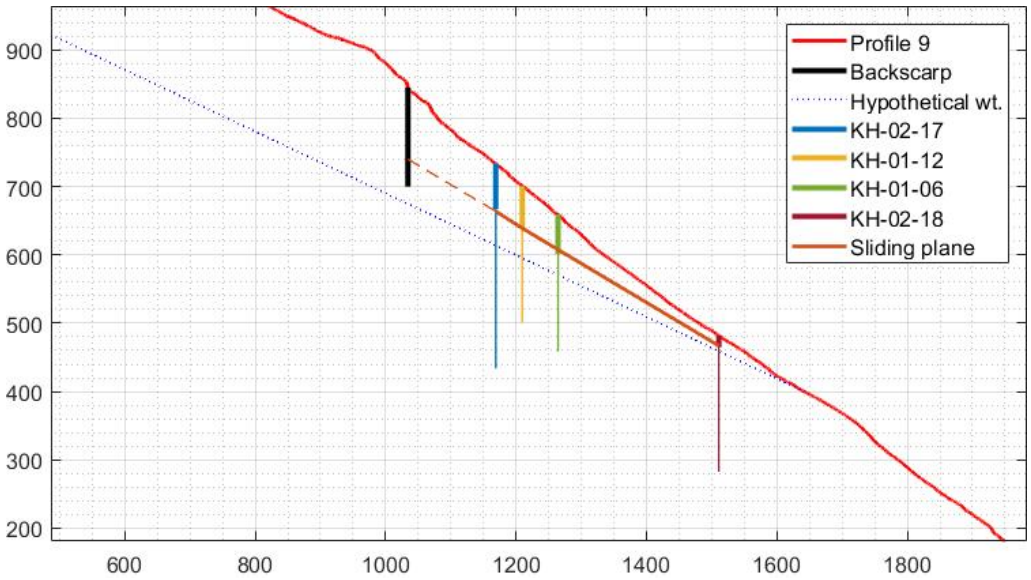

Figure 44 Close-up on sliding plane and boreholes in Figure 42.

Water flow is entirely dependent on joints or jointed sections (e.g. in connection with weakness or fault zones), but only a few open joints are necessary to make the water flow and be interconnected over long distances. Some of the foliation joints are most likely water bearing together with some vertical joints oriented North-South. The strike and dip of the foliation joints are favourable for water flow from the mountain area towards the Åknes rock slope.

Results from the Lugeon measurements show that several sections below the sliding planes have high Lugeon values. One example is **borehole KH-02-17** with 45 L around 89 mbgl and 12 L around 122 mbgl. Based on the sections with Lugeon measurements several joints are existing with high water flow, with long sections with almost no water flow. When studying the flowmeter measurements, the results showed water flowing into the borehole around 123-124 mbgl, then the water flow upwards to 88 mbgl where water is flowing out. This fits well with the sections with high Lugeon values measured. However, the heat tracing tests show a downward flow from 90 to 250 mbgl which is opposite of the flowmeter measurements.

Lugeon tests carried out in **borehole KH-01-2018** show that the borehole from depth 72.5 mbgl down to depth of 218.9 mbgl has zero hydraulic conductivity except at depth of 141 to 147 at which Lugeon value was measured to 4.2 L. Even deeper (220 mbgl) the Lugeon value was measured to 2.9 L. The core pictures from the borehole shows that there is not any visible crushed zone in the above-mentioned depth. The flowmeter measurements show large upwards flow (2400 l/hour) from the bottom of the borehole to 178 mbgl. The water seems to come from the section with Lugeon value 2.9. At a depth of 178 mbgl large flow out is registered. A flow into the borehole was registered at 86 mbgl. Then a downwards flow from 86 to 178 mbgl was registered. The heat tracing measurements show a recharge zone around 210 mbgl and upwards flow until a discharge zone started at 45 mbgl and up.

The flowmeter measurements and the heat trace tests do not fit very well. However, the results from Lugeon measurements fit well with sections showing flow either into or out of the boreholes. The measurements also show long sections with no open joints and water flow. The open boreholes give water table locally in the open borehole at that specific point of time.

Multi tracer tests have been carried out at Åknes rock slope (Frei, 2008). The results showed that the water flows over long distances, most likely also below the sliding planes, which support that the Åknes rock slope is hydraulically interconnected.

It's not unusual to meet high water pressure in tunnels beneath mountain areas with height above 800 meters. Often high water ingress is met in a few weakness zones with high water pressure typically from 40 to 70 bar. With such high water pressure, the water may enter a tunnel also through very small apertures in joints.

Profile W2 is located in the west flank, and crosses borehole KH-02-17 and KH-01-18 and is not far from borehole KH-01-12 (see Figure 45). A sketch is made illustrating the location of two sliding planes, the piezometers and the Lugeon measurements, see Figure 46 and Figure 47.

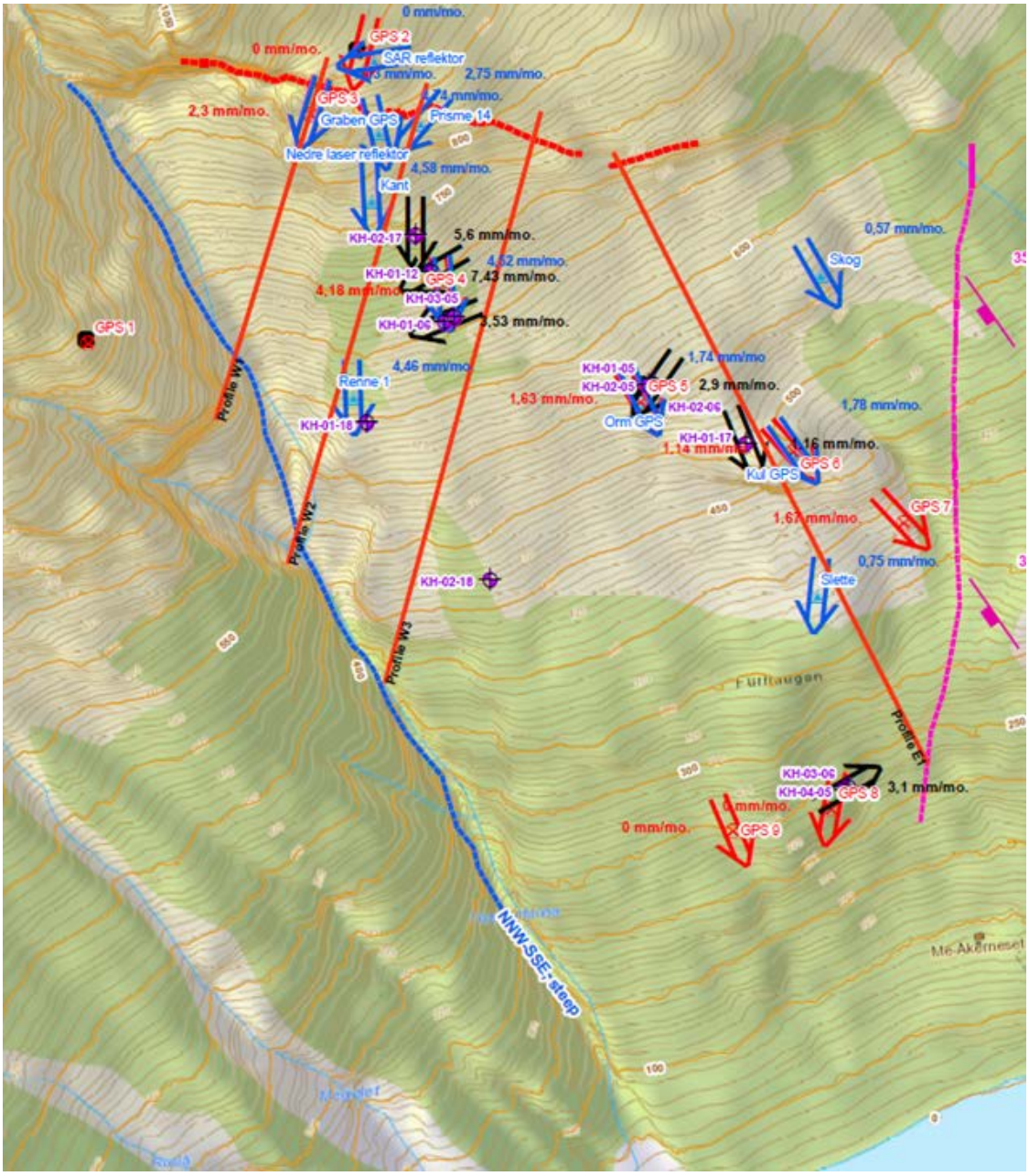

Figure 45 Map showing location of Profile W2 crossing borehole KH-02-17 and KH-01-18.

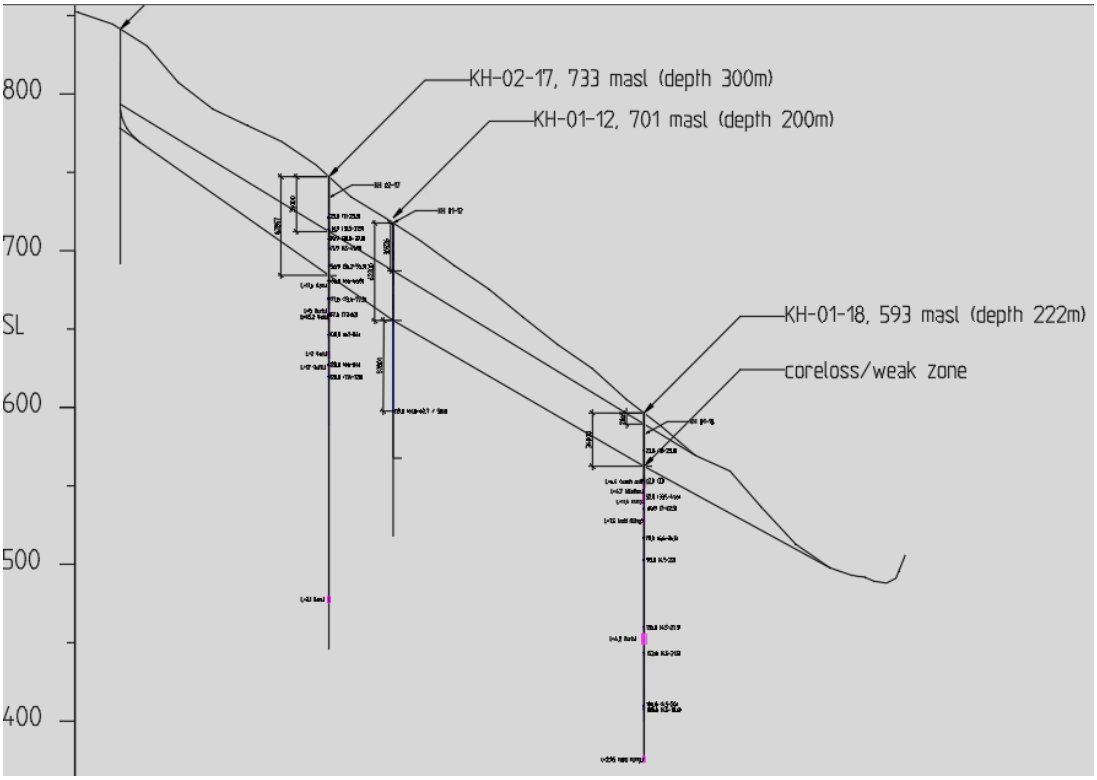

Figure 46 Sketch of profile W2 – with approximate location of two sliding planes, See a bigger version of figure in Appendix D.

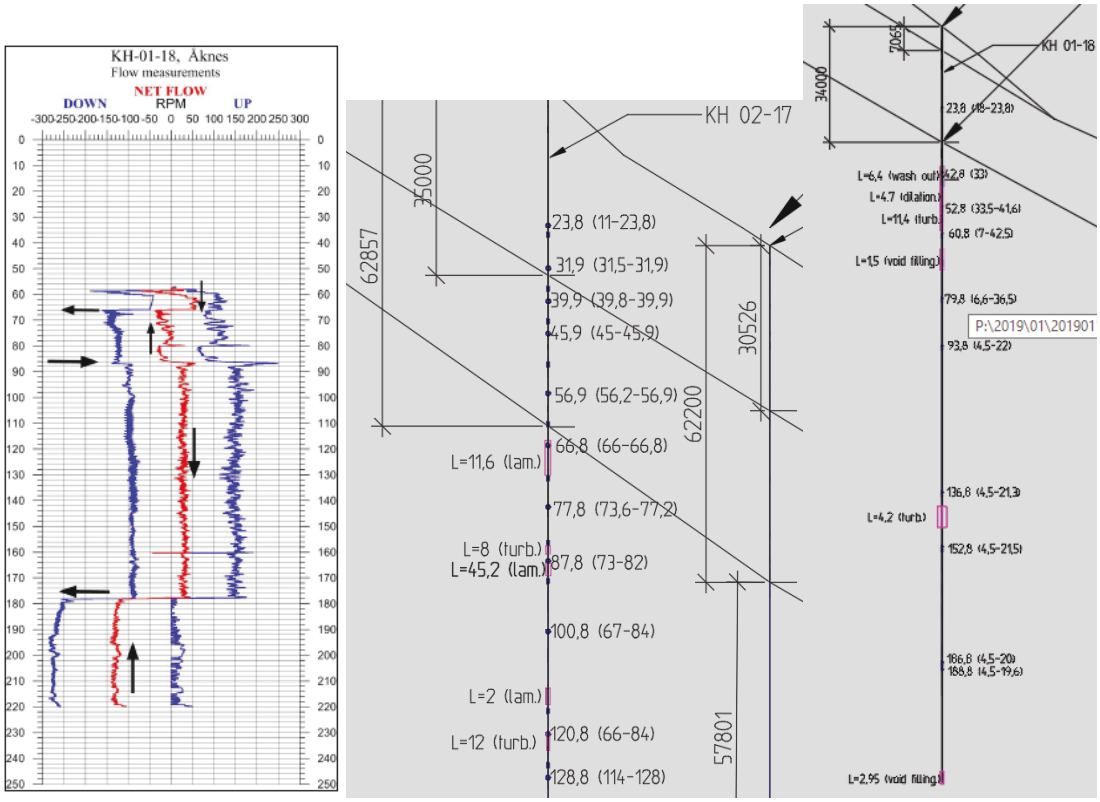

Figure 47 Left: Flowmeter measurements (autumn 2018) in Borehole KH-01-2018 (NGU, 2018). To the right: details from the sketch of profile W2 – with approximate location of two sliding planes and positioning of packers, piezometers and Lugeon-measurements (in magenta) (see also Appendix D).

5.2 Water pressure on main sliding plane

Three different approaches have been used in this report to interpret the water pressure on the sliding planes, and to some extent how it has varied over a short period of time at the location of the boreholes:

- With direct measurements at the sliding plane (if available) in the sectioned boreholes
- Measured directly from open boreholes
- Calculated based on interpretation of the water pressure measurements in the sectioned boreholes (Chapter 3.1)

All the three different methods should lead to consistent results. In addition, the water head measurements show seasonal fluctuations. To include seasonal high and low water head we selected three different dates; first of December 2019, March 2020 and September 2020.

In start of December 2019 the water head was registered to be higher than for later dates. Hence, the results from December 2019 presented in Table 14 may be wrong due to irregularities in the first months after filling the packers. It seems like the measurements

are stabilising from February 2020. The open boreholes do not show visible changes (some decimetre increase) in the water table level upon the three dates picked. Therefore, the results from March and September 2020 seems to give a good estimation for the water table and will be implemented in the hydromechanical stability analysis of Åknes.

Table 14 presents the water table calculated based on interpretation of the measurements in the sectioned boreholes, as described in Chapter 3.1. This method likewise as the direct measurements show that groundwater stands on the sliding plane for borehole KH-01-2018. The assessment based on the analysis done Chapter 3.1 shows slightly higher water head on the sliding plane compared to the direct measurements.

However, ground water head calculations as presented in Table 14 is more reliable since it considers the water head changes along the entire length of a borehole. Therefore, the data in Table 14 might be close to real conditions.

From Table 14 it can be seen that the groundwater table stands just below the sliding plane in the west flank, or 4 to 7 meters below. Only in borehole KH-01-2018 the water table is interpreted to stand above the sliding plane, 4 m above.

Table 14. Groundwater head obtained on the sliding planes with interpretation of the piezometer data from different packer modules.

Bore-hole	Water table on 01/12/ 2019 (mbgl)	Water table on 01/03/2020 and 30/09/2020 (mbgl)	Depth of major sliding plane (mbgl)	Water head on SP 01/12/2019 (m)	Water head on SP 01/03/2020 (m)	Comment
KH-01-17	-	-	35.5	-	-	No consistent data
KH-02-17	73.00	80.0	70.00	0	0	
KH-01-18	19*	30.0	34.0	4.0	4.0	*Errors in measurem. December 2019.
KH-02-18	31.70	16.0	15.0	0	0	Water table in lower parts of the borehole

* Due to errors in the measurements as explained in Chapter 3.1, it is assumed that the water head is at 30 mbgl

The water pressure on the main sliding plane is one of the most important input parameters in a stability analysis. Therefore, the main sliding plane (lowest part of the section with displacement) is studied in more detail. When studying the piezometer measurements in both open and sectioned boreholes over time, the variation in water head (water table) and water pressure on main sliding plane are presented in Table 15.

The data is based on measurements in the piezometer closest to the main sliding plane and is therefore not the same as presented in Table 14.

Table 15. Overview of registered variation of water pressure on main sliding plane (or close to the main sliding plane, as identified in Report 20180662-05-R).

Borehole number	No. of piezo-meters	Water table* (mbgl)	Depth to main sliding plane (mbgl)	Water pressure on main sliding plane (m)
BH-01-06	1	55-60	49-50	0
BH-02-06	1	43,7-45,7	33	0
BH-03-06	1	41,5-44	24	0
BH-01-12	1	~62	62	0-2,7
BH-01-17	9	~35,3	35,5	0-0,5
BH-02-17	11	~66,5	70	2,3-3,5
BH-01-18	10	~33,4	34	0,4-1,4
BH-02-18	12	~18	15	0

*Water table close to the main sliding plane.

5.3 Concluding remarks

Based on the analysis done and discussions of the results, the main conclusions are:

- Changes in water head on the sliding plane are small, only small peaks over short periods are monitored. For BH-02-17 up-to 3-4 meters water pressure on the sliding plane has been monitored over short periods. For most of the boreholes the water table is several meters below the main sliding plane.
- The hydraulic communication in the slope is high. It seems like the hydraulic system is fed from a bigger area, not only the backscarp.

NGI has used the presented results as input parameter in the coupled hydro-mechanical stability analysis UDEC model (20180662-07-R), and the monitored water head are used to calibrate the model for profile W2 on the western flank. The model is calibrated with the available boreholes with DMS and piezometers along this cross-section.

The next steps will be to do sensitivity analysis to find how the model will respond to different input parameters. When the model is calibrated and found as correct as possible, different scenarios will be modelled, trying to increase the water pressure on the main sliding plane (worst case scenario: 100 years precipitation event), and on the other hand find out how the model will respond to lowering the water pressure with drainage. Results from the modelling is summarized in Report 20180662-07-R.

6 References

ACUNA, J., MALMBERG, M., ACUNA, F. AND STOKUCA, M. 2018. *Åknes – Heat tracing tests KH-01-17 and KH 02-17*, Report 22301-1.1

AQUIFER TEST 2020. Software downloaded from site: https://www.rshydro.co.uk/groundwater-monitoring-sampling-equipment/groundwater-software/aquifertest-pro/, [sited 20.05.2020]

ALBRIGHT, S.C, WINSTON, W. AND ZAPPE, C.J. 2003: *Data Analysis & Decision Making, with Microsoft Excel*, Second Edition, 975 pp.

BEALE, G. & READ, J. 2013. *Guidelines for evaluating water in pit slope stability,* Australia and New Zealand, CSIRO Publishing.

COOPER, H.H and JAKOB, C.E. 1946. *A generalized graphical method for evaluating formation constants and summarizing wellfield history.* Transactions of the American Geophysical Union, 27, pp. 526-534

CSG Geotechnical monitoring, 2020: http://www.csgsrl.eu/eng/index.html. [cited 06.04.2020]

DIETRICH, P., HELMIG, R., SAUTER, M., HØTZL, H., KØNGETER, J., & TEUTSCH, G. 2005 *Flow and Transport in Fractured Porous Media.* Springer

FELL, R., MACGREGOR, P., STAPLEDON, D., BELL, G. & FOSTER, M. 2015. *Geotechnical Engineering of Dams, 2nd Edition,* London, CRC Press.

FREI, C. 2008 *Groundwater Flow at the Åknes rockslide site (Norway).* Master thesis at ETH Zürich

GANERØD, G.V., GRØNENG, G., RØNNING, J.S., DALSEGG, E., ELVEBAKK, H., TØNNESEN, J.F., KVELDSVIK, V., EIKEN, T., BLIKRA, L.H. AND BRAATHEN, A. 2008: "Geological model of Åknes rock slide, western Norway" Engineering Geology (102) 2008 p. 1-18

GENUCHTEN, M. TH. VAN. 1980. *A Closed-form Equation for Predicting the Hydraulic Conductivity of Unsaturated Soils.* Soil Science Society of America Journal, Volume 44, Issue 5, 892 - 898

GRIMSTAD, E. 1989. *Stabilitetsvurdering omkring Remnanae ved Åkernes i Stranda*. NGI report 85494-2

HOULSBY, A. 1976. Routine interpretation of the Lugeon water-test. *Quarterly Journal of Engineering Geology and Hydrogeology,* 9**,** 303-313.

JARSJÖ, J., PRIETO, C., AND DESTOUNI, G. 2017. *Estimation of characteristic relations for unsaturated flow through rock fractures in the Forsmark area.* Report SKB P-15-17, Swedish Nuclear Fuel and Waste Management Co.

LANGELAND, H.A. 2014. *Utvikling av revidert geologisk modell og stabilitetsanalyser for øvre deler av ustabil fjellside på Åknes.* Masteroppgave ved NTNU, 197 sider

LUGEON M., 1933. Barrage et Geologie. Dunod, Paris.

NELSON, R. A., 2001. *Geologic Analysis of Naturally Fractured Reservoirs*. Boston: Gulf Professional Publishing, 2nd edition.

NGI 2018. Data report core logging KH-01-2017. NGI report no.: 20180662-01-R

NGI 2019a. Data report core logging KH-02-2017. NGI report no.: 20180662-02-R

NGI 2019b. Data report core logging KH-01-2018. NGI report no.: 20180662-03-R

NGI 2019c. *Data report core logging KH-02-2018*. NGI report no.: 20180662-04-R

NGI 2019d. *Methodology and results from packer tests in 2017 and 2018 boreholes.* NGI Technical Note 20180662-01-TN revision no. 1 / 2020-03-27

NGI 2015. *Using the Q-system. Rock mass classification and support design*. May 2015.

NGU 2007. *Logging of drill cores from seven boreholes at Åknes, Stranda municipality, Møre og Romsdal County*, NGU Report 2007.020.

NGU 2018. *Borehullslogging Åknes, Stranda kommune, 2017-2018.* Report 2018.026

NS-EN 2012a. Geotekniske felt- og laboratorieundersøkelser. Hydraulisk prøving Del 3: Vanntapsmåling i berg. *Geotechnical investigation and testing Geohydraulic testing Part 3: Water pressure tests in rock (ISO 22282-3:2012).* Norsk Standard, EN ISO.

NS-EN 2012b. Geotekniske felt- og laboratorieundersøkelser. Hydraulisk prøving Del 2: Prøving av vannpermeabilitet I et borehull ved bruk av åpne systemer. *Geotechnical investigation and testing Geohydraulic testing Part 2: Water permeability tests in a borehole using open systems (ISO 22282-4:2012).* Norsk Standard, EN ISO.

ODA, M., 1986. *An equivalent continuum model for coupled stress and fluid flow analysis in jointed rock masses.* Water Resources Research, 22(13):1845–1856.

QUIÑONES-ROZO, C. 2010. *Lugeon test interpretation, revisited. Collaborative Management of Integrated Watersheds,* United States Society on Dams, 30th Annual Conference. Sacramento, California.

RINGSTAD S.R.S. 2019. The influence of structural discontinuities on the stability of the Åknes rockslide. M.Sc. Thesis, Oslo University.

SENA, C. 2019. *PowerPoint presentation from 28th November 2019.* Meeting in Oslo

TØNSET, L. 2019. *Verdien av kjerneborehull for økt forståelse av stabilitetsforhold ved Åknes skredområde.* Masteroppgave NTNU, 116 sider

WU, T. (2005). *Permeability prediction and drainage capillary pressure simulation in sandstone reservoirs.* PhD thesis, Texas A&M University.

Appendix A

PACKER TEST INTERPRETATION KH-02-2017,
KH-01-2018 AND KH-02-2018

Contents

A1 KH-02-2017
A2 KH-01-2018
A3 KH-02-2018

A1 KH-02-2017

Lugeon Test Summary - KH-02-2017

Project: Åknes

Number: 20180662

Client: NVE

Test Interval Top Bottom	Graphs	Result
66,500 m 73,500 m	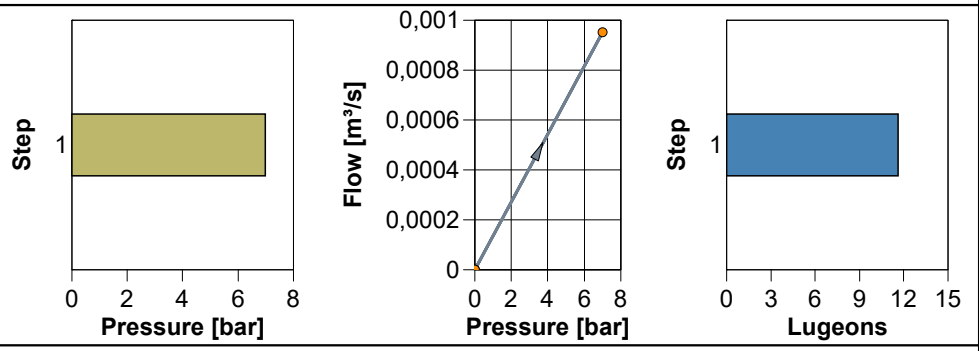	Laminar Lugeon: 11,633 Hydraulic Conductivity: 1,51E-6 m/s Hydraulic Conductivity: 1,51E-6 m/s
84,500 m 87,000 m	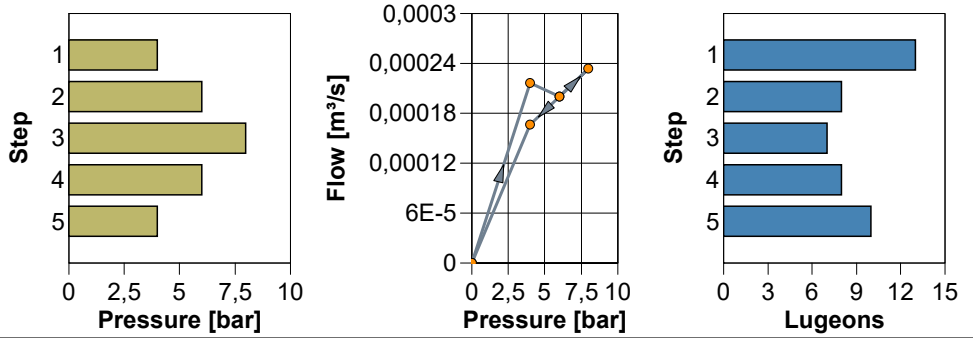	Turbulent Lugeon: 8,000 Hydraulic Conductivity: 8,23E-7 m/s Hydraulic Conductivity: 8,23E-7 m/s
88,200 m 90,500 m	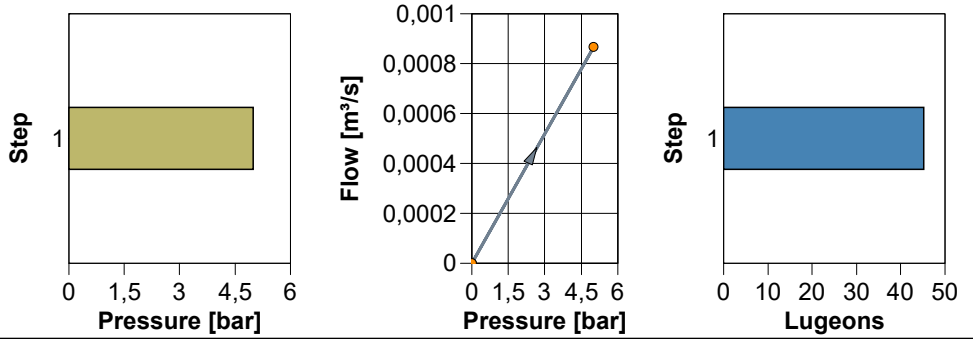	Laminar Lugeon: 45,219 Hydraulic Conductivity: 4,55E-6 m/s Hydraulic Conductivity: 4,55E-6 m/s
111,300 m 114,300 m	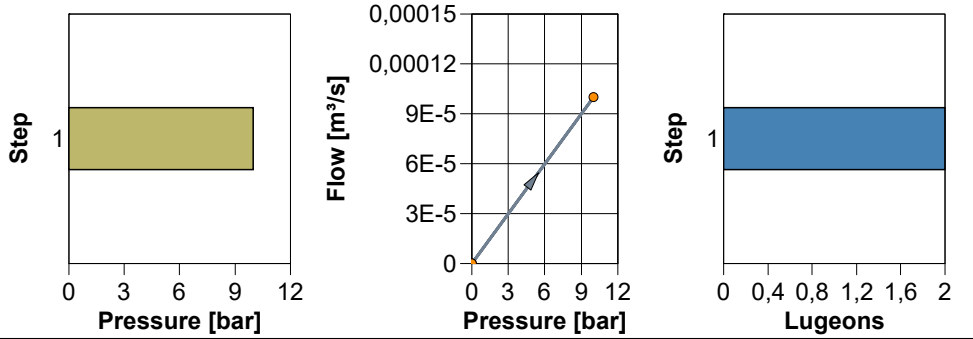	Laminar Lugeon: 2,000 Hydraulic Conductivity: 2,15E-7 m/s Hydraulic Conductivity: 2,15E-7 m/s

	Lugeon Test Summary - KH-02-2017
	Project: Åknes
	Number: 20180662
	Client: NVE

Test Interval Top Bottom	Graphs	Result
120,500 m 123,500 m	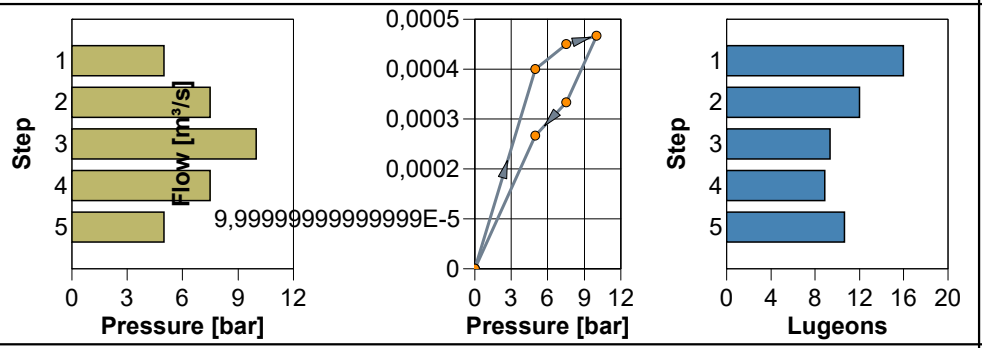	Turbulent Lugeon: 12,000 Hydraulic Conductivity: 1,29E-6 m/s Hydraulic Conductivity: 1,29E-6 m/s
268,000 m 271,500 m	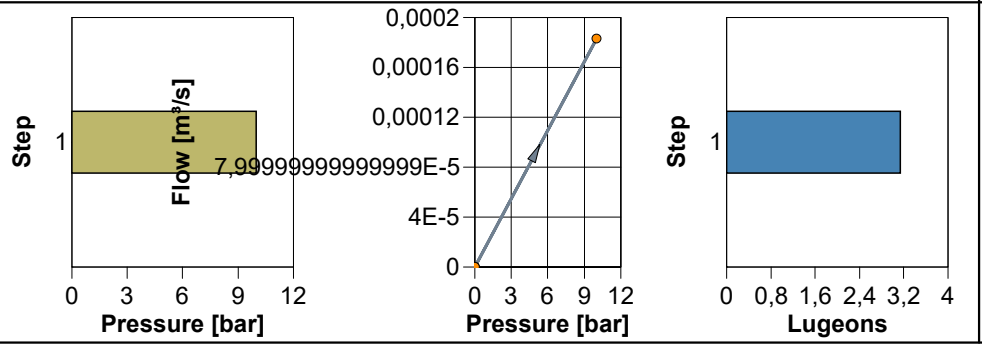	Laminar Lugeon: 3,14 Hydraulic Conductivity: 3,506238E-7 m/s Hydraulic Conductivity: 3,51E-7 m/s

	Lugeon Test Analysis Report
	Project: Åknes
	Number: 20180662
	Client: NVE

Location: Åknes	Lugeon Test: Lugeon Test 66,5-73,5	Tested bore: KH-02-2017
Test Conducted by: Geodrilling		Test Date: 25.10.2017
Analysis Performed by: HLa		Analysis Date: 20.02.2019
Lithology:		

Top of Test Interval: 66,500 m
Bottom of Test Interval: 73,500 m
Length of Test Interval: 7,000 m
Depth to Groundwater: 70,000 m
Radius of Test Section: 0,048 m

Step	Pressure [bar]	Flow Meter Readings [m³/s]	Average Flow Rate [m³/s]	Hydraulic Conductivity		
		1		[m/s]	[m/s]	Lugeon
1	7,0	0,000950	0,000950	$1,51 \times 10^{-6}$	$1,51 \times 10^{-6}$	11,633
			Average	$1,51 \times 10^{-6}$	$1,51 \times 10^{-6}$	11,633

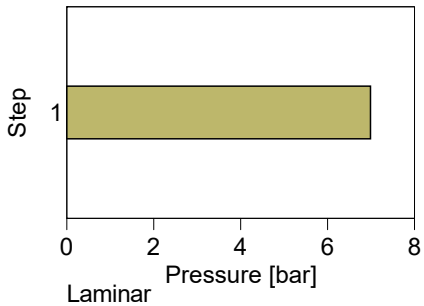

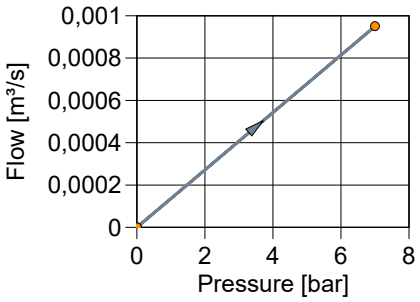

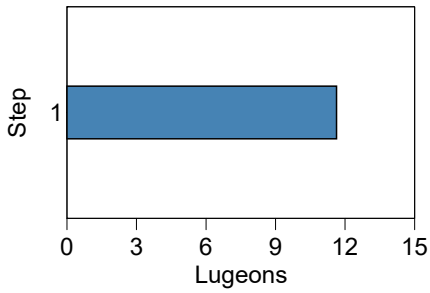

Laminar
Lugeon: 11,633
Hydraulic Conductivity: 1,51E-6 m/s
Hydraulic Conductivity: 1,51E-6 m/s

	Lugeon Test Analysis Report
	Project: Åknes
	Number: 20180662
	Client: NVE

Location: Åknes	Lugeon Test: Lugeon Test 84,5-87,0	Tested bore: KH-02-2017
Test Conducted by: Geodrilling		Test Date: 27.10.2017
Analysis Performed by: HLa		Analysis Date: 20.02.2019
Lithology:		

Top of Test Interval: 84,500 m
Bottom of Test Interval: 87,000 m
Length of Test Interval: 2,500 m
Depth to Groundwater: 78,500 m
Radius of Test Section: 0,048 m

Step	Pressure [bar]	Flow Meter Readings [m³/s]	Average Flow Rate [m³/s]	Hydraulic Conductivity		
		1		[m/s]	[m/s]	Lugeon
1	4,0	0,000217	0,000217	$1{,}34 \times 10^{-6}$	$1{,}34 \times 10^{-6}$	13,000
2	6,0	0,000200	0,000200	$8{,}23 \times 10^{-7}$	$8{,}23 \times 10^{-7}$	8,000
3	8,0	0,000233	0,000233	$7{,}20 \times 10^{-7}$	$7{,}20 \times 10^{-7}$	7,000
4	6,0	0,000200	0,000200	$8{,}23 \times 10^{-7}$	$8{,}23 \times 10^{-7}$	8,000
5	4,0	0,000167	0,000167	$1{,}03 \times 10^{-6}$	$1{,}03 \times 10^{-6}$	10,000
			Average	$9{,}46 \times 10^{-7}$	$9{,}46 \times 10^{-7}$	9,200

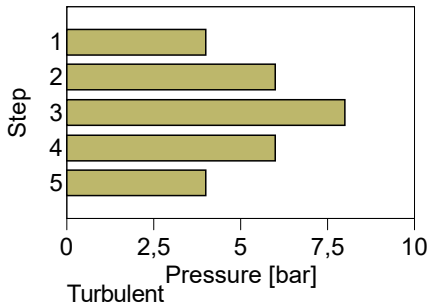

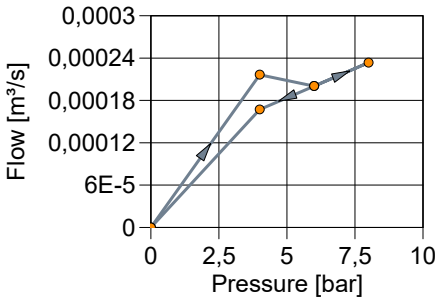

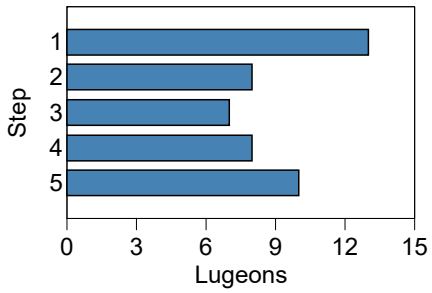

Turbulent
Lugeon: 8,000
Hydraulic Conductivity: 8,23E-7 m/s
Hydraulic Conductivity: 8,23E-7 m/s

	Lugeon Test Analysis Report
	Project: Åknes
	Number: 20180662
	Client: NVE

Location: Åknes	Lugeon Test: Lugeon Test 88,2-90,5	Tested bore: KH-02-2017
Test Conducted by: Geodrilling		Test Date: 28.10.2017
Analysis Performed by: HLa		Analysis Date: 20.02.2019
Lithology:		

Top of Test Interval: 88,200 m
Bottom of Test Interval: 90,500 m
Length of Test Interval: 2,300 m
Depth to Groundwater: 77,000 m
Radius of Test Section: 0,048 m

Step	Pressure [bar]	Flow Meter Readings [m³/s]	Average Flow Rate [m³/s]	Hydraulic Conductivity		
		1		[m/s]	[m/s]	Lugeon
1	5,0	0,000867	0,000867	$4,55 \times 10^{-6}$	$4,55 \times 10^{-6}$	45,219
			Average	$4,55 \times 10^{-6}$	$4,55 \times 10^{-6}$	45,219

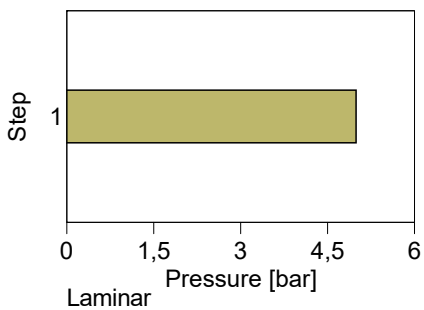

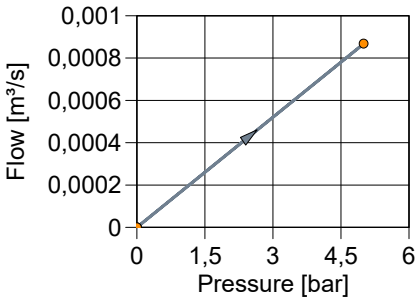

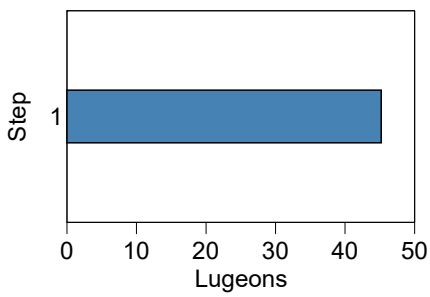

Laminar
Lugeon: 45,219
Hydraulic Conductivity: 4,55E-6 m/s
Hydraulic Conductivity: 4,55E-6 m/s

	Lugeon Test Analysis Report
	Project: Åknes
	Number: 20180662
	Client: NVE

Location: Åknes	Lugeon Test: Lugeon Test 111,3-114,3	Tested bore: KH-02-2017
Test Conducted by: Geodrilling		Test Date: 29.10.2017
Analysis Performed by: HLa		Analysis Date: 20.02.2019
Lithology:		

Top of Test Interval: 111,300 m
Bottom of Test Interval: 114,300 m
Length of Test Interval: 3,000 m
Depth to Groundwater: 77,000 m
Radius of Test Section: 0,048 m

Step	Pressure [bar]	Flow Meter Readings [m³/s]	Average Flow Rate [m³/s]	Hydraulic Conductivity		
		1		[m/s]	[m/s]	Lugeon
1	10,0	0,000100	0,000100	$2{,}15 \times 10^{-7}$	$2{,}15 \times 10^{-7}$	2,000
			Average	$2{,}15 \times 10^{-7}$	$2{,}15 \times 10^{-7}$	2,000

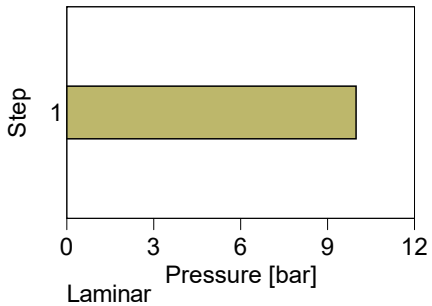

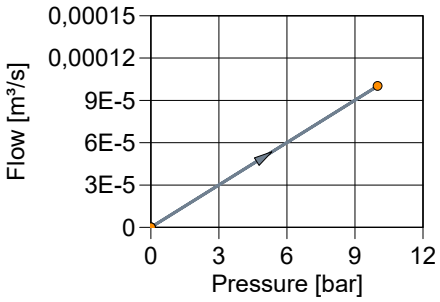

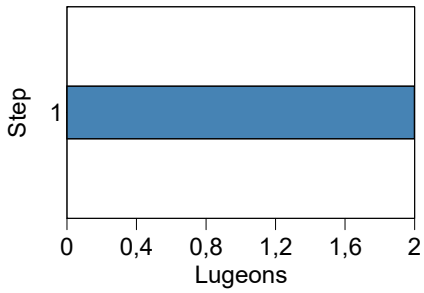

Laminar
Lugeon: 2,000
Hydraulic Conductivity: 2,15E-7 m/s
Hydraulic Conductivity: 2,15E-7 m/s

	Lugeon Test Analysis Report
	Project: Åknes
	Number: 20180662
	Client: NVE

Location: Åknes	Lugeon Test: Lugeon Test 120,5-123,5	Tested bore: KH-02-2017
Test Conducted by: Geodrilling		Test Date: 01.11.2017
Analysis Performed by: HLa		Analysis Date: 20.02.2019
Lithology:		

Top of Test Interval: 120,500 m
Bottom of Test Interval: 123,500 m
Length of Test Interval: 3,000 m
Depth to Groundwater: 77,600 m
Radius of Test Section: 0,048 m

Step	Pressure [bar]	Flow Meter Readings [m³/s]	Average Flow Rate [m³/s]	Hydraulic Conductivity		
		1		[m/s]	[m/s]	Lugeon
1	5,0	0,000400	0,000400	$1{,}72 \times 10^{-6}$	$1{,}72 \times 10^{-6}$	16,000
2	7,5	0,000450	0,000450	$1{,}29 \times 10^{-6}$	$1{,}29 \times 10^{-6}$	12,000
3	10,0	0,000467	0,000467	$1{,}00 \times 10^{-6}$	$1{,}00 \times 10^{-6}$	9,333
4	7,5	0,000333	0,000333	$9{,}56 \times 10^{-7}$	$9{,}56 \times 10^{-7}$	8,889
5	5,0	0,000267	0,000267	$1{,}15 \times 10^{-6}$	$1{,}15 \times 10^{-6}$	10,667
			Average	$1{,}22 \times 10^{-6}$	$1{,}22 \times 10^{-6}$	11,378

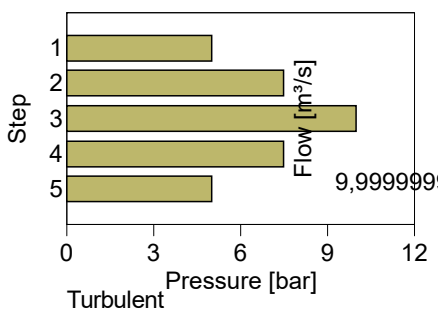

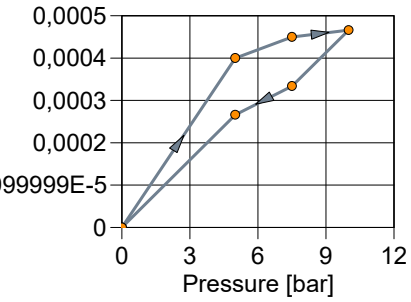

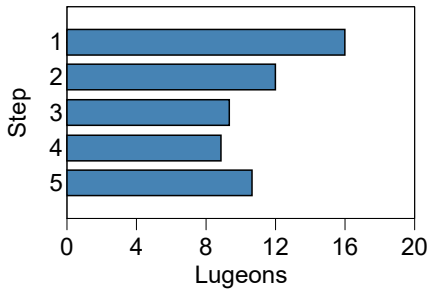

Turbulent
Lugeon: 12,000
Hydraulic Conductivity: 1,29E-6 m/s
Hydraulic Conductivity: 1,29E-6 m/s

	Lugeon Test Analysis Report
	Project: Åknes
	Number: 20180662
	Client: NVE

Location: Åknes	Lugeon Test: Lugeon Test 268-271,5	Tested bore: KH-02-2017
Test Conducted by: Geodrilling		Test Date: 02.11.2017
Analysis Performed by: HLa		Analysis Date: 20.02.2019
Lithology:		

Top of Test Interval: 268,000 m
Bottom of Test Interval: 271,500 m
Length of Test Interval: 3,500 m
Depth to Groundwater: 77,400 m
Radius of Test Section: 0,048 m

Step	Pressure [bar]	Flow Meter Readings [m³/s]	Average Flow Rate [m³/s]	Hydraulic Conductivity		
		1		[m/s]	[m/s]	Lugeon
1	10,0	0,0	0,0	$3{,}506238 \times 10^{-7}$	$3{,}51 \times 10^{-7}$	3,14
			Average	$3{,}506238 \times 10^{-7}$	$3{,}51 \times 10^{-7}$	3,14

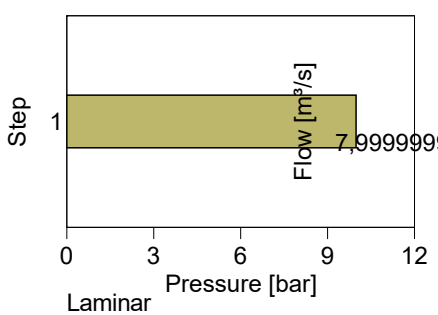

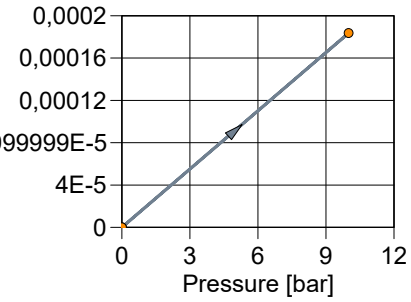

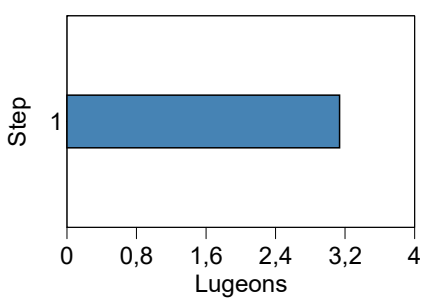

Laminar
Lugeon: 3,14
Hydraulic Conductivity: 3,506238E-7 m/s
Hydraulic Conductivity: 3,51E-7 m/s

A2 KH-01-2018

Lugeon Test Summary - KH-01-18

Project: Åknes

Number: 20180662

Client: NVE

Test Interval Top Bottom	Graphs	Result
41,000 m 47,000 m	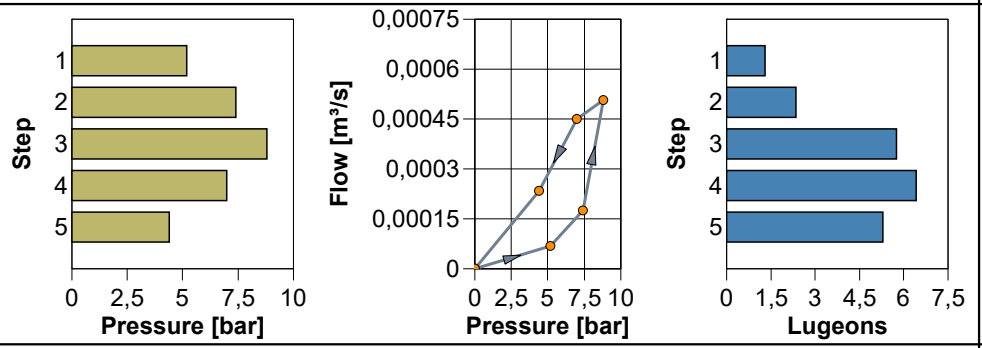	Wash out Lugeon: 6,43 Hydraulic Conductivity: 8,07E-7 m/s Hydraulic Conductivity: 8,07E-7 m/s
47,900 m 53,900 m	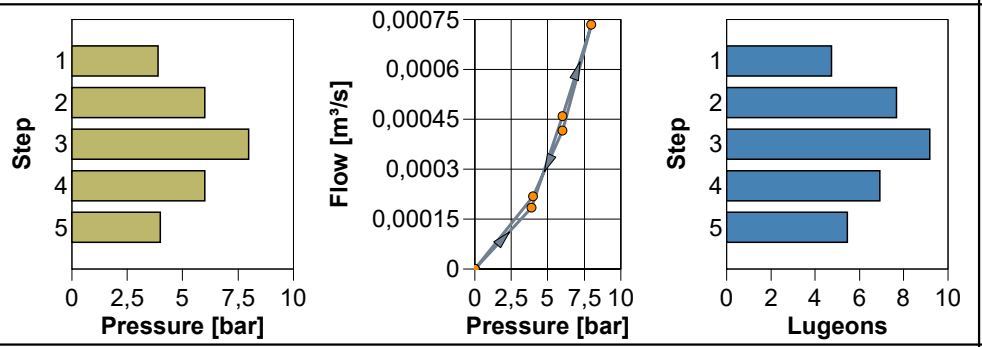	Dilation Lugeon: 4,74 Hydraulic Conductivity: 5,96E-7 m/s Hydraulic Conductivity: 5,96E-7 m/s
53,900 m 59,900 m	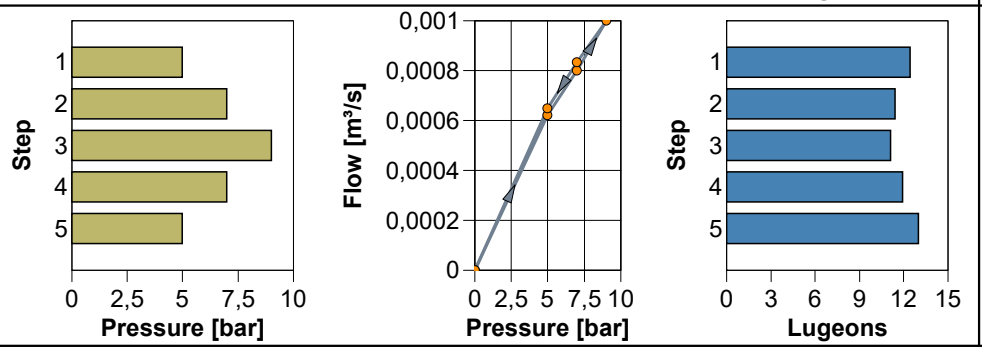	Turbulent Lugeon: 11,43 Hydraulic Conductivity: 1,44E-6 m/s Hydraulic Conductivity: 1,44E-6 m/s
65,500 m 71,500 m	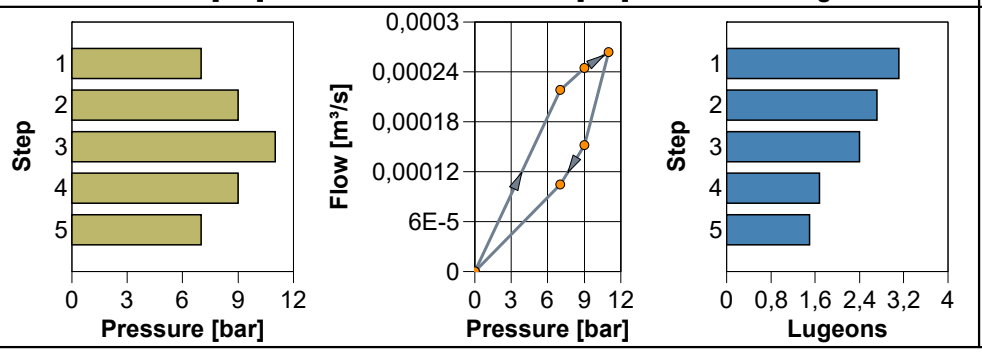	Void filling Lugeon: 1,50 Hydraulic Conductivity: 1,88E-7 m/s Hydraulic Conductivity: 1,88E-7 m/s

Lugeon Test Summary - KH-01-18

Project: Åknes

Number: 20180662

Client: NVE

Test Interval Top Bottom	Graphs	Result
72,500 m 78,500 m	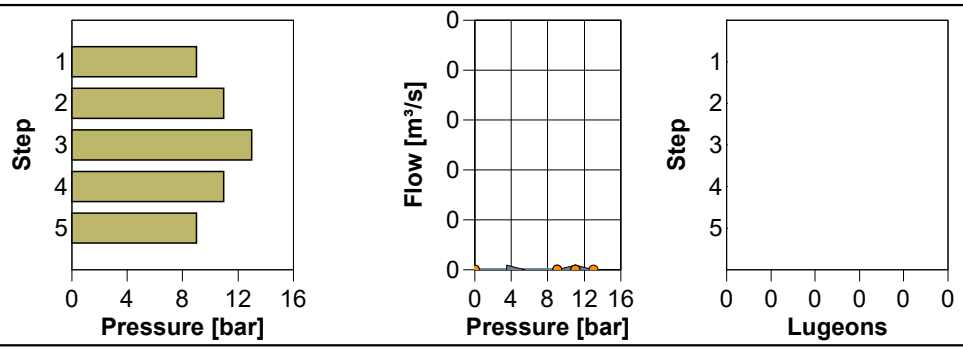	Laminar Lugeon: 0,000 Hydraulic Conductivity: 0,00E-1 m/s Hydraulic Conductivity: 0,00E-1 m/s
84,500 m 90,500 m	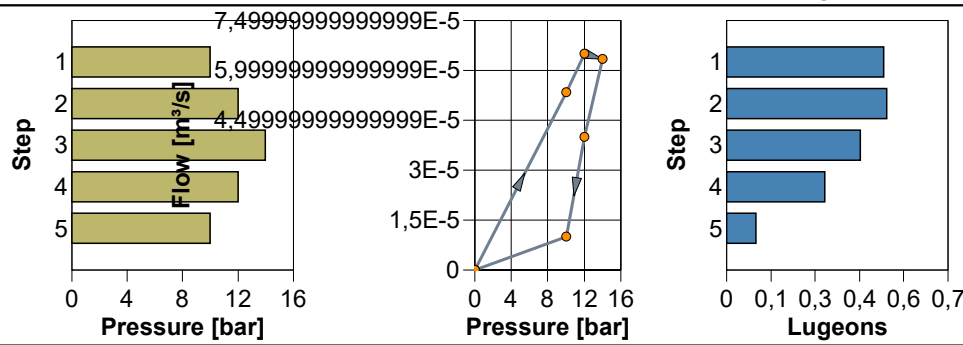	Void filling Lugeon: 0,10 Hydraulic Conductivity: 1,26E-8 m/s Hydraulic Conductivity: 1,26E-8 m/s
141,000 m 147,000 m	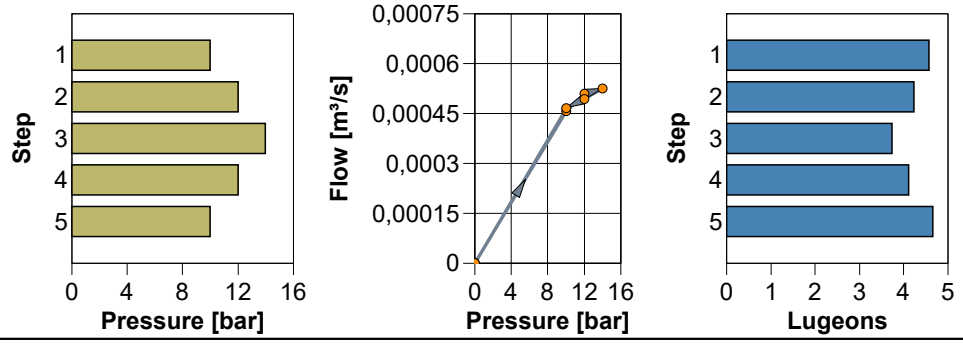	Turbulent Lugeon: 4,24 Hydraulic Conductivity: 5,32E-7 m/s Hydraulic Conductivity: 5,32E-7 m/s
158,900 m 164,900 m	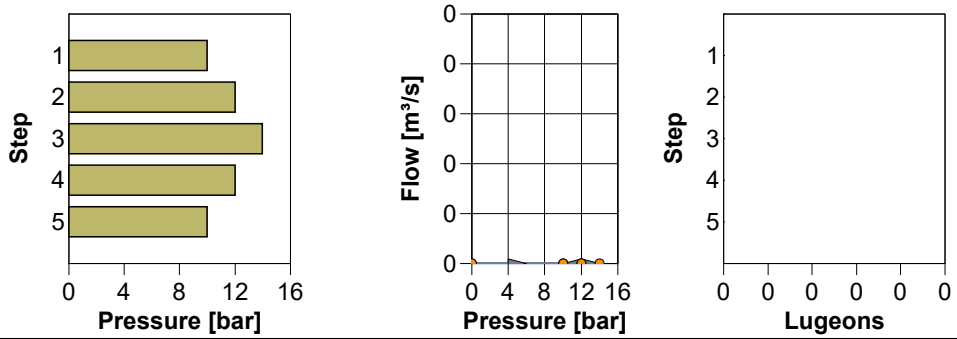	Laminar Lugeon: 0,000 Hydraulic Conductivity: 0,00E-1 m/s Hydraulic Conductivity: 0,00E-1 m/s

Lugeon Test Summary - KH-01-18

Project: Åknes

Number: 20180662

Client: NVE

Test Interval Top Bottom	Graphs	Result
164,800 m 170,800 m	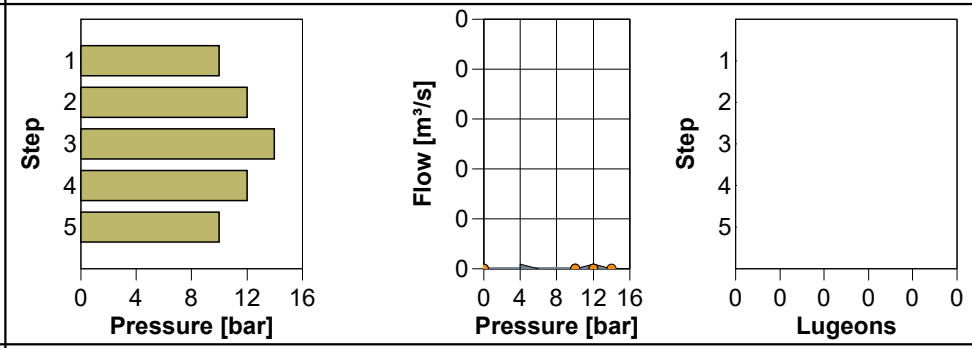	Laminar Lugeon: 0,000 Hydraulic Conductivity: 0,00E-1 m/s Hydraulic Conductivity: 0,00E-1 m/s
170,800 m 176,800 m	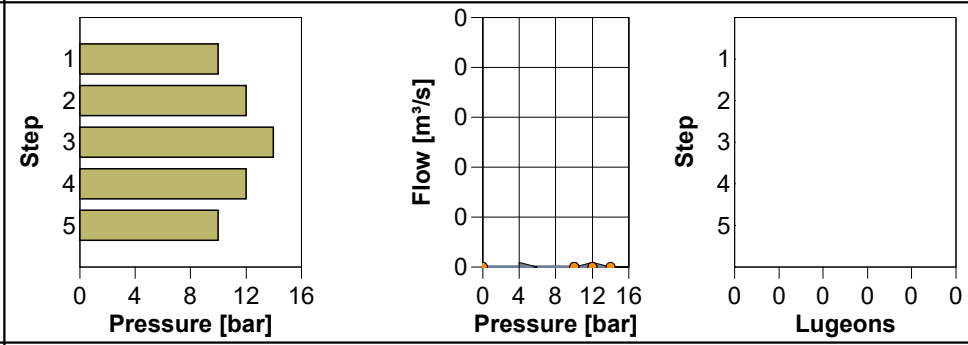	Laminar Lugeon: 0,000 Hydraulic Conductivity: 0,00E-1 m/s Hydraulic Conductivity: 0,00E-1 m/s
176,800 m 182,900 m	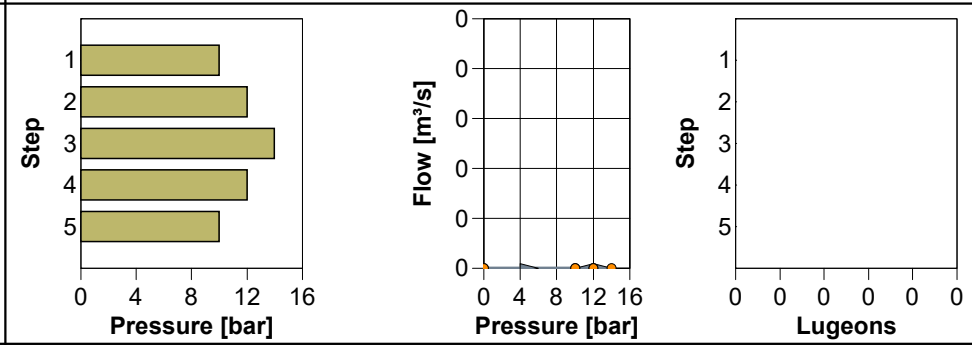	Laminar Lugeon: 0,000 Hydraulic Conductivity: 0,00E-1 m/s Hydraulic Conductivity: 0,00E-1 m/s
182,900 m 188,900 m	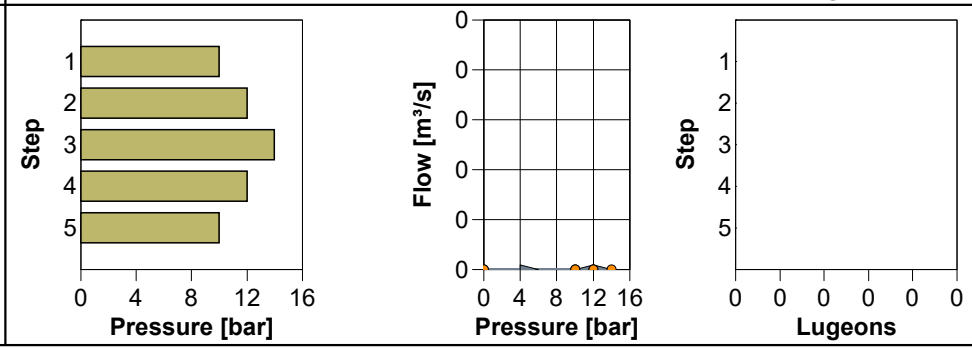	Laminar Lugeon: 0,000 Hydraulic Conductivity: 0,00E-1 m/s Hydraulic Conductivity: 0,00E-1 m/s

Lugeon Test Summary - KH-01-18

Project: Åknes

Number: 20180662

Client: NVE

Test Interval Top Bottom	Graphs	Result
188,900 m 194,900 m	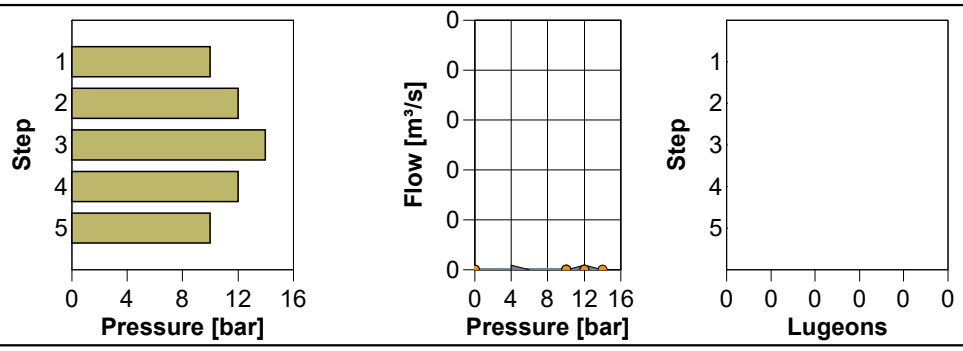	Laminar Lugeon: 0,000 Hydraulic Conductivity: 0,00E-1 m/s Hydraulic Conductivity: 0,00E-1 m/s
194,900 m 200,900 m	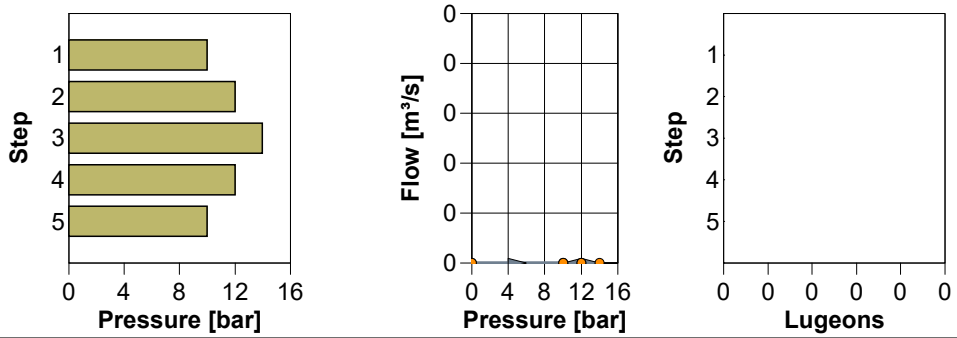	Laminar Lugeon: 0,000 Hydraulic Conductivity: 0,00E-1 m/s Hydraulic Conductivity: 0,00E-1 m/s
200,900 m 206,900 m	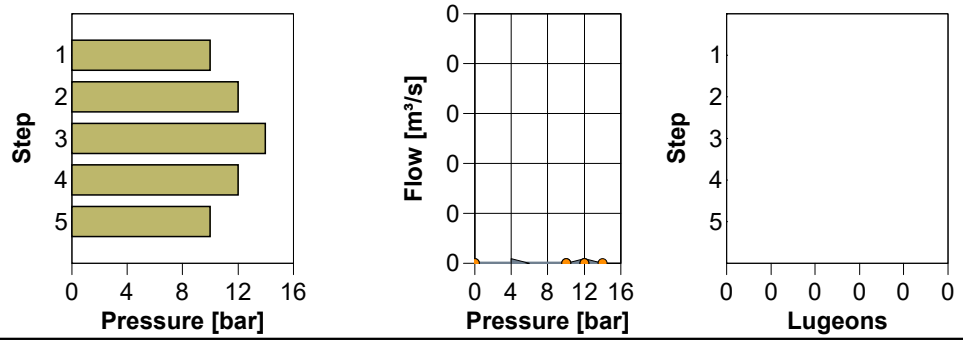	Laminar Lugeon: 0,000 Hydraulic Conductivity: 0,00E-1 m/s Hydraulic Conductivity: 0,00E-1 m/s
206,900 m 212,900 m	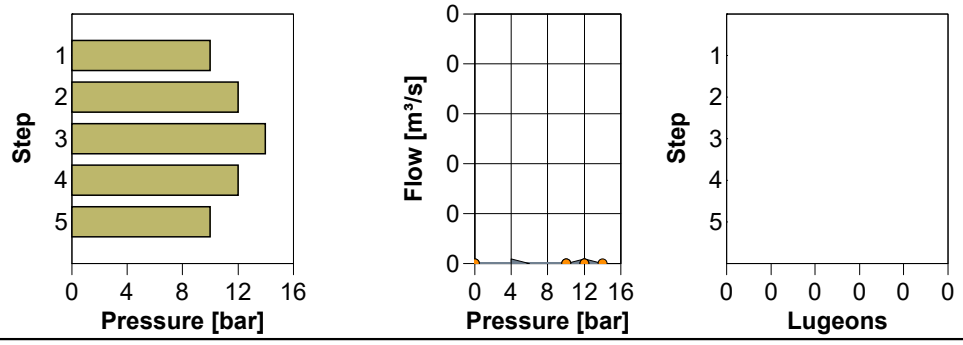	Laminar Lugeon: 0,000 Hydraulic Conductivity: 0,00E-1 m/s Hydraulic Conductivity: 0,00E-1 m/s

	Lugeon Test Analysis Report
	Project: Åknes
	Number: 20180662
	Client: NVE

Location: KH-01-2018	Lugeon Test: Lugeon Test 41,9-47,9	Tested bore: KH-01-18
Test Conducted by: Geodrilling		Test Date: 11.08.2018
Analysis Performed by: HLa		Analysis Date: 18.02.2019
Lithology:		

Top of Test Interval: 41,000 m
Bottom of Test Interval: 47,000 m
Length of Test Interval: 6,000 m
Depth to Groundwater: 5,300 m
Radius of Test Section: 0,048 m

Step	Pressure [bar]	Flow Meter Readings [m³/s]	Average Flow Rate [m³/s]	Hydraulic Conductivity		
		1		[m/s]	[m/s]	Lugeon
1	5,2	0,000068	0,000068	$1,65 \times 10^{-7}$	$1,65 \times 10^{-7}$	1,31
2	7,4	0,000175	0,000175	$2,97 \times 10^{-7}$	$2,97 \times 10^{-7}$	2,36
3	8,8	0,000507	0,000507	$7,24 \times 10^{-7}$	$7,24 \times 10^{-7}$	5,76
4	7,0	0,000450	0,000450	$8,07 \times 10^{-7}$	$8,07 \times 10^{-7}$	6,43
5	4,4	0,000233	0,000233	$6,66 \times 10^{-7}$	$6,66 \times 10^{-7}$	5,30
			Average	$5,32 \times 10^{-7}$	$5,32 \times 10^{-7}$	4,23

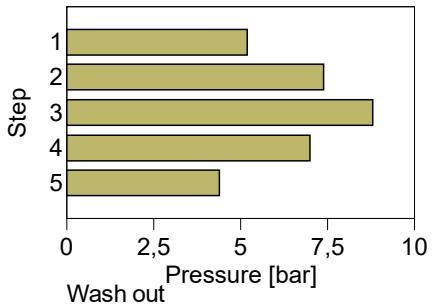

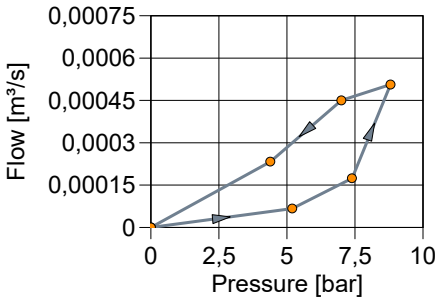

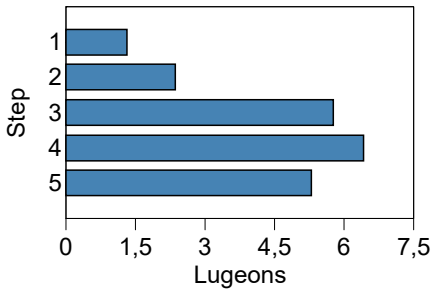

Wash out
Lugeon: 6,43
Hydraulic Conductivity: 8,07E-7 m/s
Hydraulic Conductivity: 8,07E-7 m/s

	Lugeon Test Analysis Report
	Project: Åknes
	Number: 20180662
	Client: NVE

Location: KH-01-2018	Lugeon Test: Lugeon Test 47,9-53,9	Tested bore: KH-01-18
Test Conducted by: Geodrilling		Test Date: 11.08.2018
Analysis Performed by: HLa		Analysis Date: 19.02.2019
Lithology:		

Top of Test Interval: 47,900 m
Bottom of Test Interval: 53,900 m
Length of Test Interval: 6,000 m
Depth to Groundwater: 5,300 m
Radius of Test Section: 0,048 m

Step	Pressure [bar]	Flow Meter Readings [m³/s]	Average Flow Rate [m³/s]	Hydraulic Conductivity		
		1		[m/s]	[m/s]	Lugeon
1	3,9	0,000185	0,000185	$5,96 \times 10^{-7}$	$5,96 \times 10^{-7}$	4,74
2	6,0	0,000460	0,000460	$9,63 \times 10^{-7}$	$9,63 \times 10^{-7}$	7,67
3	8,0	0,000733	0,000733	$1,15 \times 10^{-6}$	$1,15 \times 10^{-6}$	9,17
4	6,0	0,000417	0,000417	$8,72 \times 10^{-7}$	$8,72 \times 10^{-7}$	6,94
5	4,0	0,000218	0,000218	$6,86 \times 10^{-7}$	$6,86 \times 10^{-7}$	5,46
			Average	$8,54 \times 10^{-7}$	$8,54 \times 10^{-7}$	6,80

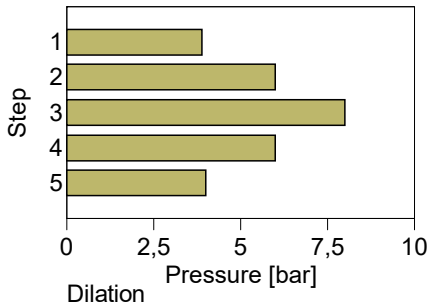

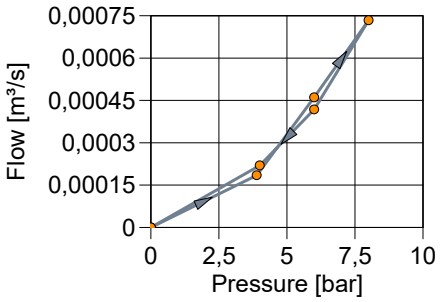

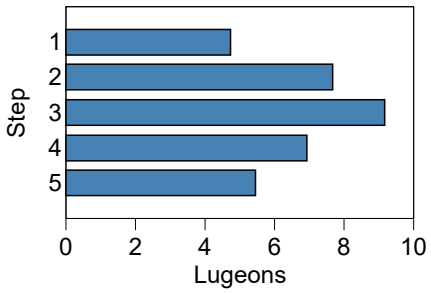

Dilation
Lugeon: 4,74
Hydraulic Conductivity: 5,96E-7 m/s
Hydraulic Conductivity: 5,96E-7 m/s

	Lugeon Test Analysis Report
	Project: Åknes
	Number: 20180662
	Client: NVE

Location: KH-01-2018	Lugeon Test: Lugeon Test 53,9-59,9	Tested bore: KH-01-18
Test Conducted by: Geodrilling		Test Date: 12.08.2018
Analysis Performed by: HLa		Analysis Date: 19.02.2019
Lithology:		

Top of Test Interval: 53,900 m
Bottom of Test Interval: 59,900 m
Length of Test Interval: 6,000 m
Depth to Groundwater: 39,600 m
Radius of Test Section: 0,048 m

Step	Pressure [bar]	Flow Meter Readings [m³/s]	Average Flow Rate [m³/s]	Hydraulic Conductivity		
		1		[m/s]	[m/s]	Lugeon
1	5,0	0,000622	0,000622	$1,56 \times 10^{-6}$	$1,56 \times 10^{-6}$	12,43
2	7,0	0,000800	0,000800	$1,44 \times 10^{-6}$	$1,44 \times 10^{-6}$	11,43
3	9,0	0,001000	0,001000	$1,40 \times 10^{-6}$	$1,40 \times 10^{-6}$	11,11
4	7,0	0,000833	0,000833	$1,50 \times 10^{-6}$	$1,50 \times 10^{-6}$	11,90
5	5,0	0,000650	0,000650	$1,63 \times 10^{-6}$	$1,63 \times 10^{-6}$	13,00
			Average	$1,50 \times 10^{-6}$	$1,50 \times 10^{-6}$	11,98

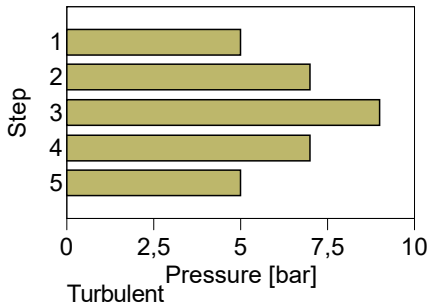

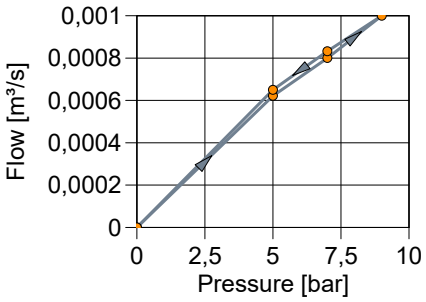

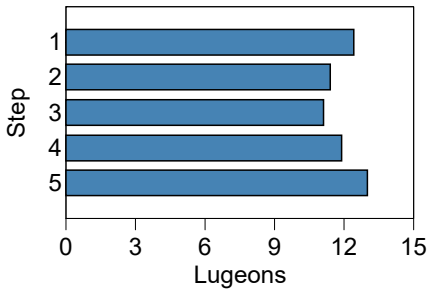

Turbulent
Lugeon: 11,43
Hydraulic Conductivity: 1,44E-6 m/s
Hydraulic Conductivity: 1,44E-6 m/s

	Lugeon Test Analysis Report
	Project: Åknes
	Number: 20180662
	Client: NVE

Location: KH-01-2018	Lugeon Test: Lugeon Test 65,5-71,5	Tested bore: KH-01-18
Test Conducted by: Geodrilling		Test Date: 30.08.2018
Analysis Performed by: HLa		Analysis Date: 19.02.2019
Lithology:		

Top of Test Interval: 65,500 m
Bottom of Test Interval: 71,500 m
Length of Test Interval: 6,000 m
Depth to Groundwater: 41,200 m
Radius of Test Section: 0,048 m

Step	Pressure [bar]	Flow Meter Readings [m³/s]	Average Flow Rate [m³/s]	Hydraulic Conductivity		
		1		[m/s]	[m/s]	Lugeon
1	7,0	0,000218	0,000218	$3,92 \times 10^{-7}$	$3,92 \times 10^{-7}$	3,12
2	9,0	0,000245	0,000245	$3,42 \times 10^{-7}$	$3,42 \times 10^{-7}$	2,72
3	11,0	0,000264	0,000264	$3,01 \times 10^{-7}$	$3,01 \times 10^{-7}$	2,40
4	9,0	0,000152	0,000152	$2,12 \times 10^{-7}$	$2,12 \times 10^{-7}$	1,69
5	7,0	0,000105	0,000105	$1,88 \times 10^{-7}$	$1,88 \times 10^{-7}$	1,50
			Average	$2,87 \times 10^{-7}$	$2,87 \times 10^{-7}$	2,29

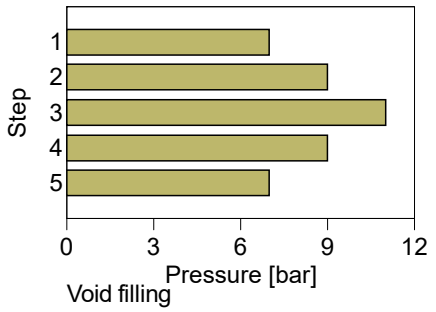

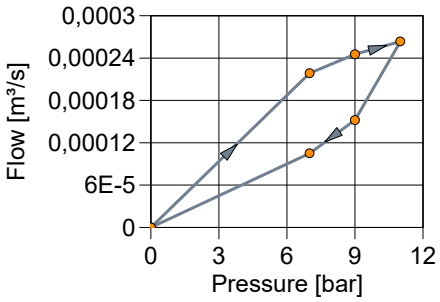

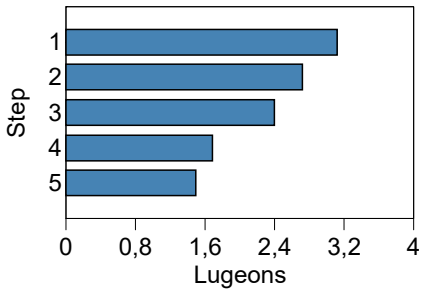

Void filling
Lugeon: 1,50
Hydraulic Conductivity: 1,88E-7 m/s
Hydraulic Conductivity: 1,88E-7 m/s

	Lugeon Test Analysis Report
	Project: Åknes
	Number: 20180662
	Client: NVE

Location: KH-01-2018	Lugeon Test: Lugeon Test 72,5-78,5	Tested bore: KH-01-18
Test Conducted by: Geodrilling		Test Date: 30.08.2018
Analysis Performed by: HLa		Analysis Date: 20.02.2019
Lithology:		

Top of Test Interval: 72,500 m
Bottom of Test Interval: 78,500 m
Length of Test Interval: 6,000 m
Depth to Groundwater: 41,200 m
Radius of Test Section: 0,048 m

Step	Pressure [bar]	Flow Meter Readings [m³/s]	Average Flow Rate [m³/s]	Hydraulic Conductivity		
		1		[m/s]	[m/s]	Lugeon
1	9,0	0,000000	0,000000	$0{,}00 \times 10^{-1}$	$0{,}00 \times 10^{-1}$	0,000
2	11,0	0,000000	0,000000	$0{,}00 \times 10^{-1}$	$0{,}00 \times 10^{-1}$	0,000
3	13,0	0,000000	0,000000	$0{,}00 \times 10^{-1}$	$0{,}00 \times 10^{-1}$	0,000
4	11,0	0,000000	0,000000	$0{,}00 \times 10^{-1}$	$0{,}00 \times 10^{-1}$	0,000
5	9,0	0,000000	0,000000	$0{,}00 \times 10^{-1}$	$0{,}00 \times 10^{-1}$	0,000
			Average	$0{,}00 \times 10^{-1}$	$0{,}00 \times 10^{-1}$	0,000

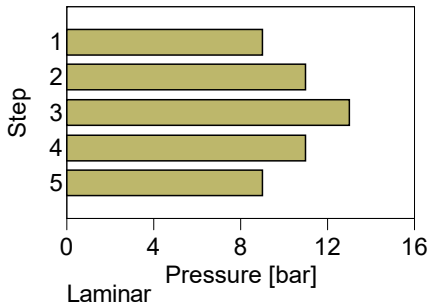

Laminar
Lugeon: 0,000
Hydraulic Conductivity: 0,00E-1 m/s
Hydraulic Conductivity: 0,00E-1 m/s

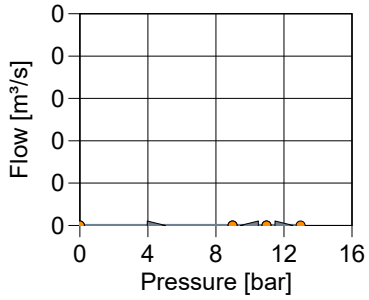

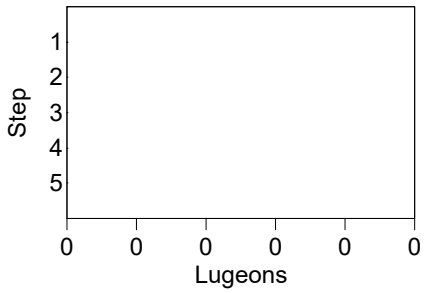

	Lugeon Test Analysis Report
	Project: Åknes
	Number: 20180662
	Client: NVE

Location: KH-01-2018	Lugeon Test: Lugeon Test 84,5-90,5	Tested bore: KH-01-18
Test Conducted by: Geodrilling		Test Date: 30.08.2018
Analysis Performed by: HLa		Analysis Date: 19.02.2019
Lithology:		

Top of Test Interval: 84,500 m
Bottom of Test Interval: 90,500 m
Length of Test Interval: 6,000 m
Depth to Groundwater: 41,200 m
Radius of Test Section: 0,048 m

Step	Pressure [bar]	Flow Meter Readings [m³/s]	Average Flow Rate [m³/s]	Hydraulic Conductivity		
		1		[m/s]	[m/s]	Lugeon
1	10,0	0,000053	0,000053	$6{,}70 \times 10^{-8}$	$6{,}70 \times 10^{-8}$	0,53
2	12,0	0,000065	0,000065	$6{,}80 \times 10^{-8}$	$6{,}80 \times 10^{-8}$	0,54
3	14,0	0,000063	0,000063	$5{,}68 \times 10^{-8}$	$5{,}68 \times 10^{-8}$	0,45
4	12,0	0,000040	0,000040	$4{,}19 \times 10^{-8}$	$4{,}19 \times 10^{-8}$	0,33
5	10,0	0,000010	0,000010	$1{,}26 \times 10^{-8}$	$1{,}26 \times 10^{-8}$	0,10
			Average	$4{,}93 \times 10^{-8}$	$4{,}93 \times 10^{-8}$	0,39

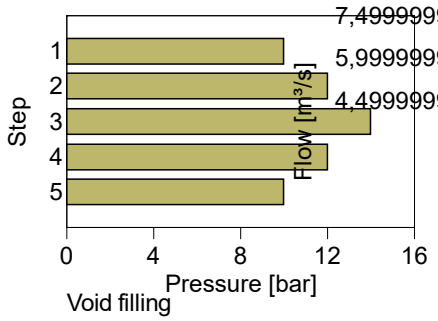

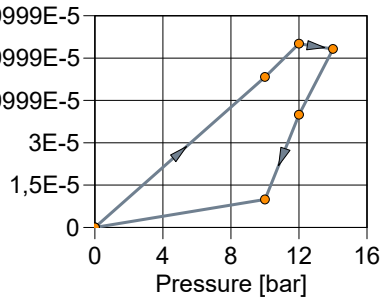

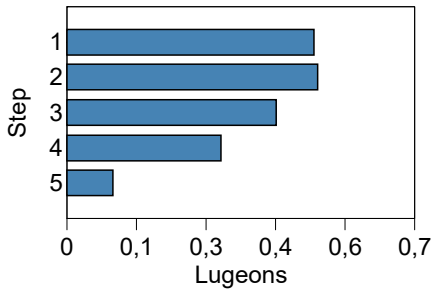

Void filling
Lugeon: 0,10
Hydraulic Conductivity: 1,26E-8 m/s
Hydraulic Conductivity: 1,26E-8 m/s

	Lugeon Test Analysis Report
	Project: Åknes
	Number: 20180662
	Client: NVE

Location: KH-01-2018	Lugeon Test: Lugeon Test 141-147	Tested bore: KH-01-18
Test Conducted by: Geodrilling		Test Date: 30.08.2018
Analysis Performed by: HLa		Analysis Date: 19.02.2019
Lithology:		

Top of Test Interval: 141,000 m
Bottom of Test Interval: 147,000 m
Length of Test Interval: 6,000 m
Depth to Groundwater: 41,200 m
Radius of Test Section: 0,048 m

Step	Pressure [bar]	Flow Meter Readings [m³/s]	Average Flow Rate [m³/s]	Hydraulic Conductivity		
		1		[m/s]	[m/s]	Lugeon
1	10,0	0,000457	0,000457	$5{,}74 \times 10^{-7}$	$5{,}74 \times 10^{-7}$	4,57
2	12,0	0,000508	0,000508	$5{,}32 \times 10^{-7}$	$5{,}32 \times 10^{-7}$	4,24
3	14,0	0,000524	0,000524	$4{,}70 \times 10^{-7}$	$4{,}70 \times 10^{-7}$	3,74
4	12,0	0,000493	0,000493	$5{,}16 \times 10^{-7}$	$5{,}16 \times 10^{-7}$	4,11
5	10,0	0,000467	0,000467	$5{,}86 \times 10^{-7}$	$5{,}86 \times 10^{-7}$	4,67
			Average	$5{,}36 \times 10^{-7}$	$5{,}36 \times 10^{-7}$	4,26

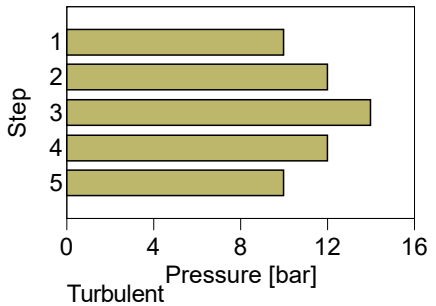

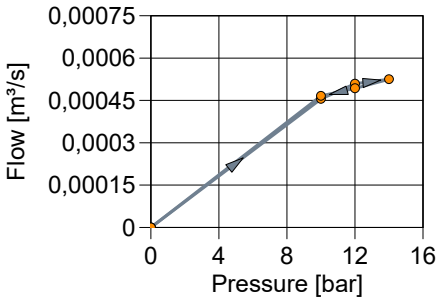

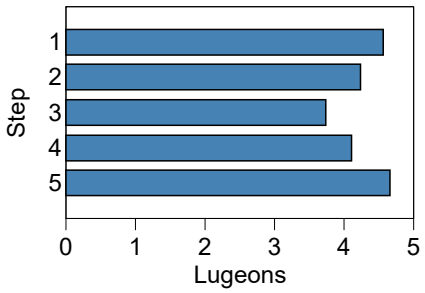

Turbulent
Lugeon: 4,24
Hydraulic Conductivity: 5,32E-7 m/s
Hydraulic Conductivity: 5,32E-7 m/s

	Lugeon Test Analysis Report
	Project: Åknes
	Number: 20180662
	Client: NVE

Location: KH-01-2018	Lugeon Test: Lugeon Test 158,9-164,9	Tested bore: KH-01-18
Test Conducted by: Geodrilling		Test Date: 21.08.2018
Analysis Performed by: HLa		Analysis Date: 20.02.2019
Lithology:		

Top of Test Interval: 158,900 m
Bottom of Test Interval: 164,900 m
Length of Test Interval: 6,000 m
Depth to Groundwater: 65,700 m
Radius of Test Section: 0,048 m

Step	Pressure [bar]	Flow Meter Readings [m³/s]	Average Flow Rate [m³/s]	Hydraulic Conductivity		
		1		[m/s]	[m/s]	Lugeon
1	10,0	0,000000	0,000000	$0{,}00 \times 10^{-1}$	$0{,}00 \times 10^{-1}$	0,000
2	12,0	0,000000	0,000000	$0{,}00 \times 10^{-1}$	$0{,}00 \times 10^{-1}$	0,000
3	14,0	0,000000	0,000000	$0{,}00 \times 10^{-1}$	$0{,}00 \times 10^{-1}$	0,000
4	12,0	0,000000	0,000000	$0{,}00 \times 10^{-1}$	$0{,}00 \times 10^{-1}$	0,000
5	10,0	0,000000	0,000000	$0{,}00 \times 10^{-1}$	$0{,}00 \times 10^{-1}$	0,000
			Average	$0{,}00 \times 10^{-1}$	$0{,}00 \times 10^{-1}$	0,000

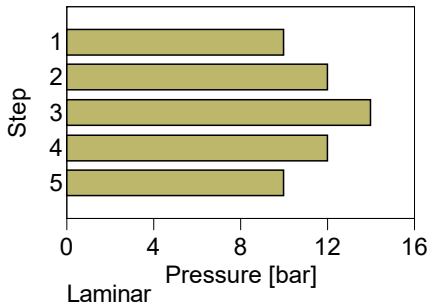

Laminar
Lugeon: 0,000
Hydraulic Conductivity: 0,00E-1 m/s
Hydraulic Conductivity: 0,00E-1 m/s

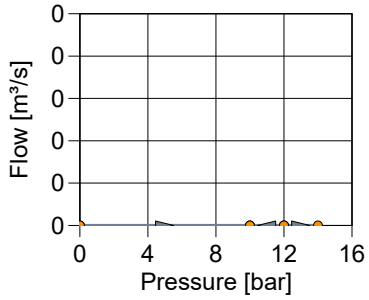

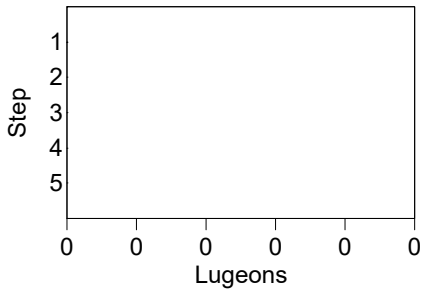

	Lugeon Test Analysis Report
	Project: Åknes
	Number: 20180662
	Client: NVE

Location: KH-01-2018	Lugeon Test: Lugeon Test 164,8-170,8	Tested bore: KH-01-18
Test Conducted by: Geodrilling		Test Date: 22.08.2018
Analysis Performed by: HLa		Analysis Date: 20.02.2019
Lithology:		

Top of Test Interval: 164,800 m
Bottom of Test Interval: 170,800 m
Length of Test Interval: 6,000 m
Depth to Groundwater: m
Radius of Test Section: 0,048 m

Step	Pressure [bar]	Flow Meter Readings [m³/s]	Average Flow Rate [m³/s]	Hydraulic Conductivity		
		1		[m/s]	[m/s]	Lugeon
1	10,0	0,000000	0,000000	$0{,}00 \times 10^{-1}$	$0{,}00 \times 10^{-1}$	0,000
2	12,0	0,000000	0,000000	$0{,}00 \times 10^{-1}$	$0{,}00 \times 10^{-1}$	0,000
3	14,0	0,000000	0,000000	$0{,}00 \times 10^{-1}$	$0{,}00 \times 10^{-1}$	0,000
4	12,0	0,000000	0,000000	$0{,}00 \times 10^{-1}$	$0{,}00 \times 10^{-1}$	0,000
5	10,0	0,000000	0,000000	$0{,}00 \times 10^{-1}$	$0{,}00 \times 10^{-1}$	0,000
			Average	$0{,}00 \times 10^{-1}$	$0{,}00 \times 10^{-1}$	0,000

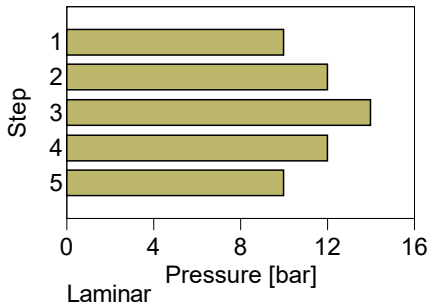

Laminar
Lugeon: 0,000
Hydraulic Conductivity: 0,00E-1 m/s
Hydraulic Conductivity: 0,00E-1 m/s

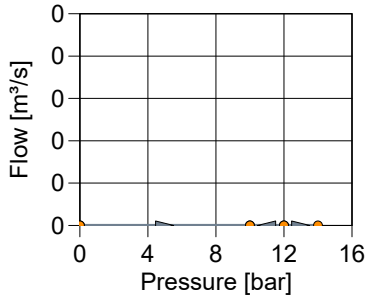

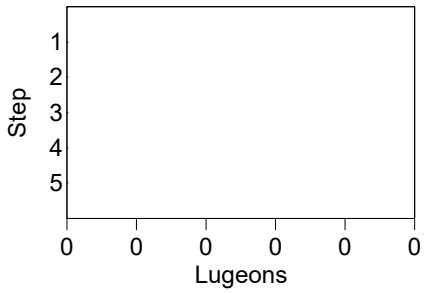

	Lugeon Test Analysis Report
	Project: Åknes
	Number: 20180662
	Client: NVE

Location: KH-01-2018	Lugeon Test: Lugeon Test 170,8-176,8	Tested bore: KH-01-18
Test Conducted by: Geodrilling		Test Date: 23.08.2018
Analysis Performed by: HLa		Analysis Date: 20.02.2019
Lithology:		

Top of Test Interval: 170,800 m
Bottom of Test Interval: 176,800 m
Length of Test Interval: 6,000 m
Depth to Groundwater: 61,000 m
Radius of Test Section: 0,048 m

Step	Pressure [bar]	Flow Meter Readings [m³/s]	Average Flow Rate [m³/s]	Hydraulic Conductivity		
		1		[m/s]	[m/s]	Lugeon
1	10,0	0,000000	0,000000	$0{,}00 \times 10^{-1}$	$0{,}00000 \times 10^{-1}$	0,000
2	12,0	0,000000	0,000000	$0{,}00 \times 10^{-1}$	$0{,}00000 \times 10^{-1}$	0,000
3	14,0	0,000000	0,000000	$0{,}00 \times 10^{-1}$	$0{,}00000 \times 10^{-1}$	0,000
4	12,0	0,000000	0,000000	$0{,}00 \times 10^{-1}$	$0{,}00000 \times 10^{-1}$	0,000
5	10,0	0,000000	0,000000	$0{,}00 \times 10^{-1}$	$0{,}00000 \times 10^{-1}$	0,000
			Average	$0{,}00 \times 10^{-1}$	$0{,}00000 \times 10^{-1}$	0,000

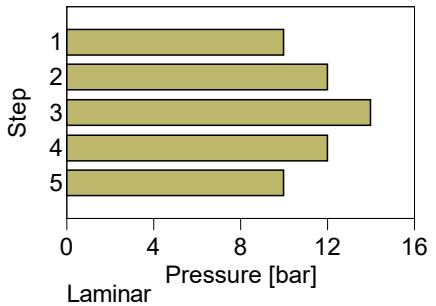

Laminar
Lugeon: 0,000
Hydraulic Conductivity: 0,00E-1 m/s
Hydraulic Conductivity: 0,00E-1 m/s

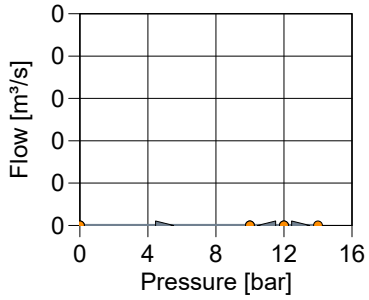

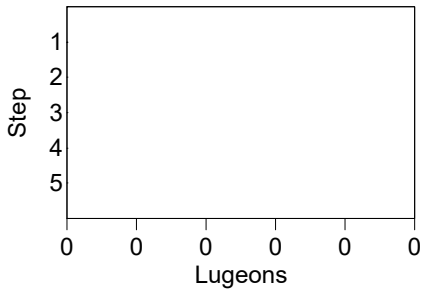

	Lugeon Test Analysis Report
	Project: Åknes
	Number: 20180662
	Client: NVE

Location: KH-01-2018	Lugeon Test: Lugeon Test 176,8-182,9	Tested bore: KH-01-18
Test Conducted by: Geodrilling		Test Date: 23.08.2018
Analysis Performed by: HLa		Analysis Date: 20.02.2019
Lithology:		

Top of Test Interval: 176,800 m
Bottom of Test Interval: 182,900 m
Length of Test Interval: 6,100 m
Depth to Groundwater: 61,000 m
Radius of Test Section: 0,048 m

Step	Pressure [bar]	Flow Meter Readings [m³/s]	Average Flow Rate [m³/s]	Hydraulic Conductivity		
		1		[m/s]	[m/s]	Lugeon
1	10,0	0,000000	0,000000	$0{,}00 \times 10^{-1}$	$0{,}00 \times 10^{-1}$	0,000
2	12,0	0,000000	0,000000	$0{,}00 \times 10^{-1}$	$0{,}00 \times 10^{-1}$	0,000
3	14,0	0,000000	0,000000	$0{,}00 \times 10^{-1}$	$0{,}00 \times 10^{-1}$	0,000
4	12,0	0,000000	0,000000	$0{,}00 \times 10^{-1}$	$0{,}00 \times 10^{-1}$	0,000
5	10,0	0,000000	0,000000	$0{,}00 \times 10^{-1}$	$0{,}00 \times 10^{-1}$	0,000
			Average	$0{,}00 \times 10^{-1}$	$0{,}00 \times 10^{-1}$	0,000

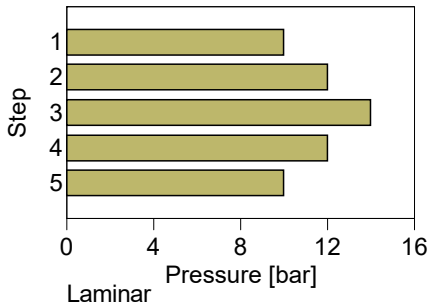

Laminar
Lugeon: 0,000
Hydraulic Conductivity: 0,00E-1 m/s
Hydraulic Conductivity: 0,00E-1 m/s

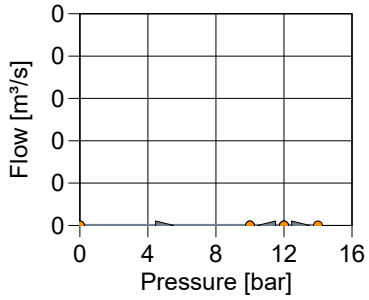

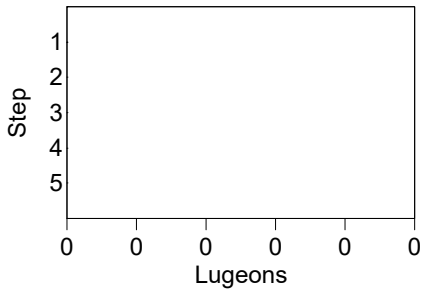

	Lugeon Test Analysis Report
	Project: Åknes
	Number: 20180662
	Client: NVE

Location: KH-01-2018	Lugeon Test: Lugeon Test 182,9-188,9	Tested bore: KH-01-18
Test Conducted by: Geodrilling		Test Date: 24.08.2018
Analysis Performed by: HLa		Analysis Date: 20.02.2019
Lithology:		

Top of Test Interval: 182,900 m
Bottom of Test Interval: 188,900 m
Length of Test Interval: 6,000 m
Depth to Groundwater: 57,000 m
Radius of Test Section: 0,048 m

Step	Pressure [bar]	Flow Meter Readings [m³/s]	Average Flow Rate [m³/s]	Hydraulic Conductivity		
		1		[m/s]	[m/s]	Lugeon
1	10,0	0,000000	0,000000	$0{,}00 \times 10^{-1}$	$0{,}00 \times 10^{-1}$	0,000
2	12,0	0,000000	0,000000	$0{,}00 \times 10^{-1}$	$0{,}00 \times 10^{-1}$	0,000
3	14,0	0,000000	0,000000	$0{,}00 \times 10^{-1}$	$0{,}00 \times 10^{-1}$	0,000
4	12,0	0,000000	0,000000	$0{,}00 \times 10^{-1}$	$0{,}00 \times 10^{-1}$	0,000
5	10,0	0,000000	0,000000	$0{,}00 \times 10^{-1}$	$0{,}00 \times 10^{-1}$	0,000
			Average	$0{,}00 \times 10^{-1}$	$0{,}00 \times 10^{-1}$	0,000

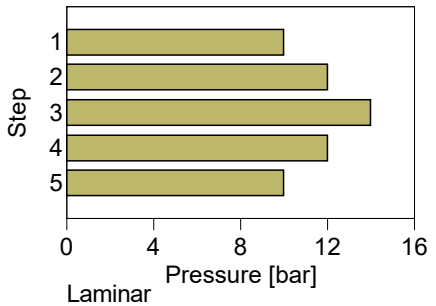

Laminar
Lugeon: 0,000
Hydraulic Conductivity: 0,00E-1 m/s
Hydraulic Conductivity: 0,00E-1 m/s

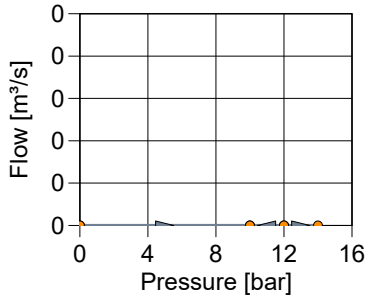

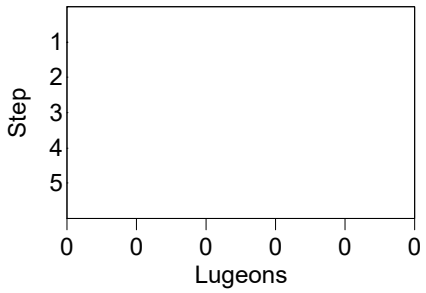

	Lugeon Test Analysis Report
	Project: Åknes
	Number: 20180662
	Client: NVE

Location: KH-01-2018	Lugeon Test: Lugeon Test 188,9-194,9	Tested bore: KH-01-18
Test Conducted by: Geodrilling		Test Date: 24.08.2018
Analysis Performed by: HLa		Analysis Date: 20.02.2019
Lithology:		

Top of Test Interval: 188,900 m
Bottom of Test Interval: 194,900 m
Length of Test Interval: 6,000 m
Depth to Groundwater: 57,000 m
Radius of Test Section: 0,048 m

Step	Pressure [bar]	Flow Meter Readings [m³/s]	Average Flow Rate [m³/s]	Hydraulic Conductivity		
		1		[m/s]	[m/s]	Lugeon
1	10,0	0,000000	0,000000	$0{,}00 \times 10^{-1}$	$0{,}00 \times 10^{-1}$	0,000
2	12,0	0,000000	0,000000	$0{,}00 \times 10^{-1}$	$0{,}00 \times 10^{-1}$	0,000
3	14,0	0,000000	0,000000	$0{,}00 \times 10^{-1}$	$0{,}00 \times 10^{-1}$	0,000
4	12,0	0,000000	0,000000	$0{,}00 \times 10^{-1}$	$0{,}00 \times 10^{-1}$	0,000
5	10,0	0,000000	0,000000	$0{,}00 \times 10^{-1}$	$0{,}00 \times 10^{-1}$	0,000
			Average	$0{,}00 \times 10^{-1}$	$0{,}00 \times 10^{-1}$	0,000

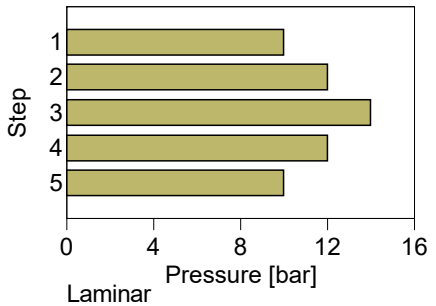

Laminar
Lugeon: 0,000
Hydraulic Conductivity: 0,00E-1 m/s
Hydraulic Conductivity: 0,00E-1 m/s

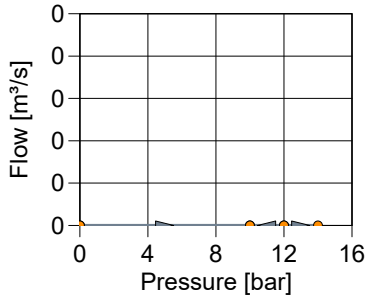

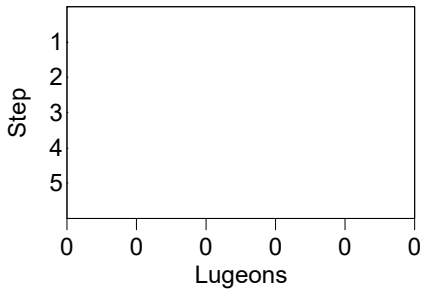

	Lugeon Test Analysis Report
	Project: Åknes
	Number: 20180662
	Client: NVE

Location: KH-01-2018	Lugeon Test: Lugeon Test 194,9-200,9	Tested bore: KH-01-18
Test Conducted by: Geodrilling		Test Date: 25.08.2018
Analysis Performed by: HLa		Analysis Date: 20.02.2019
Lithology:		

Top of Test Interval: 194,900 m
Bottom of Test Interval: 200,900 m
Length of Test Interval: 6,000 m
Depth to Groundwater: 56,000 m
Radius of Test Section: 0,048 m

Step	Pressure [bar]	Flow Meter Readings [m³/s]	Average Flow Rate [m³/s]	Hydraulic Conductivity		
		1		[m/s]	[m/s]	Lugeon
1	10,0	0,000000	0,000000	$0{,}00 \times 10^{-1}$	$0{,}00 \times 10^{-1}$	0,000
2	12,0	0,000000	0,000000	$0{,}00 \times 10^{-1}$	$0{,}00 \times 10^{-1}$	0,000
3	14,0	0,000000	0,000000	$0{,}00 \times 10^{-1}$	$0{,}00 \times 10^{-1}$	0,000
4	12,0	0,000000	0,000000	$0{,}00 \times 10^{-1}$	$0{,}00 \times 10^{-1}$	0,000
5	10,0	0,000000	0,000000	$0{,}00 \times 10^{-1}$	$0{,}00 \times 10^{-1}$	0,000
			Average	$0{,}00 \times 10^{-1}$	$0{,}00 \times 10^{-1}$	0,000

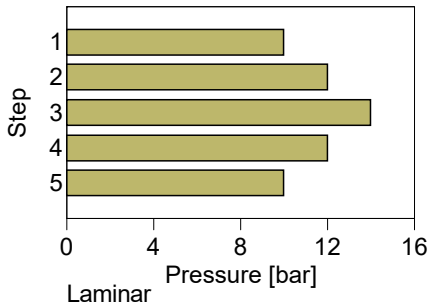

Laminar
Lugeon: 0,000
Hydraulic Conductivity: 0,00E-1 m/s
Hydraulic Conductivity: 0,00E-1 m/s

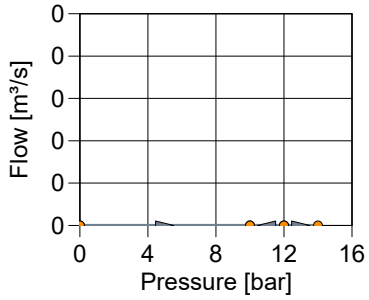

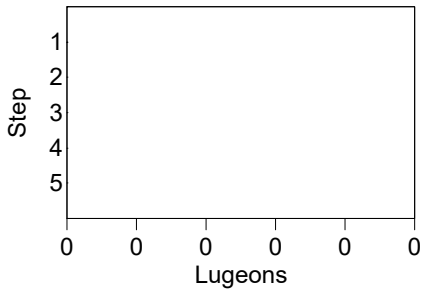

	Lugeon Test Analysis Report
	Project: Åknes
	Number: 20180662
	Client: NVE

Location: KH-01-2018	Lugeon Test: Lugeon Test 200,9-206,9	Tested bore: KH-01-18
Test Conducted by: Geodrilling		Test Date: 25.08.2018
Analysis Performed by: HLa		Analysis Date: 20.02.2019
Lithology:		

Top of Test Interval: 200,900 m
Bottom of Test Interval: 206,900 m
Length of Test Interval: 6,000 m
Depth to Groundwater: 56,000 m
Radius of Test Section: 0,048 m

Step	Pressure [bar]	Flow Meter Readings [m³/s]	Average Flow Rate [m³/s]	Hydraulic Conductivity		
		1		[m/s]	[m/s]	Lugeon
1	10,0	0,000000	0,000000	$0{,}00 \times 10^{-1}$	$0{,}00 \times 10^{-1}$	0,000
2	12,0	0,000000	0,000000	$0{,}00 \times 10^{-1}$	$0{,}00 \times 10^{-1}$	0,000
3	14,0	0,000000	0,000000	$0{,}00 \times 10^{-1}$	$0{,}00 \times 10^{-1}$	0,000
4	12,0	0,000000	0,000000	$0{,}00 \times 10^{-1}$	$0{,}00 \times 10^{-1}$	0,000
5	10,0	0,000000	0,000000	$0{,}00 \times 10^{-1}$	$0{,}00 \times 10^{-1}$	0,000
			Average	$0{,}00 \times 10^{-1}$	$0{,}00 \times 10^{-1}$	0,000

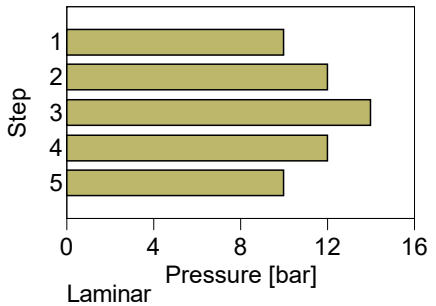

Laminar
Lugeon: 0,000
Hydraulic Conductivity: 0,00E-1 m/s
Hydraulic Conductivity: 0,00E-1 m/s

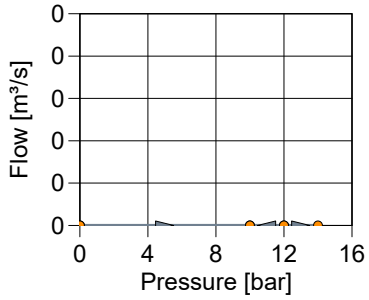

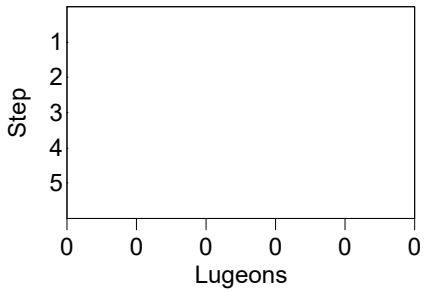

	Lugeon Test Analysis Report
	Project: Åknes
	Number: 20180662
	Client: NVE

Location: KH-01-2018	Lugeon Test: Lugeon Test 206,9-212,9	Tested bore: KH-01-18
Test Conducted by: Geodrilling		Test Date: 25.08.2018
Analysis Performed by: HLa		Analysis Date: 20.02.2019
Lithology:		

Top of Test Interval: 206,900 m
Bottom of Test Interval: 212,900 m
Length of Test Interval: 6,000 m
Depth to Groundwater: 56,000 m
Radius of Test Section: 0,048 m

Step	Pressure [bar]	Flow Meter Readings [m³/s]	Average Flow Rate [m³/s]	Hydraulic Conductivity		
		1		[m/s]	[m/s]	Lugeon
1	10,0	0,000000	0,000000	$0{,}00 \times 10^{-1}$	$0{,}00 \times 10^{-1}$	0,000
2	12,0	0,000000	0,000000	$0{,}00 \times 10^{-1}$	$0{,}00 \times 10^{-1}$	0,000
3	14,0	0,000000	0,000000	$0{,}00 \times 10^{-1}$	$0{,}00 \times 10^{-1}$	0,000
4	12,0	0,000000	0,000000	$0{,}00 \times 10^{-1}$	$0{,}00 \times 10^{-1}$	0,000
5	10,0	0,000000	0,000000	$0{,}00 \times 10^{-1}$	$0{,}00 \times 10^{-1}$	0,000
			Average	$0{,}00 \times 10^{-1}$	$0{,}00 \times 10^{-1}$	0,000

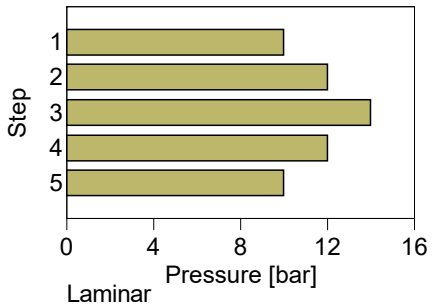

Laminar
Lugeon: 0,000
Hydraulic Conductivity: 0,00E-1 m/s
Hydraulic Conductivity: 0,00E-1 m/s

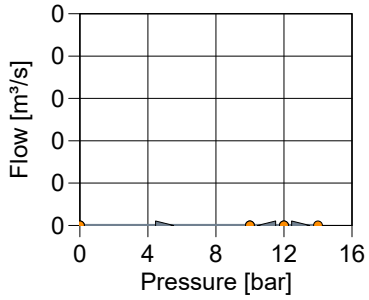

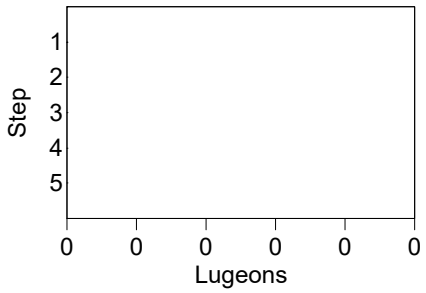

	Lugeon Test Analysis Report
	Project: Åknes
	Number: 20180662
	Client: NVE

Location: KH-01-2018	Lugeon Test: Lugeon Test 212,9-218,9	Tested bore: KH-01-18
Test Conducted by: Geodrilling		Test Date: 26.08.2018
Analysis Performed by: HLa		Analysis Date: 20.02.2019
Lithology:		

Top of Test Interval: 212,900 m
Bottom of Test Interval: 218,900 m
Length of Test Interval: 6,000 m
Depth to Groundwater: 50,000 m
Radius of Test Section: 0,048 m

Step	Pressure [bar]	Flow Meter Readings [m³/s]	Average Flow Rate [m³/s]	Hydraulic Conductivity		
		1		[m/s]	[m/s]	Lugeon
1	10,0	0,000000	0,000000	$0{,}00 \times 10^{-1}$	$0{,}00 \times 10^{-1}$	0,000
2	12,0	0,000000	0,000000	$0{,}00 \times 10^{-1}$	$0{,}00 \times 10^{-1}$	0,000
3	14,0	0,000000	0,000000	$0{,}00 \times 10^{-1}$	$0{,}00 \times 10^{-1}$	0,000
4	12,0	0,000000	0,000000	$0{,}00 \times 10^{-1}$	$0{,}00 \times 10^{-1}$	0,000
5	10,0	0,000000	0,000000	$0{,}00 \times 10^{-1}$	$0{,}00 \times 10^{-1}$	0,000
			Average	$0{,}00 \times 10^{-1}$	$0{,}00 \times 10^{-1}$	0,000

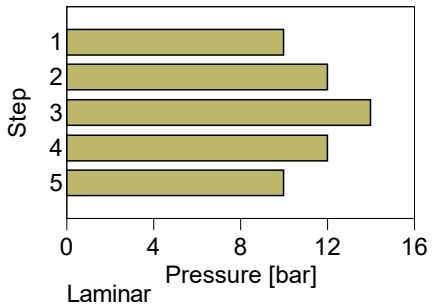

Laminar
Lugeon: 0,000
Hydraulic Conductivity: 0,00E-1 m/s
Hydraulic Conductivity: 0,00E-1 m/s

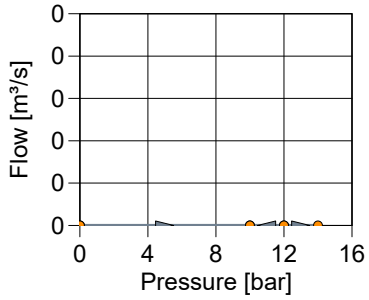

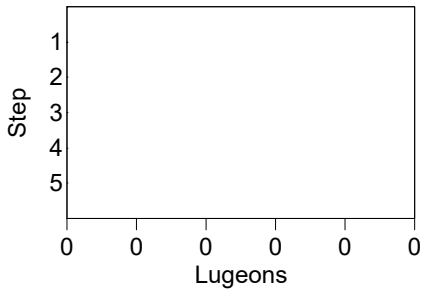

	Lugeon Test Analysis Report
	Project: Åknes
	Number: 20180662
	Client: NVE

Location: KH-01-2018	Lugeon Test: Lugeon Test 218,9-222,6	Tested bore: KH-01-18
Test Conducted by: Geodrilling		Test Date: 26.08.2018
Analysis Performed by: HLa		Analysis Date: 19.02.2019
Lithology:		

Top of Test Interval: 218,900 m
Bottom of Test Interval: 222,600 m
Length of Test Interval: 3,700 m
Depth to Groundwater: 50,000 m
Radius of Test Section: 0,048 m

Step	Pressure [bar]	Flow Meter Readings [m³/s]	Average Flow Rate [m³/s]	Hydraulic Conductivity		
		1		[m/s]	[m/s]	Lugeon
1	10,0	0,000230	0,000230	$4,22 \times 10^{-7}$	$4,22 \times 10^{-7}$	3,73
2	12,0	0,000258	0,000258	$3,95 \times 10^{-7}$	$3,95 \times 10^{-7}$	3,49
3	14,0	0,000272	0,000272	$3,56 \times 10^{-7}$	$3,56 \times 10^{-7}$	3,15
4	12,0	0,000228	0,000228	$3,49 \times 10^{-7}$	$3,49 \times 10^{-7}$	3,09
5	10,0	0,000182	0,000182	$3,33 \times 10^{-7}$	$3,33 \times 10^{-7}$	2,95
			Average	$3,71 \times 10^{-7}$	$3,71 \times 10^{-7}$	3,28

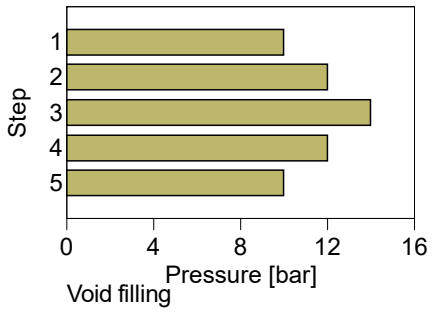

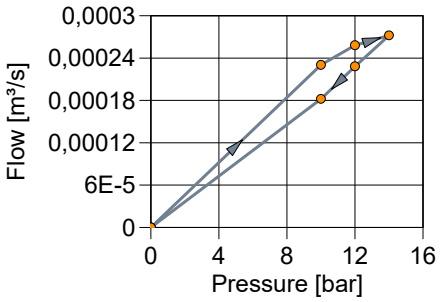

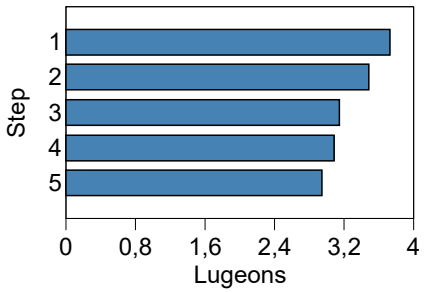

Void filling
Lugeon: 2,95
Hydraulic Conductivity: 3,33E-7 m/s
Hydraulic Conductivity: 3,33E-7 m/s

A3 KH-02-2018

Lugeon Test Summary - KH-02-18

Project: Åknes

Number: 20180662

Client: NVE

Test Interval Top Bottom	Graphs	Result
30,000 m 36,000 m	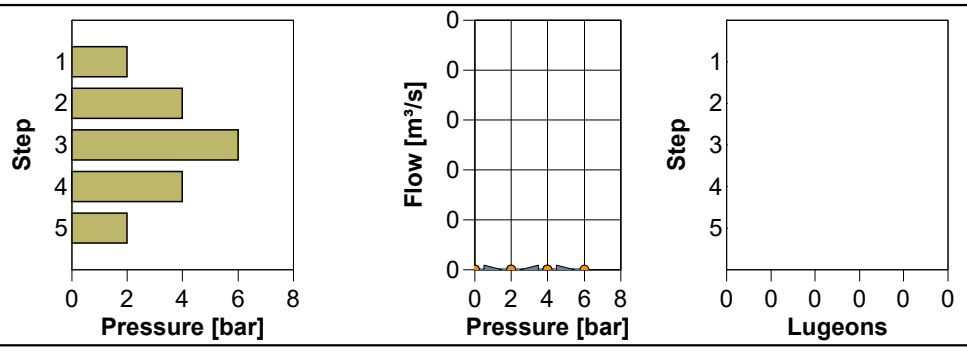	Laminar Lugeon: 0,000 Hydraulic Conductivity: 0,00E-1 m/s Hydraulic Conductivity: 0,00E-1 m/s
35,800 m 41,800 m	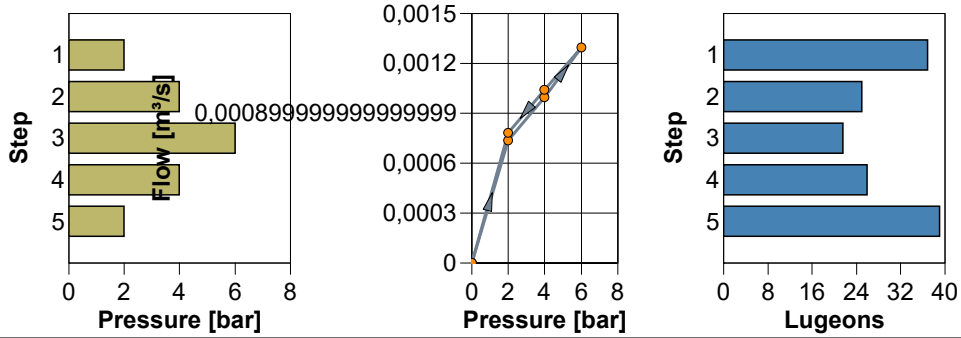	Turbulent Lugeon: 24,917 Hydraulic Conductivity: 3,13E-6 m/s Hydraulic Conductivity: 3,13E-6 m/s
51,000 m 57,100 m	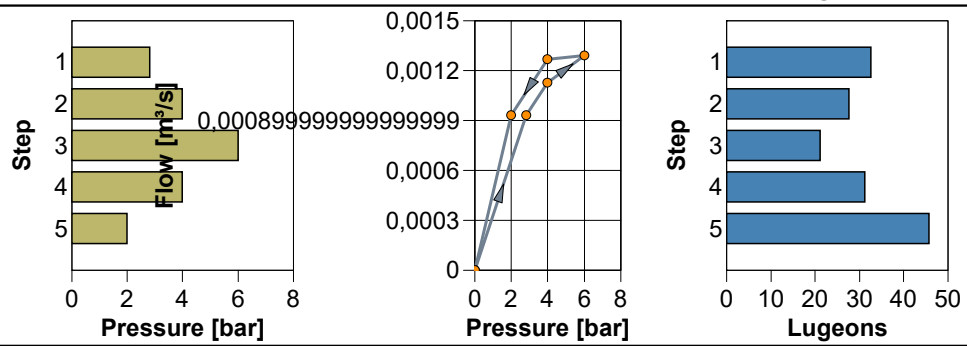	Turbulent Lugeon: 27,706 Hydraulic Conductivity: 3,49E-6 m/s Hydraulic Conductivity: 3,49E-6 m/s
57,000 m 63,000 m	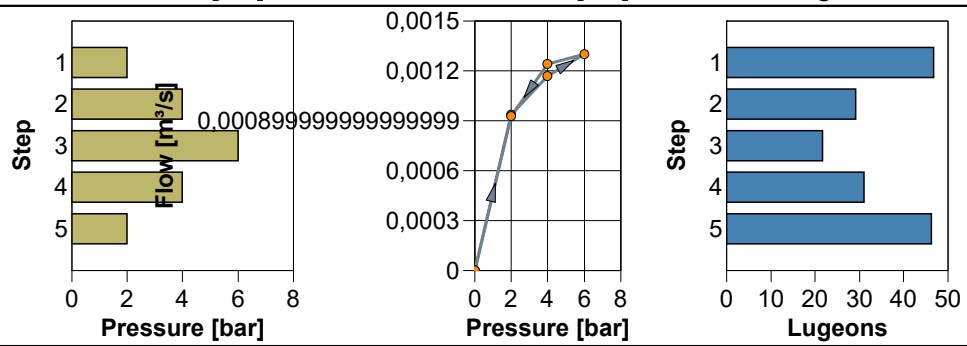	Turbulent Lugeon: 29,250 Hydraulic Conductivity: 3,67E-6 m/s Hydraulic Conductivity: 3,67E-6 m/s

Lugeon Test Summary - KH-02-18

Project: Åknes

Number: 20180662

Client: NVE

Test Interval Top Bottom	Graphs	Result
63,000 m 69,000 m	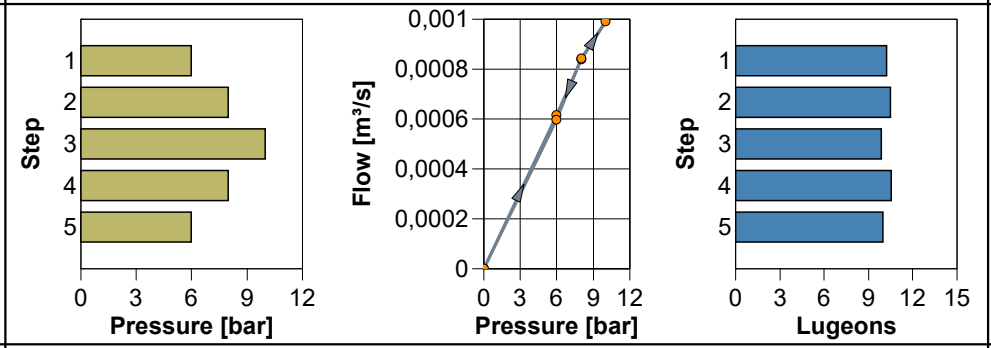	Laminar Lugeon: 10,233 Hydraulic Conductivity: 1,29E-6 m/s Hydraulic Conductivity: 1,29E-6 m/s
69,000 m 76,000 m	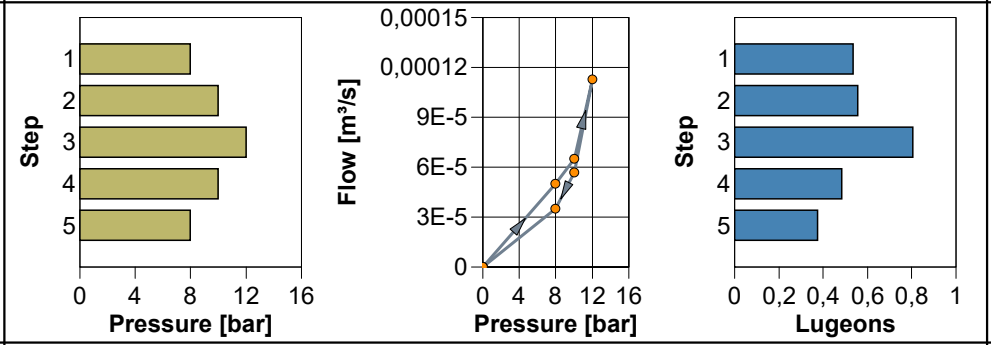	Dilation Lugeon: 0,536 Hydraulic Conductivity: 6,94E-8 m/s Hydraulic Conductivity: 6,94E-8 m/s
75,500 m 82,500 m	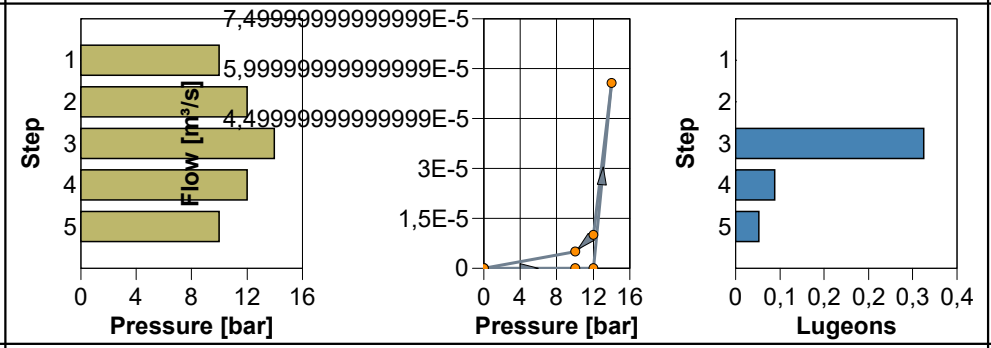	Dilation Lugeon: 0,000 Hydraulic Conductivity: 0,00E-1 m/s Hydraulic Conductivity: 0,00E-1 m/s
82,500 m 88,000 m	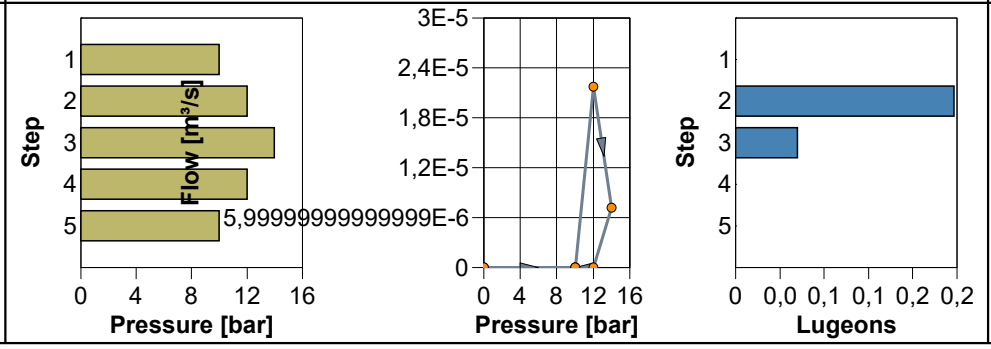	Dilation Lugeon: 0,000 Hydraulic Conductivity: 0,00E-1 m/s Hydraulic Conductivity: 0,00E-1 m/s

Lugeon Test Summary - KH-02-18

Project: Åknes

Number: 20180662

Client: NVE

Test Interval Top Bottom	Graphs	Result
93,000 m 99,000 m	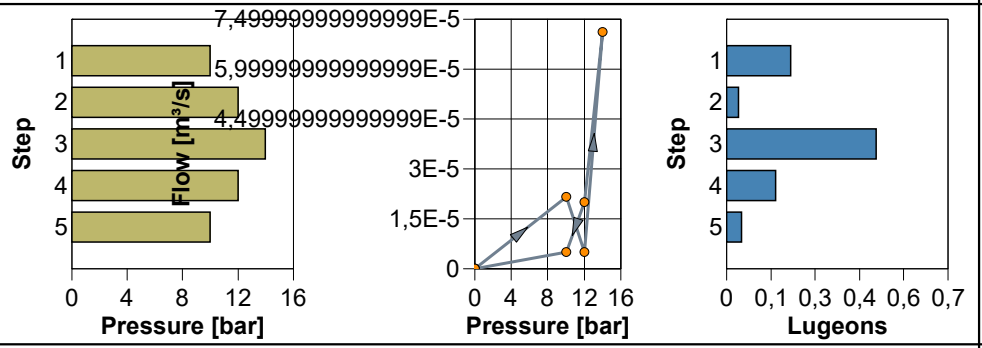	Dilation Lugeon: 0,217 Hydraulic Conductivity: 2,73E-8 m/s Hydraulic Conductivity: 2,73E-8 m/s
101,000 m 109,500 m	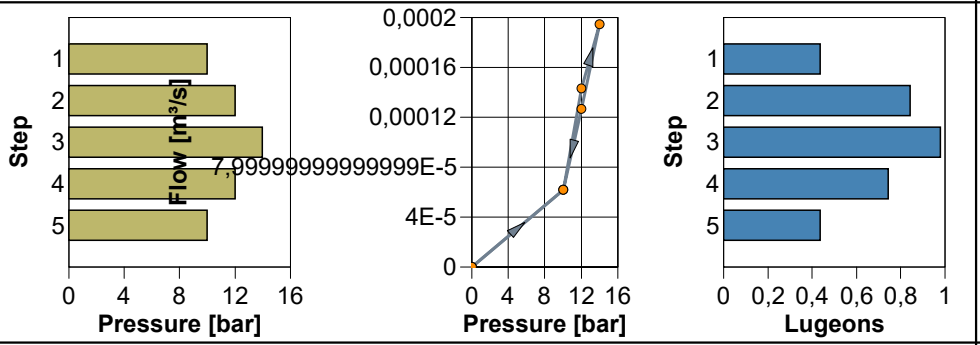	Dilation Lugeon: 0,436 Hydraulic Conductivity: 5,87E-8 m/s Hydraulic Conductivity: 5,87E-8 m/s
122,000 m 130,500 m	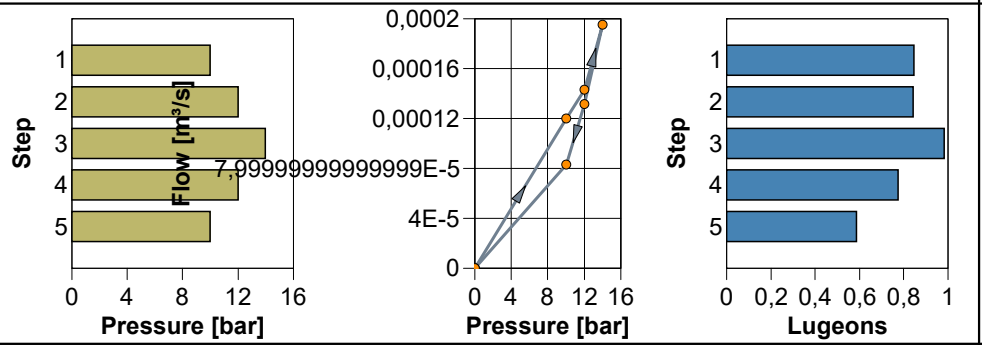	Dilation Lugeon: 0,847 Hydraulic Conductivity: 1,14E-7 m/s Hydraulic Conductivity: 1,14E-7 m/s
138,000 m 145,000 m	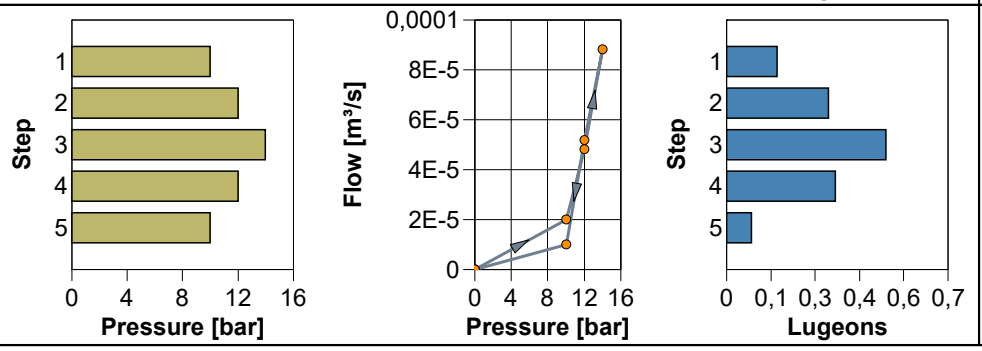	Dilation Lugeon: 0,171 Hydraulic Conductivity: 2,22E-8 m/s Hydraulic Conductivity: 2,22E-8 m/s

Lugeon Test Summary - KH-02-18

Project: Åknes

Number: 20180662

Client: NVE

Test Interval Top Bottom	Graphs	Result
148,000 m 154,000 m	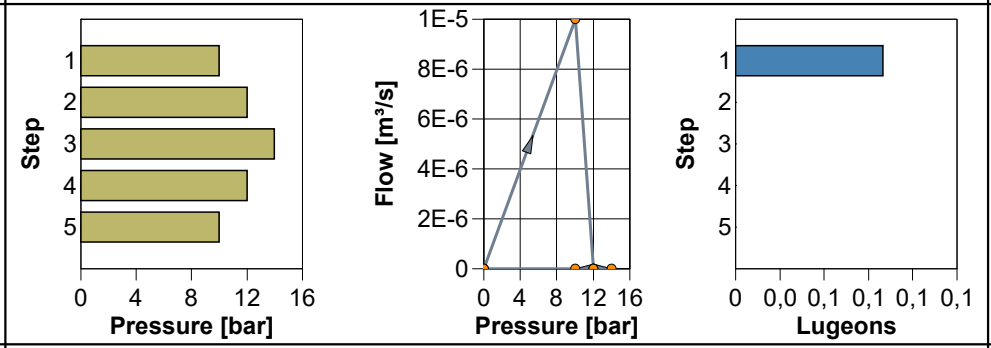	Void filling Lugeon: 0,000 Hydraulic Conductivity: 0,00E-1 m/s Hydraulic Conductivity: 0,00E-1 m/s
154,000 m 160,000 m	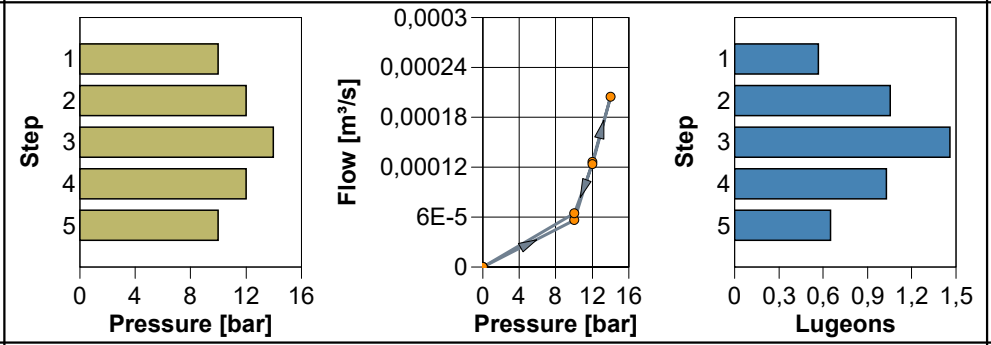	Dilation Lugeon: 0,567 Hydraulic Conductivity: 7,12E-8 m/s Hydraulic Conductivity: 7,12E-8 m/s
160,000 m 166,000 m	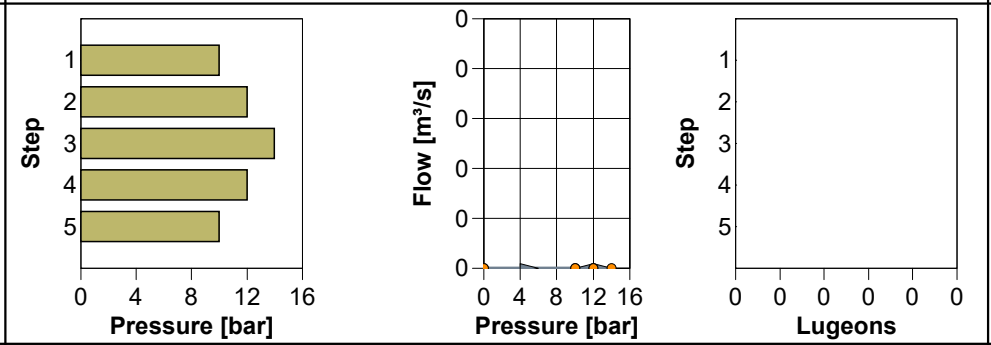	Laminar Lugeon: 0,000 Hydraulic Conductivity: 0,00E-1 m/s Hydraulic Conductivity: 0,00E-1 m/s
185,000 m 200,000 m	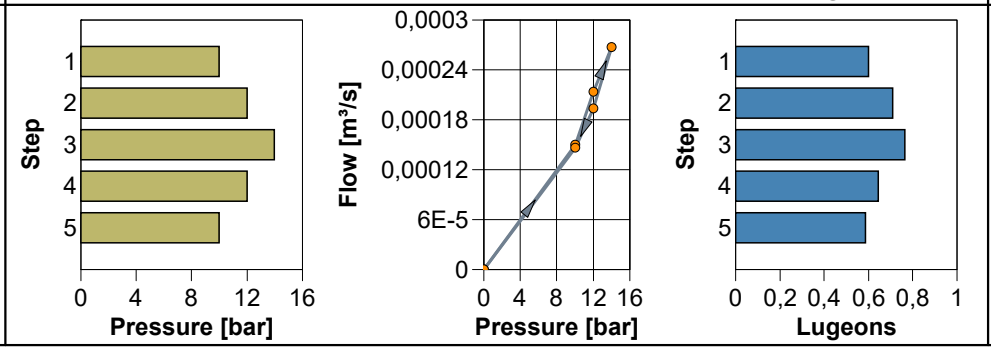	Dilation Lugeon: 0,600 Hydraulic Conductivity: 8,97E-8 m/s Hydraulic Conductivity: 8,97E-8 m/s

	Lugeon Test Analysis Report
	Project: Åknes
	Number: 20180662
	Client: NVE

Location: KH-02-2018	Lugeon Test: Lugeon Test 30-36	Tested bore: KH-02-18
Test Conducted by: Geodrilling		Test Date: 17.09.2018
Analysis Performed by: HLa		Analysis Date: 20.02.2019
Lithology:		

Top of Test Interval: 30,000 m
Bottom of Test Interval: 36,000 m
Length of Test Interval: 6,000 m
Depth to Groundwater: m
Radius of Test Section: 0,048 m

Step	Pressure [bar]	Flow Meter Readings [m³/s]	Average Flow Rate [m³/s]	Hydraulic Conductivity		
		1		[m/s]	[m/s]	Lugeon
1	2,0	0,000000	0,000000	$0{,}00 \times 10^{-1}$	$0{,}00 \times 10^{-1}$	0,000
2	4,0	0,000000	0,000000	$0{,}00 \times 10^{-1}$	$0{,}00 \times 10^{-1}$	0,000
3	6,0	0,000000	0,000000	$0{,}00 \times 10^{-1}$	$0{,}00 \times 10^{-1}$	0,000
4	4,0	0,000000	0,000000	$0{,}00 \times 10^{-1}$	$0{,}00 \times 10^{-1}$	0,000
5	2,0	0,000000	0,000000	$0{,}00 \times 10^{-1}$	$0{,}00 \times 10^{-1}$	0,000
			Average	$0{,}00 \times 10^{-1}$	$0{,}00 \times 10^{-1}$	0,000

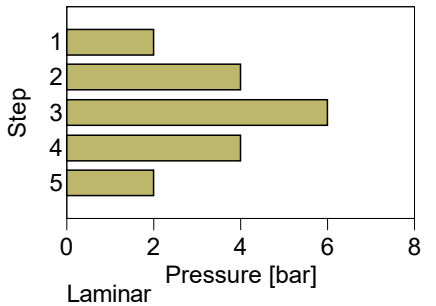

Laminar
Lugeon: 0,000
Hydraulic Conductivity: 0,00E-1 m/s
Hydraulic Conductivity: 0,00E-1 m/s

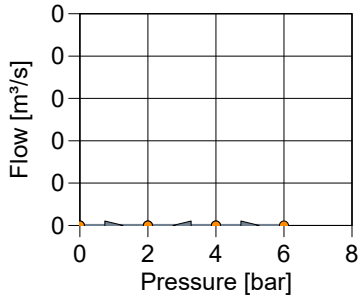

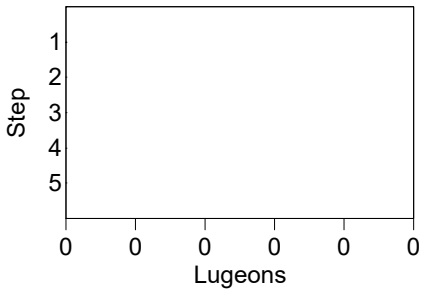

	Lugeon Test Analysis Report
	Project: Åknes
	Number: 20180662
	Client: NVE

Location: KH-02-2018	Lugeon Test: Lugeon Test 35,8-41,8	Tested bore: KH-02-18
Test Conducted by: Geodrilling		Test Date: 17.09.2018
Analysis Performed by: HLa		Analysis Date: 20.02.2019
Lithology:		

Top of Test Interval: 35,800 m
Bottom of Test Interval: 41,800 m
Length of Test Interval: 6,000 m
Depth to Groundwater: 39,600 m
Radius of Test Section: 0,048 m

Step	Pressure [bar]	Flow Meter Readings [m³/s]	Average Flow Rate [m³/s]	Hydraulic Conductivity		
		1		[m/s]	[m/s]	Lugeon
1	2,0	0,000737	0,000737	$4,63 \times 10^{-6}$	$4,63 \times 10^{-6}$	36,834
2	4,0	0,000997	0,000997	$3,13 \times 10^{-6}$	$3,13 \times 10^{-6}$	24,917
3	6,0	0,001296	0,001296	$2,71 \times 10^{-6}$	$2,71 \times 10^{-6}$	21,593
4	4,0	0,001040	0,001040	$3,27 \times 10^{-6}$	$3,27 \times 10^{-6}$	26,000
5	2,0	0,000782	0,000782	$4,91 \times 10^{-6}$	$4,91 \times 10^{-6}$	39,084
			Average	$3,73 \times 10^{-6}$	$3,73 \times 10^{-6}$	29,685

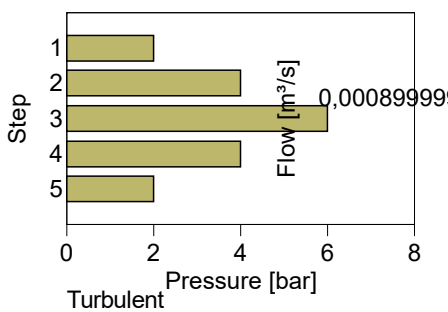

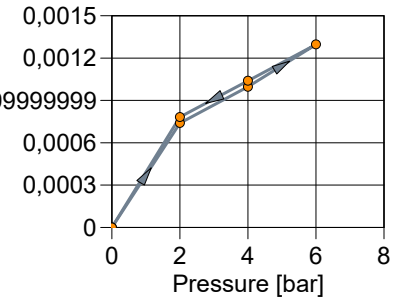

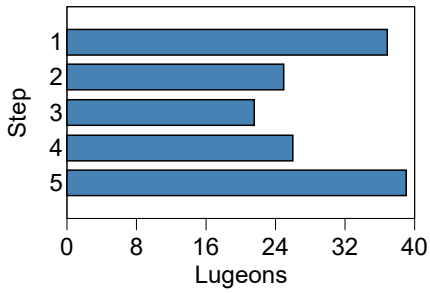

Turbulent
Lugeon: 24,917
Hydraulic Conductivity: 3,13E-6 m/s
Hydraulic Conductivity: 3,13E-6 m/s

	Lugeon Test Analysis Report
	Project: Åknes
	Number: 20180662
	Client: NVE

Location: KH-02-2018	Lugeon Test: Lugeon Test 51,0-57,1	Tested bore: KH-02-18
Test Conducted by: Geodrilling		Test Date: 18.09.2018
Analysis Performed by: HLa		Analysis Date: 20.02.2019
Lithology:		

Top of Test Interval: 51,000 m
Bottom of Test Interval: 57,100 m
Length of Test Interval: 6,100 m
Depth to Groundwater: m
Radius of Test Section: 0,048 m

Step	Pressure [bar]	Flow Meter Readings [m³/s]	Average Flow Rate [m³/s]	Hydraulic Conductivity		
		1		[m/s]	[m/s]	Lugeon
1	2,8	0,000930	0,000930	$4{,}12 \times 10^{-6}$	$4{,}12 \times 10^{-6}$	32,670
2	4,0	0,001127	0,001127	$3{,}49 \times 10^{-6}$	$3{,}49 \times 10^{-6}$	27,706
3	6,0	0,001289	0,001289	$2{,}66 \times 10^{-6}$	$2{,}66 \times 10^{-6}$	21,138
4	4,0	0,001270	0,001270	$3{,}94 \times 10^{-6}$	$3{,}94 \times 10^{-6}$	31,230
5	2,0	0,000930	0,000930	$5{,}76 \times 10^{-6}$	$5{,}76 \times 10^{-6}$	45,738
			Average	$3{,}99 \times 10^{-6}$	$3{,}99 \times 10^{-6}$	31,696

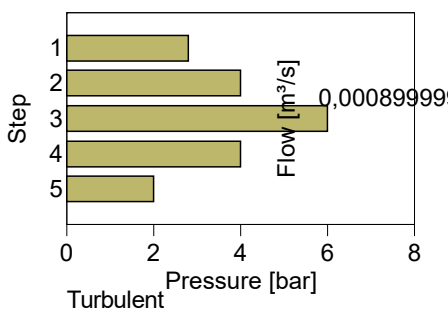

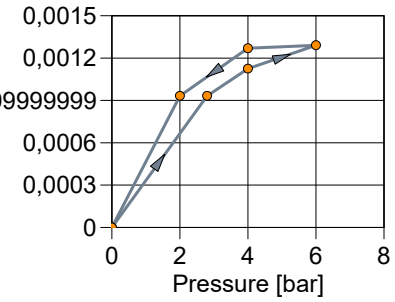

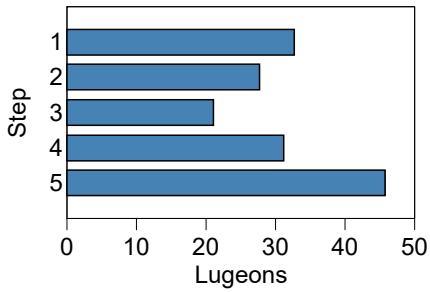

Turbulent
Lugeon: 27,706
Hydraulic Conductivity: 3,49E-6 m/s
Hydraulic Conductivity: 3,49E-6 m/s

	Lugeon Test Analysis Report
	Project: Åknes
	Number: 20180662
	Client: NVE

Location: KH-02-2018	Lugeon Test: Lugeon Test 57-63	Tested bore: KH-02-18
Test Conducted by: Geodrilling		Test Date: 19.09.2018
Analysis Performed by: HLa		Analysis Date: 20.02.2019
Lithology:		

Top of Test Interval: 57,000 m
Bottom of Test Interval: 63,000 m
Length of Test Interval: 6,000 m
Depth to Groundwater: m
Radius of Test Section: 0,048 m

Step	Pressure [bar]	Flow Meter Readings [m³/s]	Average Flow Rate [m³/s]	Hydraulic Conductivity		
		1		[m/s]	[m/s]	Lugeon
1	2,0	0,000935	0,000935	$5,87 \times 10^{-6}$	$5,87 \times 10^{-6}$	46,750
2	4,0	0,001170	0,001170	$3,67 \times 10^{-6}$	$3,67 \times 10^{-6}$	29,250
3	6,0	0,001299	0,001299	$2,72 \times 10^{-6}$	$2,72 \times 10^{-6}$	21,657
4	4,0	0,001240	0,001240	$3,89 \times 10^{-6}$	$3,89 \times 10^{-6}$	31,000
5	2,0	0,000925	0,000925	$5,81 \times 10^{-6}$	$5,81 \times 10^{-6}$	46,250
			Average	$4,39 \times 10^{-6}$	$4,39 \times 10^{-6}$	34,981

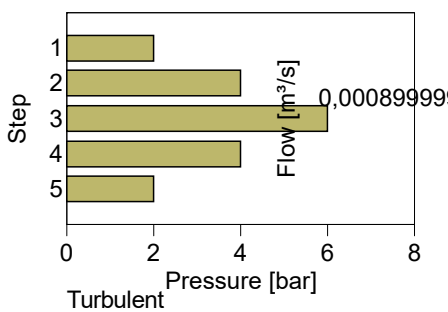

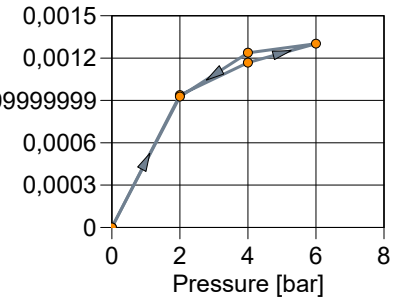

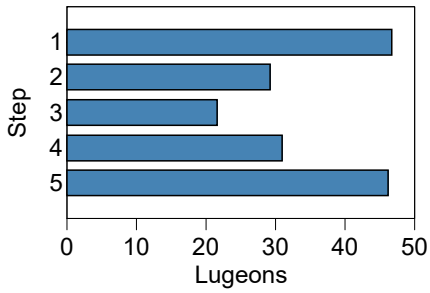

Turbulent
Lugeon: 29,250
Hydraulic Conductivity: 3,67E-6 m/s
Hydraulic Conductivity: 3,67E-6 m/s

	Lugeon Test Analysis Report
	Project: Åknes
	Number: 20180662
	Client: NVE

Location: KH-02-2018	Lugeon Test: Lugeon Test 63-69	Tested bore: KH-02-18
Test Conducted by: Geodrilling		Test Date: 04.10.2018
Analysis Performed by: HLa		Analysis Date: 20.02.2019
Lithology:		

Top of Test Interval: 63,000 m
Bottom of Test Interval: 69,000 m
Length of Test Interval: 6,000 m
Depth to Groundwater: m
Radius of Test Section: 0,048 m

Step	Pressure [bar]	Flow Meter Readings [m³/s]	Average Flow Rate [m³/s]	Hydraulic Conductivity		
		1		[m/s]	[m/s]	Lugeon
1	6,0	0,000615	0,000615	$1,29 \times 10^{-6}$	$1,29 \times 10^{-6}$	10,25
2	8,0	0,000840	0,000840	$1,32 \times 10^{-6}$	$1,32 \times 10^{-6}$	10,50
3	10,0	0,000990	0,000990	$1,24 \times 10^{-6}$	$1,24 \times 10^{-6}$	9,90
4	8,0	0,000843	0,000843	$1,32 \times 10^{-6}$	$1,32 \times 10^{-6}$	10,54
5	6,0	0,000598	0,000598	$1,25 \times 10^{-6}$	$1,25 \times 10^{-6}$	9,97
			Average	$1,29 \times 10^{-6}$	$1,29 \times 10^{-6}$	10,23

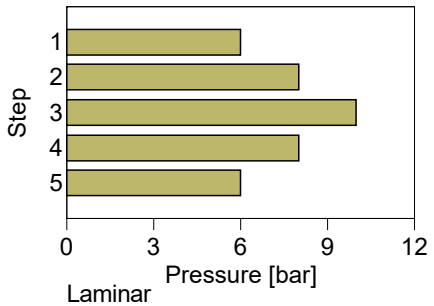

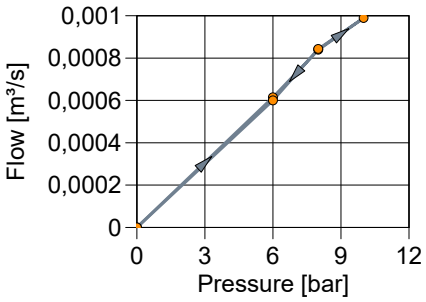

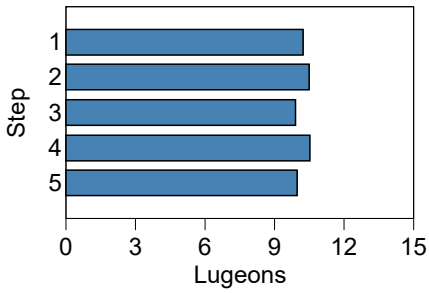

Laminar
Lugeon: 10,233
Hydraulic Conductivity: 1,29E-6 m/s
Hydraulic Conductivity: 1,29E-6 m/s

	Lugeon Test Analysis Report
	Project: Åknes
	Number: 20180662
	Client: NVE

Location: KH-02-2018	Lugeon Test: Lugeon Test 69-76	Tested bore: KH-02-18
Test Conducted by: Geodrilling		Test Date: 05.10.2018
Analysis Performed by: HLa		Analysis Date: 20.02.2019
Lithology:		

Top of Test Interval: 69,000 m
Bottom of Test Interval: 76,000 m
Length of Test Interval: 7,000 m
Depth to Groundwater: m
Radius of Test Section: 0,048 m

Step	Pressure [bar]	Flow Meter Readings [m³/s]	Average Flow Rate [m³/s]	Hydraulic Conductivity		
		1		[m/s]	[m/s]	Lugeon
1	8,0	0,000050	0,000050	$6{,}94 \times 10^{-8}$	$6{,}94 \times 10^{-8}$	0,536
2	10,0	0,000065	0,000065	$7{,}22 \times 10^{-8}$	$7{,}22 \times 10^{-8}$	0,557
3	12,0	0,000113	0,000113	$1{,}04 \times 10^{-7}$	$1{,}04 \times 10^{-7}$	0,806
4	10,0	0,000057	0,000057	$6{,}30 \times 10^{-8}$	$6{,}30 \times 10^{-8}$	0,486
5	8,0	0,000035	0,000035	$4{,}86 \times 10^{-8}$	$4{,}86 \times 10^{-8}$	0,375
			Average	$7{,}15 \times 10^{-8}$	$7{,}15 \times 10^{-8}$	0,552

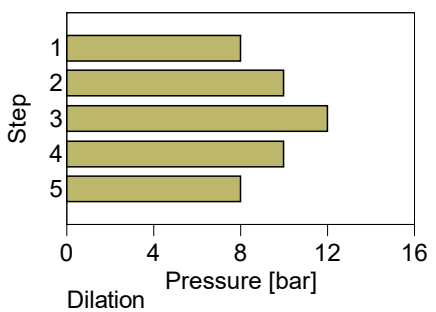

Dilation
Lugeon: 0,536
Hydraulic Conductivity: 6,94E-8 m/s
Hydraulic Conductivity: 6,94E-8 m/s

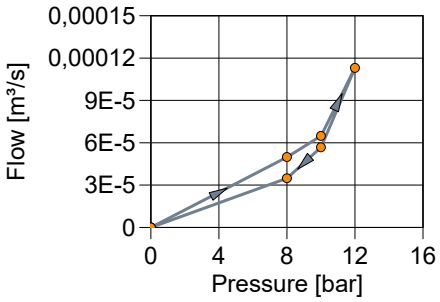

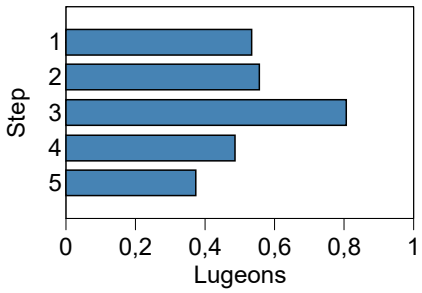

	Lugeon Test Analysis Report
	Project: Åknes
	Number: 20180662
	Client: NVE

Location: KH-02-2018	Lugeon Test: Lugeon Test 75,5-82,5	Tested bore: KH-02-18
Test Conducted by: Geodrilling		Test Date: 05.10.2018
Analysis Performed by: HLa		Analysis Date: 20.02.2019
Lithology:		

Top of Test Interval: 75,500 m
Bottom of Test Interval: 82,500 m
Length of Test Interval: 7,000 m
Depth to Groundwater: m
Radius of Test Section: 0,048 m

Step	Pressure [bar]	Flow Meter Readings [m³/s]	Average Flow Rate [m³/s]	Hydraulic Conductivity		
		1		[m/s]	[m/s]	Lugeon
1	10,0	0,000000	0,000000	$0,00 \times 10^{-1}$	$0,00 \times 10^{-1}$	0,000
2	12,0	0,000000	0,000000	$0,00 \times 10^{-1}$	$0,00 \times 10^{-1}$	0,000
3	14,0	0,000056	0,000056	$4,41 \times 10^{-8}$	$4,41 \times 10^{-8}$	0,340
4	12,0	0,000010	0,000010	$9,26 \times 10^{-9}$	$9,26 \times 10^{-9}$	0,071
5	10,0	0,000005	0,000005	$5,55 \times 10^{-9}$	$5,55 \times 10^{-9}$	0,043
			Average	$1,18 \times 10^{-8}$	$1,18 \times 10^{-8}$	0,091

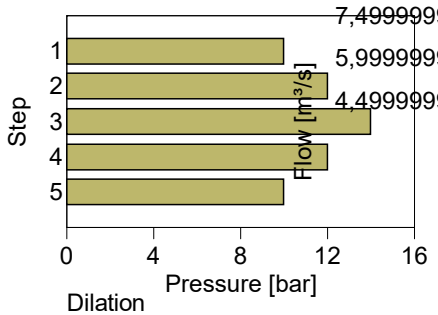

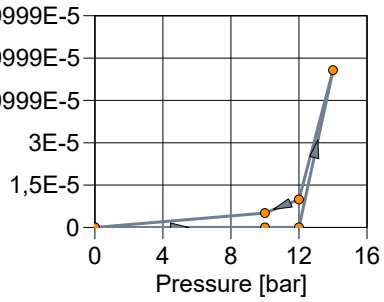

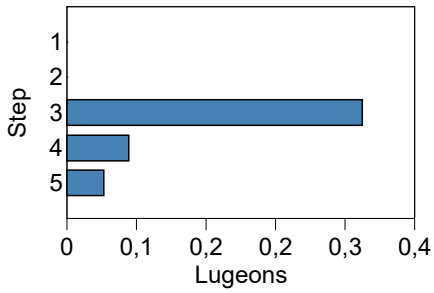

Dilation
Lugeon: 0,000
Hydraulic Conductivity: 0,00E-1 m/s
Hydraulic Conductivity: 0,00E-1 m/s

	Lugeon Test Analysis Report
	Project: Åknes
	Number: 20180662
	Client: NVE

Location: KH-02-2018	Lugeon Test: Lugeon Test 82,5-88	Tested bore: KH-02-18
Test Conducted by: Geodrilling		Test Date: 05.10.2018
Analysis Performed by: HLa		Analysis Date: 20.02.2019
Lithology:		

Top of Test Interval: 82,500 m
Bottom of Test Interval: 88,000 m
Length of Test Interval: 5,500 m
Depth to Groundwater: m
Radius of Test Section: 0,048 m

Step	Pressure [bar]	Flow Meter Readings [m³/s]	Average Flow Rate [m³/s]	Hydraulic Conductivity		
		1		[m/s]	[m/s]	Lugeon
1	10,0	0,000000	0,000000	$0,00 \times 10^{-1}$	$0,00 \times 10^{-1}$	0,000
2	12,0	0,000022	0,000022	$2,43 \times 10^{-8}$	$2,43 \times 10^{-8}$	0,197
3	14,0	0,000007	0,000007	$6,92 \times 10^{-9}$	$6,92 \times 10^{-9}$	0,056
4	12,0	0,000000	0,000000	$0,00 \times 10^{-1}$	$0,00 \times 10^{-1}$	0,000
5	10,0	0,000000	0,000000	$0,00 \times 10^{-1}$	$0,00 \times 10^{-1}$	0,000
			Average	$6,25 \times 10^{-9}$	$6,25 \times 10^{-9}$	0,051

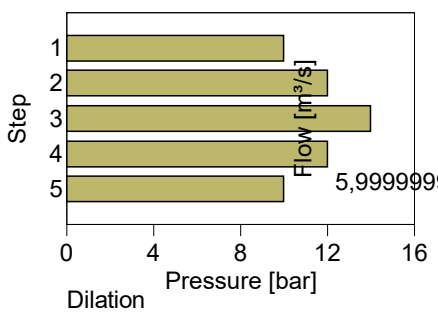

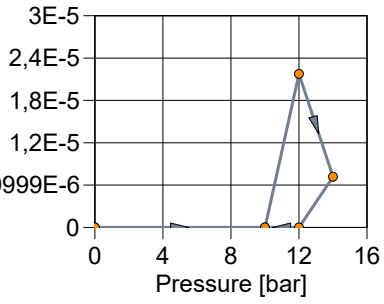

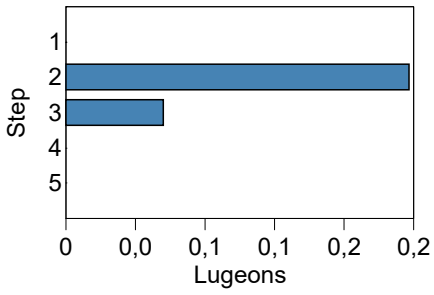

Dilation
Lugeon: 0,000
Hydraulic Conductivity: 0,00E-1 m/s
Hydraulic Conductivity: 0,00E-1 m/s

	Lugeon Test Analysis Report
	Project: Åknes
	Number: 20180662
	Client: NVE

Location: KH-02-2018	Lugeon Test: Lugeon Test 93-99	Tested bore: KH-02-18
Test Conducted by: Geodrilling		Test Date: 05.10.2018
Analysis Performed by: HLa		Analysis Date: 20.02.2019
Lithology:		

Top of Test Interval: 93,000 m
Bottom of Test Interval: 99,000 m
Length of Test Interval: 6,000 m
Depth to Groundwater: m
Radius of Test Section: 0,048 m

Step	Pressure [bar]	Flow Meter Readings [m³/s]	Average Flow Rate [m³/s]	Hydraulic Conductivity		
		1		[m/s]	[m/s]	Lugeon
1	10,0	0,000022	0,000022	$2,73 \times 10^{-8}$	$2,73 \times 10^{-8}$	0,217
2	12,0	0,000005	0,000005	$5,23 \times 10^{-9}$	$5,23 \times 10^{-9}$	0,042
3	14,0	0,000071	0,000071	$6,38 \times 10^{-8}$	$6,38 \times 10^{-8}$	0,508
4	12,0	0,000020	0,000020	$2,09 \times 10^{-8}$	$2,09 \times 10^{-8}$	0,167
5	10,0	0,000005	0,000005	$6,28 \times 10^{-9}$	$6,28 \times 10^{-9}$	0,050
			Average	$2,47 \times 10^{-8}$	$2,47 \times 10^{-8}$	0,197

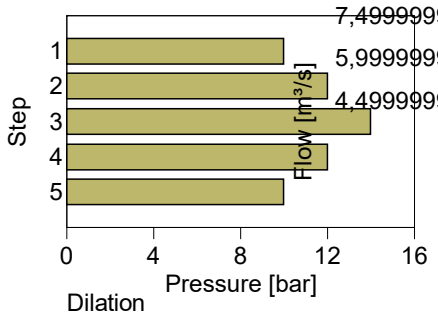

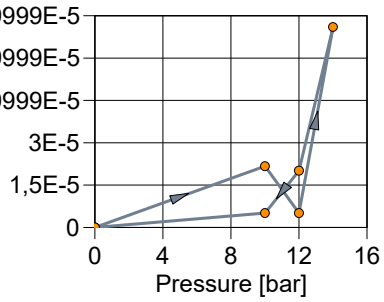

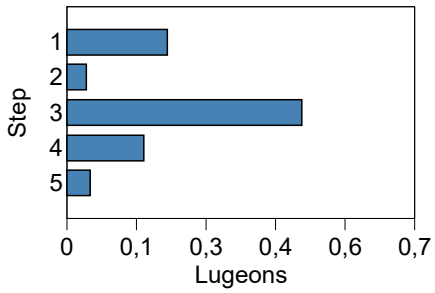

Dilation
Lugeon: 0,217
Hydraulic Conductivity: 2,73E-8 m/s
Hydraulic Conductivity: 2,73E-8 m/s

	Lugeon Test Analysis Report
	Project: Åknes
	Number: 20180662
	Client: NVE

Location: KH-02-2018	Lugeon Test: Lugeon Test 101-109,5	Tested bore: KH-02-18
Test Conducted by: Geodrilling		Test Date: 05.10.2018
Analysis Performed by: HLa		Analysis Date: 20.02.2019
Lithology:		

Top of Test Interval: 101,000 m
Bottom of Test Interval: 109,500 m
Length of Test Interval: 8,500 m
Depth to Groundwater: m
Radius of Test Section: 0,048 m

Step	Pressure [bar]	Flow Meter Readings [m³/s]	Average Flow Rate [m³/s]	Hydraulic Conductivity		
		1		[m/s]	[m/s]	Lugeon
1	10,0	0,000062	0,000062	$5{,}87 \times 10^{-8}$	$5{,}87 \times 10^{-8}$	0,436
2	12,0	0,000143	0,000143	$1{,}14 \times 10^{-7}$	$1{,}14 \times 10^{-7}$	0,843
3	14,0	0,000194	0,000194	$1{,}32 \times 10^{-7}$	$1{,}32 \times 10^{-7}$	0,980
4	12,0	0,000127	0,000127	$1{,}00 \times 10^{-7}$	$1{,}00 \times 10^{-7}$	0,745
5	10,0	0,000062	0,000062	$5{,}87 \times 10^{-8}$	$5{,}87 \times 10^{-8}$	0,436
			Average	$9{,}26 \times 10^{-8}$	$9{,}26 \times 10^{-8}$	0,688

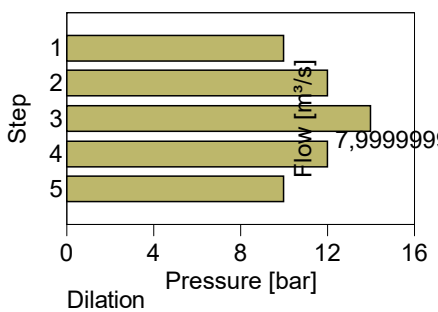

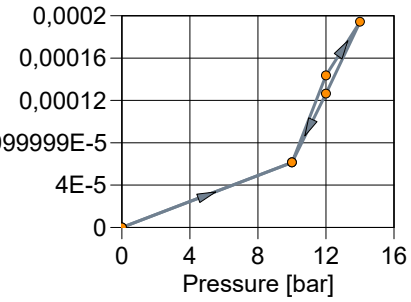

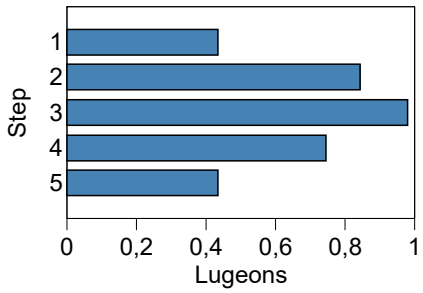

Dilation
Lugeon: 0,436
Hydraulic Conductivity: 5,87E-8 m/s
Hydraulic Conductivity: 5,87E-8 m/s

	Lugeon Test Analysis Report
	Project: Åknes
	Number: 20180662
	Client: NVE

Location: KH-02-2018	Lugeon Test: Lugeon Test 122-130,5	Tested bore: KH-02-18
Test Conducted by: Geodrilling		Test Date: 05.10.2018
Analysis Performed by: HLa		Analysis Date: 20.02.2019
Lithology:		

Top of Test Interval: 122,000 m
Bottom of Test Interval: 130,500 m
Length of Test Interval: 8,500 m
Depth to Groundwater: m
Radius of Test Section: 0,048 m

Step	Pressure [bar]	Flow Meter Readings [m³/s]	Average Flow Rate [m³/s]	Hydraulic Conductivity		
		1		[m/s]	[m/s]	Lugeon
1	10,0	0,000120	0,000120	$1{,}14 \times 10^{-7}$	$1{,}14 \times 10^{-7}$	0,847
2	12,0	0,000143	0,000143	$1{,}14 \times 10^{-7}$	$1{,}14 \times 10^{-7}$	0,843
3	14,0	0,000195	0,000195	$1{,}32 \times 10^{-7}$	$1{,}32 \times 10^{-7}$	0,983
4	12,0	0,000132	0,000132	$1{,}04 \times 10^{-7}$	$1{,}04 \times 10^{-7}$	0,775
5	10,0	0,000083	0,000083	$7{,}92 \times 10^{-8}$	$7{,}92 \times 10^{-8}$	0,588
			Average	$1{,}09 \times 10^{-7}$	$1{,}09 \times 10^{-7}$	0,807

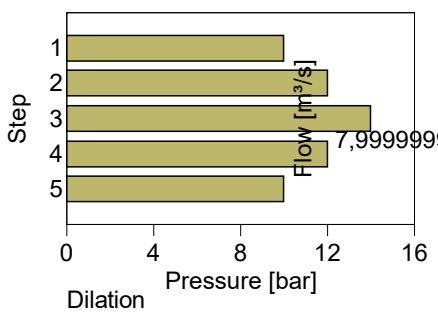

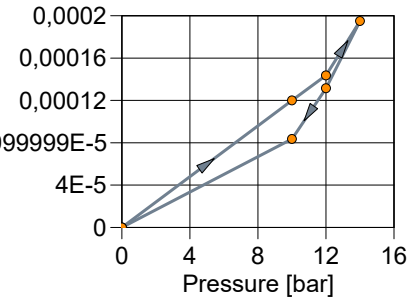

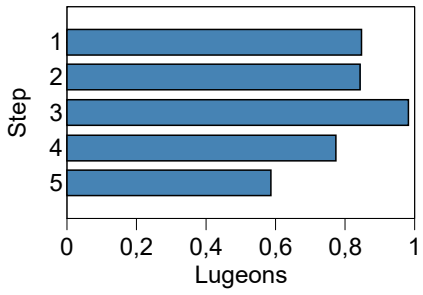

Dilation
Lugeon: 0,847
Hydraulic Conductivity: 1,14E-7 m/s
Hydraulic Conductivity: 1,14E-7 m/s

	Lugeon Test Analysis Report
	Project: Åknes
	Number: 20180662
	Client: NVE

Location: KH-02-2018	Lugeon Test: Lugeon Test 138-145	Tested bore: KH-02-18
Test Conducted by: Geodrilling		Test Date: 05.10.2018
Analysis Performed by: HLa		Analysis Date: 20.02.2019
Lithology:		

Top of Test Interval: 138,000 m
Bottom of Test Interval: 145,000 m
Length of Test Interval: 7,000 m
Depth to Groundwater: m
Radius of Test Section: 0,048 m

Step	Pressure [bar]	Flow Meter Readings [m³/s]	Average Flow Rate [m³/s]	Hydraulic Conductivity		
		1		[m/s]	[m/s]	Lugeon
1	10,0	0,000020	0,000020	$2,22 \times 10^{-8}$	$2,22 \times 10^{-8}$	0,171
2	12,0	0,000048	0,000048	$4,47 \times 10^{-8}$	$4,47 \times 10^{-8}$	0,345
3	14,0	0,000088	0,000088	$7,01 \times 10^{-8}$	$7,01 \times 10^{-8}$	0,541
4	12,0	0,000052	0,000052	$4,79 \times 10^{-8}$	$4,79 \times 10^{-8}$	0,369
5	10,0	0,000010	0,000010	$1,11 \times 10^{-8}$	$1,11 \times 10^{-8}$	0,086
			Average	$3,92 \times 10^{-8}$	$3,92 \times 10^{-8}$	0,302

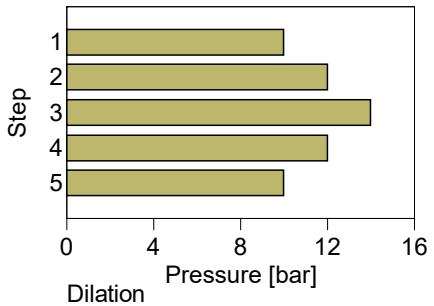

Dilation
Lugeon: 0,171
Hydraulic Conductivity: 2,22E-8 m/s
Hydraulic Conductivity: 2,22E-8 m/s

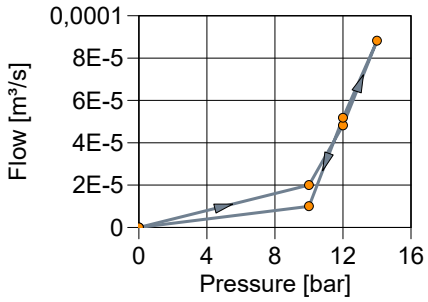

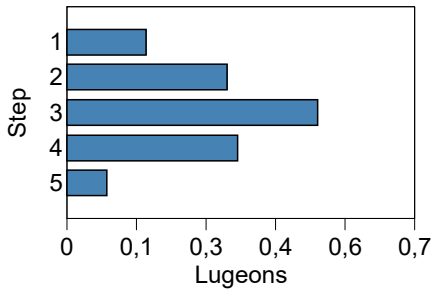

	Lugeon Test Analysis Report
	Project: Åknes
	Number: 20180662
	Client: NVE

Location: KH-02-2018	Lugeon Test: Lugeon Test 148-154	Tested bore: KH-02-18
Test Conducted by: Geodrilling		Test Date: 05.10.2018
Analysis Performed by: HLa		Analysis Date: 20.02.2019
Lithology:		

Top of Test Interval: 148,000 m
Bottom of Test Interval: 154,000 m
Length of Test Interval: 6,000 m
Depth to Groundwater: m
Radius of Test Section: 0,048 m

Step	Pressure [bar]	Flow Meter Readings [m³/s]	Average Flow Rate [m³/s]	Hydraulic Conductivity		
		1		[m/s]	[m/s]	Lugeon
1	10,0	0,000010	0,000010	$1,26 \times 10^{-8}$	$1,26 \times 10^{-8}$	0,100
2	12,0	0,000000	0,000000	$0,00 \times 10^{-1}$	$0,00 \times 10^{-1}$	0,000
3	14,0	0,000000	0,000000	$0,00 \times 10^{-1}$	$0,00 \times 10^{-1}$	0,000
4	12,0	0,000000	0,000000	$0,00 \times 10^{-1}$	$0,00 \times 10^{-1}$	0,000
5	10,0	0,000000	0,000000	$0,00 \times 10^{-1}$	$0,00 \times 10^{-1}$	0,000
			Average	$2,51 \times 10^{-9}$	$2,51 \times 10^{-9}$	0,020

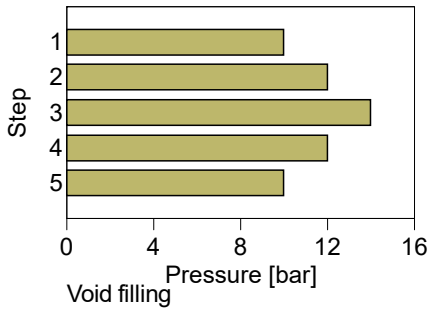

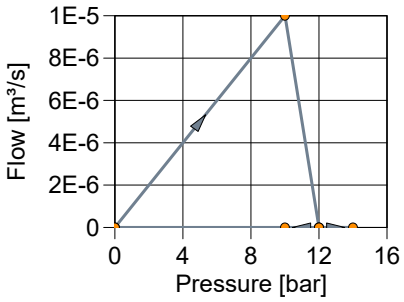

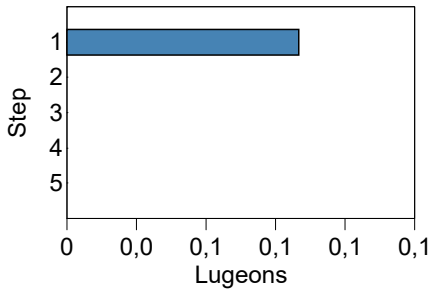

Void filling
Lugeon: 0,000
Hydraulic Conductivity: 0,00E-1 m/s
Hydraulic Conductivity: 0,00E-1 m/s

	Lugeon Test Analysis Report
	Project: Åknes
	Number: 20180662
	Client: NVE

Location: KH-02-2018	Lugeon Test: Lugeon Test 154-160	Tested bore: KH-02-18
Test Conducted by: Geodrilling		Test Date: 05.10.2018
Analysis Performed by: HLa		Analysis Date: 20.02.2019
Lithology:		

Top of Test Interval: 154,000 m
Bottom of Test Interval: 160,000 m
Length of Test Interval: 6,000 m
Depth to Groundwater: m
Radius of Test Section: 0,048 m

Step	Pressure [bar]	Flow Meter Readings [m³/s]	Average Flow Rate [m³/s]	Hydraulic Conductivity		
		1		[m/s]	[m/s]	Lugeon
1	10,0	0,000057	0,000057	$7{,}12 \times 10^{-8}$	$7{,}12 \times 10^{-8}$	0,567
2	12,0	0,000127	0,000127	$1{,}33 \times 10^{-7}$	$1{,}33 \times 10^{-7}$	1,056
3	14,0	0,000204	0,000204	$1{,}83 \times 10^{-7}$	$1{,}83 \times 10^{-7}$	1,460
4	12,0	0,000123	0,000123	$1{,}29 \times 10^{-7}$	$1{,}29 \times 10^{-7}$	1,027
5	10,0	0,000065	0,000065	$8{,}16 \times 10^{-8}$	$8{,}16 \times 10^{-8}$	0,650
			Average	$1{,}20 \times 10^{-7}$	$1{,}20 \times 10^{-7}$	0,952

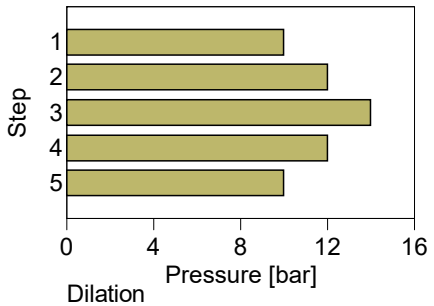

Dilation
Lugeon: 0,567
Hydraulic Conductivity: 7,12E-8 m/s
Hydraulic Conductivity: 7,12E-8 m/s

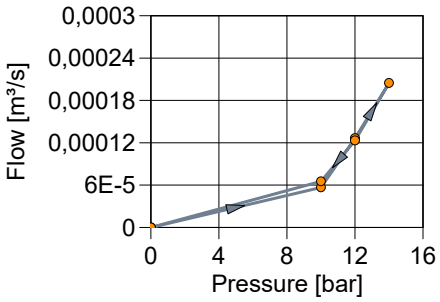

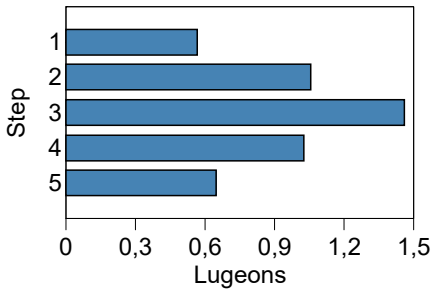

	Lugeon Test Analysis Report
	Project: Åknes
	Number: 20180662
	Client: NVE

Location: KH-02-2018	Lugeon Test: Lugeon Test 160-166	Tested bore: KH-02-18
Test Conducted by: Geodrilling		Test Date: 05.10.2018
Analysis Performed by: HLa		Analysis Date: 20.02.2019
Lithology:		

Top of Test Interval: 160,000 m
Bottom of Test Interval: 166,000 m
Length of Test Interval: 6,000 m
Depth to Groundwater: m
Radius of Test Section: 0,048 m

Step	Pressure [bar]	Flow Meter Readings [m³/s]	Average Flow Rate [m³/s]	Hydraulic Conductivity		
		1		[m/s]	[m/s]	Lugeon
1	10,0	0,000000	0,000000	$0{,}00 \times 10^{-1}$	$0{,}00 \times 10^{-1}$	0,000
2	12,0	0,000000	0,000000	$0{,}00 \times 10^{-1}$	$0{,}00 \times 10^{-1}$	0,000
3	14,0	0,000000	0,000000	$0{,}00 \times 10^{-1}$	$0{,}00 \times 10^{-1}$	0,000
4	12,0	0,000000	0,000000	$0{,}00 \times 10^{-1}$	$0{,}00 \times 10^{-1}$	0,000
5	10,0	0,000000	0,000000	$0{,}00 \times 10^{-1}$	$0{,}00 \times 10^{-1}$	0,000
			Average	$0{,}00 \times 10^{-1}$	$0{,}00 \times 10^{-1}$	0,000

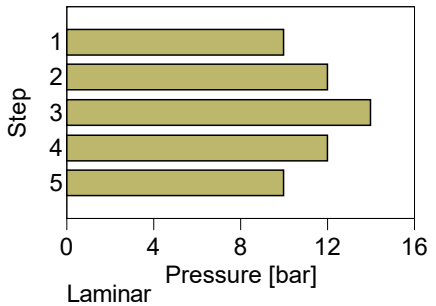

Laminar
Lugeon: 0,000
Hydraulic Conductivity: 0,00E-1 m/s
Hydraulic Conductivity: 0,00E-1 m/s

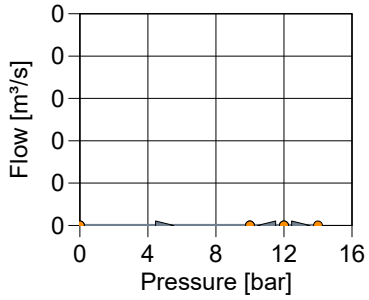

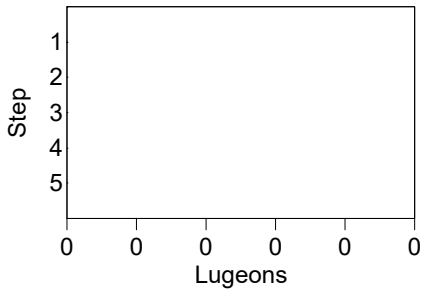

	Lugeon Test Analysis Report
	Project: Åknes
	Number: 20180662
	Client: NVE

Location: KH-02-2018	Lugeon Test: Lugeon Test 185-200	Tested bore: KH-02-18
Test Conducted by: Geodrilling		Test Date: 05.10.2018
Analysis Performed by: HLa		Analysis Date: 20.02.2019
Lithology:		

Top of Test Interval: 185,000 m
Bottom of Test Interval: 200,000 m
Length of Test Interval: 15,000 m
Depth to Groundwater: m
Radius of Test Section: 0,048 m

Step	Pressure [bar]	Flow Meter Readings [m³/s]	Average Flow Rate [m³/s]	Hydraulic Conductivity		
		1		[m/s]	[m/s]	Lugeon
1	10,0	0,000150	0,000150	$8,97 \times 10^{-8}$	$8,97 \times 10^{-8}$	0,600
2	12,0	0,000213	0,000213	$1,06 \times 10^{-7}$	$1,06 \times 10^{-7}$	0,711
3	14,0	0,000267	0,000267	$1,14 \times 10^{-7}$	$1,14 \times 10^{-7}$	0,763
4	12,0	0,000193	0,000193	$9,63 \times 10^{-8}$	$9,63 \times 10^{-8}$	0,644
5	10,0	0,000147	0,000147	$8,77 \times 10^{-8}$	$8,77 \times 10^{-8}$	0,587
			Average	$9,88 \times 10^{-8}$	$9,88 \times 10^{-8}$	0,661

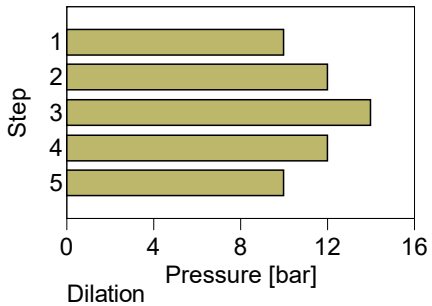

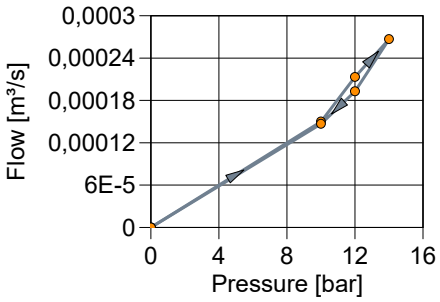

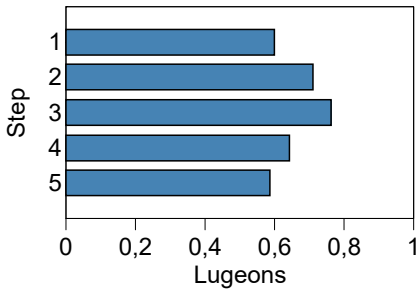

Dilation
Lugeon: 0,600
Hydraulic Conductivity: 8,97E-8 m/s
Hydraulic Conductivity: 8,97E-8 m/s

Appendix B

DETAILS ON POSITION OF PACKERS AND PIEZOMETERS IN THE FOUR BOREHOLES

DMS ROCK PLUS ÅKNES: AKN008 (BH1-17)

Depth (m)	Stratigraphy	Completation					DMS							
		Pipe	Slotted pipe	Drainage	Seals Compactonit	Grouting	I sensor	T sensor	U sensor	S100 sensor	A3 sensor	Digital Compass	Packer	Joint
1														
2							103	103			103			1
3							102	102			102			1
4							101	101			101			1
5							100	100			100			1
6							99	99			99			1
7							98	98			98			1
8							97	97			97			1
9							96	96			96			1
10							95	95			95			1
11							94	94			94			1
12							93	93		93	93			1
13							92	92			92			1
14							91	91			91			1
15							90	90			90			1
16							89	89			89			1
17							88	88			88			1
18							87	87			87			1
19							86	86			86			1
20							85	85			85			1
21							84	84			84			1
22							83	83	83		83			1
23							82	82			82			1
24							81	81			81			1
25							80	80			80			1
26							79	79			79			1
27							78	78			78		78	1
28							77	77			77			1
29							76	76		76	76			1
30							75	75	75		75			1
31							74	74			74			1
32							73	73			73		73	1
33							72	72			72			1
34							71	71			71			1
35							70	70			70			1
36							69	69	69		69			1
37							68	68			68			1
38							67	67		67	67			1
39							66	66			66			1
40							65	65			65			1
41							64	64			64			1
42							63	63			63		63	1
43							62	62			62			1
44							61	61			61			1
45							60	60			60			1
46							59	59			59			1
47							58	58			58			1
48							57	57			57			1
49							56	56	56		56			1
50							55	55			55			1
51							54	54		54	54			1
52							53	53			53			1
53							52	52			52			1
54							51	51			51			1
55							50	50			50			1
56							49	49			49			1
57							48	48			48		48	1
58							47	47			47			1
59							46	46			46			1
60							45	45			45			1
61							44	44			44			1
62							43	43			43			1
63							42	42			42			1
64							41	41			41			1
65							40	40	40		40			1
66							39	39			39			1
67							38	38		38	38			1
68							37	37			37			1
69							36	36			36			1
70							35	35			35			1
71							34	34			34			1
72							33	33			33			1
73							32	32			32			1
74							31	31			31			1
75							30	30			30			1
76							29	29			29		29	1
77							28	28			28			1
78							27	27			27			1
79							26	26	26		26			1
80							25	25		25	25			1
81							24	24			24			1
82							23	23			23		23	1
83							22	22			22			1
84							21	21			21			1
85							20	20		20	20			1
86							19	19	19		19			1
87							18	18			18			1
88							17	17			17			1
89							16	16			16			1
90							15	15			15			1
91							14	14			14		14	1
92							13	13			13			1
93							12	12			12			1
94							11	11			11			1
95							10	10			10			1
96							9	9	9		9			1
97							8	8			8			1
98							7	7			7			1
99							6	6		6	6			1
100							5	5			5			1
101							4	4			4			1
102							3	3			3		3	1
103							2	2			2			1
104							1	1	1		1			1
105							0	0			0	0		1

Sensors Legend

- I = biaxial inclinometric sensor ±45°
- 1 = twin sensor
- T = PT1000
- U = piezometric sensor range 250 psi
- S100 = linear displacement transducer 100 mm
- A3 = triaxial accelerometric sensor ±2g
- M = digital compass
- Packer
- DMS Joint 40 kN

DMS ROCK PLUS ÅKNES: AKN009 (BH2-17)

Depth (m)	Stratigraphy	Completation					DMS							
		Pipe	Slotted pipe	Drainage	Seals Compactonit	Grouting	I sensor	T sensor	U sensor	S100 sensor	A3 sensor	Digital Compass	Packer	Joint
1							129	129			129			1
2							128	128			128			1
3							127	127			127			1
4							126	126			126			1
5							125	125			125			1
6							124	124			124			1
7							123	123			123			1
8							122	122			122			1
9							121	121			121			1
10							120	120			120			1
11							119	119			119			1
12							118	118			118			1
13							117	117		117	117			1
14							116	116			116			1
15							115	115			115			1
16							114	114			114			1
17							113	113			113			1
18							112	112			112			1
19							111	111			111			1
20							110	110			110			1
21							109	109			109			1
22							108	108			108			1
23							107	107			107			1
24							106	106	106		106			1
25							105	105			105			1
26							104	104			104			1
27							103	103			103			1
28							102	102			102		102	1
29							101	101			101			1
30							100	100			100			1
31							99	99			99			1
32							98	98	98		98			1
33							97	97		97	97			1
34							96	96			96			1
35							95	95			95			1
36							94	94			94			1
37							93	93			93			1
38							92	92			92		92	1
39							91	91			91			1
40							90	90	90		90			1
41							89	89		89	89			1
42							88	88			88			1
43							87	87			87			1
44							86	86			86		86	1
45							85	85			85			1
46							84	84	84		84			1
47							83	83		83	83			1
48							82	82			82			1
49							81	81			81			1
50							80	80			80			1
51							79	79			79			1
52							78	78			78		78	1
53							77	77			77			1
54							76	76			76			1
55							75	75			75			1
56							74	74			74			1
57							73	73	73		73			1
58							72	72		72	72			1
59							71	71			71			1
60							70	70			70			1
61							69	69			69			1
62							68	68			68			1
63							67	67			67		67	1
64							66	66			66			1
65	?						65	65			65			1
66							64	64			64			1
67							63	63	63		63			1
68							62	62		62	62			1
69							61	61			61			1
70							60	60			60			1
71							59	59			59			1
72							58	58			58			1
73							57	57			57		57	1
74							56	56			56			1
75							55	55			55			1
76							54	54			54			1
77							53	53			53			1
78							52	52	52		52			1
79							51	51			51			1
80							50	50		50	50			1
81							49	49			49			1
82							48	48			48			1
83							47	47			47			1
84							46	46			46			1
85							45	45			45		45	1
86							44	44			44			1
87							43	43			43			1
88							42	42	42		42			1
89							41	41		41	41			1
90							40	40			40			1
91							39	39			39			1
92							38	38			38		38	1
93							37	37			37			1
94							36	36			36			1
95							35	35			35			1
96							34	34			34			1
97							33	33			33			1
98							32	32			32			1
99							31	31			31			1
100							30	30			30			1
101							29	29	29		29			1
102							28	28			28			1
103							27	27			27			1
104							26	26		26	26			1
105							25	25			25			1
106							24	24			24			1
107							23	23			23			1
108							22	22			22			1
109							21	21			21			1
110							20	20			20			1
111							19	19			19			1
112							18	18			18			1
113							17	17			17			1
114							16	16			16			1
115							15	15			15			1
116							14	14			14		14	1
117							13	13			13			1
118							12	12			12			1
119							11	11			11			1
120							10	10			10			1
121							9	9	9		9			1
122							8	8		8	8			1
123							7	7			7			1
124							6	6			6			1
125							5	5			5			1
126							4	4			4		4	1
127							3	3			3			1
128							2	2			2			1
129							1	1	1		1			1
130							0	0			0	0		1

Sensors Legend

- I = biaxial inclinometric sensor ±45°
- T = PT1000
- U = piezometric sensor range 250 psi
- S100 = linear displacement transducer 100 mm
- A3 = triaxial accelerometric sensor ±2g
- M = digital compass
- Packer
- DMS Joint 40 kN
- twin sensor

DMS ROCK PLUS ÅKNES: AKN010 1960 flank (BH01-18)

Depth (m)	Stratigraphy	Completation					DMS								
		Pipe	Slotted pipe	Drainage	Seals Compactonit	Grouting	I sensor	T sensor	U sensor	S100 sensor	A3 sensor	Digital Compass	Packer	Joint	Modular extension
1							105	105			105			1	
2							104	104			104			1	
3							103	103			103			1	
4							102	102			102			1	
5							101	101			101			1	
6							100	100			100			1	
7							99	99			99			1	
8							98	98			98			1	
9							97	97			97			1	
10							96	96			96			1	
11							95	95			95			1	
12							94	94			94			1	
13							93	93		93	93			1	
14							92	92			92			1	
15							91	91			91			1	
16							90	90			90			1	
17							89	89			89			1	
18							88	88			88			1	
19							87	87			87			1	
20							86	86			86			1	
21							85	85			85			1	
22							84	84			84			1	
23							83	83			83			1	
24							82	82	82		82			1	
25							81	81			81		81	1	
26							80	80			80			1	
27							79	79			79			1	
28							78	78			78			1	
29							77	77			77			1	
30							76	76			76			1	
31							75	75			75			1	
32							74	74			74			1	
33							73	73		73	73			1	
34							72	72			72			1	
35							71	71			71			1	
36							70	70			70			1	
37							69	69			69			1	
38							68	68			68			1	
39							67	67			67			1	
40							66	66			66			1	
41							65	65			65			1	
42							64	64			64			1	
43							63	63	63		63			1	
44							62	62			62		62	1	
45							61	61			61			1	
46							60	60			60			1	
47							59	59			59			1	
48							58	58		58	58			1	
49							57	57			57			1	
50							56	56			56			1	
51							55	55			55			1	
52							54	54			54			1	
53							53	53	53		53			1	
54							52	52			52		52	1	
55							51	51			51			1	
56							50	50			50			1	
57							49	49			49			1	
58							48	48		48	48			1	
59							47	47			47			1	
60							46	46			46			1	
61							45	45	45		45			1	
62							44	44			44		44	1	
63							43	43			43			1	
64							42	42			42			1	
65							41	41			41			1	
66							40	40			40			1	
67							39	39			39			1	
68							38	38			38			1	
69							37	37			37			1	
70							36	36			36			1	
71							35	35		35	35			1	
72							34	34			34			1	
73							33	33			33			1	
74							32	32			32			1	
75							31	31			31			1	
76							30	30			30			1	
77							29	29			29			1	
78							28	28			28			1	
79							27	27			27			1	
80							26	26	26		26			1	
81							25	25			25		25	1	
82							24	24			24			1	
83							23	23			23			1	
84							22	22			22			1	
85							21	21			21			1	
86							20	20			20			1	
87							19	19		19	19			1	
88							18	18			18			1	
89							17	17			17			1	
90							16	16			16			1	
91							15	15			15			1	
92							14	14			14			1	
93							13	13			13			1	
94							12	12	12		12			1	
95							11	11			11		11	1	
96														1	1
97														1	1
98														1	1
99														1	1
100														1	1
101														1	1
102														1	1
103														1	1
104														1	1
105														1	1
106														1	1
107														1	1
108														1	1
109														1	1
110														1	1
111														1	1
112														1	1
113							10	10		10	10			1	
114														1	1
115														1	1
116														1	1
117														1	1
118														1	1
119														1	1
120														1	1
121														1	1
122														1	1
123														1	1
124														1	1
125														1	1
126														1	1
127														1	1
128														1	1
129														1	1
130														1	1
131														1	1
132														1	1
133														1	1
134														1	1
135														1	1
136														1	1
137							9	9	9		9			1	
138							8	8			8		8	1	
139														1	1
140														1	1
141														1	1
142														1	1
143														1	1
144														1	1
145							7	7		7	7			1	
146														1	1
147														1	1
148														1	1
149														1	1
150														1	1
151														1	1
152														1	1
153							6	6	6		6			1	
154							5	5			5		5	1	
155														1	1
156							4	4		4	4			1	
157														1	1
158														1	1
159														1	1
160														1	1
161														1	1
162														1	1
163														1	1
164														1	1
165														1	1
166														1	1
167														1	1
168														1	1
169														1	1
170														1	1
171														1	1
172														1	1
173														1	1
174														1	1
175														1	1
176														1	1
177														1	1
178														1	1
179														1	1
180														1	1
181														1	1
182														1	1
183														1	1
184														1	1
185														1	1
186														1	1
187							3	3	3		3			1	
188							2	2			2		2	1	
189							1	1	1		1			1	
190							0	0			0	0		1	

Sensors Legend

- I = biaxial inclinometric sensor ±45°
- *twin sensor
- T = PT1000
- U = piezometric sensor range 250 psi
- S100 = linear displacement transducer 100 mm
- A3 = triaxial accelerometric sensor ±2g
- M = digital compass
- Pneumatic packer
- DMS Joint 40 kN
- Modular extension

DMS ROCK PLUS ÅKNES: AKN011 (BH-02-18)

Depth (m)	Stratigraphy	Completation					DMS								
		Pipe	Slotted pipe	Drainage	Seals Compactonit	Grouting	I sensor	T sensor	U sensor	S100 sensor	A3 sensor	Digital Compass	Packer	Joint	Modular extension
1							153	153			153			1	
2							152	152			152			1	
3							151	151			151			1	
4							150	150			150			1	
5							149	149			149			1	
6							148	148			148			1	
7							147	147			147			1	
8							146	146			146			1	
9							145	145			145			1	
10							144	144			144			1	
11							143	143			143			1	
12							142	142			142			1	
13							141	141		141	141			1	
14							140	140			140			1	
15							139	139			139			1	
16							138	138			138			1	
17							137	137			137			1	
18							136	136			136			1	
19							135	135			135			1	
20							134	134	134		134			1	
21							133	133			133		133	1	
22							132	132			132			1	
23							131	131			131			1	
24							130	130			130			1	
25							129	129			129			1	
26							128	128			128			1	
27							127	127			127			1	
28							126	126			126			1	
29							125	125			125			1	
30							124	124			124			1	
31							123	123			123			1	
32							122	122			122			1	
33							121	121		121	121			1	
34							120	120			120			1	
35							119	119			119			1	
36							118	118			118			1	
37							117	117			117			1	
38							116	116			116			1	
39							115	115			115			1	
40							114	114			114			1	
41							113	113			113			1	
42							112	112	112		112			1	
43							111	111			111		111	1	
44							110	110			110			1	
45							109	109			109			1	
46							108	108			108			1	
47							107	107			107			1	
48							106	106			106			1	
49							105	105			105			1	
50							104	104		104	104			1	
51							103	103			103			1	
52							102	102			102			1	
53							101	101			101			1	
54							100	100			100			1	
55							99	99			99			1	
56							98	98			98			1	
57							97	97	97		97			1	
58							96	96			96		96	1	
59							95	95			95			1	
60							94	94			94			1	
61							93	93			93			1	
62							92	92			92			1	
63							91	91		91	91			1	
64							90	90			90			1	
65							89	89			89			1	
66							88	88			88			1	
67							87	87	87		87			1	
68							86	86			86		86	1	
69							85	85			85			1	
70							84	84			84			1	
71							83	83			83			1	
72							82	82			82			1	
73							81	81			81			1	
74							80	80			80			1	
75							79	79			79			1	
76							78	78			78			1	
77							77	77			77			1	
78							76	76		76	76			1	
79							75	75			75			1	
80							74	74			74			1	
81							73	73			73			1	
82							72	72			72			1	
83							71	71			71			1	
84							70	70			70			1	
85							69	69			69			1	
86							68	68			68			1	
87							67	67	67		67			1	
88							66	66			66		66	1	
89							65	65			65			1	
90							64	64			64			1	
91							63	63			63			1	
92							62	62			62			1	
93							61	61			61			1	
94							60	60			60			1	
95							59	59			59			1	
96							58	58			58			1	
97							57	57			57			1	
98							56	56			56			1	
99							55	55			55			1	
100							54	54			54			1	
101							53	53		53	53			1	
102							52	52			52			1	
103							51	51			51			1	
104							50	50			50			1	
105							49	49			49			1	
106							48	48			48			1	
107							47	47			47			1	
108							46	46			46			1	
109							45	45			45			1	
110							44	44			44			1	
111							43	43	43		43			1	
112							42	42			42		42	1	
113							41	41			41			1	
114							40	40			40			1	
115							39	39			39			1	
116							38	38			38			1	
117							37	37			37			1	
118							36	36			36			1	
119							35	35		35	35			1	
120							34	34			34			1	
121							33	33			33			1	
122							32	32			32			1	
123							31	31			31			1	
124							30	30			30			1	
125							29	29			29			1	
126							28	28			28			1	
127							27	27	27		27			1	
128							26	26			26		26	1	
129							25	25			25			1	
130							24	24			24			1	
131							23	23			23			1	
132							22	22		22	22			1	
133							21	21			21			1	
134							20	20			20			1	
135							19	19			19			1	
136							18	18	18		18			1	
137							17	17			17		17	1	
138							16	16			16			1	
139							15	15			15			1	
140							14	14			14			1	
141							13	13		13	13			1	
142							12	12			12			1	
143							11	11			11			1	
144							10	10			10			1	
145							9	9	9		9			1	
146							8	8			8		8	1	
147														1	1
148														1	1
149														1	1
150														1	1
151							7	7		7	7			1	
152														1	1
153														1	1
154														1	1
155														1	1
156														1	1
157														1	1
158							6	6	6		6			1	
159							5	5			5		5	1	
160														1	1
161														1	1
162														1	1
163							4	4		4	4			1	
164														1	1
165														1	1
166														1	1
167														1	1
168							3	3	3		3			1	
169							2	2			2		2	1	
170							1	1	1		1			1	
171							0	0			0	0		1	

Sensors Legend

- I = biaxial inclinometric sensor ±45°
- T = PT1000
- U = piezometric sensor range 250 psi
- S100 = linear displacement transducer 100 mm
- A3 = triaxial accelerometric sensor ±2g
- M = digital compass
- Pneumatic packer
- DMS Joint 40 kN
- Modular extension
- *twin sensor

Appendix C

WATER PRESSURE VARIATION VERSUS PRECIPITATION IN THE BOREHOLES FROM 2017 AND 2018

Water pressure variation versus precipitation in borehole KH-01-17.

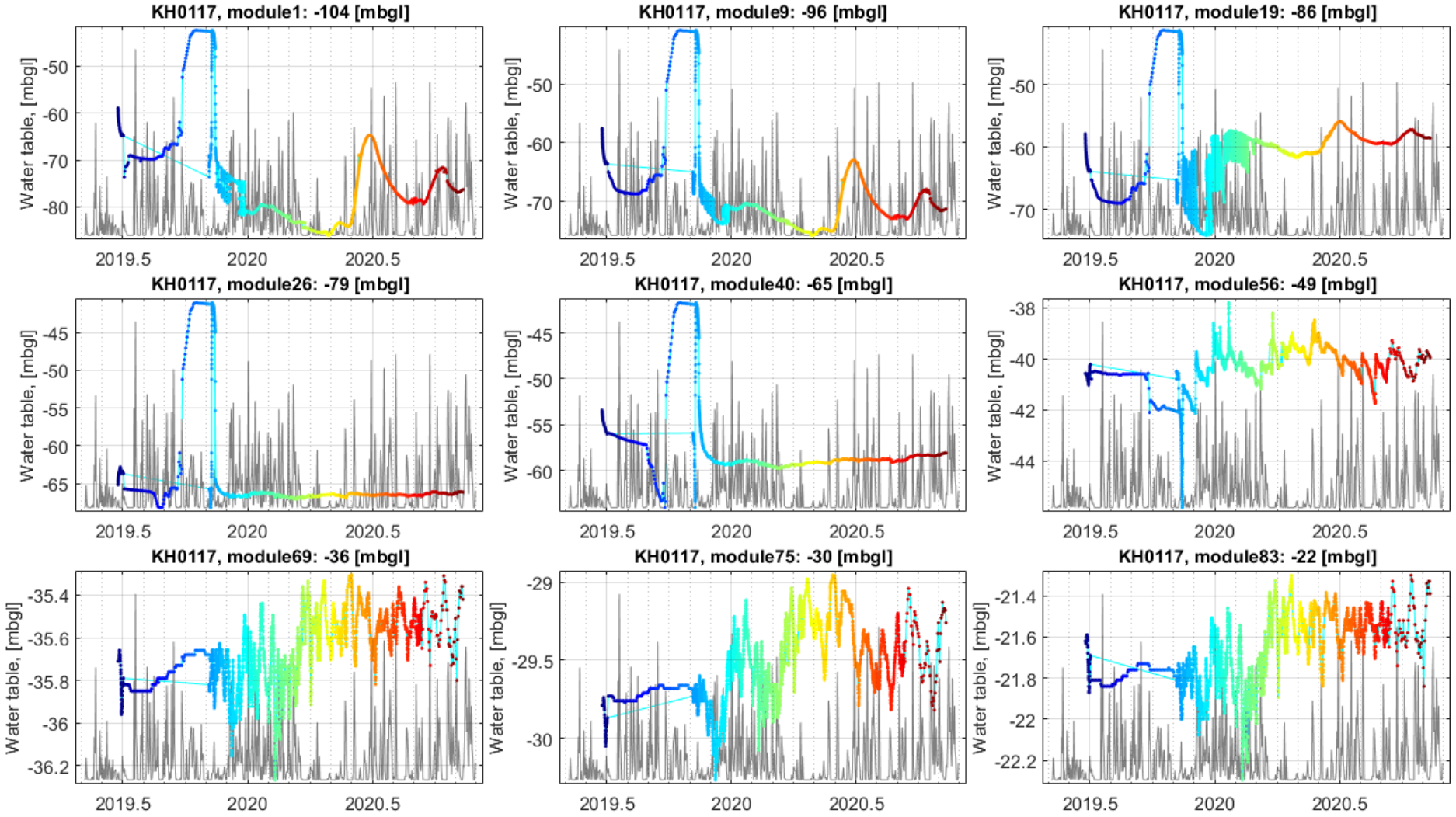

Water pressure variation versus precipitation in borehole KH-02-17.

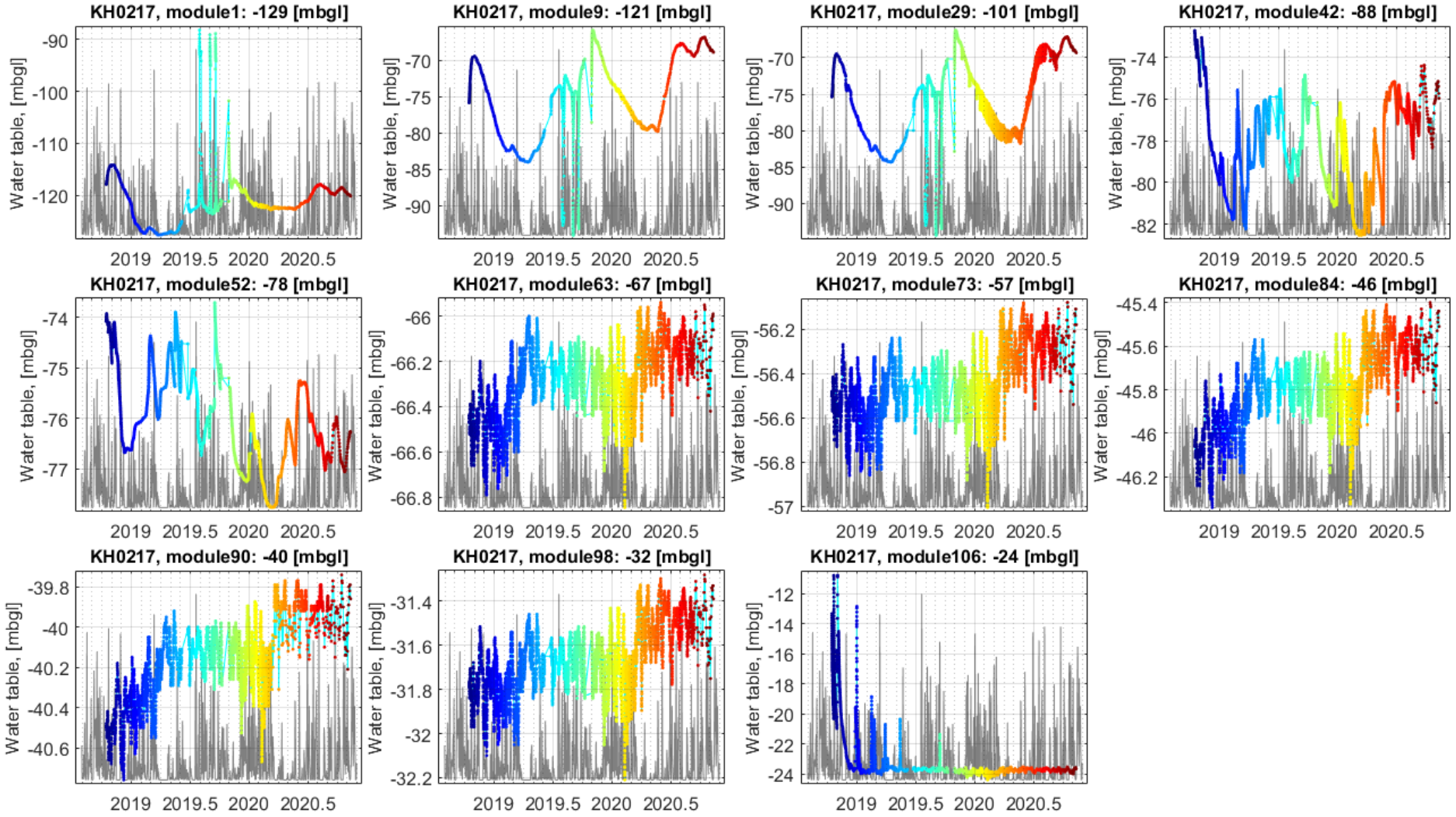

Water pressure variation versus precipitation in borehole KH-01-18.

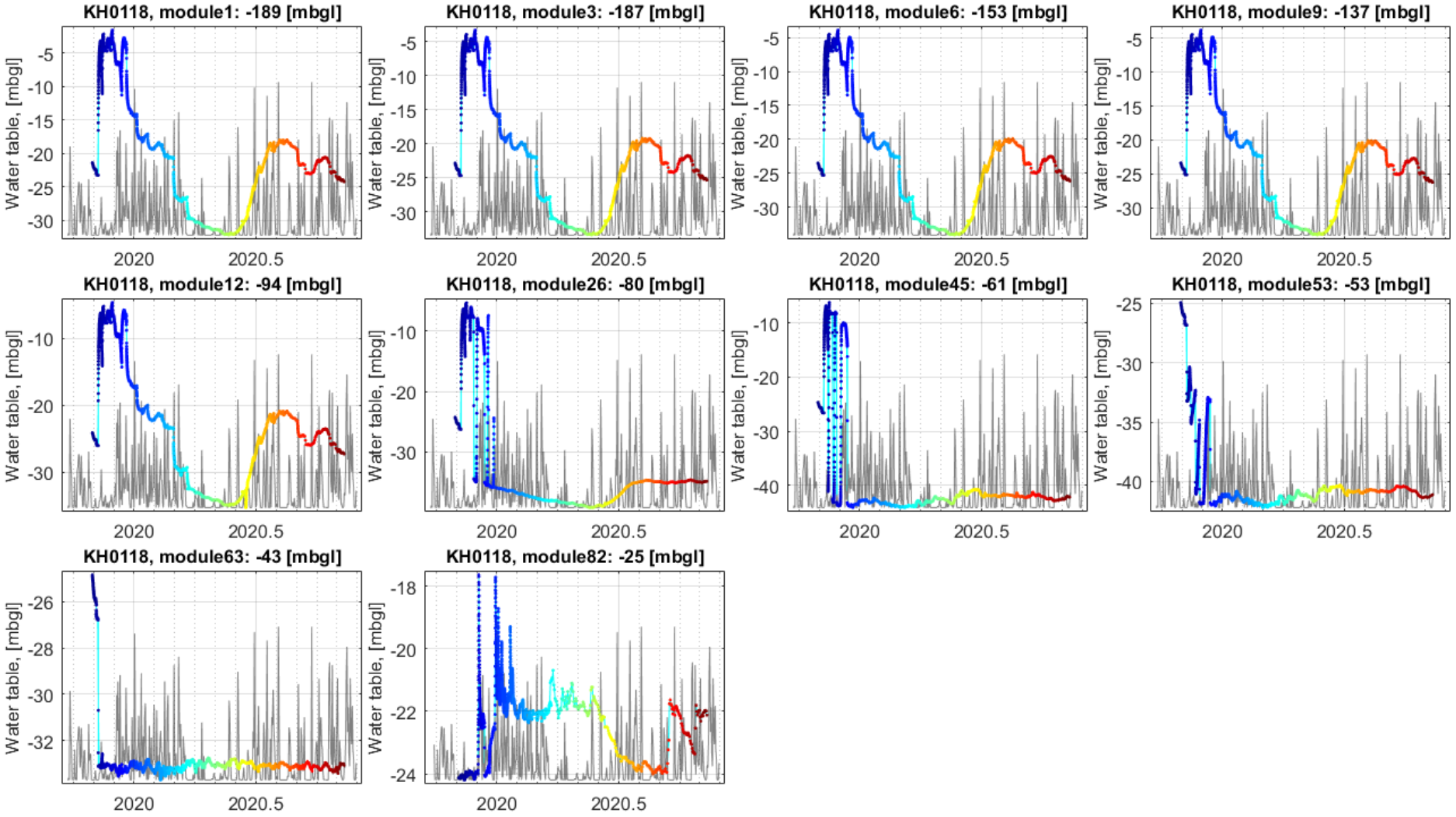

Water pressure variation versus precipitation in borehole KH-02-18.

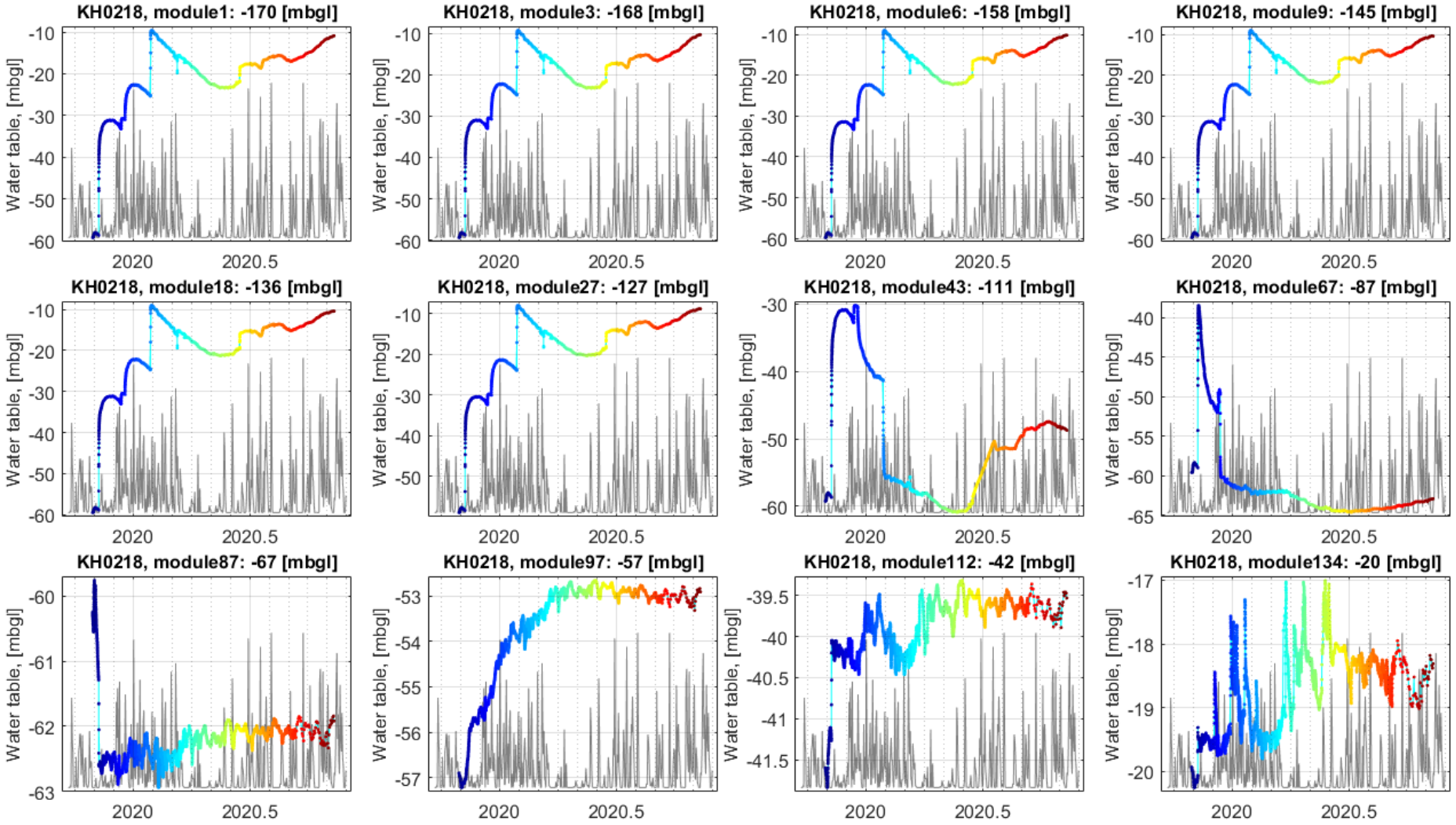

Appendix D

ILLUSTRATION OF PROFILE W2

Illustration of profile W2 – with approximate location of two sliding planes and positioning of packers, piezometers and Lugeon-measurements (in magenta):

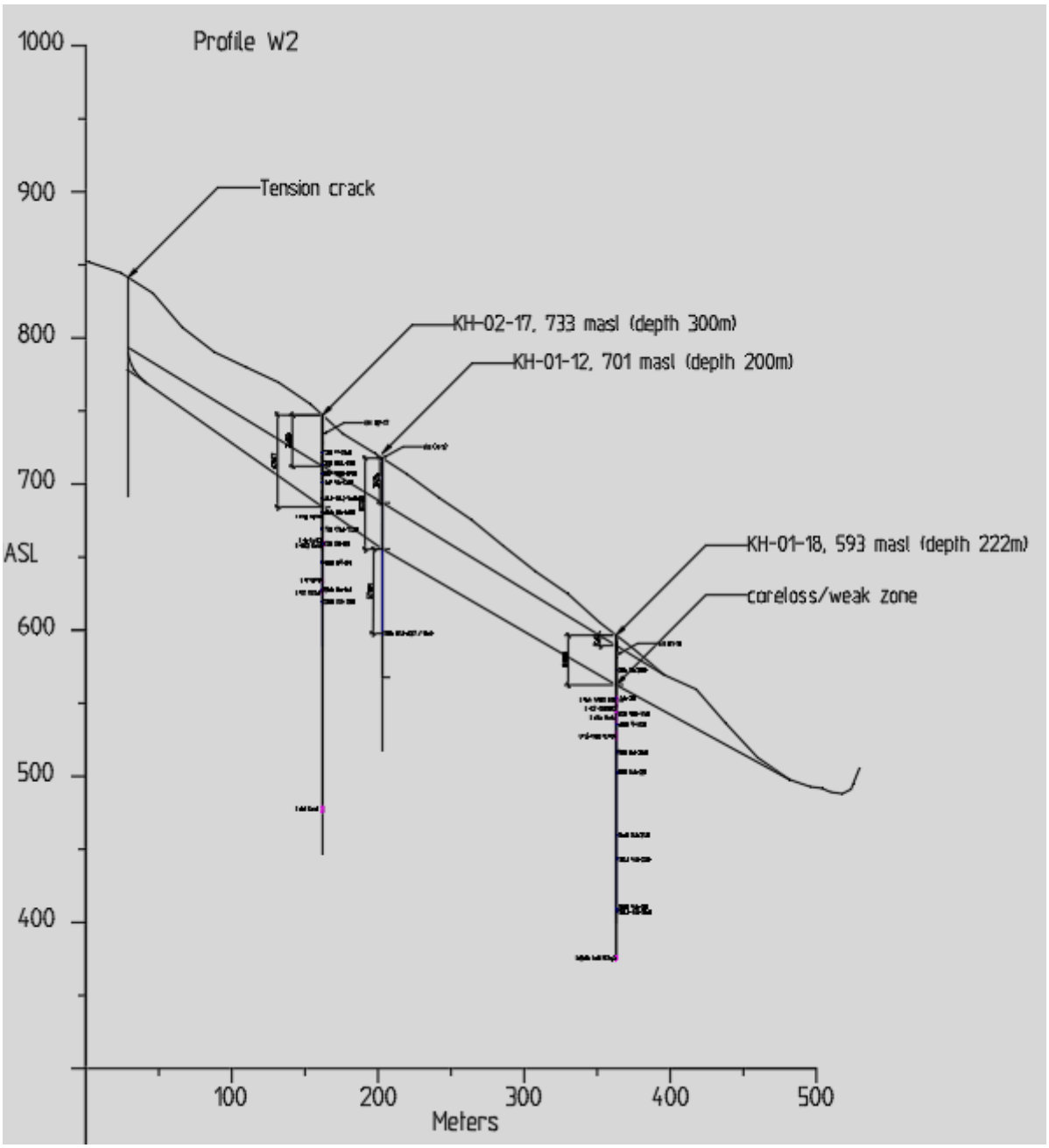

Details from profile W2 with focus on borehole KH-02-17

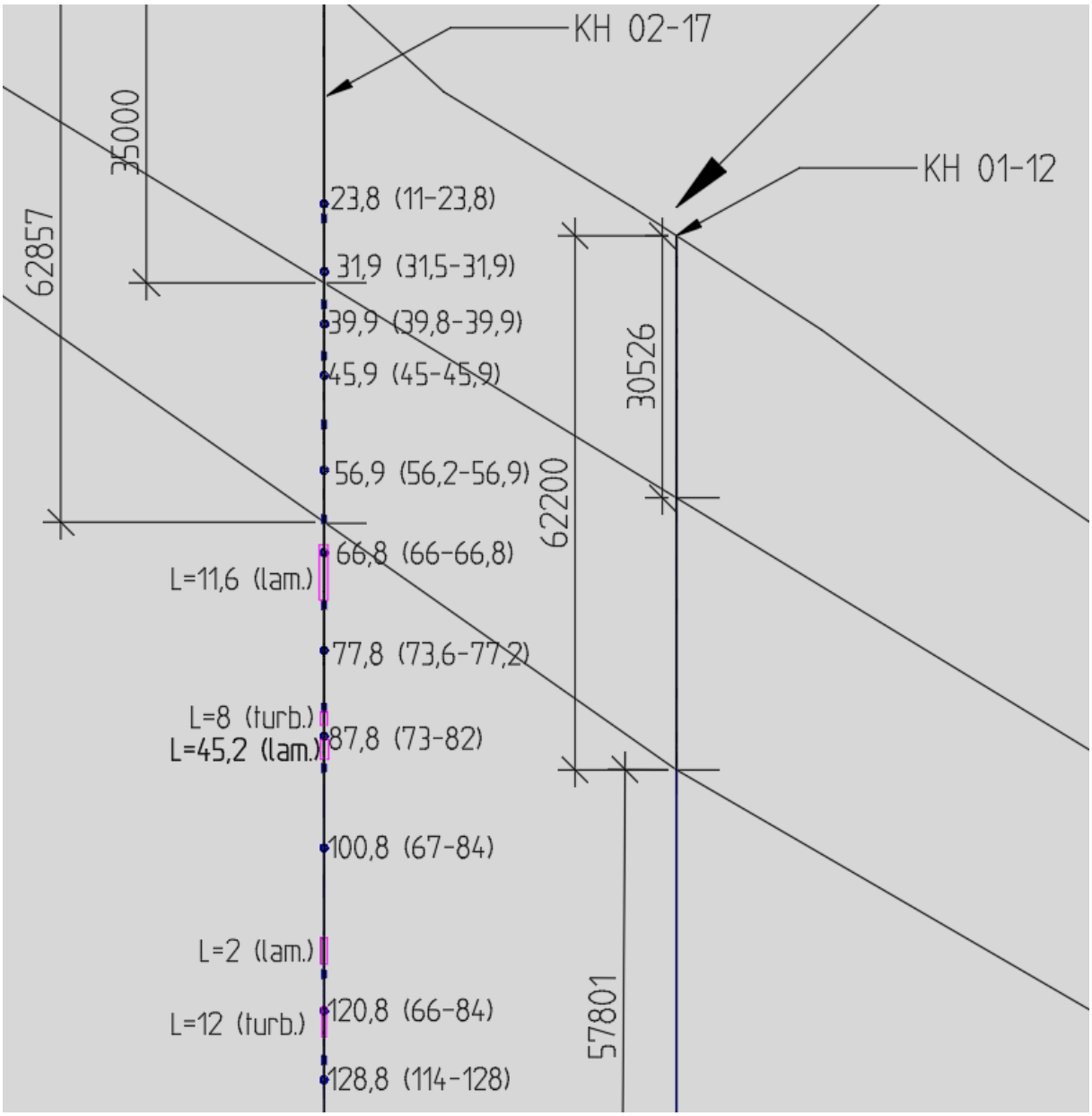

Details from profile W2 with focus on borehole KH-01-18

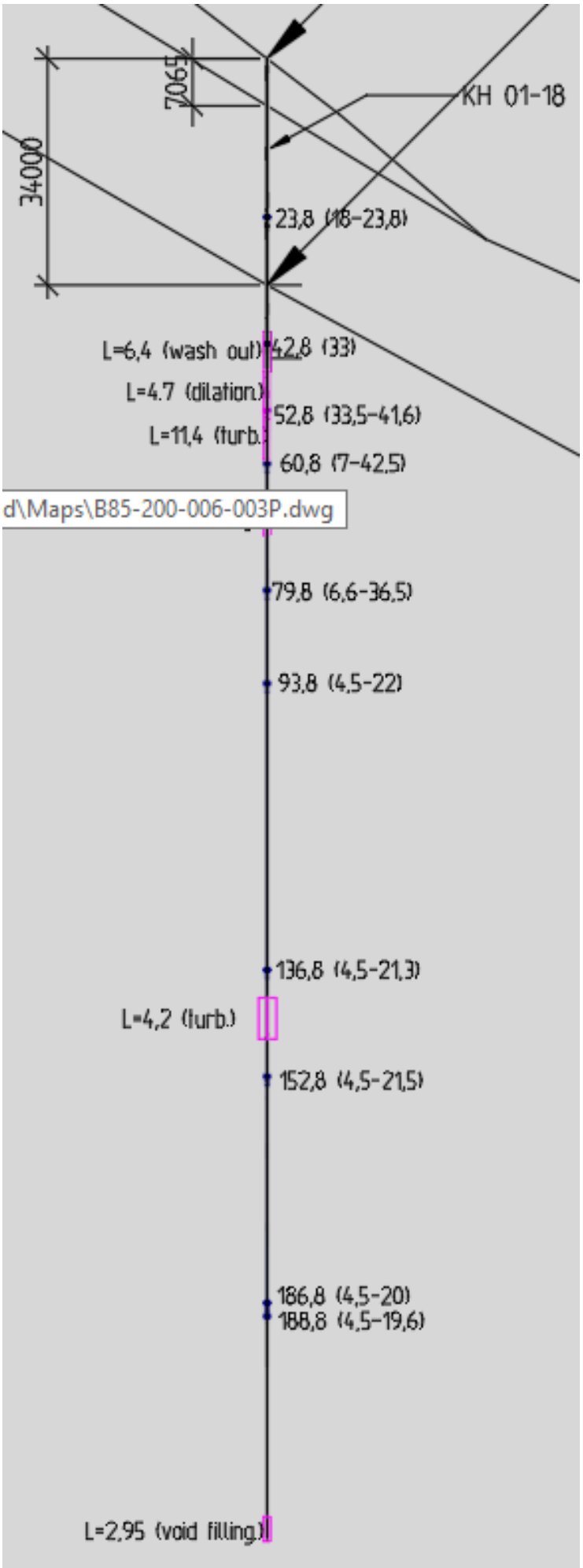
7065
34000
KH 01-18
23,8 (18-23,8)
L=6,4 (wash out)
42,8 (33)
L=4.7 (dilation)
52,8 (33,5-41,6)
L=11,4 (turb.)
60,8 (7-42,5)
d\Maps\B85-200-006-003P.dwg
79,8 (6,6-36,5)
93,8 (4,5-22)
136,8 (4,5-21,3)
L=4,2 (turb.)
152,8 (4,5-21,5)
186,8 (4,5-20)
188,8 (4,5-19,6)
L=2,95 (void filling)

Appendix E

WEATHER DATA: PRECIPITATION AND TEMPERATURE

1 Precipitation

A detailed analysis of the effect of temperature, and the implications on Åknes for e.g. freezing and thawing is not done.

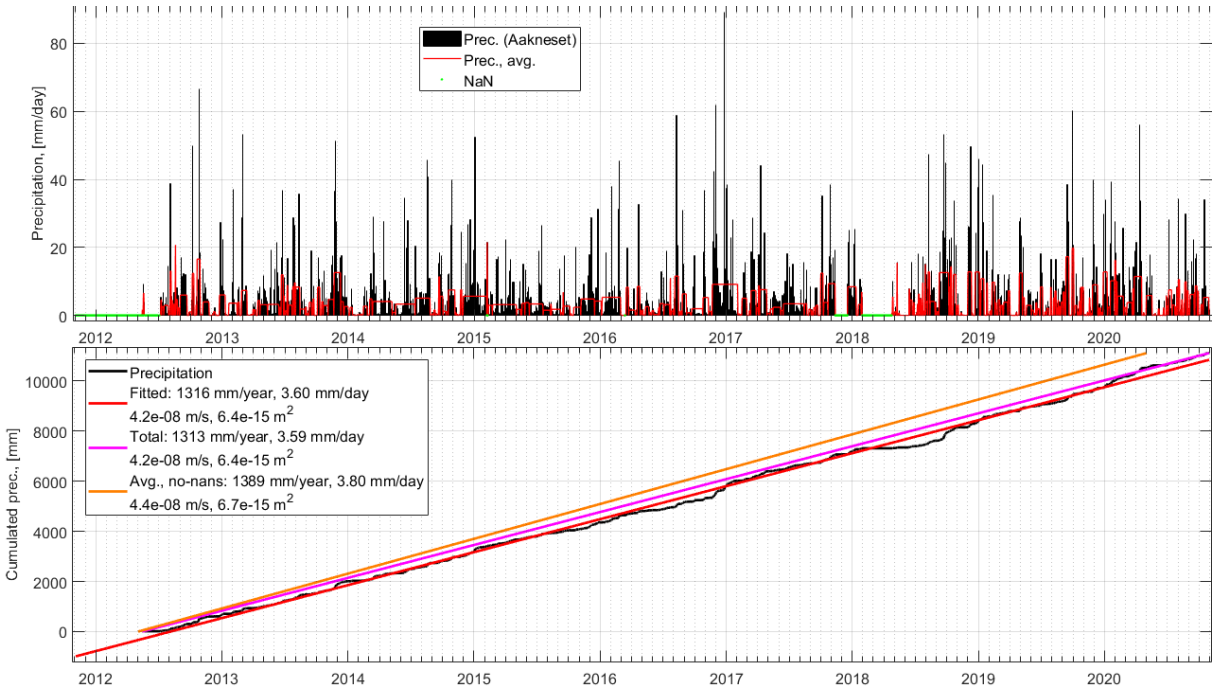

Figure 1.1. Precipitation at Åknes. Top figure is a bar plot of the daily precipitation levels at Åknes, the green dots represents missing data and the thin red lines outlines the average precipitation of continuous periods of rain (precipitation more than 0.1 mm/day).

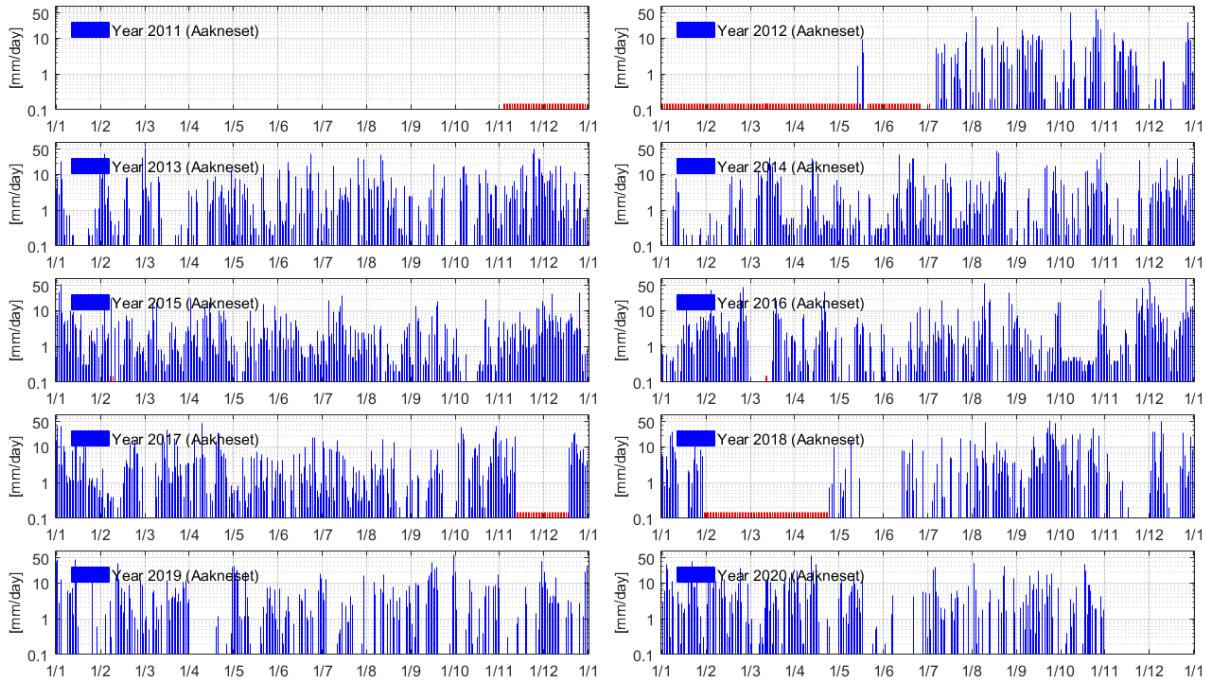

Figure 1.2. Daily precipitation from Åknes. Note that the precipitation is in logarithmic scale. Red bars indicate missing data.

2 Temperature

Temperature data is available at eKlima (web-page moderated by MET.no). The temperature and precipitation from Åknes are recorded at station number 60240 (latitude 62.191 and longitude 6.9933) at 900 m elevation with recordings from October 2011. The temperature can be fitted to the correlation:

$$T = T_{mean} + T_{amp}\sin(2\pi t - \theta) \qquad Eq.\ 1$$

where t is the fraction of a year.

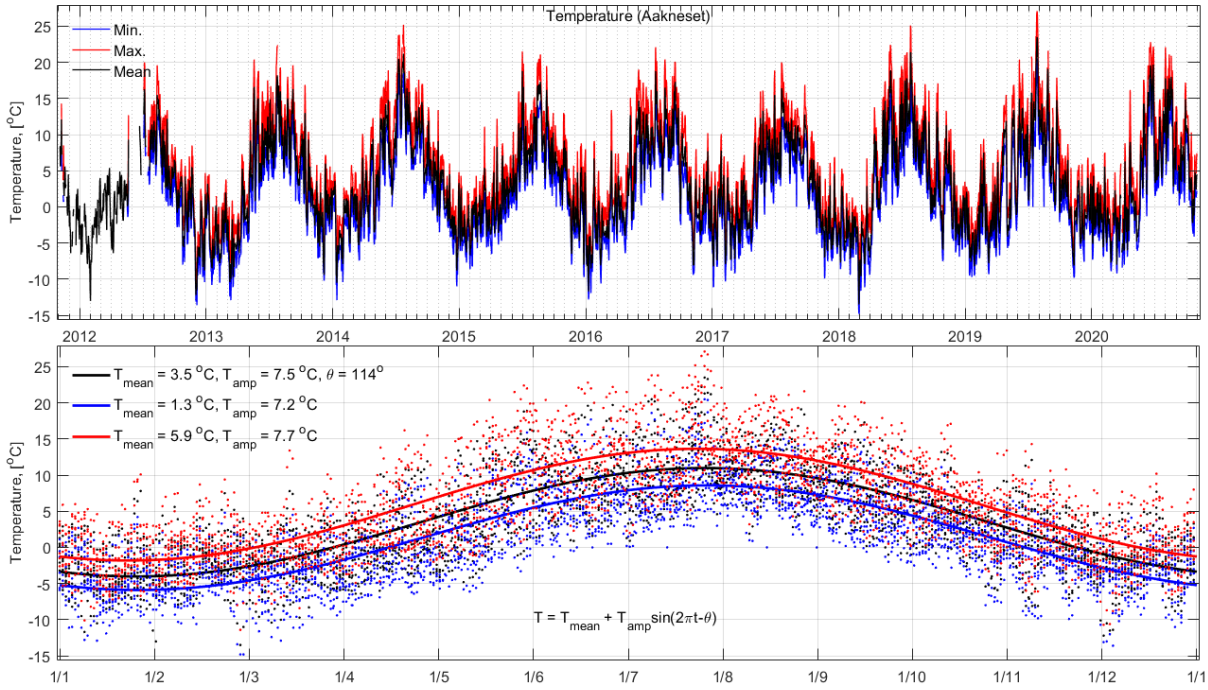

Figure 2.1. Temperature evolution in Åknes (900 m elevation): daily mean temperature (black), daily minimum (blue) and daily maximum temperature (red). Bottom: All timeseries-data plotted together and fitted to a seasonal variation.

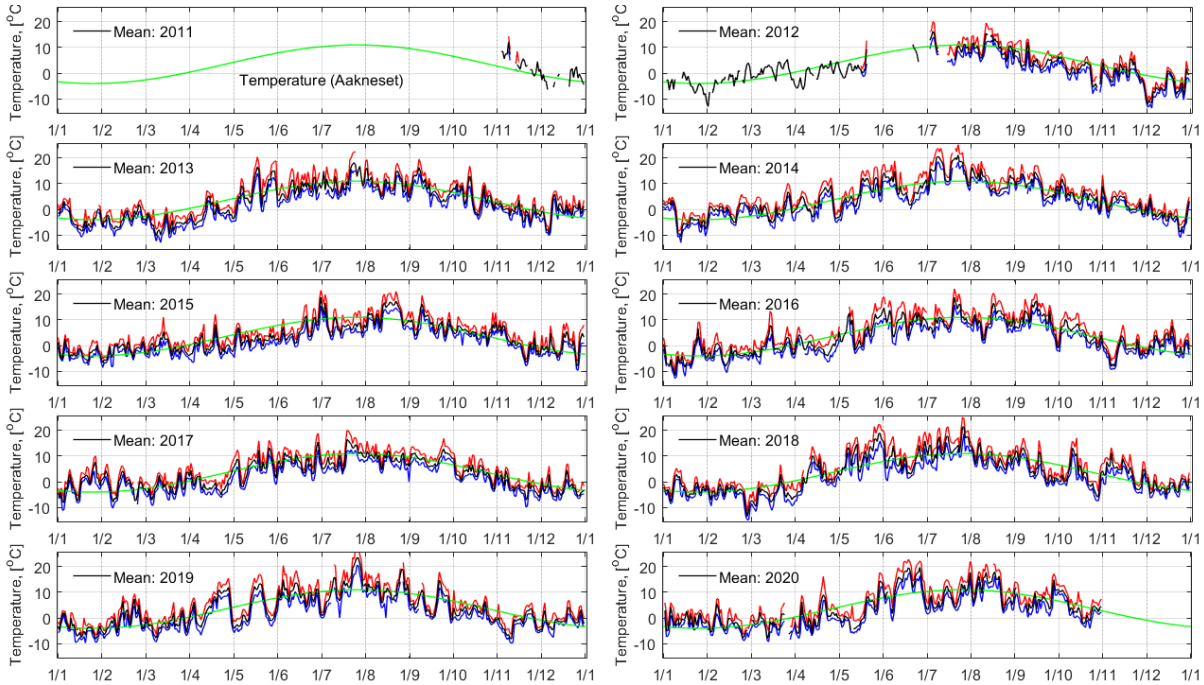

Figure 2.2. Annual temperature from Åknes (900 m elevation): daily mean temperature (black), daily minimum (blue) and daily maximum temperature (red).

The average temperature at 900 m above sea level is app. 3.5 °C with a seasonal amplitude of ±7.5 °C. The recorded daily temperatures show a large variation, up to 20 °C temperature change, over short periods of time.

Appendix F

HYDRAULIC CONDUCTIVITY AND FRACTURE STATISTICS

1 Hydraulic conductivity and fracture statistics

Statistics of the Lugeon-tests from wells KH-02-17, KH-01-18 and KH-02-18, and fracture frequency of various boreholes based on core logging and televiewer data (from NGU and NGI reports, 2007 until 2019).

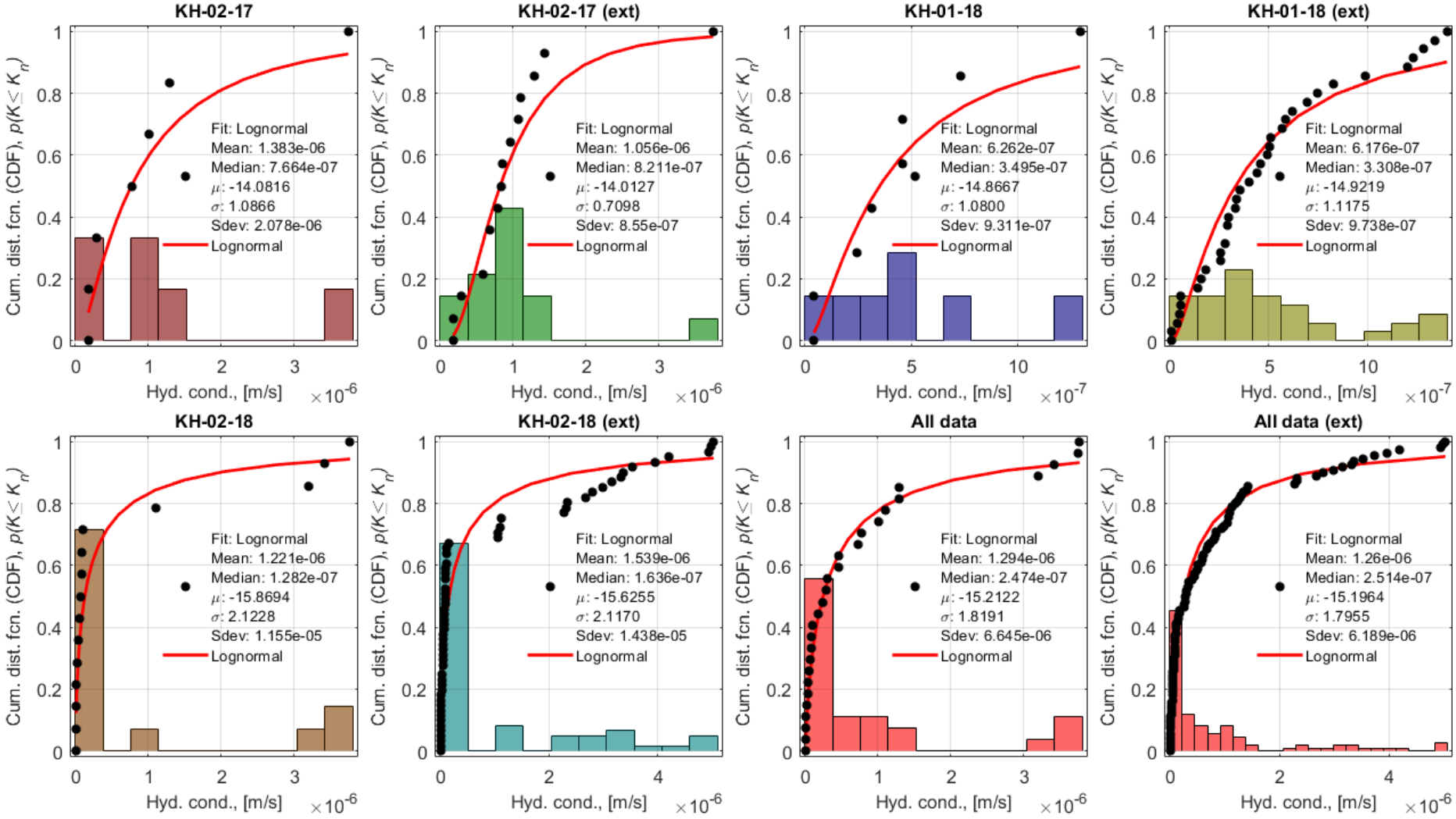

Figure 1. Bar plot of hydraulic conductivity fitted to a log-normal cumulative distribution function. The plots with (ext.) in the title contain all the measurement data in every Lugeon-test interval.

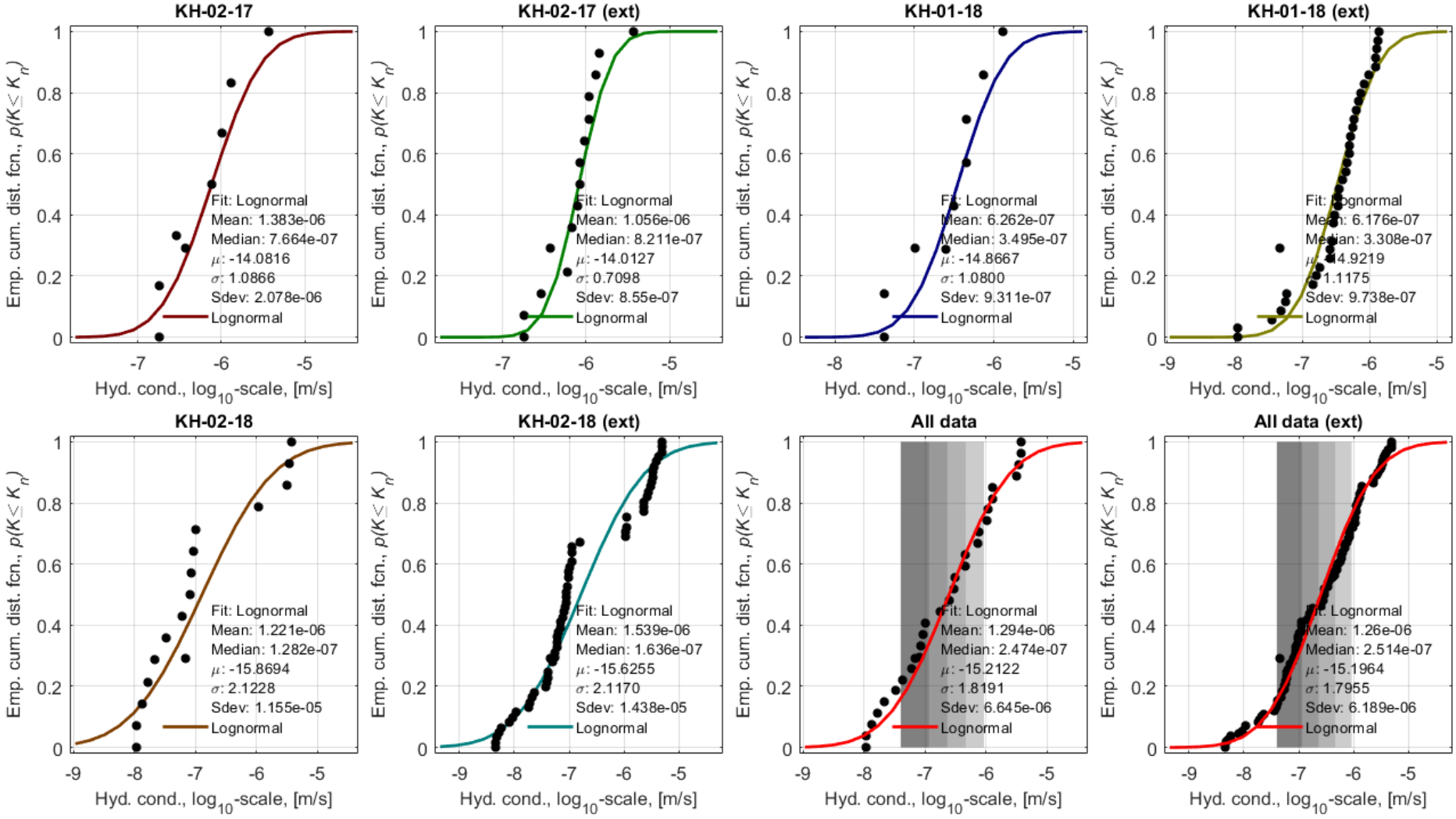

Figure 2. Hydraulic conductivity fitted to a log-normal empirical cumulative distribution function. The plots with (ext) in the title contain all the measurement data in every Lugeon-test interval. Four ranges of precipitation rates are represented by grey rectangles (from dark grey to light grey): 0.04 0.12 μm/s (equivalent to 3.5 10 mm/day), 0.12 0.23 μm/s (equivalent to 10 20 mm/day), 0.23 0.46 μm/s (equivalent to 20 40 mm/day), and finally 0.46 0.95 μm/s (equivalent to 40 80 mm/day).

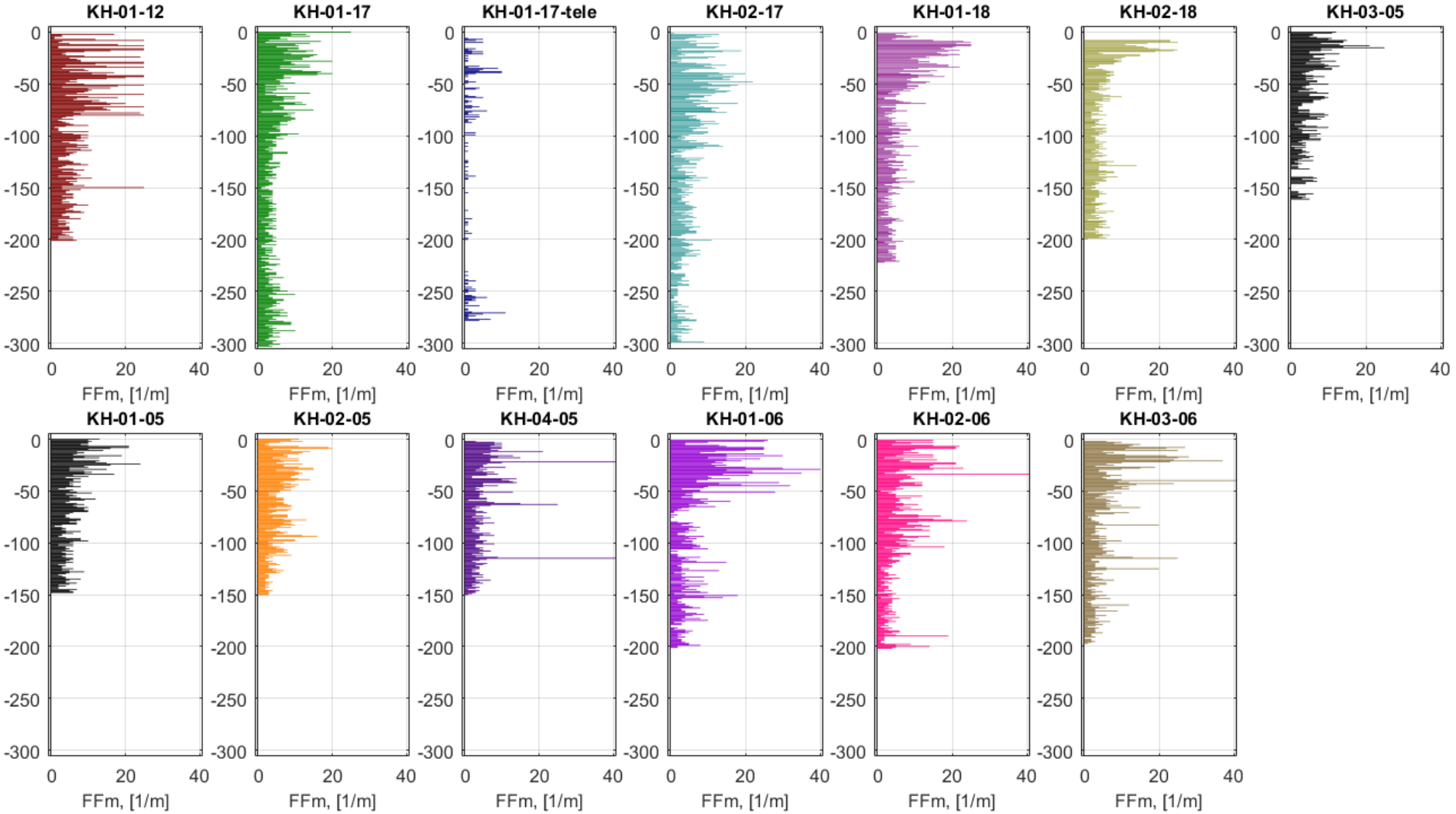

Figure 3. Fracture frequency (number of fractures per meter) with depth of various boreholes. The fracture frequency diagrams are based on core logging, except for KH-01-17 which is from a televiewer (from NGU and NGI reports, 2007 until 2019).

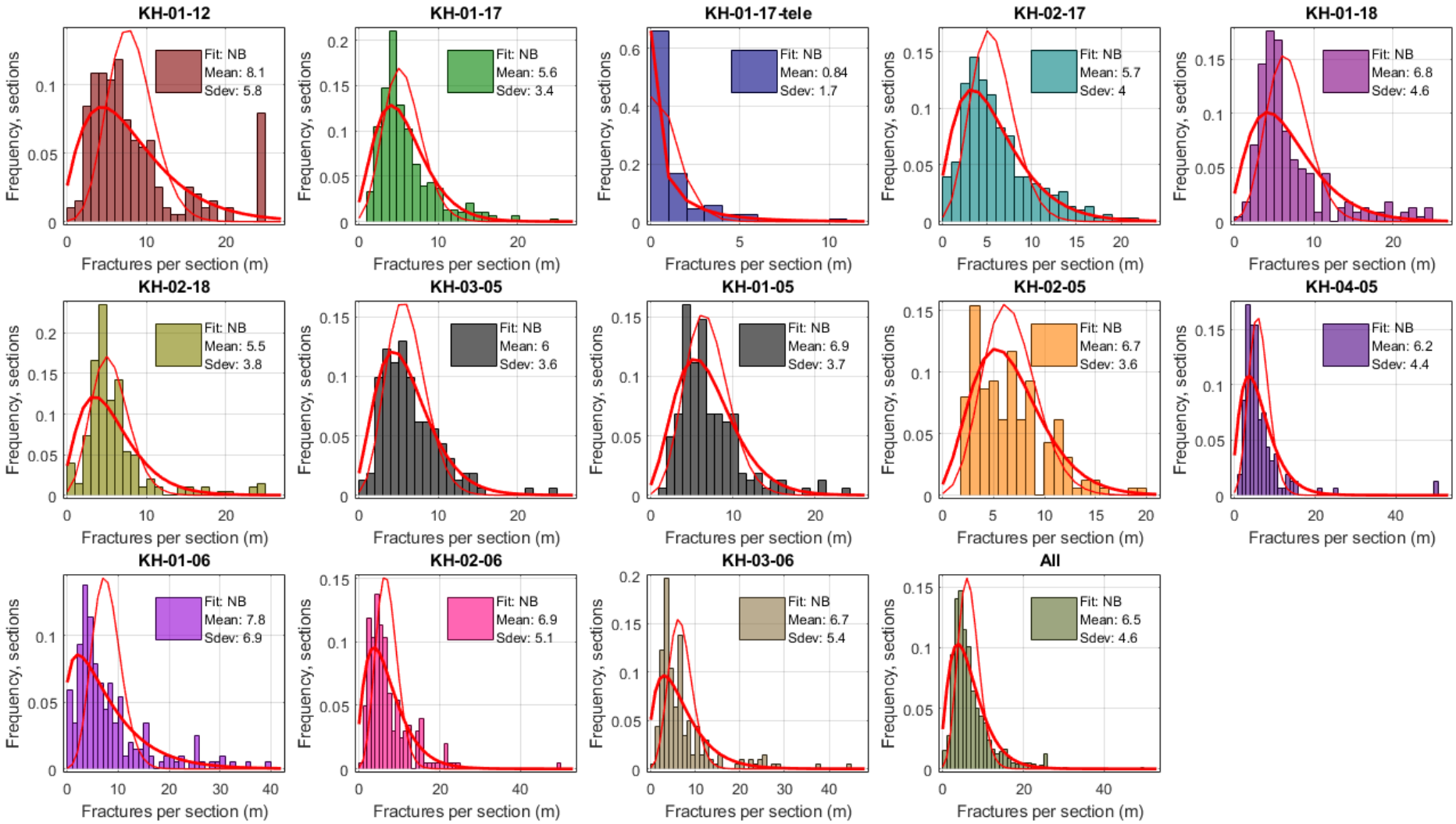

Figure 4. Bar plot of fracture frequency (number of fractures per meter) of various boreholes fitted to a Negative Binomial (NB) distribution function (thick red line) and a Poisson distribution function (thin red line). The last figure (lower right) is the statistical distribution of all the fracture datasets. The fracture frequency diagrams are based on core-logging, except for "KH 01 17 tele", which is from a televiewer.

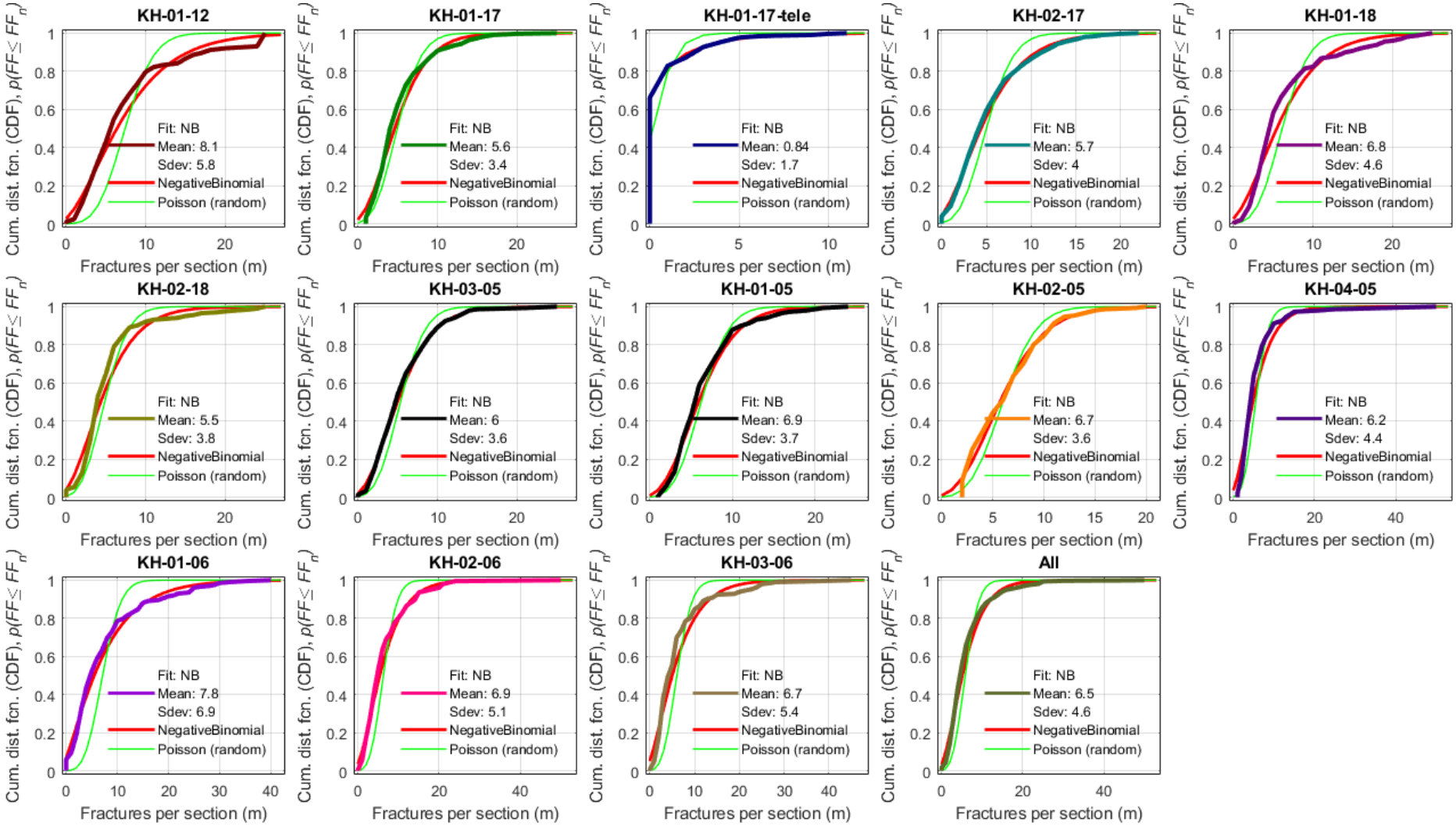

Figure 5. Cumulative distribution of fractures (number of fractures per meter) of various boreholes (thick coloured lines, not red) fitted to two cumulative distribution functions: Negative Binomial (thick red line) and Poisson (thin green line). The last figure (lower right) is the statistical distribution of all the fracture datasets. The frequency diagrams are based on core-logging, except for "KH-01-17 tele" which is from a televiewer.

Appendix G

VARIABLE HEAD TESTS IN BOREHOLES

Variable head tests in boreholes

Variable head tests were only performed in KH-02-2017. The performed variable head test follow the procedure of Norwegian standard (ISO) (NS-EN 2012b) and Beale and Read (2013);

- Rising head test; rapidly empty the borehole (or borehole section) and measure time for recovery of head to original level
- Falling head test; instantaneous increase in head by pumping water into the borehole and then measure time for the head to decline to original level

Hydraulic conductivity can be calculated from the rate at which water returns to original depth (Beale and Read, 2013), where a fast recovery of water head indicates high hydraulic conductivity and slow recovery indicates low hydraulic conductivity.

1.1.1 Instruments

Test was performed with Vanessen TD-Diver DI802, Grundfos submersible pump, and the same packers in borehole as for Lugeon Tests (NGI, 2019d).

TD-Diver is a small scale submersible datalogger. The diver is positioned in the well at a given depth from where it monitors variations in pressure from the water column (Figure 1). The Diver log pressure, temperature and data in an internal memory. The diver was located on top of the Grundfos submersible pump during tests.

The Grundfos submersible pump is about 1 m long and connected with pumping hose and power supply. The pump was equipped with a non-return valve mounted directly above the pump to stop the water in the pump-hose to flow back into the borehole after pumping stopped and the recovery time started. The pump was submerged all the way down to the packer, limiting the test section during pumping.

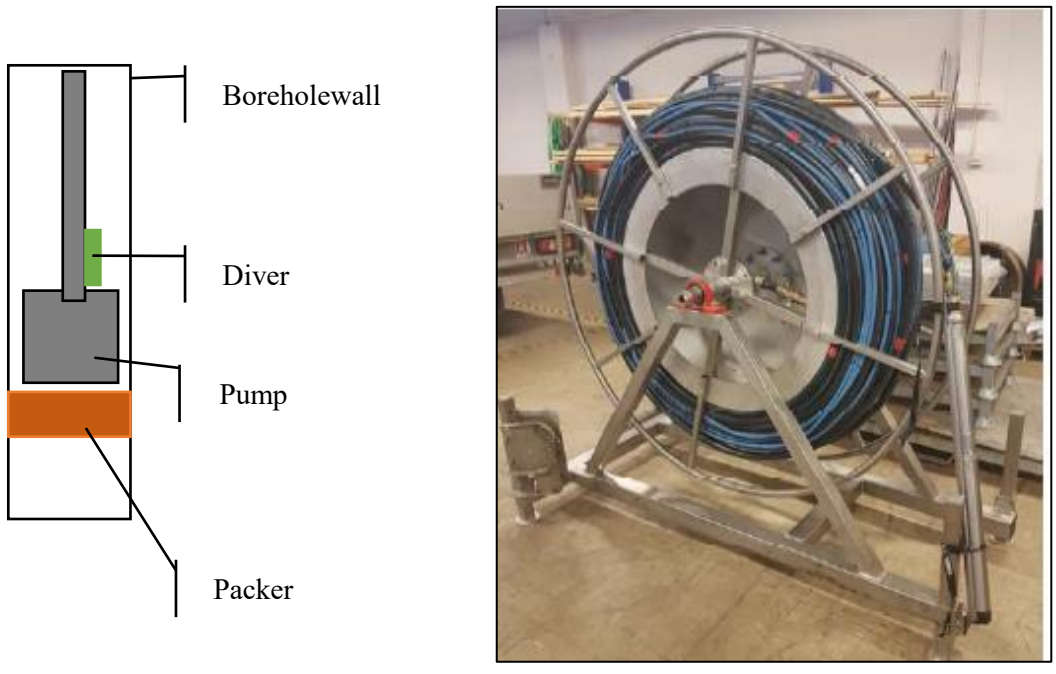

Figure 1 Left; Location of packer, pump and Diver in borehole. Right; Pump assembled.

1.1.2 Pumping tests

Some of the tests performed in KH-02-17 were unsuccessful where a constant pumping rate was not possible, but some tests were successful.

Table 1. Overview of test sections and type of variable head tests in KH-02-2017.

Zone	Variable head test	Packer placement		Length	Test status/Comment
		From	To		
		m	m	m	
Zone 1	Falling head	66,5	73,5	7	Successful / Above water level in borehole. Zone with clay from core drilling
Zone 2	Rising head	84,5	87,0	2,5	Successful / Below water level in borehole. Flowmeter measurements indicate flow
Zone 3	Rising head	88,2	90,5	2,3	Successful / No flow identified, however registered large open fracture below water level
Zone 4	Rising head	111,3	114,3	3	Not successful / No flow identified, however registered several large open fractures below water level
Zone 5	Rising head	120,5	123,5	3	Not successful / Flowmeter measurements indicate flow
Zone 6	Rising head	268,0	271,5	3,5	Successful / No flowmeter measurements performed at this depth, however registered large open fracture

Although successful, the documentation is a bit unclear as to the conditions under the various tests, so here we only report on the measured data (Figure 2 to Figure 5) and the theory to convert changes in hydraulic head over time to hydraulic properties such as hydraulic conductivity and rock mass storage coefficient (Figure 6). The test numbers in Figure 2 to Figure 5 refer to the chronological sorting of the result-datasets, and time periods are extracted from the Diver log-files.

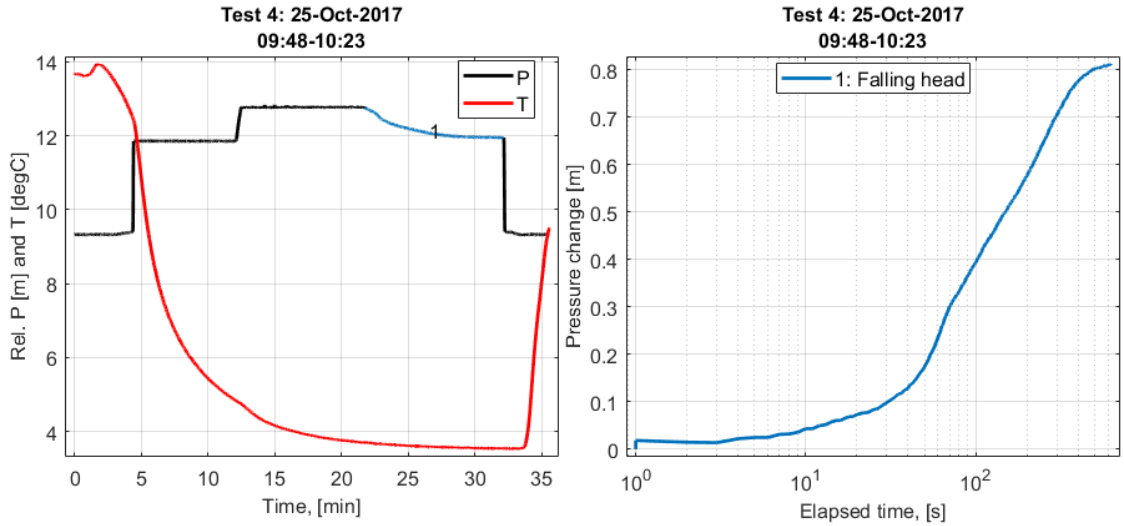

Figure 2 Falling head test zone 1, 66,5-73,5 m depth, above water level in borehole. Zone with clay from core drilling.

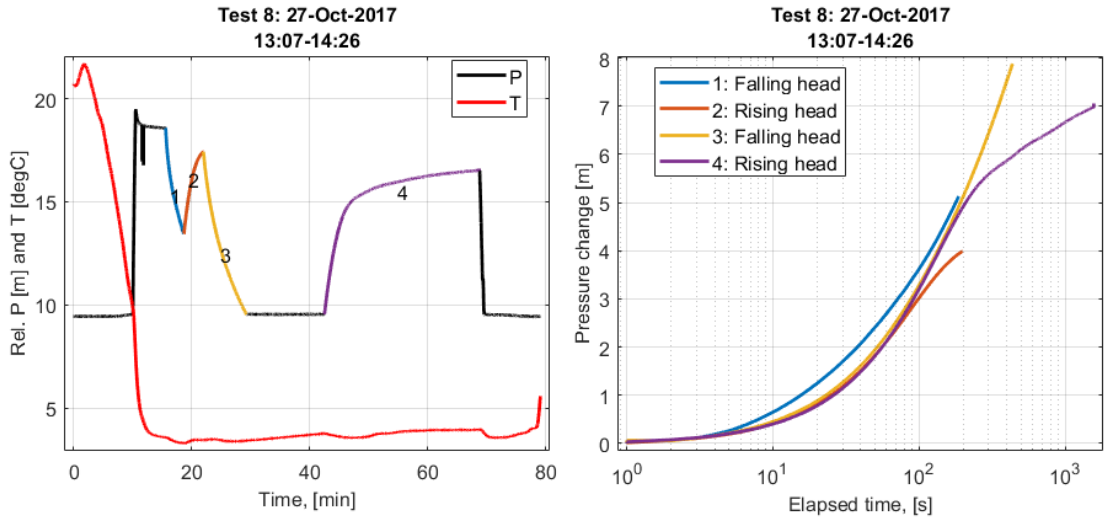

Figure 3 Repeated rising head test zone 2, 84,5-87,0 m depth, below water level in borehole. Flowmeter measurements indicate flow.

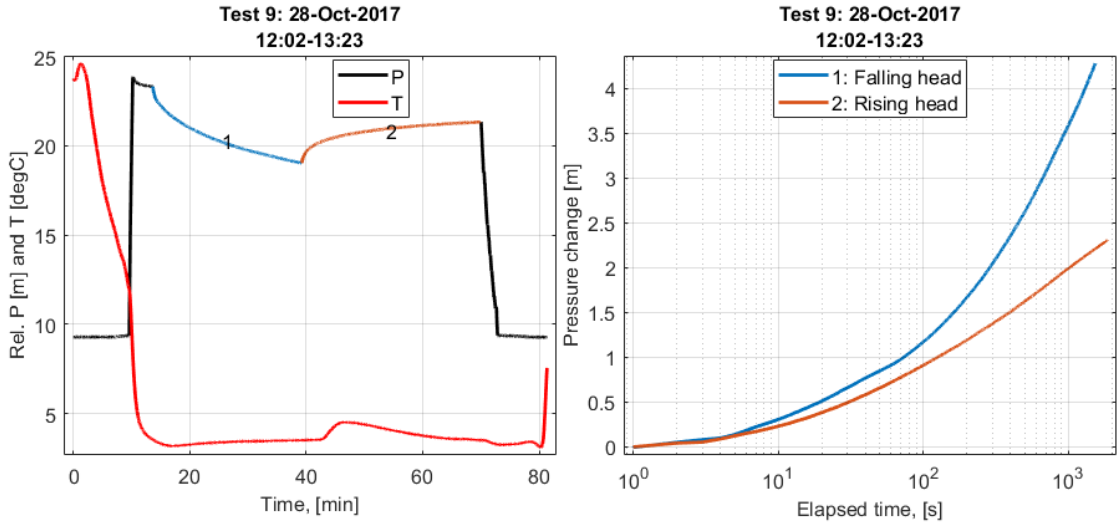

Figure 4 Rising head test zone 3, 88,2-90,5 m depth, no flow identified, however registered large open fracture below water level.

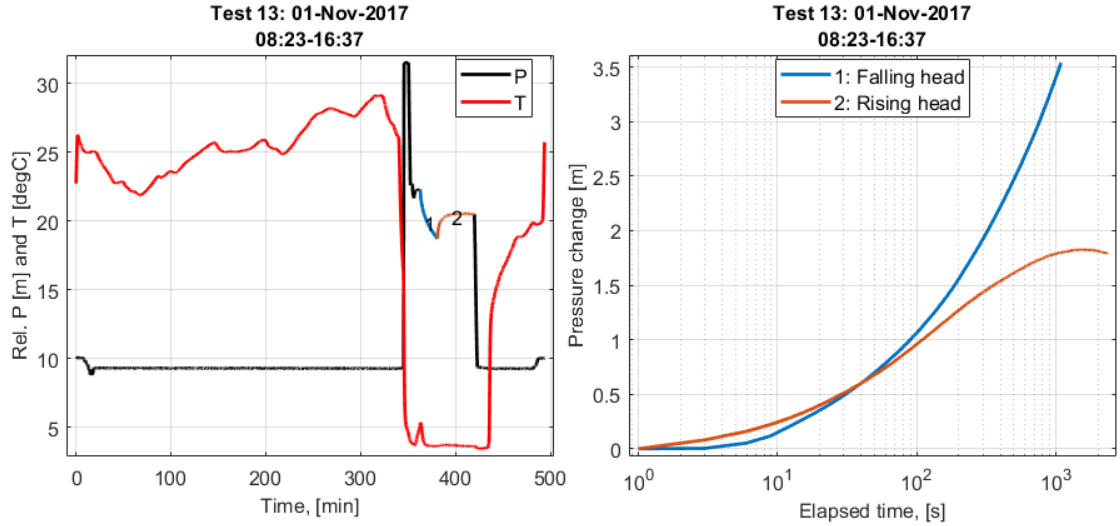

Figure 5 Rising head test zone 6, 268,0-271,5 m depth, no flowmeter measurement performed at this depth, however registered large open fracture.

The hydraulic conductivity K [m/s] can be estimated from the following formula (Cooper and Jacob, 1946):

$$K = \frac{0.1833}{\Delta s_{10}} \frac{Q}{L} \qquad \textit{Eq. 1}$$

where Q [m^3/s] is volumetric flow rate (withdrawal or recharge), Δs_{10} [m] is the change in hydraulic head (drawdown or recharge) over one decade of time on $\log_{10}$-scale and L [m] is length (thickness) of interval.

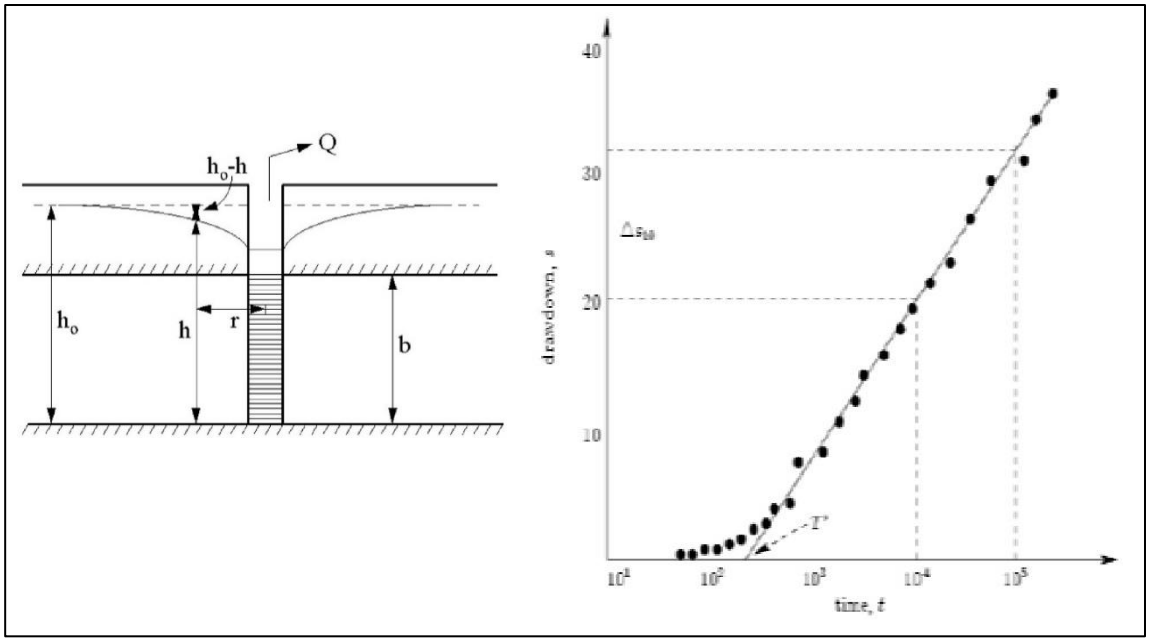

Figure 6 Left: Illustration of unsteady state drawdown of a confined aquifer. Right: Illustration of Cooper-Jacob analysis (Cooper and Jacob, 1946) for drawdown ($s = h - h_0$) of a confined aquifer. The linear part (time in log-scale) of the drawdown-curve can be used to infer hydraulic conductivity and the storage coefficient of the rock mass.

The confined storage S_c [-] coefficient can be determined from the extrapolation of the straight part of the drawdown curve in Figure 6 to zero drawdown (Cooper and Jacob, 1946):

$$S_c = 2.246KL\frac{t^*}{r^2} \qquad \textit{Eq. 2}$$

where t^* [s] is where the extrapolation of the straight part of the drawdown curve in Figure 6 crosses zero drawdown and r [m] is the radius of the borehole (here the borehole diameter is 96 mm, so r = 0,048 m). The storage coefficient S is related to the confined storage coefficient S_c in the mass conservation equations for the fluid and can be derived theoretically as:

$$S = \frac{S_c}{\rho g L} = \frac{(\alpha - \phi_{fr})}{K_s} + \frac{\phi_{fr}}{K_f} + \frac{\alpha^2}{M} \qquad \textit{Eq. 3}$$

where K_s [Pa] is the effective bulk modulus of the solid grains in the rock mass, K_f [Pa] is the inverse of the compressibility of water, α [-] is Biot's parameter (equal to 1 for soft rocks), ϕ_{fr} [-] is the fracture void fraction of the rock mass (fracture porosity) and M [Pa] is equivalent to the Oedometer modulus. Because both K_s and K_f are large (compared to the stiffness of the rock mass), Eq. 3 can be simplified to

$$S = \frac{S_c}{\rho g L} \approx \frac{1}{M} \qquad \textit{Eq. 4}$$

The Oedometer modulus is related to the mechanical stiffness of the rock mass:

$$M = \frac{E(1-\nu)}{(1+\nu)(1-2\nu)} \qquad \textit{Eq. 5}$$

where E [Pa] is Young's modulus and ν [-] is the Poisson's ratio.

Although a bit theoretical, Eq. 2, Eq. 4 and Eq. 5 can be used to derive an effective rock mass stiffness from a measured storage coefficient.

Considering the single withdraw in Figure 2 (test of zone 1), we have that $\Delta s_{10} = 0.6$ m, the volumetric flow rate is either $Q = 81$ l/min or 55 l/min (conflicting documentation), the length of the segment is $L = 7$ m and the extrapolated $t^* = 23$ s. This results in a hydraulic conductivity $K = 59$ μm/s (from Eq. 1) which is 40-1500 times higher than the range measured in the Lugeon tests. The storage coefficient is estimated to be $S = 3 \cdot 10^{-5}$ 1/Pa which implies a very soft rock mass (equivalent to a soft clay). This might be the case in a weakness zone but is not correct for a competent rock mass (gneiss in this case) in general. A similar calculation could be done for the other withdrawal and/or recharge tests, but because of uncertainty in the test-setup, particularly the parameters Q and L, it is difficult to get reliable results.

Also, based on the shape of the transient pressure change curves (not linear on a log-scale), the applicability of the method used here to estimate hydraulic conductivity and storage coefficient may be in question. It is evident that the results are not directly applicable and to get more meaningful information from the test a more thorough and detailed investigation is needed. Therefore, the hydraulic conductivity of the rock mass will rely on the Lugeon-tests described in section hydrological borehole investigations in the main report.

Kontroll- og referanseside/ Review and reference page

Dokumentinformasjon/*Document information*		
Dokumenttittel/*Document title* Hydrogeological report		**Dokumentnr./*Document no.*** 20180662-06-R
Dokumenttype/*Type of document* Rapport / Report	**Oppdragsgiver/*Client*** NVE	**Dato/*Date*** 2020-06-11
Rettigheter til dokumentet iht kontrakt/ *Proprietary rights to the document according to contract* Oppdragsgiver / Client		**Rev.nr.&dato/*Rev.no.&date*** 1 / 2021-01-14
Distribusjon/*Distribution* BEGRENSET: Distribueres til oppdragsgiver og er tilgjengelig for NGIs ansatte / LIMITED: Distributed to client and available for NGI employees		
Emneord/*Keywords* Åknes, rock slope, hydrogeology, borehole monitoring		

Stedfesting/*Geographical information*	
Land, fylke/*Country* Norway	**Havområde/*Offshore area***
Kommune/*Municipality* Stranda	**Feltnavn/*Field name***
Sted/*Location* Åknes	**Sted/*Location***
Kartblad/*Map* Geiranger 1219 II	**Felt, blokknr./*Field, Block No.***
UTM-koordinater/*UTM-coordinates* **Zone: East: North:** UTM32 X 395170 Y 6891861	**Koordinater/*Coordinates*** **Projection, datum: East: North:**

Dokumentkontroll/*Document control*
Kvalitetssikring i henhold til/*Quality assurance according to NS-EN ISO9001*

Rev/ *Rev.*	**Revisjonsgrunnlag/*Reason for revision***	**Egenkontroll av/ *Self review by:***	**Sidemanns-kontroll av/ *Colleague review by:***	**Uavhengig kontroll av/ *Independent review by*:**	**Tverrfaglig kontroll av/ *Interdisciplinary review by:***
0	Original document	2020-06-05 Kristin H. Holmøy	2020-06-08 Vidar Kveldsvik		
1	Revision 1 / Comments from NVE and UiO	2021-01-07 Kristin H. Holmøy	2021-01-13 Vidar Kveldsvik		

Dokument godkjent for utsendelse/ *Document approved for release*	**Dato/*Date***	**Prosjektleder/*Project Manager***
	14 January 2021	Kristin H. Holmøy

NGI (Norwegian Geotechnical Institute) is a leading international centre for research and consulting within the geosciences. NGI develops optimum solutions for society and offers expertise on the behaviour of soil, rock and snow and their interaction with the natural and built environment.

NGI works within the following sectors: Offshore energy – Building, Construction and Transportation – Natural Hazards – Environmental Engineering.

NGI is a private foundation with office and laboratories in Oslo, a branch office in Trondheim and daughter companies in Houston, Texas, USA and in Perth, Western Australia

www.ngi.no

NGI (Norges Geotekniske Institutt) er et internasjonalt ledende senter for forskning og rådgivning innen ingeniørrelaterte geofag. Vi tilbyr ekspertise om jord, berg og snø og deres påvirkning på miljøet, konstruksjoner og anlegg, og hvordan jord og berg kan benyttes som byggegrunn og byggemateriale.

Vi arbeider i følgende markeder: Offshore energi – Bygg, anlegg og samferdsel – Naturfare – Miljøteknologi.

NGI er en privat næringsdrivende stiftelse med kontor og laboratorier i Oslo, avdelingskontor i Trondheim og datterselskaper i Houston, Texas, USA og i Perth, Western Australia.

www.ngi.no

NGI
OSLO
TRONDHEIM
HOUSTON
PERTH

NORWEGIAN GEOTECHNICAL INSTITUTE
NGI.NO

Main office
PO Box 3930 Ullevaal St.
NO-0806 Oslo
Norway

Trondheim office
PO Box 5687 Torgarden
NO-7485 Trondheim
Norway

T (+47)22 02 30 00
F (+47)22 23 04 48
NGI@ngi.no

BIC NO. DNBANOKK
IBAN NO26 5096 0501 281
ORGANISATION NO.
958 254 318MVA

ISO 9001/14001
CERTIFIED BY BSI
FS 32989/EMS 612006